

DESIGN AND SYNTHESIS OF
CONJUGATED MACROCYCLES AND POLYMERS

by

Julian M. W. Chan

B.S. Chemistry

University of Illinois at Urbana-Champaign, 2005

Submitted to the Department of Chemistry
In Partial Fulfillment of the Requirements for the Degree of

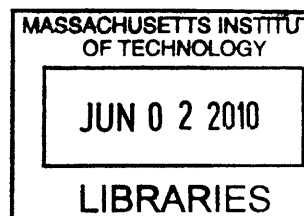
DOCTOR OF PHILOSOPHY IN CHEMISTRY

at the

MASSACHUSETTS INSTITUTE OF TECHNOLOGY

June 2010

ARCHIVES



© 2010 Massachusetts Institute of Technology. All Rights Reserved.

Signature of Author: _____

Department of Chemistry
May 20, 2010

Certified by: _____

Timothy M. Swager
Thesis Supervisor

Accepted by: _____

Robert W. Field
Chairman, Departmental Committee on Graduate Students

This doctoral thesis has been examined by a Committee at the Department of Chemistry as follows:

Professor Rick L. Danheiser: _____

Chairman

Professor Timothy M. Swager: _____

Thesis Advisor

Professor Mounji Bawendi: _____

*Dedicated to my family and Puiyee,
for all their love and support*

DESIGN AND SYNTHESIS OF CONJUGATED MACROCYCLES AND POLYMERS

By

Julian M. W. Chan

Submitted to the Department of Chemistry on May 20, 2010
In Partial Fulfillment of the Requirements for the Degree of
Doctor of Philosophy in Chemistry

ABSTRACT

The design, synthesis and characterization of conjugated macrocycles and polymers are presented in this dissertation. In particular, work involving the exploration of unusual and/or novel aromatic structures for various materials applications is described in detail, along with appropriate discussions of relevant structure-property relationships.

A brief general introduction to J-aggregates and conjugated polymers is given in Chapter 1, which represents two major areas that are dealt with throughout this thesis. Besides providing an overview of the basic principles, this introductory chapter will hopefully serve to give insight into the motivation behind the work discussed herein.

In Chapter 2, the facile one-step construction of highly functionalized cyclohexa-*m*-phenylene macrocycles from simple monobenzenoid building blocks is presented. This methodology is based on a six-fold Suzuki-Miyaura coupling, and represents an improvement over preceding cyclohexa-*m*-phenylene preparations.

In Chapter 3, the development of novel J-aggregating dibenz[*a,j*]anthracene-based macrocycles are reported. These materials are uniquely non-polar compared to all other known J-aggregates, and are also much more photostable relative to the classic J-aggregating cyanine dyes. A variation on the dibenzanthracene theme was extended to the work described in Chapter 4, which features poly(aryleneethynylene)s containing dibenz[*a,h*]anthracene repeat units. These polymers have unusual stair-stepped structures that confer unto them spectroscopic properties that are atypical of the more common poly(phenyleneethynylene)s. Chapter 5 details recent efforts aimed at utilizing the J-aggregate design principles discussed in Chapter 3 in our search for new J-aggregate candidates in various conjugated polymers and small molecules (e.g. the dibenz[*a,m*]rubicenes).

Thesis Supervisor: Timothy M. Swager

Title: John D. MacArthur Professor of Chemistry and Department Head

Table of Contents

Dedication.....	3
Abstract.....	5
Table of Contents.....	7
List of Abbreviations.....	10
List of Figures.....	11
List of Schemes.....	14
List of Tables.....	16
Chapter 1: Introduction to J-aggregates and Conjugated Polymers.....	17
1.1 J-aggregates: History and General Considerations.....	18
1.2 Exciton Theory.....	19
1.3 Designing J-aggregates.....	21
1.4 Conjugated Polymers.....	22
References and Notes.....	23
Chapter 2: Efficient Synthesis of Arylethynylated Cyclohexa-<i>m</i>-phenylenes.....	27
2.1 Introduction.....	28
2.2 Synthesis of Functionalized Cyclohexa- <i>m</i> -phenylenes.....	31
2.3 Physical Properties.....	35
2.4 Further Synthetic Studies using Cyclohexa- <i>m</i> -phenylene 4	37
2.5 Conclusions.....	40
2.6 Experimental Section.....	41
References and Notes.....	43
Appendix.....	45

Chapter 3: Synthesis of J-aggregating Dibenz[<i>a,j</i>]anthracene-based Macrocycles	49
3.1 Introduction.....	50
3.2 Synthesis.....	51
3.3 Photophysical studies.....	55
3.4 Molecular modelling.....	66
3.5 Conclusion.....	68
3.6 Experimental Section.....	68
References and Notes.....	84
Appendix	89
Chapter 4: Synthesis of Stair-stepped Polymers Containing Dibenz[<i>a,h</i>]anthracene Subunits	109
4.1 Introduction.....	110
4.2 Results and Discussion.....	111
4.3 Conclusions.....	119
4.4 Experimental Section.....	120
References and Notes.....	134
Appendix	137
Chapter 5: Towards Novel J-aggregating Structures	151
5.1 Introduction.....	152
5.2 Extension of the dibenz[<i>a,j</i>]anthracene dimer motif.....	153
5.3 Polymer prototype and model studies.....	157
5.4 Dibenz[<i>a,m</i>]rubicenes.....	161
5.5 Conclusion.....	166
5.6 Experimental Section.....	166
References and Notes.....	183

Appendix.....185

Curriculum Vitae.....205

Acknowledgments.....207

List of Abbreviations

1D	one dimensional
2D	two dimensional
3D	three dimensional
DBU	1,8-diazabicyclo[5.4.0]undec-7-ene
DCM	dichloromethane
DMAc	<i>N,N</i> -dimethylacetamide
DMF	<i>N,N</i> -dimethylformamide
DMSO	dimethyl sulfoxide
dppp	1,3-bis(diphenylphosphino)propane
EI	electron impact ionization
ESI	electrospray
GPC	gel permeation chromatography
HOMO	highest occupied molecular orbital
HRMS	high resolution mass spectrometry
LED	light-emitting diode
LUMO	lowest unoccupied molecular orbital
MALDI	matrix-assisted laser desorption/ionization
MIT	Massachusetts Institute of Technology
M_n	number-average molecular weight
MS	mass spectrometry
M_w	weight-average molecular weight
m/z	mass-to-charge ratio
NBS	<i>N</i> -bromosuccinimide
NMR	nuclear magnetic resonance
PAE	poly(aryleneethynylene)
PDI	polydispersity index
PhMe	toluene
PMMA	poly(methyl methacrylate)
PPE	poly(<i>p</i> -phenyleneethynylene)
PPP	poly(<i>p</i> -phenylene)
PPV	poly(<i>p</i> -phenylenevinylene)
PS	polystyrene
QY	quantum yield
rt (or r.t.)	room temperature
TBAF	tetra- <i>n</i> -butylammonium fluoride
TFA	trifluoroacetic acid
THF	tetrahydrofuran
TIPS	triisopropyl
TLC	thin layer chromatography
TMS	trimethylsilyl
TOF	time-of-flight
UV	ultraviolet
UV-vis	ultraviolet-visible
v/v	volume to volume ratio

List of Figures

Figure 1.1. Examples of J-aggregating cyanine dyes (where R is an alkyl group, e.g. Et)

Figure 1.2. State energy diagram showing a monomer dye, an H-aggregate, and a J-aggregate. The small arrows depict transition dipole moments of the interacting chromophores.

Figure 1.3. General structure of a perylene bisimide dye, where X and Y are bay substituents.

Figure 1.4. a) Schematic of a poly(aryleneethynylene) b) A poly(*para*-phenyleneethynylene)

Figure 2.1. Normalized absorbance (blue line) and emission (pink line) spectra of **4**

Figure 2.2. a) Energy-minimized (PM3) structure of compound **4**. b) Inset of congested cavity.

Figure 2.3. Energy-minimized (PM3) 3D structure of the proposed kekulene

Figure 3.1. Normalized absorbance (solid lines) and emission (dotted lines) spectra of **6a**, **6b**, **12** and **15** in chloroform.

Figure 3.2. Absorption spectra of **6a**, solution (blue line) vs. film (red line), normalized to the absorbance at 340 nm.

Figure 3.3. Normalized absorption (blue line) and fluorescence (pink line) spectra of **6a** (film).

Figure 3.4. Absorption spectra of **6a** (film), before and after annealing under toluene (PhMe) and THF vapor, normalized to the absorbance at 340 nm.

Figure 3.5. Absorption spectra of **6b** (film) and **12** (film), before and after annealing under THF vapor, normalized to the absorbance at 340 nm.

Figure 3.6. Photoluminescence intensity vs. concentration of **6a** in thin films (PL scaled by subtracting the background and scaling by integrated intensity at all wavelengths).

Figure 3.7. Excitation vs. concentration of **6a** in thin films (PLE scaled by subtracting background and scaling by integrated intensity at all wavelengths).

Figure 3.8. PM3-calculated models (a) top-down view of geometry-optimized macrocyclic structure, (b) molecular electrostatic potential map, (c) optimized structure tilted to emphasize steric crowding, (d) edge-on view of optimized structure, (e) frontier HOMO, and (f) frontier LUMO, (g) edge-on view of the acyclic model structure, (h) top-down view of the acyclic structure.

Figure 4.1. Anthracene (left), dibenz[*a,h*]anthracene (center), dibenz[*a,j*]anthracene (right).

Figure 4.2. UV-vis (solid lines) and fluorescence (dashed lines) spectra of polymers **8**, **9**, **13**, **19** in chloroform solution (black) and in thin films (red; normalized).

Figure 5.1 a) Absorption and emission spectra of **8** in chloroform. b) UV-vis absorption spectra of **8** (film vs. solution).

Figure 5.2 a) Absorption and emission spectra of **9** in chloroform. b) UV-vis absorption spectra of **9** (film vs. solution), with a sharp J-band observed in the film spectrum.

Figure 5.3 a) Absorption and emission spectra of polymer **12** in chloroform. b) Solutions of **12** under ultraviolet irradiation.

Figure 5.4 a) Spartan model of a substituted dibenz[*a,m*]rubicene (from top), b) Side-on view showing a dihedral angle of 16.6°, c) Two-dimensional representation of the molecule.

Figure 5.5 Absorption and emission spectra of **32** in chloroform solution

List of Schemes

Scheme 2.1. Synthesis of the parent cyclohexa-*m*-phenylene by Staab *et al.*

Scheme 2.2. Synthesis of Kekulene by Staab and Diederich.

Scheme 2.3. Synthesis of the diboronate building block

Scheme 2.4. Synthesis of cyclohexa-*m*-phenylene **4** via six-fold Suzuki coupling

Scheme 2.5. Proposed conversion of cyclohexa-*m*-phenylene to kekulene.

Scheme 3.1. Synthesis of macrocycles **6a** and **6b**.

Scheme 3.2. Synthesis of macrocycle **12**.

Scheme 3.3. Synthesis of acyclic **15**.

Scheme 4.1. Synthesis of monomers **3** and **5**.

Scheme 4.2. Synthesis of polymers **8** and **9**.

Scheme 4.3. Synthesis of polymer **13**.

Scheme 4.4. Synthesis of polymer **19**.

Scheme 5.1. Synthesis of a network polymer containing dibenz[*a,j*]anthracene repeat units

Scheme 5.2. Synthesis of polymer **16**

Scheme 5.3. Synthesis of model compound **21**

Scheme 5.4. Attempted synthesis of a substituted dibenz[*a,m*]rubicene

Scheme 5.5. Synthesis of dibenz[*a,m*]rubicene 32

List of Tables

Table 2.1. Scope of the one-step macrocyclization

Table 2.2. Attempted conditions for the key electrophilic cyclization step

Table 3.1. Photophysical properties of **6a**, **6b**, **12**, and **15**.

Table 3.2. Fluorescence lifetimes of **6a** (solutions and films) at different concentrations.

Table 4.1. Characterization and Spectroscopic Data for Polymers **8**, **9**, **13**, **19**

Chapter 1
Introduction to J-aggregates and
Conjugated Polymers

1.1 J-aggregates: History and General Considerations

In the 1930s, it was observed that the aggregation of pseudoisocyanine dyes in concentrated solutions gave rise to the appearance of an intense and very narrow absorption band that was red-shifted relative to the absorption band of monomeric pseudoisocyanine.¹ Along with the observation of this so-called J-band, the pseudoisocyanines also displayed narrow resonance fluorescence bands and extremely small Stokes shifts. This rare and interesting phenomenon was reported independently by Edwin E. Jelley (Kodak) and Günter Scheibe in 1936, and these special dye aggregates were henceforth known as J-aggregates or Scheibe aggregates.² Apart from these features, J-aggregates typically also exhibit extremely high quantum yields that can approach 100%, coherently-coupled transition dipole moments, delocalized excitons and sometimes non-linear optical behavior as well. As one can imagine, materials having such properties would have significant technological implications (e.g. fluorescent sensors, organic photoconductors, and photovoltaics).³ However, despite being around for almost 80 years, J-aggregates still have not found widespread applications in today's modern optoelectronic technology. In fact, J-aggregating cyanine dyes (Figure 1.1) have thus far only been used as spectral sensitizers of the photographic process in silver halides⁴, a process that takes advantage of their strong absorption.

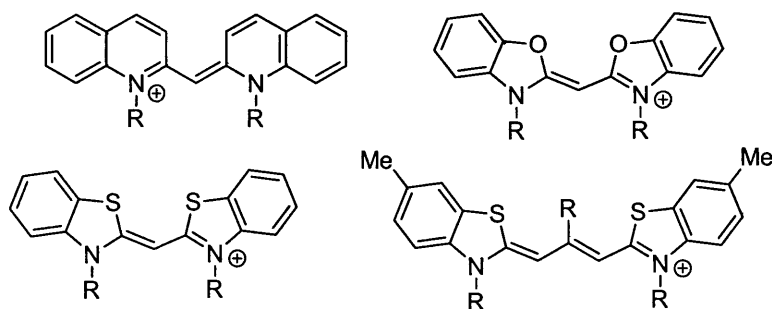


Figure 1.1. Examples of J-aggregating cyanine dyes (where R is an alkyl group, e.g. Et)

There are several reasons for the current lack of technological applications of J-aggregates. One reason is the paucity of known J-aggregates beyond the cyanine class of dyes. Furthermore, these dyes are mostly water-soluble compounds with poor photostability, thus imposing a huge limitation on the range of technological applications where they may be applied. Finally, the structure-property relationship behind J-aggregating molecules is also not well-developed, and until the appearance of some recent works⁵ by the group of Frank Würthner, the past eight decades have seen virtually no attempts at the rational design of J-aggregating molecules. In order to fully take advantage of the unique properties of J-aggregates, additional classes of J-aggregates will have to be developed. In particular, J-aggregating molecules that are photochemically robust as well as processible need to be discovered, and to do this, the structure-property relationships of J-aggregates have to be more thoroughly studied and understood.

1.2 Exciton Theory

In order to account for some of the spectroscopic properties observed in J-aggregates, a brief discussion of molecular exciton theory⁶ is appropriate. First, consider two chromophores coming into close proximity to each other to form a dimeric aggregate (Figure 1.2). Aromatic dye molecules with flat extended π -systems may aggregate in a parallel fashion (plane-to-plane stacking) to give either a sandwich arrangement (H-dimer) or a slip-stacked arrangement (J-dimer), depending on the magnitude of the slip angle between the two aggregating molecules. Next, the individual transition dipoles of each molecule must be considered. These may be arranged such that they align in the same direction, or point in opposite directions.

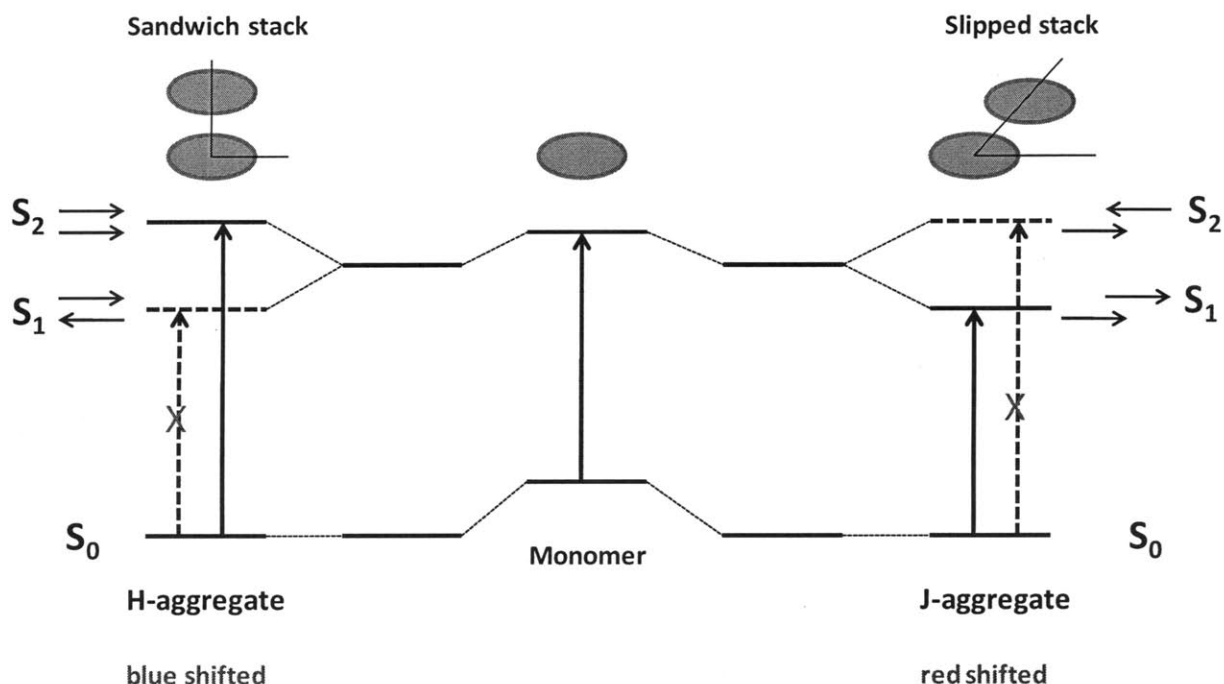


Figure 1.2. State energy diagram showing a monomer dye, an H-aggregate, and a J-aggregate. The small arrows depict transition dipole moments of the interacting chromophores.

In the case of the sandwich H-dimer, the lower energy state S_1 is the one where transition dipoles are anti-aligned, since electrostatic repulsions are minimized during an electronic transition. However, since this lower energy state has a net transition dipole of zero, electronic transitions to this state do not take place. Instead, transition to the higher energy state S_2 occurs in H-dimers/aggregates. Accordingly, a blue-shift, or hypsochromic shift, is observed, hence the term H-aggregate. In the case of the J-dimer, the lower energy state S_1 with head-to-tail dipole arrangements is the state with a non-zero net transition dipole moment, a consequence of the slip-stacking. Electronic transitions to this lower energy state are thus allowed, thereby accounting for red-shifted absorption relative to the monomeric species. This red-shifted absorption band in J-aggregates (J-band) tends to be intense, owing to the fact that the transition dipole moments of individual molecules are coherently coupled, giving the entire system a very

large oscillator strength. Since electrons in H-aggregates are excited into the higher energy state S_2 , non-radiative processes to the lower energy state S_1 can occur, resulting in weak fluorescence. In J-aggregates however, electrons are photoexcited into the lower energy state S_1 , and as a result, a similar non-radiative decay pathway does not exist, manifesting in strong unquenched fluorescence.

1.3 Designing J-aggregates

As mentioned earlier, the rational design of J-aggregating materials has received attention only in recent years, with most of the important work being done by the group of Frank Würthner in Germany. Slip-stacking appears to be one of the important criteria in bringing about J-aggregation, akin to the slipped arrangement of chromophores in both natural and artificial light-harvesting systems.⁷ Many works by Würthner involving the rational design and synthesis of J-aggregates have thus focused on twisted perylene bisimide dyes⁵ (Figure 1.3).

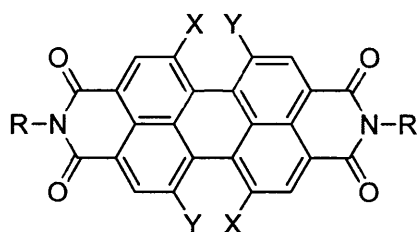


Figure 1.3. General structure of a perylene bisimide dye, where X and Y are bay substituents.

By installing a variety of bulky substituents in the bay region of the perylene bisimide, the otherwise planar molecule becomes twisted in order to minimize the steric interactions. Consequently, it becomes difficult for the twisted dye molecules to associate in a sandwich, H-aggregate fashion, but instead, adopt slip-stacked arrangements that lead to J-aggregation. This

approach by Würthner represents the first approach towards the rational design of J-aggregates, and can serve as a launch pad for the future syntheses of new J-aggregate candidates. Our own work⁸ on J-aggregates draws on some of these design principles, and will form the subject of Chapters 3 and 5.

1.4 Conjugated Polymers

With the discovery of polyacetylene back in 1977, the field of conjugated polymers/electroactive polymers was born.⁹ Conjugated polymers are organic semiconductors and have been the focus of much research over the past three decades.¹⁰ In general, these polymers are macromolecules that possess a backbone chain of alternating single and multiple C-C bonds, forming an extended linear π -system. Some examples of conjugated polymers include, but are not limited to, poly(aryleneethynylene)s (PAEs), poly(*para*-phenylene)s (PPPs), poly(*para*-phenylene vinylene)s (PPVs), and polythiophenes. Many of these fluorescent conjugated polymers have found important technological applications in the form of chemical sensors¹¹, organic photovoltaics¹², etc. For the purpose of this thesis, only the poly(aryleneethynylene)¹³ class of conjugated polymers will be relevant. These are polymers consisting of aryl units connected together by alkyne linkers throughout the entire backbone. The most widely studied subclass of these polymers are the poly(*para*-phenyleneethynylene)s, where the aryl units are simply benzene rings (Figure 1.4).

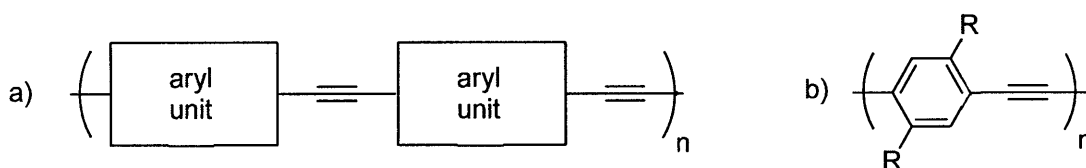


Figure 1.4. a) Schematic of a poly(aryleneethynylene) b) A poly(*para*-phenyleneethynylene)

While the PAEs do not have any special properties that set them apart from the other classes of conjugated polymers, they are attractive to researchers due to the fact that they can be easily synthesized by various organometallic polycondensations¹⁴ (e.g. Sonogashira-Hagihara coupling) between the appropriate monomers. Their facile preparation allows for easy tuning of polymer properties, since the repeat units can be varied readily, and a small library of PAEs can be built up fairly quickly. In addition, the PAEs also tend to have high fluorescence quantum yields and good photostability. The specific PAEs that will be dealt with in this dissertation are those in which the aryl units are polycyclic aromatic moieties, covered in Chapter 4. The work discussed therein will describe successful efforts to explore unusual structures as PAE precursors, thus pushing the limits of structural diversity within the field of PAEs.¹⁵

References and Notes

- [1] (a) Jelley, E. E. *Nature* **1936**, *138*, 1009–1010 (b) Jelley, E. E. *Nature* **1937**, *139*, 631–632 (c) Scheibe, G. *Angew. Chem.* **1936**, *49*, 563 (d) Scheibe, G. *Angew. Chem.* **1937**, *50*, 51; (e) Scheibe, G. *Kolloid-Z.* **1938**, *82*, 1–14; (f) Scheibe, G., Schöntag, A. and Katheder, F. *Naturwissenschaften* **1939**, *29*, 499–501.
- [2] (a) Mübicus, D. *Adv. Mater.* **1995**, *7*, 437–444. (b) Kobayashi, T., Ed. *J-Aggregates*; World Science: Singapore, 1996. (c) Dähne, S. *Bunsen-Magazin* **2002**, *4*, 81–92 (d) Knoester, J. *Int. J. Photoenergy* **2006**, *5*, 4(1–10) (e) Kirstein, S.; Dähne, S. *Int. J. Photoenergy* **2006**, *5*, 3(1–21) (f) Shapiro, B. I. *Russ. Chem. Rev.* **2006**, *75*, 433–456 (g) Egorov, V. V.; Alfimov, M. V. *Phys.-Usp.* **2007**, *50*, 985–1029.

- [3] (a) Hannah, K. C.; Armitage, B. A. *Acc. Chem. Res.* **2004**, *37*, 845–853 (b) Whitten, D. G.; Achyuthan, K. E.; Lopez, G. P.; Kim, O.-K. *Pure Appl. Chem.* **2006**, *78*, 2313–2323 (c) Law, K. Y. *Chem. Rev.* **1993**, *93*, 449–86 (d) Meng, F.; Chen, K.; Tian, H.; Zuppiroli, L.; Nuesch, F. *Appl. Phys. Lett.* **2003**, *82*, 3788–3790 (e) Sayama, K.; Tsukagoshi, S.; Mori, T.; Hara, K.; Ohga, Y.; Shinpou, A.; Abe, Y.; Suga, S.; Arakawa, H. *Sol. Energy Mater. Sol. Cells* **2003**, *80*, 47–71 (f) Kawasaki, M.; Aoyama, S. *Chem. Commun.* **2004**, 988–989 (g) Tameev, A. R.; Vannikov, A. V.; Schoo, H. F. M. *Thin Solid Films* **2004**, *451/452*, 109–111.
- [4] a) Herz, A. H. *The Theory of the Photographic Process*, 4th ed.; James, T. H., Ed.; MacMillan: New York, 1977; Chapter 9 and references therein. b) Herz, A. H. *Adv. Colloid Interface Sci.* **1977**, *8*, 237–298.
- [5] a) Kaiser, T. E.; Stepanenko, V.; Würthner, F. *J. Am. Chem. Soc.* **2009**, *131*, 6719–6732 b) Kaiser, T. E., Wang, H., Stepanenko, V., Würthner, F. *Angew. Chem. Int. Ed.* **2007**, *46*, 5541–5544; c) Yagai, S., Seki, T., Karatsu, T., Kitamura, A., Würthner, F. *Angew. Chem. Int. Ed.* **2008**, *47*, 3367–3371; d) Li, X.-Q., Zhang, X., Ghosh, S., Würthner, F. *Chem. Eur. J.* **2008**, *14*, 8074–8078; e) Würthner, F., Bauer, C., Stepanenko, V., Yagai, S. *Adv. Mater.* **2008**, *20*, 1695–1698. f) Wang, H., Kaiser, T. E., Uemura, S., Würthner, F. *Chem. Commun.* **2008**, 1181–1183. g) Würthner, F. *Chem. Commun.* **2004**, 1564–1579; h) Würthner, F. *Pure Appl. Chem.* **2006**, *78*, 2341–2349.
- [6] Kasha, M.; Rawls, H. R.; El-Bayoumi, M. A. *Pure Appl. Chem.* **1965**, *11*, 371–392.
- [7] (a) Hoeben, F. J. M.; Jonkheim, P.; Meijer, E. W.; Schenning, A. P. H. *J. Chem. Rev.* **2005**, *105*, 1491–1546 (b) Wasielewski, M. R. *J. Org. Chem.* **2006**, *71*, 5051–5066 (c) Yamamoto, Y.; Fukushima, T.; Suna, Y.; Ishii, N.; Saeki, A.; Seki, S.; Tagawa, S.; Taniguchi, M.;

Kawai, T.; Aida, T. *Science* **2006**, *314*, 1761–1764 (d) Miller, R. A.; Presley, A. D.; Francis, M. B. *J. Am. Chem. Soc.* **2007**, *129*, 3104–3109 (e) *Photosynthetic Light-Harvesting Systems: Organization and Function*; Scheer, H.; Schneider, S., Eds.; de Gruyter: Berlin, 1988. (f) Prokhorenko, V. I.; Steensgard, D. B.; Holzwarth, A. R. *Biophys. J.* **2000**, *79*, 2105–2120 (g) Takahashi, R.; Kobuke, Y. *J. Am. Chem. Soc.* **2003**, *125*, 2372–2373 (h) Yamaguchi, T.; Kimura, T.; Matsuda, H.; Aida, T. *Angew. Chem. Int. Ed.* **2004**, *43*, 6350–6355 (i) Elemans, J. A. A. W.; van Hameren, R.; Nolte, R. J. M.; Rowan, A. E. *Adv. Mater.* **2006**, *18*, 1251–1266.

[8] Chan, J. M. W., Tischler, J. R., Kooi, S. E., Bulović, V., Swager, T. M. *J. Am. Chem. Soc.* **2009**, *131*, 5659-5666.

[9] Shirakawa, H.; Louis, E. J.; MacDiarmid, A. G.; Chiang, C. K.; Heeger, A. J. *J. Chem. Soc. Chem. Commun.* **1977**, 578-580.

[10] a) Shirakawa, H. *Angew. Chem. Int. Ed.* **2001**, *40*, 2575–2580; b) MacDiarmid, A. G. *Angew. Chem. Int. Ed.* **2001**, *40*, 2581–2590; c) Heeger, A. J. *Angew. Chem. Int. Ed.* **2001**, *40*, 2591–2611. c)

[11] a) Burnworth, M.; Rowan, S. J.; Weder, C. *Chem. Eur. J.* **2007**, *13*, 7828-7836; b) Knapton, D.; Burnworth, M.; Rowan, S. J.; Weder, C. *Angew. Chem. Int. Ed.* **2006**, *45*, 5825-5829; c) Zhang, S. W.; Swager, T. M. *J. Am. Chem. Soc.* **2003**, *125*, 3420-3421.

[12] a) Bendikov, M.; Wudl, F.; Perepichka, D. F.; *Chem. Rev.* **2004**, *104*, 4891-4946; b) Benanti, T. L.; Venkataraman, D. *Photosynthesis Res.* **2006**, *87*, 73-81; c) Gunes, S.; Neugebauer, H.; Sariciftci, N. S. *Chem. Rev.* **2007**, *107*, 1324-1338; d) Spanggaard, H.; Krebs, F. C. *Solar Energy Materials, Solar Cells* **2004**, *83*, 125-146; e) Bundgaard, E.;

Krebs, F. C. *Solar Energy Materials, Solar Cells* **2007**, *91*, 954-985; f) Segura, J. L.; Martin, N.; Guldi, D. M. *Chem. Soc. Rev.* **2005**, *34*, 31-47.

[13] a) Bunz, U. H. F. *Macromol. Rapid. Commun.* **2009**, *30*, 772-805; b) Bunz, U. H. F. *Chem. Rev.* **2000**, *100*, 1605-1644; c) Skotheim, T. A.; Reynolds, J. *Conjugated Polymers: Theory, Synthesis, Properties, and Characterization*; CRC Press: USA, 2006.

[14] a) Pinto, M. R.; Schanze, K. S. *Synthesis* **2002**, 1293-1309; b) Yamamoto, T. *Macromol. Rapid Commun.* **2002**, *23*, 583-606; c) Mangel, T.; Eberhardt, A.; Scherf, U.; Bunz, U. H. F.; Müllen, K. *Macromol. Rapid Commun.* **1995**, *16*, 571-580; d) Giesa, R. J. *Macromol. Sci.-Rev. Macromol. Chem. Phys.* **1996**, *36*, 631; e) Babudri, F.; Farinola, G. M.; Naso, F. J. *Mater. Chem.* **2004**, *14*, 11-34; f) Yamamoto, T. *Synlett* **2003**, 0425-0450; g) Yamamoto, T. *Bull. Chem. Soc. Jpn.* **1999**, *72*, 621-638.

[15] Chan, J. M. W., Kooi, S. E., Swager, T. M. *Macromolecules* **2010**, *43*, 2789-2793.

Chapter 2

Efficient Synthesis of Arylethynylated Cyclohexa-*m*-phenylenes

Adapted and reprinted from:

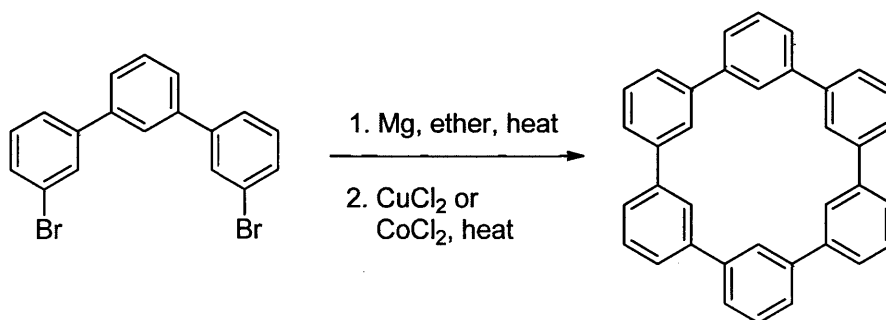
Chan, J. M. W., Swager, T. M. *Tetrahedron Lett.* **2008**, *49*, 4912-4914

with permission from Elsevier

2.1 Introduction

Cyclohexa-*m*-phenylenes are conjugated macrocycles possessing the same oligobenzene-based backbone as the poly(*p*-phenylene)s (PPPs). Ever since the first syntheses of cyclohexa-*m*-phenylenes by the Heinz Staab group in the 1960s¹, there has generally been little attention given to these interesting macrocyclic species, with the notable exception of some work on cyclohexa-*m*-phenylene-based cation hosts conducted by Donald Cram and co-workers in the 1980s.² In recent years, other than a publication³ in 2007 by the Klaus Müllen group, there have been no reports of cyclohexa-*m*-phenylenes bearing functional groups more complex than alkyl and alkoxy substituents. Furthermore, those synthetic strategies utilized by Staab *et. al.* for making cyclohexa-*m*-phenylenes involve the cumbersome preparation of terphenyl precursors prior to the final macrocyclization step, which is effected by a reductive coupling (Scheme 2.1). The terphenyl strategy not only restricts the diversity of symmetries that can be achieved in the final product, but also limits the range of functional groups that can be tolerated, considering the harsh conditions used in the annulation step.

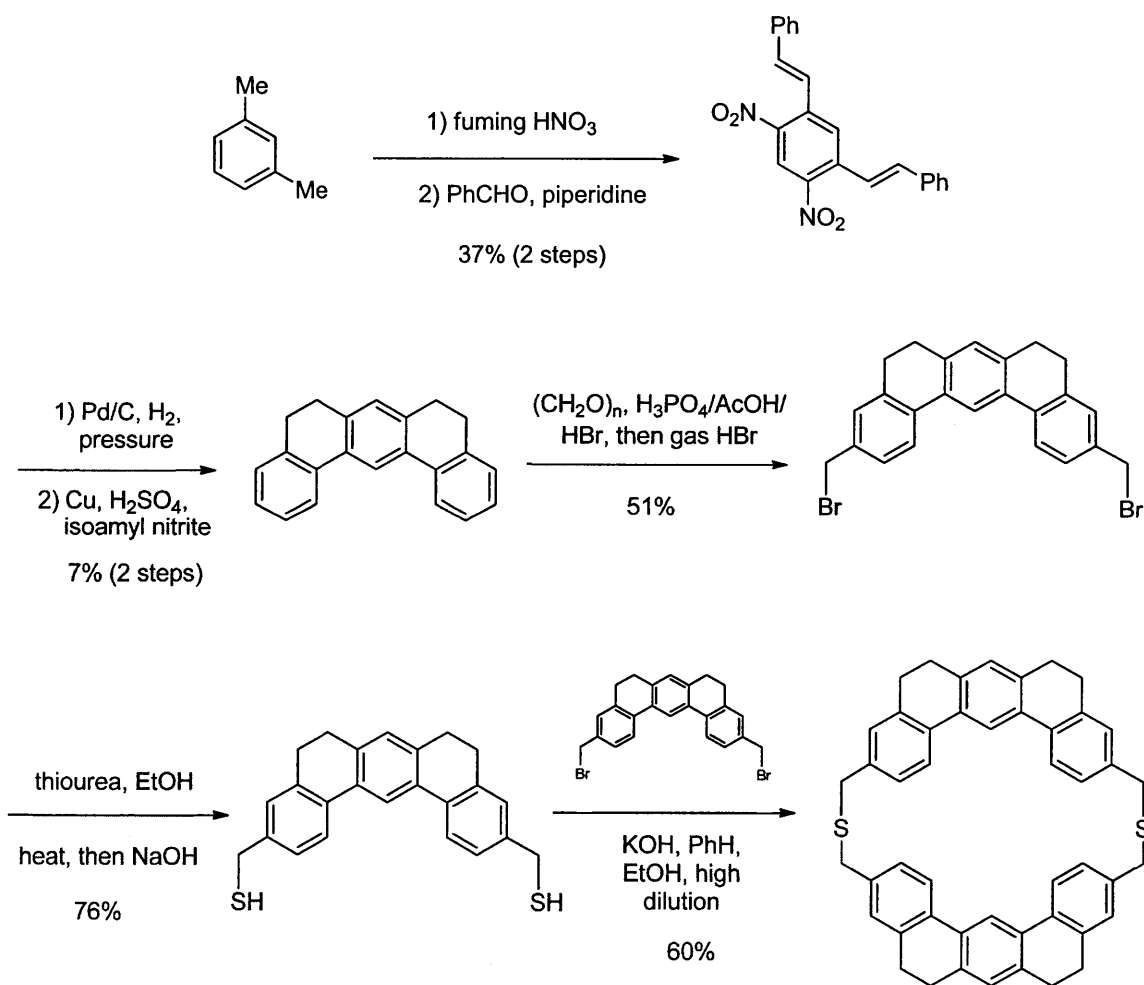
Scheme 2.1. Synthesis of the parent cyclohexa-*m*-phenylene by Staab *et al.*

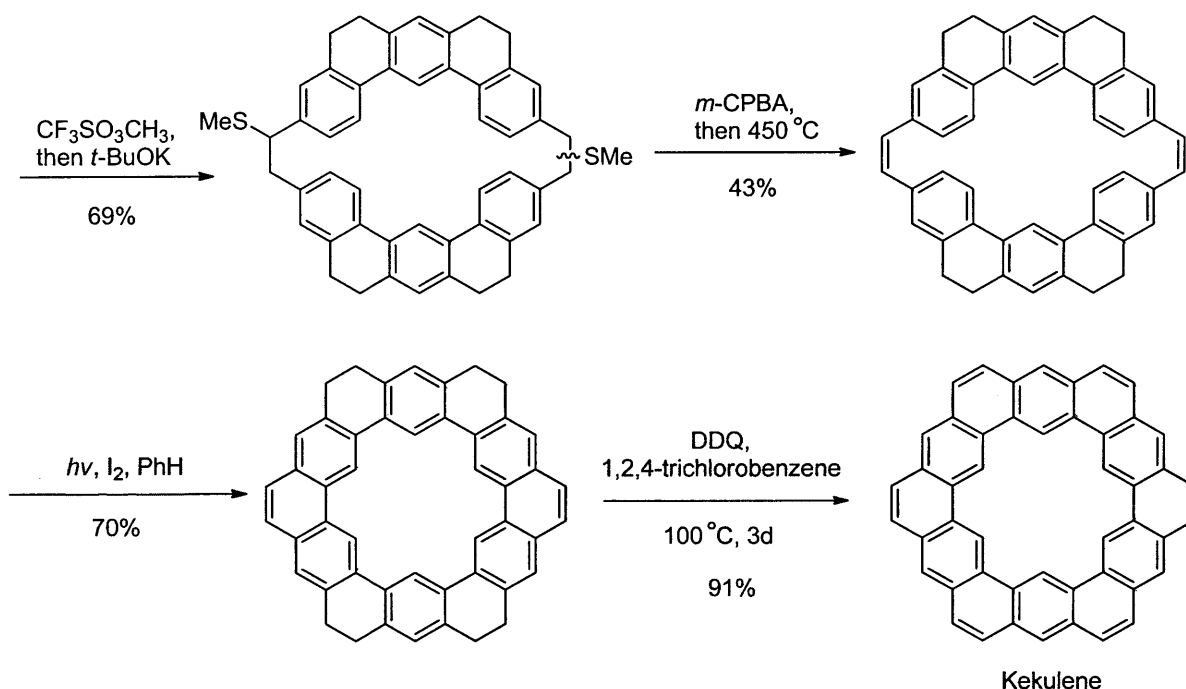


Given the worldwide interest in developing novel functional materials, more efficient methods for the synthesis of cyclohexa-*m*-phenylenes need to be developed, so that this class of

compounds can be more thoroughly investigated for their materials properties. The methodology discussed below adds another technique to the ever-growing arsenal of synthetic tools in the field of organic materials chemistry. It was also hoped that by using this method to synthesize a highly decorated cyclohexa-*m*-phenylene bearing six arylethynyl substituents on the periphery, we could subsequently gain rapid access to a host of soluble, functionalized kekulene structures by carrying out multiple electrophilic cyclizations in a single operation. The parent kekulene molecule itself was synthesized in 1983 by Diederich and Staab via a moderately lengthy and very laborious synthetic route containing several low-yielding steps (see Scheme 2.2 below).⁴

Scheme 2.2. Synthesis of Kekulene by Staab and Diederich.





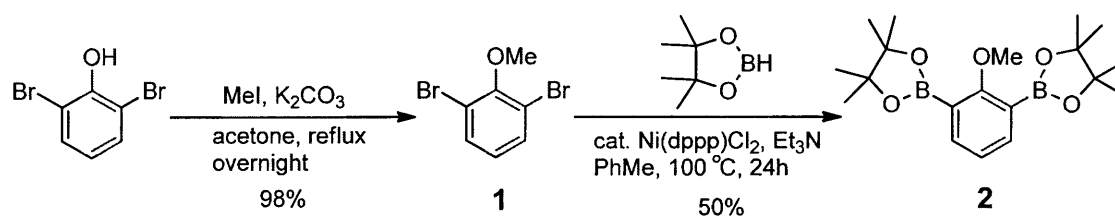
Furthermore, the kekulene product was highly insoluble and challenging to characterize due to the absence of any solubilizing substituents. Such an intractable compound would hardly be ideal as an electronic material, since the ease of processability is of paramount importance when it comes to incorporation into devices. However, the yellow-green color of kekulene (indicating a band gap corresponding to energies within the visible spectrum), along with its fluorescent properties and its lack of precedent as a structural motif in the field of materials science, was sufficient justification for new synthetic attempts at making functionalized versions of the parent molecule. In particular, we envisioned the possibility of designing soluble kekulenes that had the ability to chelate metal cations within the central cavity, and form self-assembled columns via π - π stacking interactions and/or metal-metal interactions. The self-assembly of rigid disk-like cores bearing flexible peripheral sidechains are known to bring about discotic liquid crystalline behavior.⁵ Unfortunately, even after a protracted period of research by us, conversion of the cyclohexa-*m*-phenylene precursor to the substituted kekulene was never

successfully achieved, despite the plethora of reliable electrophilic cyclization conditions that were tried. The precise mechanism of failure remains undetermined, but some plausible hypotheses will be discussed below.

2.2 Synthesis of Functionalized Cyclohexa-*m*-phenylenes

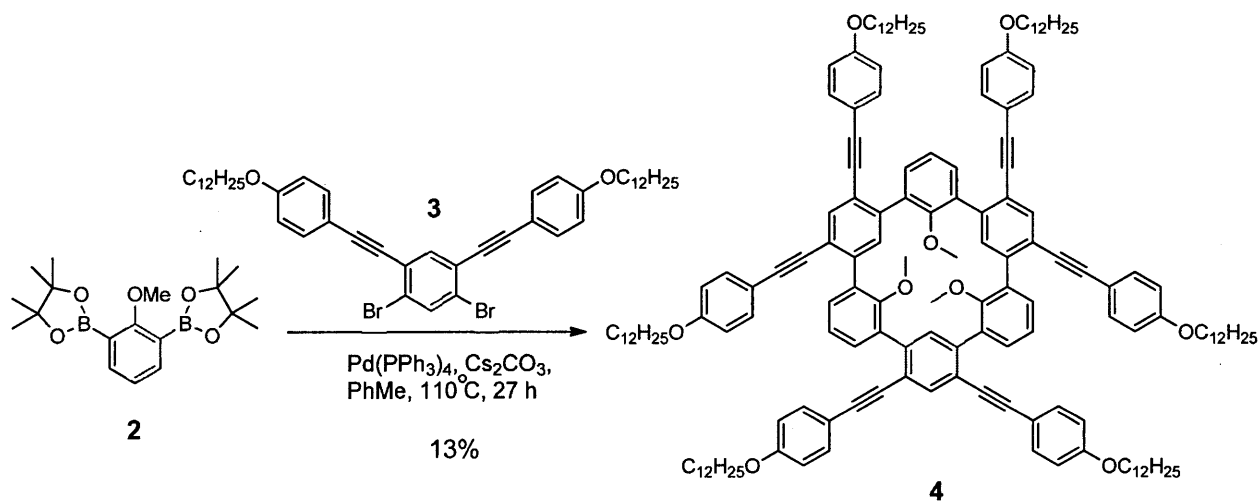
We reported an efficient one-step assembly of the cyclohexa-*m*-phenylene framework via a six-fold Suzuki-Miyaura coupling between *meta*-difunctionalized, monobenzenoid precursors.⁶ Prior to the macrocyclization step, we prepared the two simple building blocks, namely pinacol-protected diboronic acid **2** and dibromide **3**. The synthesis of the dibromide has been described in previous work performed in our group,⁷ whilst the bis-pinacolboronate was a new compound that had to be separately prepared in two steps (Scheme 2.3). The first step involved a routine *O*-methylation of 2,6-dibromophenol with methyl iodide in the presence of potassium carbonate base, whilst the second step saw a nickel-catalyzed double borylation reaction using a method described by Tour *et al.*⁸ Interestingly, the use of an analogous palladium catalyst proved ineffective compared with the nickel-based one, giving only the mono-borylation product. It is worth noting that the use of pinacol protecting groups allowed for the complete purification of the diboronic acid coupling partner by column chromatography. In contrast, a structurally similar but unprotected 1-alkoxyphenyl-2,6-diboronic acid employed by Cram *et al.*^{2a} could only be used in the subsequent step without further purification. The difficulties associated in obtaining pure samples of this sort of diboronic acid was corroborated during our own attempts to prepare the unprotected 1-methoxyphenyl-2,6-diboronic acid. With pinacol protecting groups however, complete purification was possible, and thus allowed us to avoid stoichiometric uncertainties and imbalances in the macrocyclization step.

Scheme 2.3. Synthesis of the diboronate building block



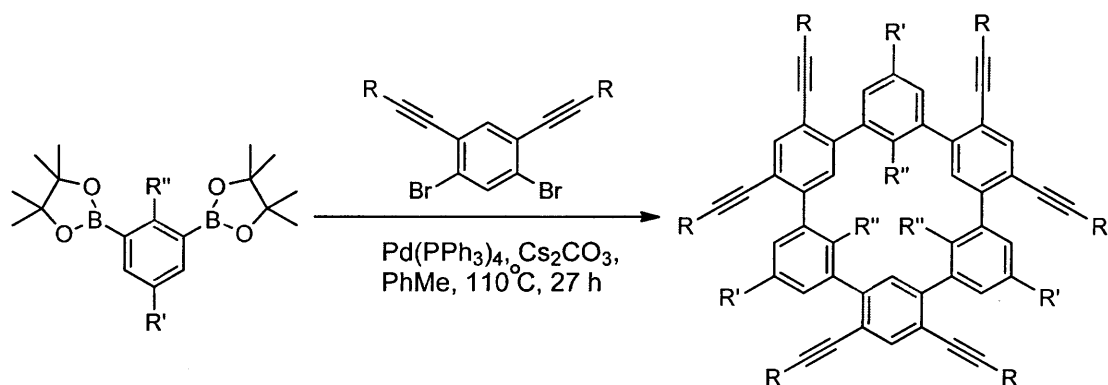
In the final macrocyclization step, equimolar quantities of both coupling partners were mixed together with catalytic Pd(PPh₃)₄ (6 mol%), anhydrous cesium carbonate and dry toluene, and refluxed for 27 hours under argon to give the functionalized cyclohexa-*m*-phenylene **4** as a white powder in 13% isolated yield following purification (Scheme 2.4). A variety of oligomeric byproducts (ca. 37%) was also formed alongside the macrocycle. Empirically, the use of this particular set of conditions appears to be crucial to the success of the reaction. Increasing the scale of the reaction ten-fold had a tendency to decrease the yield to about 9-10%, implying that the reaction may be quite sensitive to mass and/or heat transfer issues.

Scheme 2.4. Synthesis of cyclohexa-*m*-phenylene **4** via six-fold Suzuki coupling



Following the isolation of the cyclohexa-*m*-phenylene, the more polar oligomeric mixture was then successfully eluted from the silica gel column and subsequently analyzed by NMR and gel permeation chromatography (GPC). The chemical shifts from the ^1H NMR spectra showed that the functionality present in the oligomers was the same as those found in the cyclohexa-*m*-phenylene. The GPC results indicated a number-average molecular weight of 4400 amu, and a polydispersity index of about 1.2. This corresponds to species containing about six repeat units (or 12 benzene rings) in their structure. Whether the oligomeric species in this mixture were linear or cyclic could not be determined with certainty, but judging from the much higher polarity, it would not be unreasonable to assume that linear oligomers bearing polar terminal groups (e.g. boronate) were present. The use of high-dilution/slow-addition techniques was found to be unnecessary (and in fact detrimental) to macrocycle formation. When such conditions were applied, a grand mixture of inseparable and unidentifiable products was obtained, with the distinctive absence of the desired cyclohexa-*m*-phenylene **4**. A multitude of emissive (under UV light) and non-emissive spots were observed by thin-layer chromatography (TLC), with the dibromide starting material being one of the components within the crude mixture. The emissive species were presumed to be oligomers, and subsequent analysis of the crude mixture by MALDI-TOF confirmed the presence of molecules in the 4900-4950 amu mass range, which correspond to oligomers containing about 6.5 repeat units. Trials employing tetrahydrofuran or dioxane as solvent did not give successful reactions. The use of cesium carbonate under anhydrous conditions was also found to be more effective compared with the use of potassium and sodium carbonates in the presence of water. The introduction of water to the reaction mixture proved deleterious to the formation of cyclohexa-*m*-phenylene. For example, when $\text{K}_2\text{CO}_3/\text{H}_2\text{O}$ was used instead of Cs_2CO_3 , no macrocycle was obtained. Instead,

up to 60% of the starting dibromide could be recovered after column chromatography, and an analysis of the remaining mixture of substances by MALDI-TOF revealed only very low molecular weight species (i.e. < 1150 amu). It is highly likely that under protic conditions, hydrolytic deborylation of the pinacolboronate ester predominates, leading to very little coupling being effected. An additional experiment in which the methoxy group of the diboronic acid component was deliberately omitted was performed, keeping all other reaction conditions unchanged. In this case (Table 2.1, entry 4), no macrocycle was detected by either TLC or MALDI-TOF. Instead, numerous unresolvable emissive spots were observed on TLC. After partial purification and attempted separation by silica gel column chromatography, several (emissive) fractions were analyzed by NMR and MALDI. The ^1H NMR spectra of the partially purified mixtures showed typical aromatic peaks between 6.5 to 8.0 ppm, as well as signals around 3.5 to 4.0 ppm (OCH_2), suggesting the kind of functionality that would be expected in any oligomer or macrocycle formed. MALDI studies on these fractions indicated the presence of numerous species with exact masses ranging from 1100 to 4900 amu. These could correspond to oligomers containing between 2 to 7 repeat units. When the methoxy groups were kept in place, macrocyclization occurred even as the ethynyl substituents were varied. Isolated yields tended to be below 20%, with greater steric hindrance (bulkier substituents) resulting in lower yields. Finally, a macrocyclization reaction between pinacolboronate **2** and 1,3-dibromobenzene was attempted. This reaction did not proceed cleanly, leading to the formation of numerous products. TLC showed no less than ten unresolvable non-emissive spots, and MALDI analysis failed to show any peak that would correspond to the desired target. Thus, the reaction appears to be quite sensitive to the type of substituents employed in the coupling partners.

Table 2.1. Scope of the one-step macrocyclization

Entry	R	R'	R''	Yield ^a (%)
1		H	OMe	13
2		Me	OMe	ca. 5 ^b
3	$n\text{-C}_{10}\text{H}_{21}$	H	OMe	15
4		H	H	0

^aIsolated yields based on 0.14 mmol scale.

^bYield could not be determined with sufficient accuracy.

2.3 Physical Properties

Cyclohexa-*m*-phenylene **4** was characterized by ¹H NMR, ¹³C NMR, high-resolution mass spectrometry (MALDI-TOF), UV-vis and fluorescence spectroscopy. The ¹H NMR spectrum showed all the expected splitting patterns and chemical shifts. The three sets of methoxy protons within the macrocycle cavity turned out to be magnetically equivalent ($\delta = 3.33$

ppm), suggesting a symmetrical optimum conformation that placed the internal substituents in identical environments, or that the ring system was reasonably fluxional. There were also no unusual chemical shifts associated with the benzene protons within the central cavity, suggesting the absence of any diatropic ring current. This was not surprising given the fact that the puckered macrocyclic system would preclude the possibility of any π -system overlap between the benzene rings. Also, Clar's rule⁹ of aromatic sextets would indicate that the $4n + 2$ π -electrons be localized within each benzene ring rather than being delocalized over the internal 18-membered ring. Figure 2.1 shows the normalized absorbance and emission spectra of **4**, with the absorption and emission maxima at 311 nm and 388 nm respectively. The large bandgap of the material (3.4 eV) suggests the lack of conjugation between the rings of the cyclic system due to twisting relative to each other, not unlike the rings of unsubstituted cyclohexa-*m*-phenylene (bandgap = 3.9 eV, based on its 320 nm band edge).¹⁰

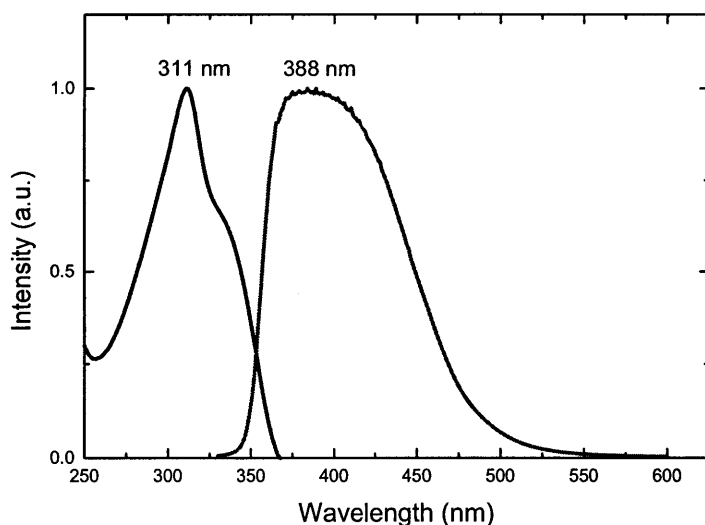


Figure 2.1. Normalized absorbance (blue line) and emission (pink line) spectra of **4**

2.4 Further Synthetic Studies using Cyclohexa-*m*-phenylene 4

Further synthetic manipulations involving the cyclohexa-*m*-phenylene targets are envisioned and we were particularly interested in cyclization reactions promoted by electrophilic additions to the acetylene groups (Scheme 2.5).¹¹ The appeal of these reactions is that they would provide an efficient synthesis of kekulene structures.^{4,12} Unfortunately, all our attempts using various well-known electrophilic cyclization conditions have been unsuccessful, resulting in either the recovery of unchanged starting material or complex inseparable mixtures (Table 2.2). Given the reliability of these methods, it was reasonable to assume that the failure of the six-fold electrophilic cyclization lies in the nature of the cyclohexa-*m*-phenylene substrate.

Scheme 2.5. Proposed conversion of cyclohexa-*m*-phenylene to kekulene.

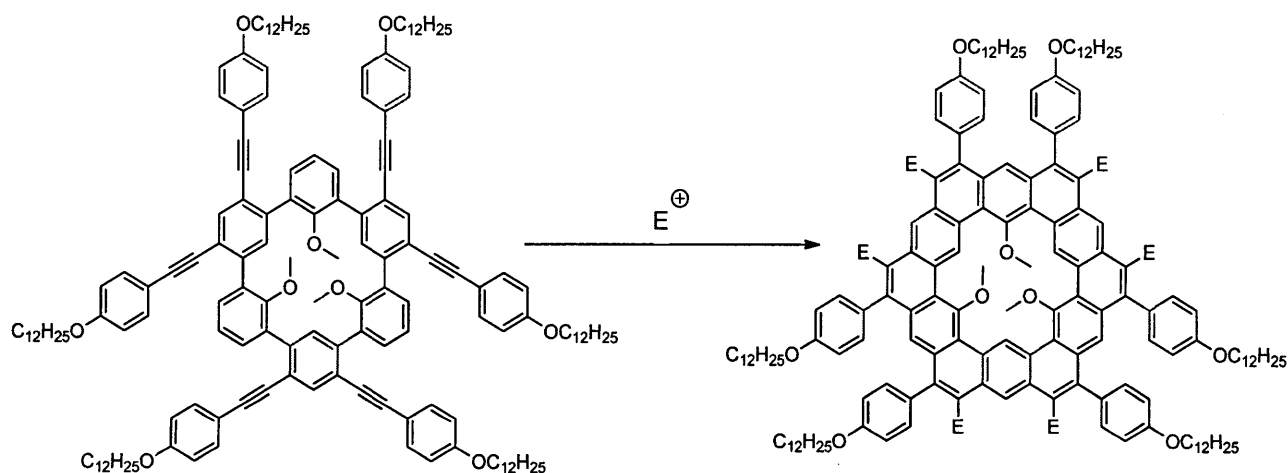


Table 2.2. Attempted conditions for the key electrophilic cyclization step

Conditions	E	Result
CF ₃ CO ₂ H, CH ₂ Cl ₂ , room temp, 4 h	H	Inseparable, unidentifiable mixture
Hg(CF ₃ CO ₂) ₂ , I ₂ , 2,6-lutidine, 0 °C, 2 h	I	Inseparable, unidentifiable mixture

ICl, CH ₂ Cl ₂ , -78 °C, 1 h	I	Inseparable, unidentifiable mixture
I ₂ , CH ₂ Cl ₂ , NaHCO ₃ room temp, 24 h	I	No reaction
<i>N</i> -bromosuccinimide, silica gel, CH ₂ Cl ₂ , room temp, 6 days	Br	No reaction
Cat. PtCl ₂ , PhMe, 80 °C, 24 h	H	No reaction
Cat. InCl ₃ , PhMe, 80 °C, 24 h	H	Inseparable, unidentifiable mixture

Semi-empirical calculations (PM3) using Spartan '08 showed macrocycle **4** to be quite puckered, due to significant steric interactions between the three methoxy groups within the central cavity (see Figure 2.2, dodecyloxy groups have been simplified to methoxy groups for the purpose of the calculation).

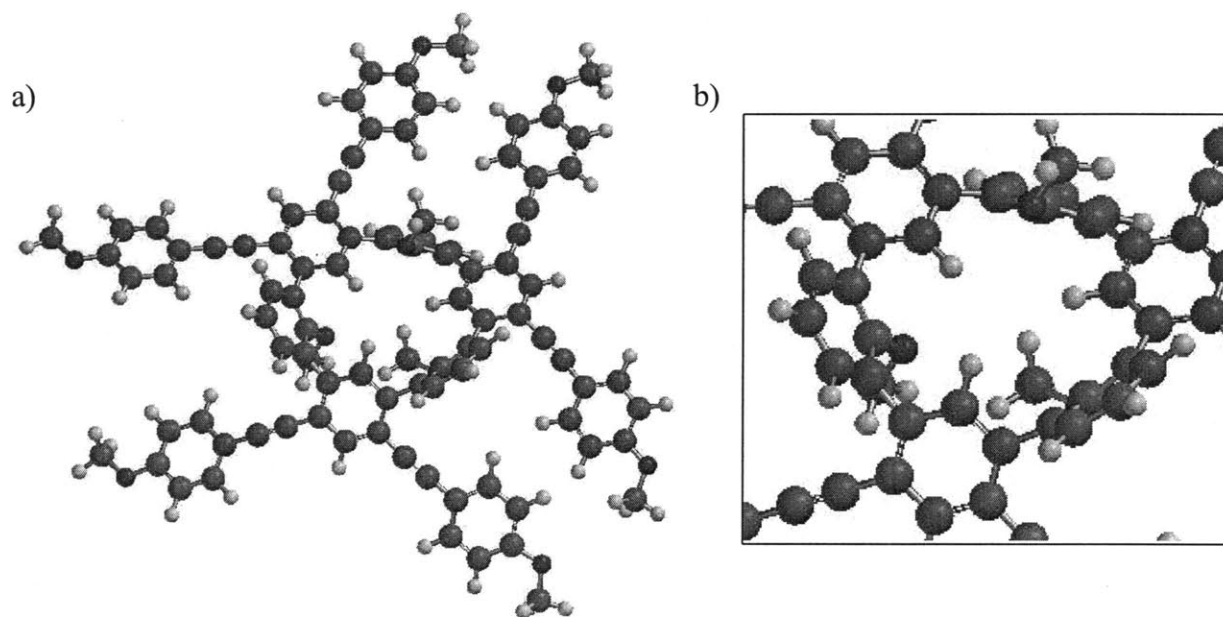


Figure 2.2. a) Energy-minimized (PM3) structure of compound **4**. b) Inset of congested cavity.

One can imagine that after the first electrophilic cyclization takes place, some degree of planarization is enforced in that part of the molecule, resulting in local rigidification and simultaneously bringing the bulky peripheral substituents on the more flexible portion of the macrocycle closer together in space. Thus, overall steric repulsions between peripheral groups increase with each electrophilic cyclization, making subsequent ones energetically more difficult and eventually causing side reactions to predominate. It should also be recognized that the target kekulene must be a very high energy molecule by virtue of its planarity and the immense steric repulsions that exist between the three methoxy groups and three hydrogen atoms within its small cavity (Figure 2.3).

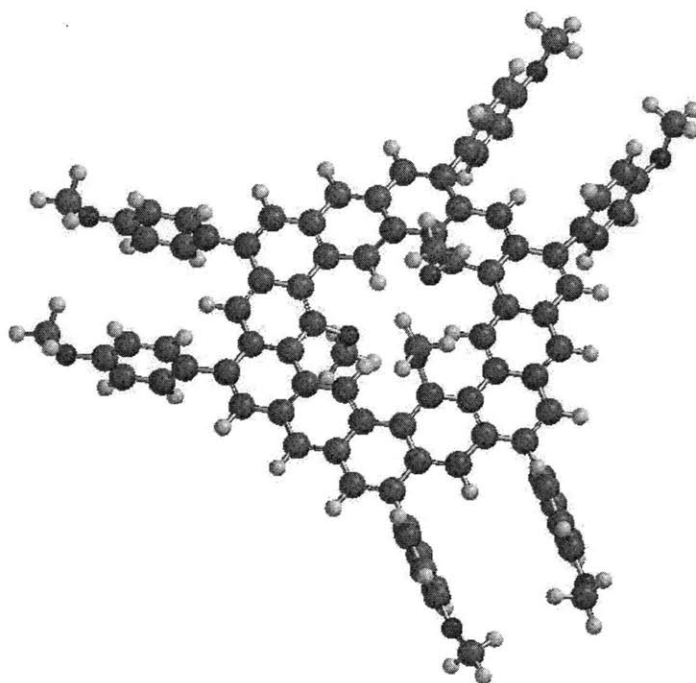


Figure 2.3. Energy-minimized (PM3) 3D structure of the proposed kekulene

As a result, the sequence of planarizing ring closures from cyclohexa-*m*-phenylene to kekulene must be energetically uphill, since the cavity substituents are brought closer and closer

together with each successful electrophilic cyclization. Our attempt to address this problem of cavity crowding was to deprotect the methoxy groups prior to the six-fold ring closure. However, the harsher demethylation reactions employed were found to be unselective for the methoxy groups, whilst the milder conditions proved to be completely ineffective probably as a result of the sterically encumbered environment. Furthermore, the problem peripheral crowding remains unaddressed with this approach, since the aryl groups are necessary synthetic handles for successful electrophilic cyclization. Ultimately, it is currently not possible to access kekulene structures via the cyclohexa-*m*-phenylene strategy.

2.5 Conclusions

In summary, we have discovered an expeditious one-step construction of arylolethynylated cyclohexa-*m*-phenylenes from simple building blocks, with the carbon-carbon bond formations being based on the Suzuki-Miyaura reaction. Compared with previous preparations of oligophenylene macrocycles, all the carbon-carbon bond-forming processes of this method take place within a single step. Besides allowing for the quick assembly of the cyclohexa-*m*-phenylene framework, the relatively mild conditions employed can also accommodate the introduction of more complex functionality into any designed target molecule, and thus provides access to a wider range of potentially useful materials. Numerous attempts to convert an arylolethynylated cyclohexa-*m*-phenylene to a substituted kekulene via multiple electrophilic cyclizations proved unsuccessful, probably due to steric reasons within the target molecule as well as the intermediates leading up to it.

2.5 Experimental Section

2,6-Dibromoanisole (1). A 250 mL two-neck round-bottom flask containing a magnetic stir-bar was charged with 2,6-dibromophenol (5.0 g, 19.85 mmol), methyl iodide (3.7 mL, 61.5 mmol), potassium carbonate (5.49 g, 39.7 mmol), and acetone (45 mL). The mixture was stirred and heated at 60 °C under argon for 17 hours, after which it was cooled down to room temperature. The acetone was removed *in vacuo*, leaving a residue to which water and diethyl ether was added. The mixture was extracted with diethyl ether (3 x 40 mL) and the combined organic extracts were dried over anhydrous sodium sulfate and concentrated by rotary evaporation to give a yellow-orange oil. This crude product was purified by silica gel column chromatography (3:2 v/v hexane/dichloromethane) to give **1** (5.15 g, 19.35 mmol, 98%) as a colorless oil. ¹H NMR (300 MHz, CH₂Cl₂-d₂): δ 7.51 (d, 2H, *J* = 8.1 Hz), 6.88 (t, 1H, *J* = 8.1 Hz), 3.85 (s, 3H). ¹³C NMR (300 MHz, CH₂Cl₂-d₂): δ 133.0, 126.6, 118.4, 60.7. HRMS (EI-MS): *m/z* calcd for C₁₅H₁₉O₉: 263.8785, found 265.8758 [M + H]⁺.

1-Methoxy-2,6-benzenedipinacolboronate (2). A two-neck round-bottom flask containing a magnetic stir-bar was charged with 2,6-dibromoanisole (4.5 g, 16.9 mmol), anhydrous triethylamine (19 mL), (1,3-diphenylphosphinopropane)nickel(II) chloride (0.551 g, 1.01 mmol) and dry toluene (60 mL). The mixture was stirred and then 4,4',5,5'-tetramethyl-1,3,2-dioxaborolane (7.38 mL, 50.9 mmol) was added via syringe. The reaction mixture was refluxed under argon at 100 °C for 24 hours before it was cooled down and subsequently quenched with saturated aqueous ammonium chloride. The mixture was extracted with diethyl ether (3 x 30 mL) and the combined organic extracts were dried over anhydrous magnesium sulfate, partially decolorized with Norit A, and finally filtered through a bed of Celite. The organic solution was

then subjected to rotary evaporation to give an oily orange residue. Titration of the crude residue with cold hexane gave an off-white precipitate, which was recrystallized from hot hexane to afford a crystalline white solid of **2** (3.05 g, 8.47 mmol, 50%). ¹H NMR (300 MHz, CH₂Cl₂-d₂): δ 7.73 (d, 2H, *J* = 7.2 Hz), 7.08 (t, 1H, *J* = 7.2 Hz), 3.77 (s, 3H), 1.33 (s, 24H). ¹³C NMR (300 MHz, CH₂Cl₂-d₂): δ 171.3, 139.5, 123.0, 83.7, 63.7, 24.8. HRMS (EI-MS): *m/z* calcd for C₁₅₉H₁₉₈O₉: 360.2279, found 361.2370 [M + H]⁺.

Cyclohexa-*m*-phenylene (4). A 250 mL two-neck round-bottom flask containing a magnetic stir-bar was charged with 1,5-dibromo-2,4-bis(*p*-dodecyloxyphenylethynyl)benzene (0.112g, 0.14 mmol), 1-methoxy-2,6-benzenedipinacolboronate (0.050 g, 0.14 mmol), cesium carbonate (0.113g, 0.35 mmol), tetrakis(triphenylphosphine)palladium (4.8 mg, 0.0042 mmol), , and dry toluene (8 mL). After sparging the stirred mixture with argon gas over 10 minutes, the reaction mixture was refluxed under argon at 110 °C for 27 hours. Upon cooling, the crude mixture was partitioned between diethyl ether and deionized water. After extraction with diethyl ether (3 x 30 mL), the combined organic extracts were dried over anhydrous magnesium sulfate, before being concentrated *in vacuo* to give a viscous brown oil. This was then subjected to flash chromatography on a silica gel column (3:2 v/v hexane/dichloromethane). Upon the complete removal of solvent from the desired fractions, the target cyclohexa-*m*-phenylene **4** (13.7 mg, 0.0061 mmol) was obtained as an off-white solid. ¹H NMR (300 MHz, CH₂Cl₂-d₂): δ 7.96 (s, 3H), 7.94 (s, 3H), 7.81 (d, 6H, *J* = 7.8 Hz) 7.38 (d, 12H, *J* = 9.0 Hz), 7.29 (t, 3H, *J* = 7.8 Hz), 6.85 (d, 12H, *J* = 9.0 Hz), 3.97 (t, 12H, *J* = 6.6 Hz), 3.33 (s, 9H), 1.80 (m, 12H), 1.2-1.6 (108H), 0.90 (t, 18H, *J* = 6.9 Hz). ¹³C NMR (300 MHz, CH₂Cl₂-d₂): δ 159.6, 138.8, 134.0, 133.1, 131.4,

120.8, 115.3, 114.7, 93.2, 87.4, 68.4, 32.2, 30.0, 29.9, 29.8, 29.70, 29.6, 29.5, 26.3, 22.94, 14.1.

HRMS (MALDI-TOF): m/z calcd for $C_{159}H_{198}O_9$: 2253.2680, found 2252.9891 (M^+).

References and Notes

- [1] a) Staab, H. A.; Binnig, F. *Chem. Ber.* **1967**, *100(1)*, 293-305; b) Staab, H. A.; Binnig, F. *Tetrahedron Lett.* **1964**, *5*, 319-321.
- [2] a) Cram, D. J.; Kaneda, T.; Helgeson, R. C.; Brown, S. B.; Knobler, C. B.; Maverick, E.; Trueblood, K. N. *J. Am. Chem. Soc.* **1985**, *107(12)*, 3645-3657; b) Cram, D. J.; Carmack, R. A.; Helgeson, R. C. *J. Am. Chem. Soc.* **1988**, *110(2)*, 571-577; c) Cram, D. J.; Lein, G. M. *J. Am. Chem. Soc.* **1985**, *107(12)*, 3657-3658; d) Lein, G. M.; Cram, D. J. *J. Chem. Soc. Chem. Commun.* **1982**, *5*, 301-304; e) Cram, D. J.; Lein, G. M.; Kaneda, T.; Helgeson, R. C.; Knobler, C. B.; Maverick, E.; Trueblood, K. N. *J. Am. Chem. Soc.* **1981**, *103(20)*, 6228-6232; f) Trueblood, K. N.; Knobler, C. B.; Maverick, E.; Helgeson, R. C.; Brown, S. B.; Cram, D. J. *J. Am. Chem. Soc.* **1981**, *103(18)*, 5594-5596; g) Cram, D. J.; Kaneda, T.; Helgeson, R. C.; Lein, G. M. *J. Am. Chem. Soc.* **1979**, *101(22)*, 6752-6754.
- [3] Pisula, W.; Kastler, M.; Yang, C.; Enkelmann, V.; Müllen, K. *Chem. Asian J.* **2007**, *2*, 51-56.
- [4] Staab, H. A.; Diederich, F. *Chem. Ber.* **1983**, *116*, 3487-3503.
- [5] (a) Kumar, S. *Chem. Soc. Rev.* **2006**, *35*, 83-109; (b) Meier, H. *Synthesis* **2002**, *9*, 1213-1228.
- [6] Chan, J. M. W.; Swager, T. M. *Tetrahedron Lett.* **2008**, *49*, 4912-4914.

- [7] Goldfinger, M. B.; Crawford, K. B.; Swager, T. M. *J. Am. Chem. Soc.* **1997**, *119*, 4578.
- [8] Morgan, A. B.; Jurs, J. L.; Tour, J. M. *J. Appl. Polym. Sci.* **2000**, *76*, 1257-1268.
- [9] Harvey, R. G. *Polycyclic Aromatic Hydrocarbons*; Wiley-VCH: New York, 1997.
- [10] Fujioka, Y. *Bull. Chem. Soc. Jpn.* **1984**, *57*, 3494-3506.
- [11] a) Goldfinger, M. B.; Crawford, K. B.; Swager, T. M. *J. Org. Chem.* **1998**, *63*, 1676; b) Zhang, X.; Larock, R. C. *J. Am. Chem. Soc.* **2005**, *127*, 12230; c) Yao, T.; Campo, M. A.; Larock, R. C. *J. Org. Chem.* **2005**, *70*, 3511; d) Mamane, V.; Hannen, P.; Fürstner, A. *Chem. Eur. J.*, **2004**, *10*, 4556-4575.
- [12] a) Steiner, E.; Fowler, P. W.; Acocella, A.; Jenneskens, L. W. *Chem. Commun.* **2001**, *7*, 659-660; b) Jiao, H.; Schleyer, P. v. R. *Angew. Chem. Int. Ed.* **1996**, *35*, 2383-2386. c) Aihara, J. *J. Am. Chem. Soc.* **1992**, *114*, 865-868; d) Cioslowski, J.; O'Connor, P. B.; Fleischmann, E. D. *J. Am. Chem. Soc.* **1991**, *113*, 1086-1089.

Chapter 2 Appendix

^1H -NMR and ^{13}C -NMR Spectra

Adapted and reprinted from:

Chan, J. M. W., Swager, T. M. *Tetrahedron Lett.* **2008**, *49*, 4912-4914

with permission from Elsevier

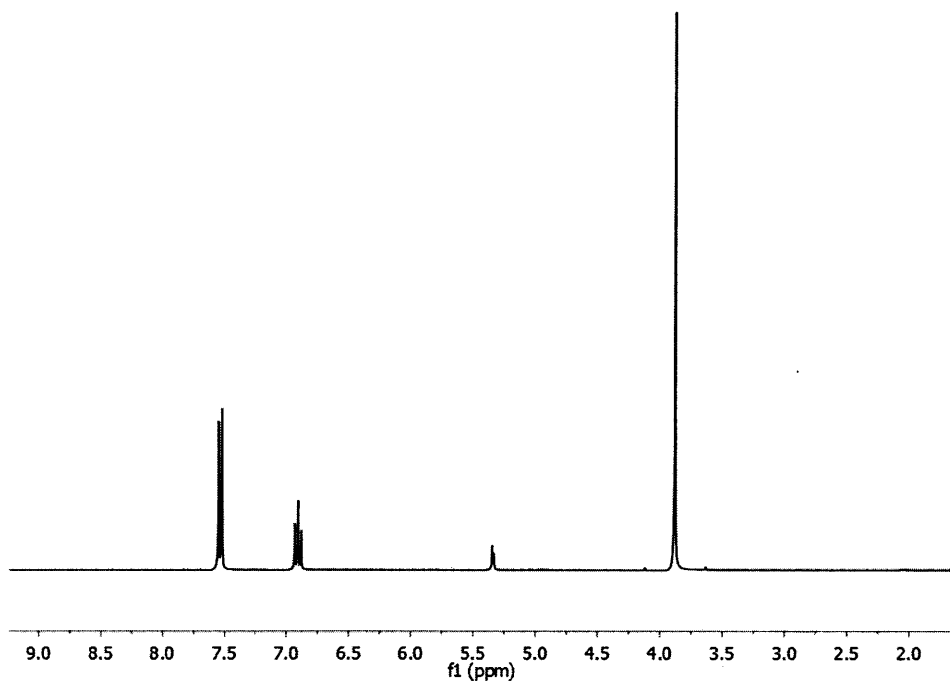


Figure 2.A.1. ^1H -NMR spectrum of **1** (300 MHz, CD_2Cl_2).

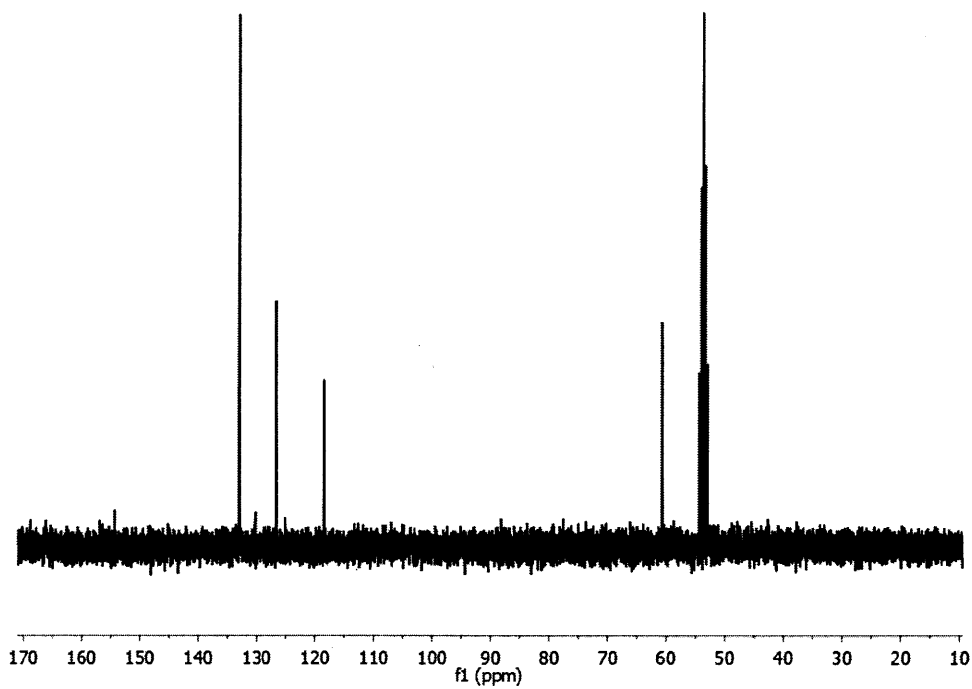


Figure 2.A.2. ^{13}C -NMR spectrum of **1** (300 MHz, CD_2Cl_2).

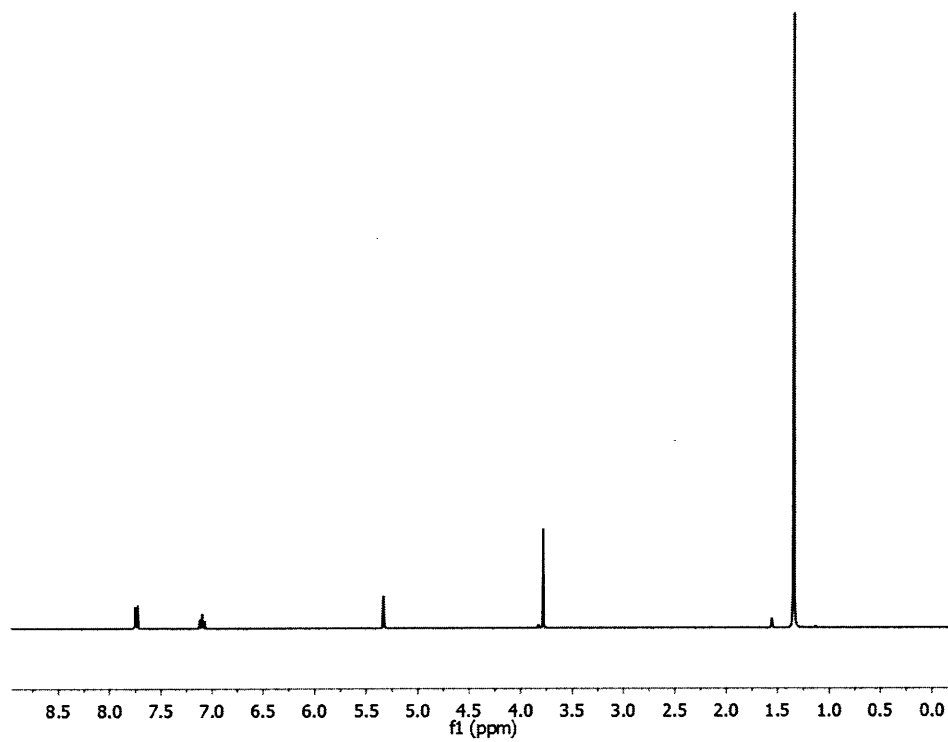


Figure 2.A.3. ^1H -NMR spectrum of **2** (300 MHz, CD_2Cl_2).

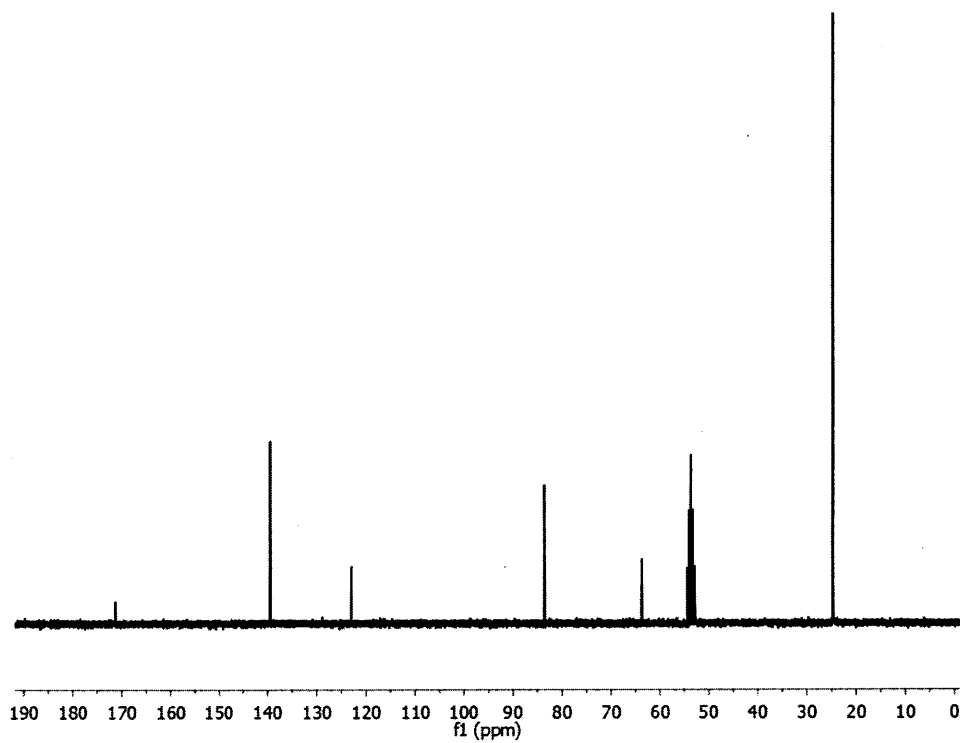


Figure 2.A.4. ^{13}C -NMR spectrum of **2** (300 MHz, CD_2Cl_2).

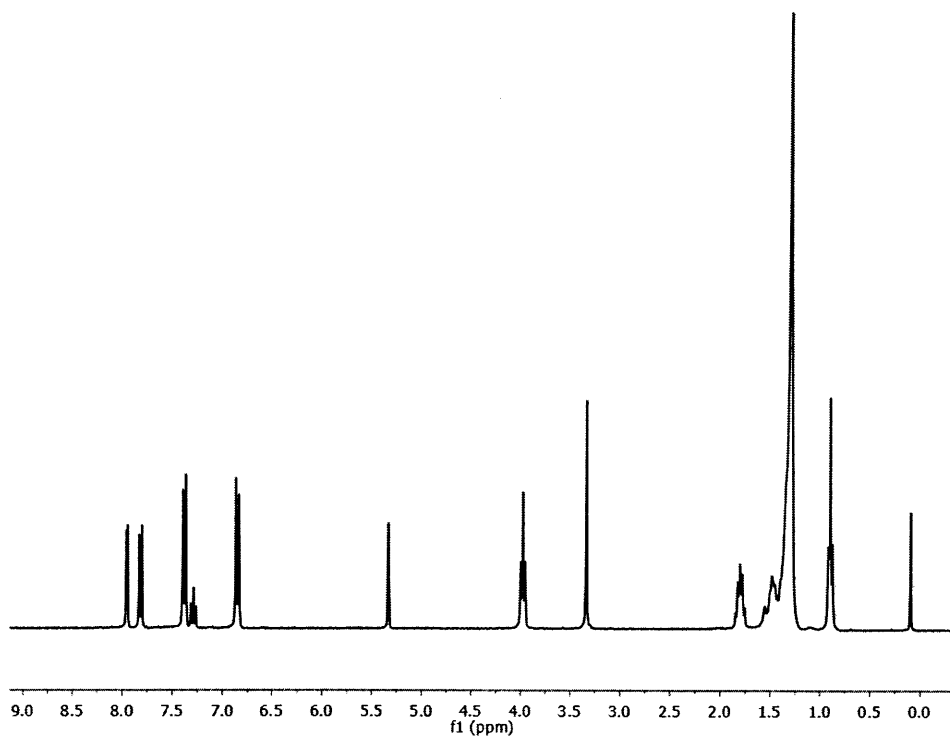


Figure 2.A.5. ^1H -NMR spectrum of **4** (300 MHz, CD_2Cl_2).

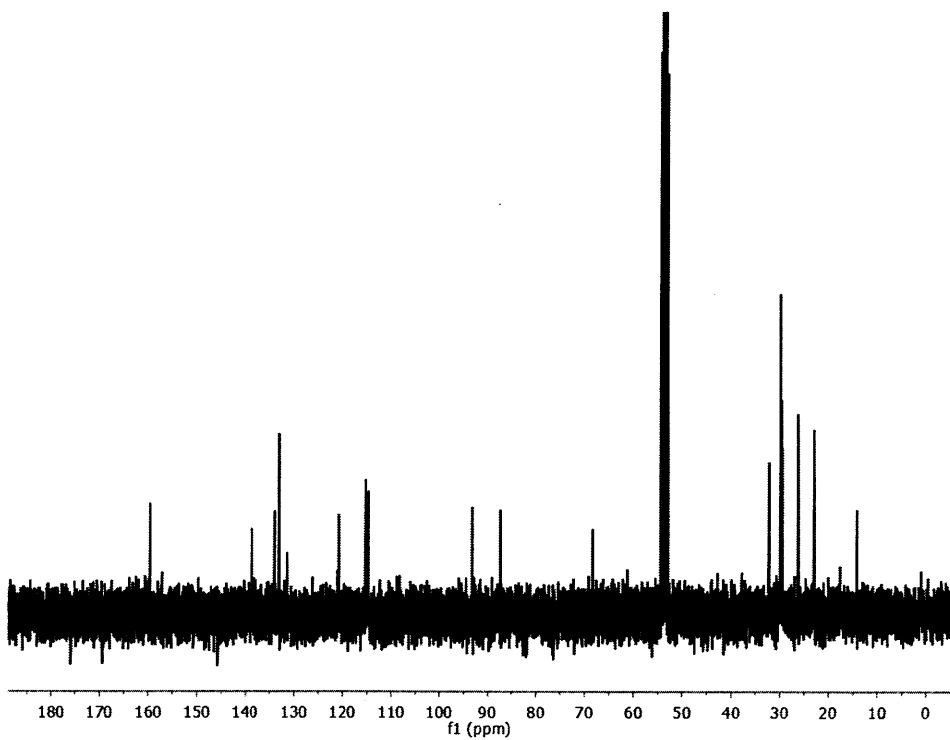


Figure 2.A.6. ^{13}C -NMR spectrum of **4** (300 MHz, CD_2Cl_2).

Chapter 3

Synthesis of J-aggregating Dibenz[*a,j*]anthracene- Based Macrocycles

Adapted and reproduced with permission from:

Chan, J. M. W., Tischler, J. R., Kooi, S. E., Bulović, V., Swager, T. M. *J. Am. Chem. Soc.* **2009**, *131*, 5659-5666.

I thank my collaborators Steve Kooi (ISN) and Jonathan Tischler (Bulović lab) for their help with fluorescence lifetimes and concentration dependence studies respectively.

3.1 Introduction

Shape-persistent macrocycles have received much attention in the field of materials science, particularly in the area of nanoscale architectures.¹ The first macrocycle featuring two unfunctionalized anthracenes linked by 1,3-butadiyne bridges was reported in 1960, but due to the lack of modern synthetic and characterization methods, the nature of the resulting material was not rigorously elucidated.² Following little interest in such systems over the next four decades, reports of anthrylene-ethynylene oligomers and macrocycles have surfaced in the past 5 years.³ However, the molecular rigidity and lack of solubilizing groups resulted in the reported compounds having poor solubilities in common solvents. To create a class of molecules that could have potentially interesting photophysical and materials properties, we embarked on the design of conjugated macrocycles based on rigid dibenz[*a,j*]anthracene units bridged by butadiyne π -linkers (see compound **6**, p. 53). This was a logical choice since arylenethynylene and 1,3-butadiyne linkages are frequently used in conjugated systems (e.g. polymers) for their ability to maintain rigidity and π -conjugation.⁴ The polycyclic aromatic motifs are commonly seen in other areas of materials science, notably in the fields of discotic liquid crystals and graphitic materials.⁵ By employing various modern synthetic transformations, it was possible to introduce numerous functionalities (e.g. sidechains) into the structure to give better solubility and processability. In particular, bulky 4-alkoxyphenyl substituents located near the middle of the macrocycles serve several purposes: 1) as synthetic handles to allow for the facile electrophilic cyclizations⁶ used to establish the dibenz[*a,j*]anthracene framework, 2) as solubilizing groups, and most importantly, 3) as a source of steric hindrance to bring about twisting of the π -system. Such distortion of the rigid framework by steric bulk has been known to induce slipped stacking arrangements,⁷ resulting in aggregate structures with unique optical properties. Similar slipped

structures are also known in nature: for example, the arrangement of J-aggregated chlorophyll chromophores is crucial to the light-harvesting efficiency of photosynthetic systems.⁸ Using natural photosystems as a guide and inspiration, researchers have found ways to emulate this J-aggregate design in various porphyrins and perylene bisimides.⁹ More recently, the laboratories of Frank Würthner have also successfully implemented the rational synthesis of several J-aggregated systems using supramolecular design principles.¹⁰ Ever since their serendipitous discovery in 1936, J-aggregates have been of great theoretical interest because they display coherent, cooperative phenomena like superradiance and giant oscillator strength, a consequence of their electronic excitation being delocalized over several molecules.¹¹ Besides being theoretical curiosities, J-aggregates also have a myriad of practical applications, such as their use as organic photoconductors,¹² photopolymerization initiators,¹³ and nonlinear optical devices,¹⁴ as well as the emerging applications such as the recently demonstrated critically coupled resonators¹⁵ and strongly QED coupled microcavity LEDs.¹⁶

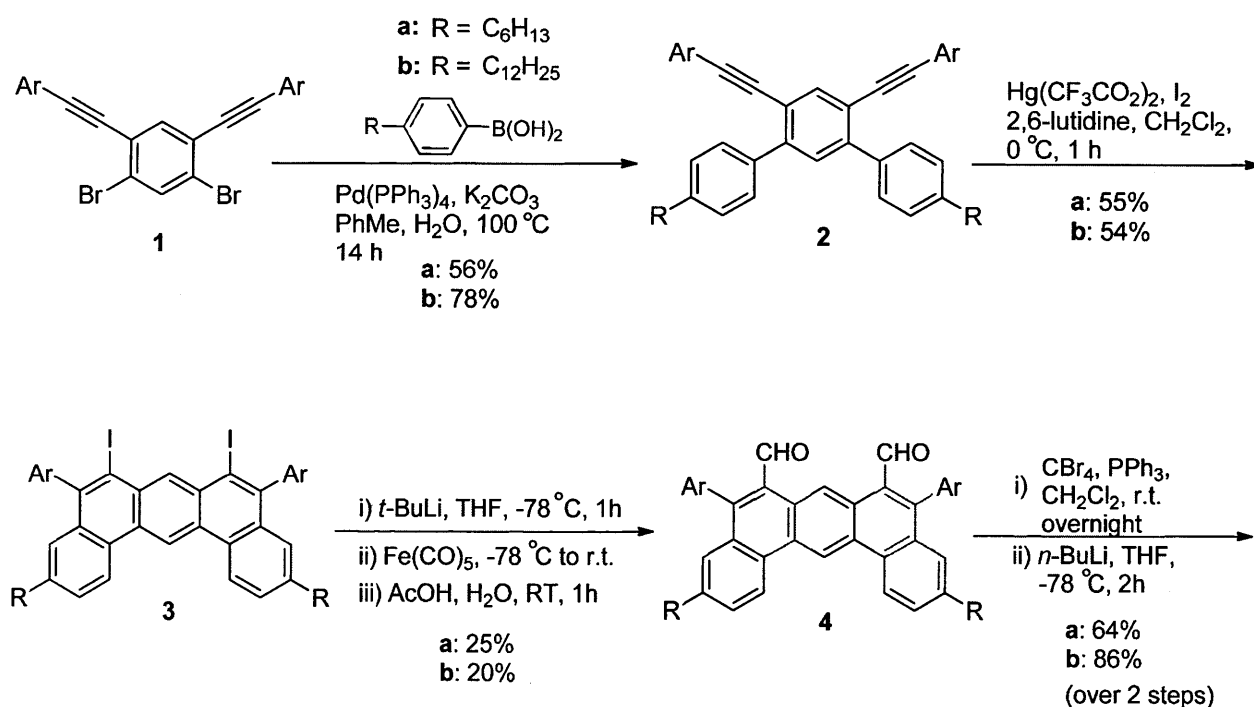
Herein, we report the synthesis and characterization of a series of J-aggregating macrocycles based on functionalized dibenz[*a,j*]anthracene fragments linked at the 6- and 8-positions by a pair of 1,3-butadiyne bridges, in which the ring interior can be viewed as an octadehydro[18]annulene system. The results of their photophysical studies are also detailed.

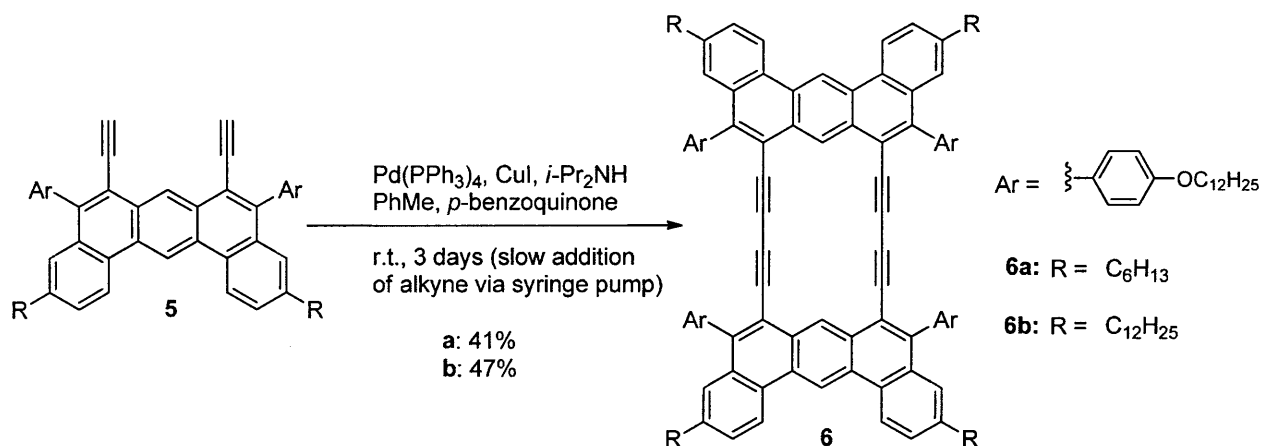
3.2 Synthesis

Macrocycles **6a** and **6b** were prepared in six steps (Scheme 3.1) from the previously reported dibromide **1**¹⁷, which is itself made in two steps from 1,3-dibromobenzene. Subjecting the dibromide to a double Suzuki coupling with 4-alkylphenylboronic acids afforded terphenyl derivatives **2**, which were then converted to the required 6,8-diiododibenz[*a,j*]anthracenes via a

double iodonium-induced electrophilic cyclization.^{17,18} Numerous attempts to convert the diiodide to the *bis*-acetylene **5** via Sonogashira and Castro-Stephens reactions proved unsuccessful, instead resulting in complex, undefined mixtures. However, an indirect method involving a lithiation/carbonylation sequence to give **4**, followed by Corey-Fuchs homologation¹⁹, successfully afforded dialkyne **5**. Owing to the sterically encumbered environment of the reaction centers, dialdehyde **4** was always accompanied by the formation of monoaldehyde byproduct **13**. Separation of the two could however, be easily achieved by column chromatography. Finally, an oxidative coupling utilizing conditions previously developed²⁰ in our group was performed, furnishing macrocycles **6a** and **6b** in reasonable yields.

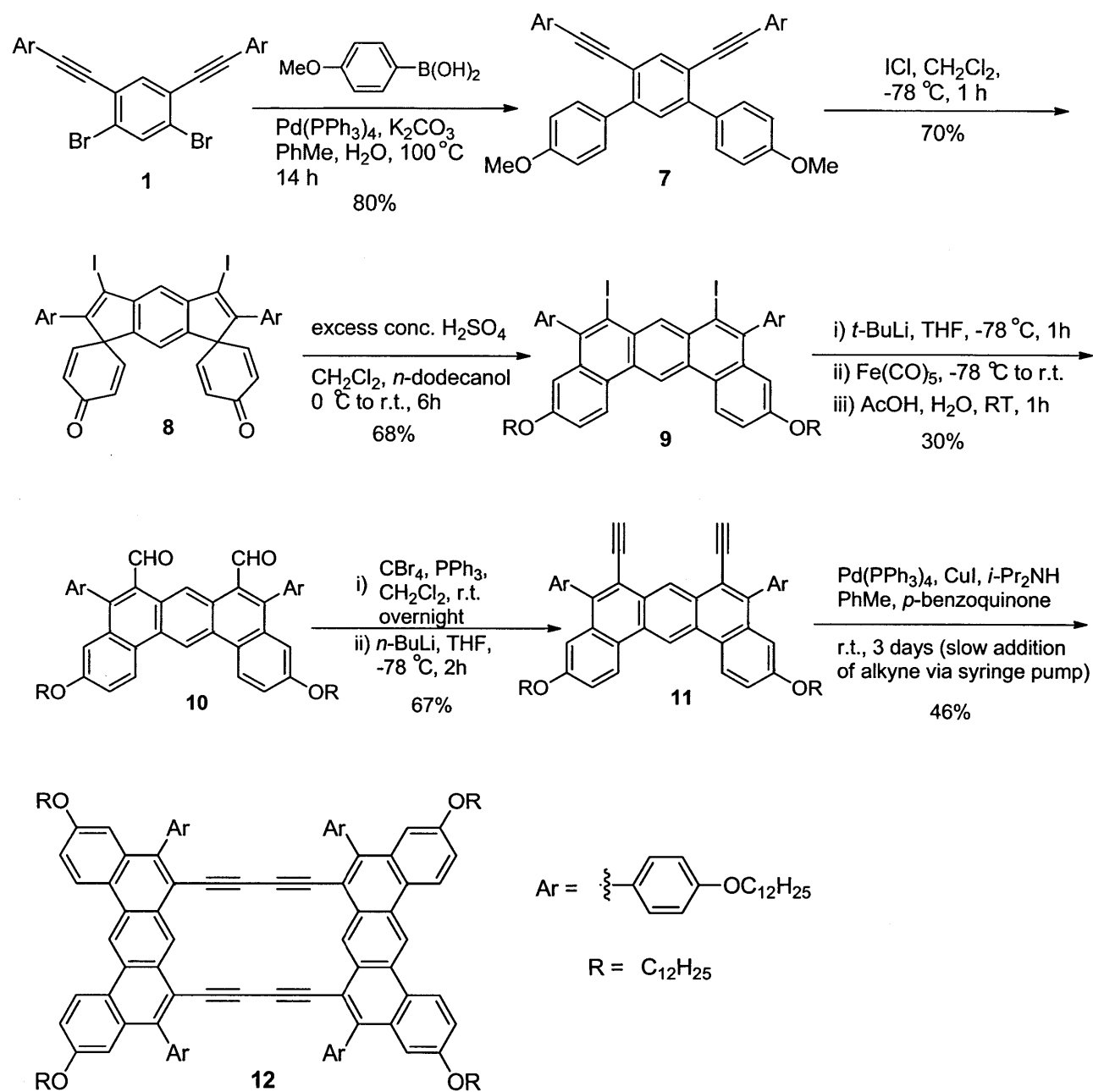
Scheme 3.1. Synthesis of macrocycles **6a** and **6b**.





The synthesis of macrocycle **12** (Scheme 3.2) involved a similar sequence of transformations employed in the preparation of **6a** and **6b**, with the exception that the dialkoxyterphenyl **7** could only be converted to the desired diiodide **9** in two steps, via a skeletal rearrangement of the structurally intriguing **8**, using modifications of known reactions.^{6, 21} A second alkoxy-based macrocycle bearing branched farnesol-derived sidechains was also synthesized in a manner analogous to **12**, with its existence confirmed by MALDI-TOF. Unfortunately, this fourth and final macrocycle could not be satisfactorily separated from a trimeric byproduct even after repeated column chromatography and attempted fractional recrystallizations. In addition to the three macrocycles, compound **15** (the acyclic analog of **6a**) was also prepared to study the effect of the number of bridges on the photophysical properties. This was made in three steps (Scheme 3.3) starting from monoaldehyde **13**, which is a byproduct isolated during the purification of dialdehyde **4a**.

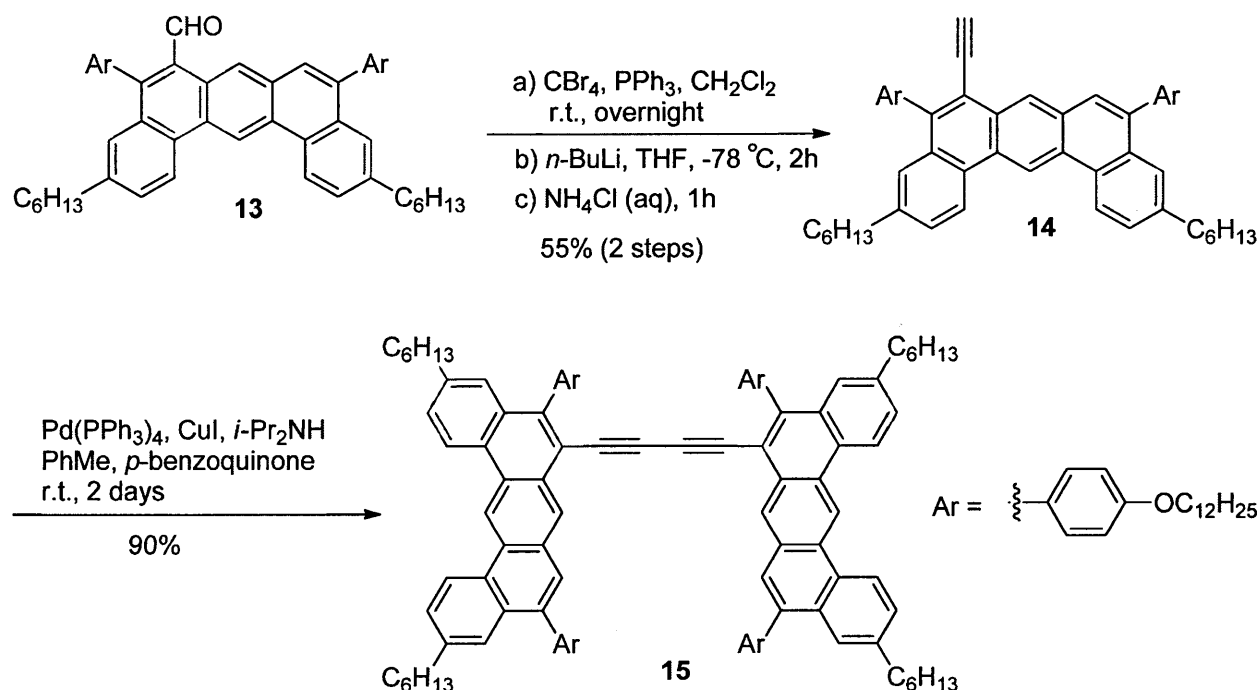
Scheme 3.2. Synthesis of macrocycle **12**.



The abovementioned target compounds were characterized by ^1H NMR, ^{13}C NMR, high-resolution mass spectrometry (MALDI-TOF), UV/Vis and fluorescence spectroscopy. In the ^1H

NMR spectra of the macrocycles, the two protons located within the ring were found to be shifted downfield ($\delta \approx 9.5$ ppm) as a result of Van der Waals deshielding brought about by steric interactions. The lack of any upfield shift of those internal protons implies the absence of a ring current²² in these systems (i.e. no diatropic effect observed). Brief polarized optical microscopy experiments were also performed on the macrocycles in hope of finding liquid crystalline behavior as well, but the compounds had extremely high melting points (between 200°C and 330°C) and were also observed to decompose and discolor at those elevated temperatures.

Scheme 3.3. Synthesis of acyclic 15.



3.3 Photophysical studies.

A SPEX fluorolog, with dual monochromators, was used to collect photoluminescence (PL) and photoluminescence excitation (PLE) spectra. The instrument is wavelength and

intensity calibrated and it compensates for variations in excitation intensity by monitoring the incident optical power level. In PL measurements, the **6a** films were optically excited at a wavelength $\lambda = 375$ nm. For PLE spectra, emission at $\lambda = 508$ nm was collected. Figure 3.1 shows the UV-Vis absorption and fluorescence spectra of the four compounds in chloroform. Macrocycles **6a** and **6b** displayed essentially identical spectral profiles, with absorption and emission maxima occurring at around 440 nm and 455 nm respectively. Changing the peripheral alkyl groups to alkoxy chains (e.g. **12**) resulted in a slight bathochromic shift, with the spectral shape remaining similar otherwise. The spectra of the acyclic **15** differed somewhat from the macrocycles, which was expected due to the major structural difference. Its absorption spectrum was blue-shifted relative to the others, possibly due to reduced conjugation resulting from the absence of the second diyne linker. A much larger Stokes shift was also observed, which could indicate reduced rigidity, once again as a result of having only a single linker. Fluorescence quantum yields of the compounds were measured against quinine sulfate in 0.1N H₂SO₄ (Table 3.1). The three macrocycles in chloroform solution showed fairly high quantum yields between 0.40 and 0.50, whereas the singly-bridged **15** had a lower value of 0.35.

Table 3.1. Photophysical properties of **6a**, **6b**, **12**, and **15**.

Compound	Absorption max (nm)	Emission max (nm)	Quantum yield, Φ_F	Extinction coefficient (M ⁻¹ cm ⁻¹)
6a	443	456	0.45	90141 (at 443 nm)
6b	443	456	0.43	63569 (at 443 nm)
12	448	461	0.47	79113 (at 448 nm)
15	395	440	0.35	38206 (at 395 nm)

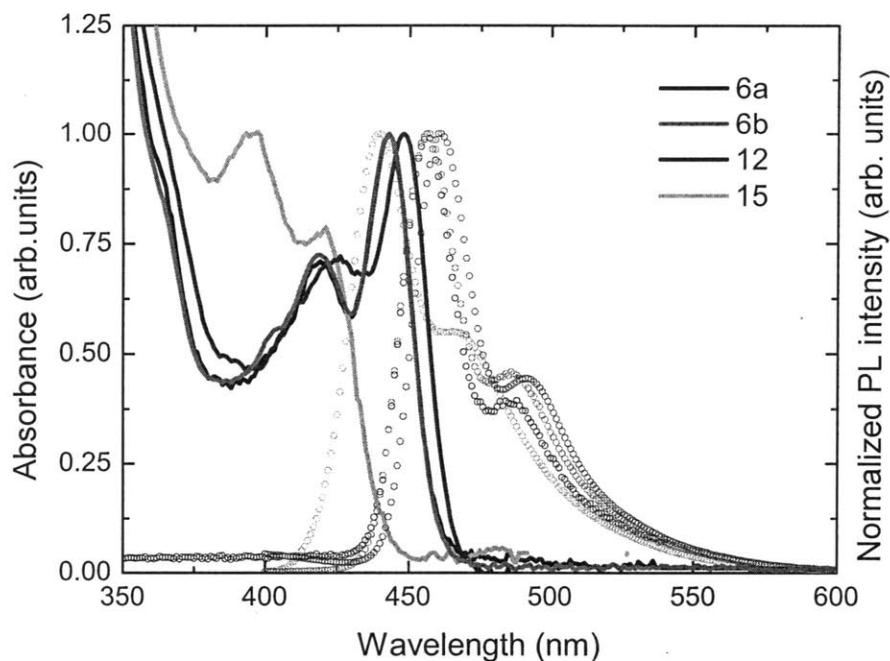


Figure 3.1. Normalized absorbance (solid lines) and emission (dotted lines) spectra of **6a**, **6b**, **12** and **15** in chloroform.

To test for the presence of J-aggregates, we investigated the thin film photophysics of the macrocycles. As **6a** was synthesized in the largest quantity, films of this compound were studied in greatest detail. The initial films were produced by spin-coating a fairly concentrated (5 mg/mL) toluene solution of **6a** on to glass or quartz cover-slips (18 x 18 mm). Fortuitously, the first few films showed promising UV-Vis absorption features consistent with J-aggregates (Figure 3.2).

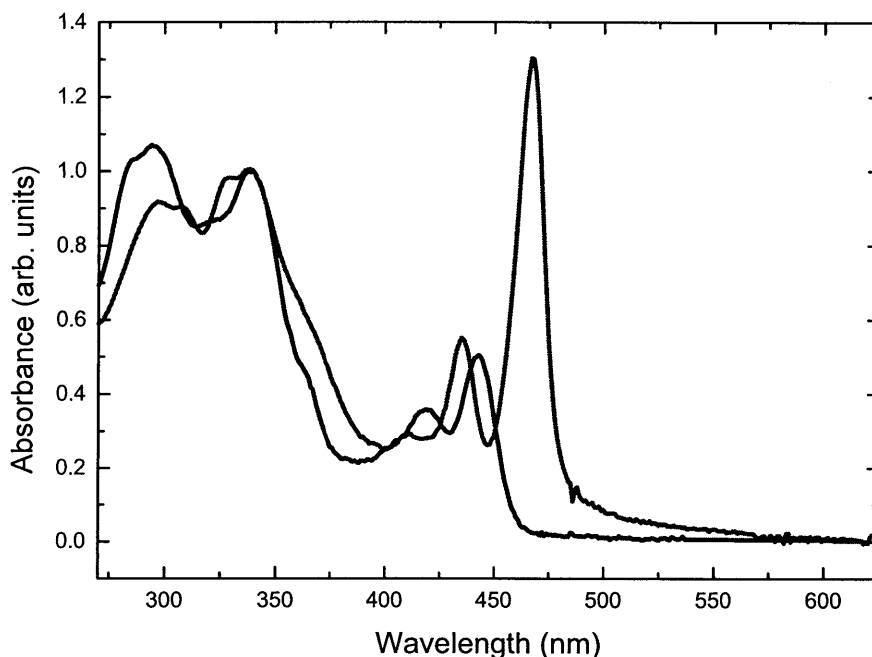


Figure 3.2. Absorption spectra of **6a**, solution (blue line) vs. film (red line), normalized to the absorbance at 340 nm.

Compared with the solution spectrum, the **6a** film spectrum shows an aggregate absorption peak at 467 nm (red-shifted by (23 ± 1) nm from the solution). Even more notable is the high intensity and narrow linewidth of this peak (J-band), which dominates all other spectral features. This is in stark contrast to the solution spectrum, in which the peak at 443 nm shows much lower intensity than those between 300 nm and 360 nm (absorptions due to pendant *p*-alkoxyphenyl moieties). Normalizing the solution and film absorbances at 340 nm, the enhancement in the peak intensity (at 467 nm) relative to the other spectral features becomes evident (Figure 3.2). The bathochromic shift and the strong intensity of the aggregate peak, are photophysical characteristics of J-aggregates.²³ From the emission spectra of the **6a** films we find the Stokes shift to be only 4 nm (Figure 3.3), versus 13 nm in solution phase. Such minimal Stokes shift is also consistent with the existence of J-aggregates.²⁴ It is notable that the fluorescence band is a mirror image of the low energy edge of the J-band absorption.

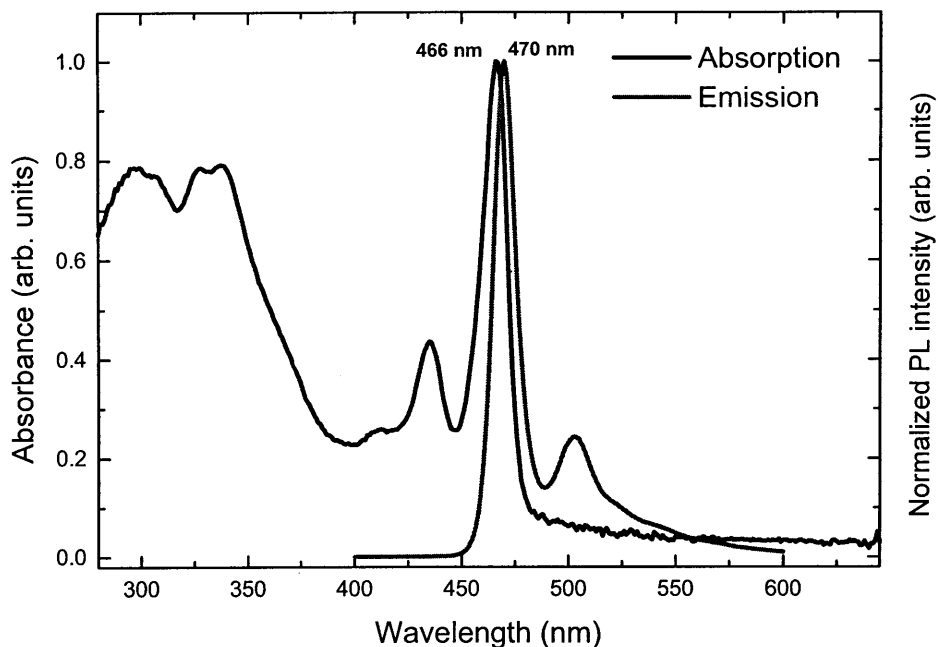


Figure 3.3. Normalized absorption (blue line) and fluorescence (pink line) spectra of **6a** (film).

We also find that it is possible to spin-coat films of **6a** that did not display a J-band. These less strongly absorbing films could be produced when: the spin rate (of the spin-coating process) was high (e.g. 4000 rpm), a lower concentration (< 2 mg/mL) of **6a** in solvent was used, or when a more volatile solvent (e.g. THF) was employed. The use of these parameters provided for less-than-favorable conditions for aggregate formation. But when these ‘non-aggregated’ (i.e. monomeric) films were then subjected to conditions conducive to aggregate formation, the typical J-aggregate spectral features were found to emerge with time. This was achieved by vapor-annealing the films in a solvent chamber saturated with toluene vapor for 45 minutes, and then retrieving them for spectral (UV-Vis) re-acquisition. It can be seen (Figure 4) that the vapor-annealing, which should result in more ordered thin films²⁵, precipitates the appearance of the highly intense J-band, confirming that molecular organization was indeed important in

producing the desired J-aggregate photophysics. When the volatile THF is used as the spin-casting solvent (particularly with low **6a** concentration) the resulting films lacked J-aggregate features. However, J-aggregate features can be recovered when these films are placed in a solvent chamber containing THF vapor (Figure 3.4).

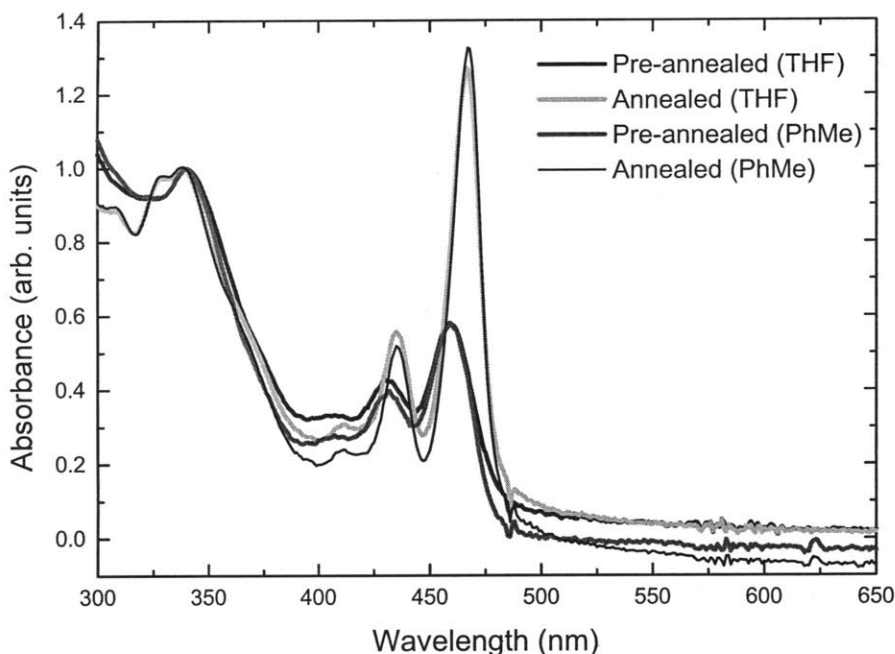


Figure 3.4. Absorption spectra of **6a** (film), before and after annealing under toluene (PhMe) and THF vapor, normalized to the absorbance at 340 nm.

Similar photophysical experiments were also performed on films of the two longer-chained macrocyclic analogs **6b** and **12**. In both cases, the films were cast from THF solutions of the macrocycles, and subsequently annealed under THF vapor for 45 minutes. UV-Vis data were acquired before and after the annealing process, and the spectra of **6b** and **12** are shown in Figure 3.5. The spectra of the pre-annealed films did not show J-bands, but these appeared in both cases upon annealing. Therefore, the results obtained with **6b** and **12** were analogous to those of **6a**, suggesting that the doubling of chain length of the peripheral alkyl/alkoxy groups had little effect on the photophysics, be it in solution or in the film-state. Similar J-aggregate photophysics could

not be observed with the non-cyclic **15**, implying that the aggregate formation may require approximate molecular planarity (steric hindrance in the non-cyclic **15** produces a larger deviation from planarity, since the two dibenzanthracene sub-units are less constrained). It is likely that J-aggregation of these polycyclic aromatics in the solid-state relies on π - π stacking interactions that could be disrupted if the non-planarity became too pronounced.

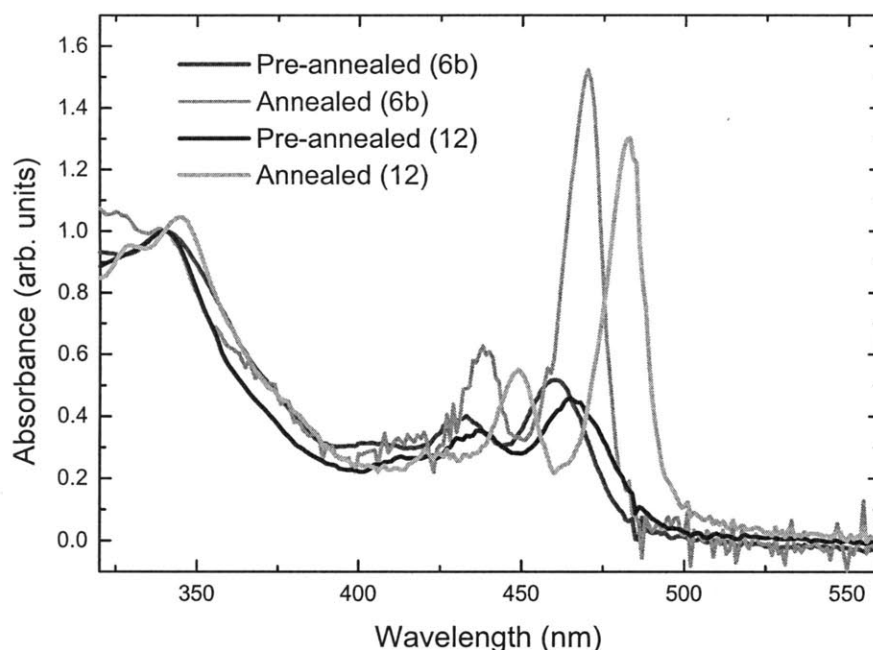


Figure 3.5. Absorption spectra of **6b** (film) and **12** (film), before and after annealing under THF vapor, normalized to the absorbance at 340 nm.

Additional experiments examining the photophysics of **6a** as a function of concentration were also undertaken. A series of films were spin-coated using **6a** solutions (polyisobutylene matrix /chlorobenzene as solvent) of varying concentrations, and their photoluminescence spectra, excitation spectra, and fluorescence lifetimes were measured. Chlorobenzene was chosen as it provided for optimal co-miscibility of **6a**, polyisobutylene, and solvent. When a film containing a very low concentration of **6a** (i.e. 0.0005 mg in a 1 mL solution of 40 mg/mL polyisobutylene (PIB) in chlorobenzene) was used, its emission peak was at 455 nm (Figure 3.6),

identical to that observed in solution spectra. As the amount of **6a** used in the spin-coating process was increased to 0.002 mg/mL of PIB/chlorobenzene, aggregate peaks began to emerge at 470 nm with a shoulder at 500 nm, while the 455 nm “monomer” peak diminished. A further increase in **6a** concentration to 0.005 mg/mL resulted in further reduction in the 455 nm peak, so that at 0.02 mg/mL the monomer peak can no longer be observed, at which point the emission spectrum begins to resemble those obtained with neat films discussed above (pure **6a**, no PIB matrix). From the excitation spectra (Figure 3.7), no J-band at 470 nm could be observed at the lowest concentration of 0.0005 mg/mL, but as the concentration was increased ten-fold, a peak at 470 nm appeared, becoming more pronounced with increasing **6a** concentrations. Fluorescence lifetimes (at 470 nm) for a series of solutions and films of different concentrations were also measured. Solution lifetimes were found to be between (1.7 ± 0.1) ns regardless of concentration. In the film state, it can be observed from Table 3.2 that the lifetimes generally decrease as the concentration of **6a** was increased from 0.0005 to 2.000 mg/mL (only a small incidence of scatter is observed in the trends). In particular, with a concentration of 0.0005 mg/mL, a lifetime of $\tau_m = 1.3$ ns was obtained, comparable to what was observed in chlorobenzene solutions, while at higher concentrations, lifetimes of about $\tau_f = 0.24$ ns are observed. Higher doping concentration also leads to a measureable increase in thin film photoluminescence (PL) quantum yield (QY) from $\Phi_m = 43 \pm 6$ % for the monomeric film to $\Phi_f = 92 \pm 8$ % for the aggregate films. To determine PL QY, we compared the PL counts from the **6a** film to a thin film standard of known QY, accounting for relative differences in absorption strength of the films. The standard was a thin film of thickness 75 nm of the small molecule *tris*(8-hydroxyquinolino)aluminum (Alq₃). The Alq₃ film was prepared by thermally evaporating recrystallized Alq₃ in ultra high vacuum (growth pressure below 10^{-6} Torr) onto a quartz substrate

that was carefully solvent cleaned and oxygen plasma treated to remove trace impurities. The published QY for Alq₃ in thin film is $32 \pm 2\%$.²⁶ We erred on the side of caution and used a value of QY = 30% for our calculations. To make a fair comparison of QY, for each film in consideration, the percentage of absorbed optical excitation was determined from optical transmission measurements. Measured PL counts were then normalized to the percent absorption values, on a film by film basis. For **6a** in monomeric form, we calculated the PL QY to be $43 \pm 6\%$, which is similar to the QY for **6a** in solution, and for **6a** at high doping concentrations, we determined the QY to be $92 \pm 8\%$.

The emergence of a red-shifted narrower linewidth optical transition at higher **6a** concentrations, the corresponding reduction in lifetime, and increase in quantum yield of aggregates as compared to monomers are indicative of J-aggregate formation.²⁷ In J-aggregates, strong coupling between the monomer transition dipoles produces a new cooperative molecular state. The coupling results in a new optical transition called the J-band, when the interaction strength exceeds the monomeric dephasing processes.²⁸ The interaction between monomeric transition dipoles lowers the overall energy of the cooperative state; hence the J-band absorption/fluorescence is red-shifted relative to that of the monomer. In the J-aggregate state, multiple molecules coherently couple, the number being denoted by N_c , and the J-aggregate exciton delocalizes over all of them²⁹. Coherent coupling amongst the N_c molecules leads to the acceleration of the radiative rate of the J-band states by a factor of N_c relative to the monomer³⁰, which translates into shorter excited state lifetime and higher PL QY. The radiative rate enhancement is typically referred to as a superradiance phenomenon since it is caused by coherent exciton coupling,³¹ though in J-aggregates the mechanism for the coupling is near-field Coulombic interactions while in classic superradiant systems, the origin is interference effects in

the spontaneous light emission process.³² Since the radiative rate of a J-aggregate increases relative to that of the monomer by a factor of N_c , from a comparison of lifetimes (τ_J vs. τ_m) and quantum yields (Φ_J vs. Φ_m), N_c can be determined using the equation³³:

$$N_c = \frac{\tau_m}{\tau_J} \frac{\Phi_J}{\Phi_m}$$

The data obtained suggest that N_c is on the order of 12 for our **6a** J-aggregate films. Coherent coupling also leads to a narrower total linewidth for the J-aggregate optical transition relative to the monomer, because the delocalized exciton averages out site-to-site variations, and suppresses the inhomogeneous broadening.³⁴ The linewidths of the monomer optical transition and the J-band are dominated by inhomogeneous broadening. Nevertheless, the width of the J-band relative to the monomer spectrum does characterize the coherence of the system. The linewidth of the J-band is narrower than the monomer optical transition because in the J-aggregate state, the exciton is delocalized over the N_c molecules that are coherently coupled, which tends to average out site-to-site inhomogeneities in the exciton energy. This motional narrowing is manifest in the smaller linewidth for J-aggregate absorption and emission spectra. This coherent coupling also results in the accelerated radiative process in the J-aggregate state, which translates into the higher observed QY and shorter exciton lifetime for the J-aggregate compared to the monomer.

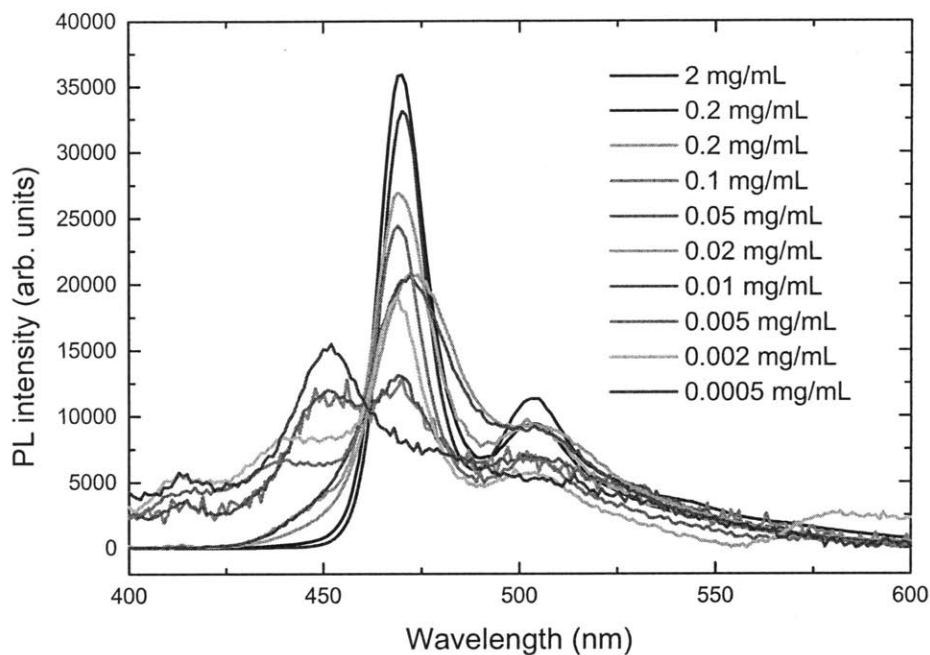


Figure 3.6. Photoluminescence intensity vs. concentration of **6a** in thin films (PL scaled by subtracting the background and scaling by integrated intensity at all wavelengths).

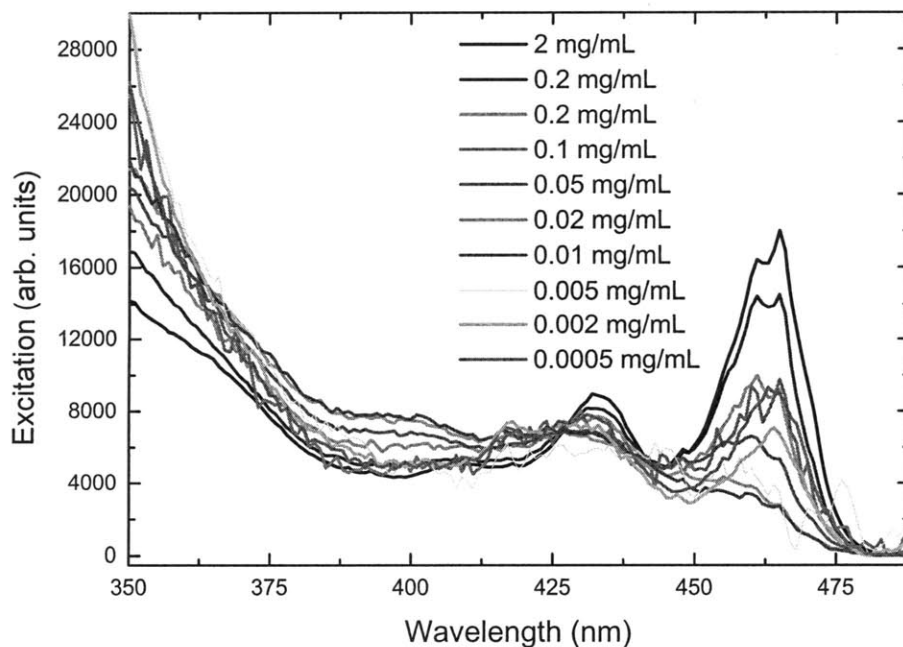


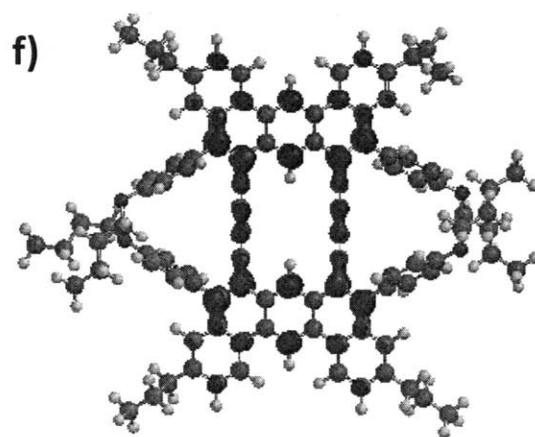
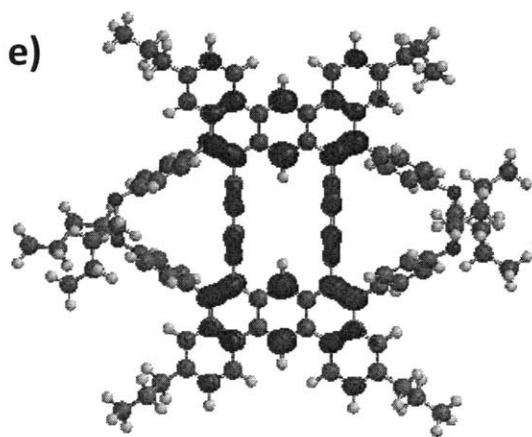
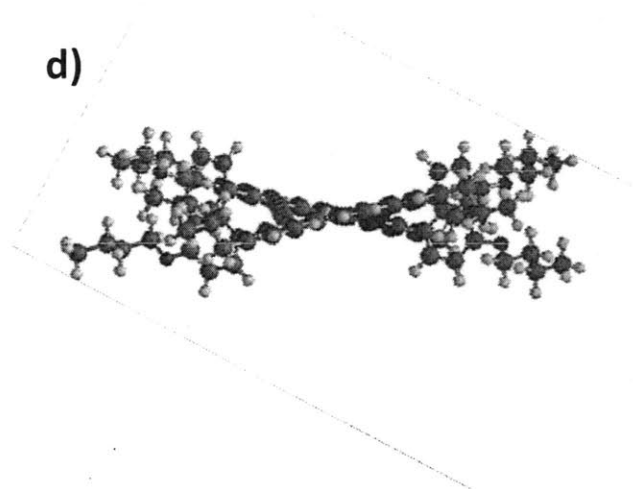
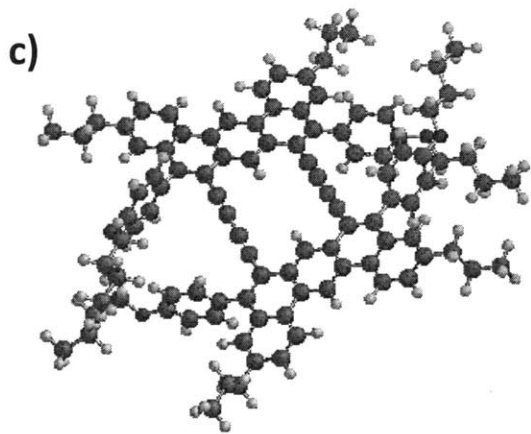
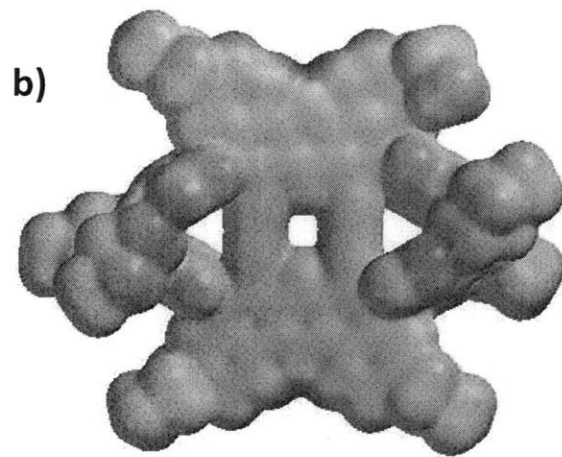
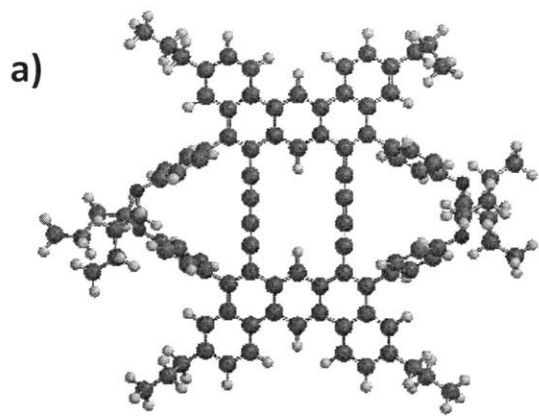
Figure 3.7. Excitation vs. concentration of **6a** in thin films (PLE scaled by subtracting background and scaling by integrated intensity at all wavelengths).

Table 3.2. Fluorescence lifetimes of **6a** (solutions and films) at different concentrations.

Concentration (mg/mL)	Lifetimes (bimodal) (ns)		State
0.002	1.7 (100%)	-	Solution (PhCl)
0.02	1.7 (100%)	-	Solution (PhCl)
0.2	1.8 (100%)	-	Solution (PhCl)
0.0005	1.3 (99.9%)	4.8 (0.1%)	Film
0.002	0.2 (96.7%)	1.3 (3.3%)	Film
0.005	0.3 (96.6%)	1.2 (3.4%)	Film
0.01	0.3 (97.4%)	1.0 (2.6%)	Film
0.02	0.2 (98.1%)	1.1 (1.9%)	Film
0.05	0.6 (84.5%)	1.5 (15.5%)	Film
0.10	0.4 (82.7%)	1.4 (17.3%)	Film
0.20	0.4 (94.9%)	1.4 (5.1%)	Film
2.00	0.2 (97.4%)	0.7 (2.6%)	Film

3.4 Molecular modelling.

In order to better visualize the equilibrium geometry of the macrocycles **6a**, **6b**, and **12**, molecular calculations³⁵ were performed at the semi-empirical PM3 level, using a model compound (Figure 3.8) with deliberately shortened alkyl sidechains to enable more rapid completion of the calculation. As can be seen in Figure 8, the macrocycle is composed of two 1,3-butadiyne-linked planar dibenz[*a,j*]anthracene sub-units that are slightly staggered relative to each other as a result of steric crowding in the middle of the molecule. Despite this structural distortion, the core of the macrocycle retains some overall planarity, which would still allow for intermolecular π - π stacking interactions. By comparison, the acyclic analog shows greater non-planarity (Figure 8g), since the two non-restrained aromatic sub-units have more freedom to minimize steric repulsions. As a result, π - π stacking interactions in acyclic **15** may be weakened.



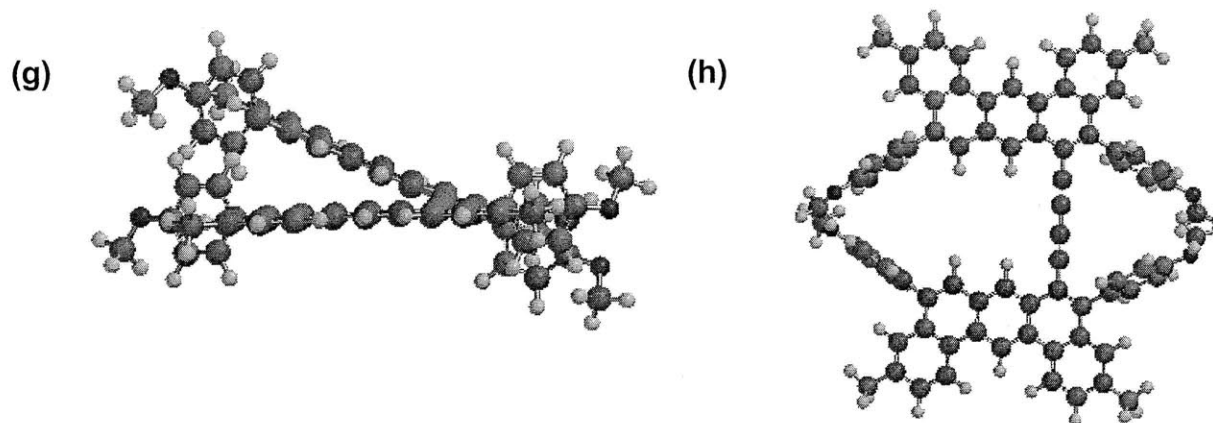


Figure 3.8. PM3-calculated models (a) top-down view of geometry-optimized macrocyclic structure, (b) molecular electrostatic potential map, (c) optimized structure tilted to emphasize steric crowding, (d) edge-on view of optimized structure, (e) frontier HOMO, and (f) frontier LUMO, (g) edge-on view of the acyclic model structure, (h) top-down view of the acyclic structure.

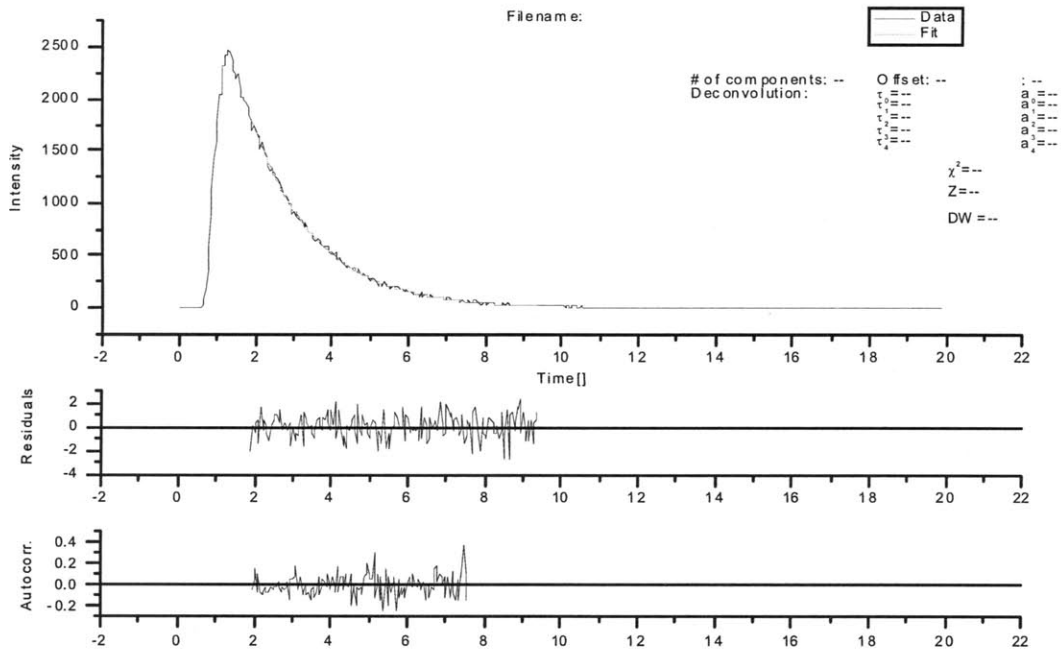
3.5 Conclusion

In summary, three dibenz[*a,j*]anthracene-based macrocycles have been synthesized and spectroscopically characterized. The conjugated macrocycles display pronounced photophysical properties in the solid-state, such as the intense red-shifted absorbances, narrow linewidths, and small Stokes shifts, indicating J-aggregate formation. These new compounds may have the potential to be utilized in various optoelectronic devices (e.g. lasers, photovoltaics, and polaritonic devices^{16a, 36}).

3.6 Experimental Section

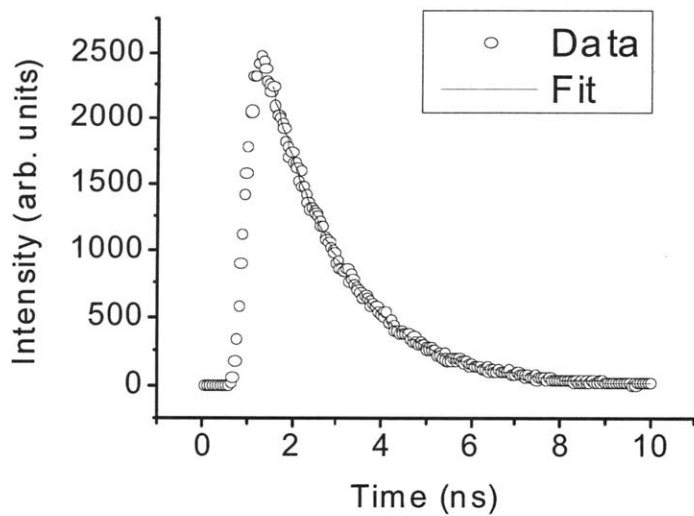
General Methods and Instrumentation: All reactions were performed under an argon atmosphere, using over-dried glassware and standard Schlenk techniques. Tetrakis-(triphenylphosphine)palladium(0) was purchased from Strem Chemicals, Inc. All other reagents were obtained from Aldrich Chemical Co., Inc., and used as received. Anhydrous toluene,

tetrahydrofuran, and dichloromethane were obtained from a solvent purification system (Innovative Technologies). Dry diisopropylamine (DIPA) was obtained by distilling reagent-grade DIPA over sodium hydroxide pellets. Nuclear Magnetic Resonance (NMR) spectra were recorded on a Varian Mercury (300 MHz) NMR spectrometer located in the MIT Department of Chemistry Instrumentation Facility (DCIF). Mass spectra were obtained on a Bruker Omnix MALDI-TOF instrument. UV/Vis spectra were recorded on an Agilent 8453 diode-array spectrophotometer. Emission spectra were acquired on a SPEX Fluorolog fluorometer (model FL-321, 450 W xenon lamp) using either right-angle detection (solution measurements) or front-face detection (thin film measurements). Fluorescence lifetime measurements were performed by exciting both thin film and solution samples with 160 fs pulses at 390 nm obtained by frequency doubling the output of a Coherent RegA Ti:Sapphire amplifier laser system. A Hamamatsu C4780 DynaSpect Picosecond Fluorescence Lifetime System operating in photon counting mode and triggered by an Agilent 81104A Pulse Pattern Generator was used to spectrally and temporally resolve the resulting fluorescence. The instrument response function (IRF) of the fluorescence lifetime system was 40 ps. A representative figure showing photoluminescence decay (compound **6a**, 0.02 mg/mL in PhCl) is included below:



of components: 1 Offset: -3.60779 :0
 Deconvolution: $\tau_0 = 1.68172$ $a_0 = 5591.805$
 $\tau_1 = --$ $a_1 = --$
 $\tau_2 = --$ $a_2 = --$
 $\tau_3 = --$ $a_3 = --$
 $\tau_4 = --$ $a_4 = --$

$\chi^2 = 1.00014$
 Z = 0.00133
 DW = 2.07295



4',6'-Bis-(*p*-(dodecyloxy)phenylethynyl)-4,4''-dihexyl-[1,1':3',1'']terphenyl (2a): A 500 mL two-neck round-bottom flask containing a magnetic stir-bar was charged with the dibromide **1** (or 1,5-dibromo-2,4-bis-(4-dodecyloxyphenylethynyl)benzene) (10.355 g, 16.83 mmol), 4-hexylphenyl-boronic acid (8.33 g, 40.4 mmol), tetrakis-(triphenylphosphine)-palladium(0) (0.583 g, 0.505 mmol), potassium carbonate (5.81 g, 42.1 mol), toluene (180 mL), and water (5 mL) under an atmosphere of argon. The mixture was stirred and briefly sparged by bubbling argon through it for 5-10 minutes using a long needle. Following the degassing, the mixture was then stirred vigorously and heated at 100 °C for 16 hours. After allowing the reaction mixture to cool down to room temperature, it was diluted with diethyl ether and transferred into a separatory funnel, and extracted with additional portions of ether (3 x 60 mL). The combined organic extracts were dried over anhydrous magnesium sulfate, filtered through a piece of fluted filter paper into a 500 mL round-bottom flask, and then concentrated by rotary evaporate to give a residue of the crude product. This was purified by flash chromatography on a silica gel column (15% v/v dichloromethane/hexane) to afford **2a** (9.028 g, 56%). ¹H NMR (300 MHz, CD₂Cl₂, δ ppm): 7.85 (1H, s), 7.66 (4H, d, *J* = 8.1 Hz), 7.50 (1H, s), 7.30 (4H, d, *J* = 8.1 Hz), 7.30 (4H, d, *J* = 8.1 Hz), 6.84 (4H, d, *J* = 8.7 Hz), 3.96 (4H, t, *J* = 6.6 Hz), 2.69 (4H, d, *J* = 7.5 Hz), 0.8-1.8 (68H). ¹³C NMR (300 MHz, CD₂Cl₂, δ ppm): 159.6, 143.2, 143.1, 137.4, 136.9, 133.0, 129.3, 128.3, 120.7, 115.2, 114.7, 93.0, 87.5, 68.3, 35.9, 32.2, 32.0, 31.8, 29.9, 29.87, 29.83, 29.81, 29.6, 29.4, 29.3, 26.2, 22.93, 22.90, 14.1. HRMS (MALDI-TOF): calcd: 966.7254 (M)⁺, found: 966.1416.

4',6'-Bis-(*p*-(dodecyloxy)phenylethynyl)-4,4''-didodecyl[1,1':3',1'']terphenyl (2b): **2b** was synthesized in a manner analogous to **2a**, but starting with **1** (2.88 g, 3.58 mmol) and 4-

dodecylphenylboronic acid (2.84 g, 9.78 mmol) instead. The crude product was also purified by column chromatography (10% v/v dichloromethane/hexane) to give **2b** (3.16 g, 78%). ¹H NMR (300 MHz, CD₂Cl₂, δ ppm): 7.86 (1H, s), 7.68 (4H, s), 7.50 (1H, s), 7.32 (8H, d, *J* = 7.5 Hz), 6.84 (4H, d, *J* = 8.7 Hz), 3.96 (4H, t, *J* = 6.6 Hz), 2.70 (4H, t, *J* = 7.5 Hz), 0.8-1.8 (92H). ¹³C NMR (300 MHz, CD₂Cl₂, δ ppm): 159.8, 159.6, 143.2, 143.1, 137.4, 136.9, 134.2, 133.4, 133.3, 133.0, 130.7, 129.3, 128.3, 120.7, 115.2, 114.8, 114.7, 93.0, 87.5, 68.3, 35.9, 32.2, 31.8, 30.0, 29.9, 29.8, 29.6, 29.4, 26.2, 23.0, 14.1. HRMS (MALDI-TOF): calcd: 1134.9132 (M)⁺, found: 1134.4322.

5,9-Bis-(4-dodecyloxyphenyl)-3,11-dihexyl-6,8-diiododibenz[*a,j*]anthracene (3a): A 250 mL two-neck round-bottom flask containing a magnetic stir-bar was charged with mercury (II) trifluoroacetate (7.92 g, 18.6 mmol) and iodine (17.0 g, 66.7 mmol). The flask was placed under an argon atmosphere, after which dry dichloromethane was introduced via syringe. The contents were stirred for about 15 minutes to dissolve as much of the solid reagents as possible. Then, the purple mixture was cooled down in an ice-water bath and stirred for an additional 5-10 minutes before 2,6-lutidine (2.13 mL, 0.0184 mol) was added dropwise to the stirred mixture via a syringe. Upon stirring for an additional 5 minutes, a solution of **2a** (7.82 g, 8.08 mmol) in dichloromethane (20 mL) was added slowly via syringe, and the resulting mixture was allowed to stir at a temperature 0 to 5 °C for 1 hour. Upon completion of the reaction, the mixture was diluted with dichloromethane, and then transferred into a 500 mL separatory funnel. The organic layer was shaken with aqueous sodium hydroxide, with its color changing from purple to yellow in the process. After the organic phase was collected in a clean 250 mL Erlenmeyer flask, the remaining aqueous layer was further extracted with additional dichloromethane (2 x 60 mL). The

combined organic phases were dried over anhydrous magnesium sulfate and then filtered through a piece of fluted filter paper. The clear yellow filtrate was collected in a 500 mL round-bottom flask, and the solvent was removed by rotary evaporation, leaving behind a crude product that was subsequently purified by flash chromatography on a silica gel column (15% v/v dichloromethane/hexane). The relevant fractions were combined and the solvent was removed, affording **3a** (5.41 g, 55%) as an off-white solid. ¹H NMR (300 MHz, CD₂Cl₂, δ ppm): 9.83 (1H, s), 9.45 (1H, s), 8.88 (2H, d, *J* = 8.7 Hz), 7.58 (2H, d, *J* = 7.8 Hz), 7.26 (2H, s), 7.21 (4H, d, *J* = 8.7 Hz), 7.07 (4H, d, *J* = 8.7 Hz), 4.08 (4H, t, *J* = 6.6 Hz), 2.66 (4H, t, *J* = 7.8 Hz), 0.8-1.9 (68H). ¹³C NMR (300 MHz, CD₂Cl₂, δ ppm): 159.1, 145.9, 142.9, 141.3, 137.8, 133.3, 132.0, 129.5, 128.5, 128.4, 128.3, 123.1, 116.4, 114.4, 107.3, 68.3, 36.1, 32.2, 31.9, 31.7, 30.0, 29.9, 29.8, 29.7, 29.6, 29.2, 26.4, 23.0, 22.9, 14.2, 14.1. HRMS (MALDI-TOF): calcd: 964.7097 (M-I₂)⁺, found: 964.4381.

5,9-Bis-(4-dodecyloxyphenyl)-3,11-dihexyl-6,8-diiododibenz[*a,j*]anthracene (3b): **3b** was synthesized in a fashion analogous to **3a**, but starting from **2b** (3.155 g, 2.78 mmol) instead. The crude product was purified by column chromatography (20% v/v dichloromethane/hexane) to give pure **3b** (2.06 g, 54%). ¹H NMR (300 MHz, CD₂Cl₂, δ ppm): 9.79 (1H, s), 9.44 (1H, s), 8.85 (2H, d, *J* = 8.7 Hz), 7.56 (2H, d, *J* = 8.1 Hz), 7.26 (2H, s), 7.19 (4H, d, *J* = 8.4 Hz), 7.07 (4H, d, *J* = 8.7 Hz), 4.07 (4H, t, *J* = 6.3 Hz), 2.65 (4H, t, *J* = 7.5 Hz), 1.87 (4H, m, *J* = 7.5 Hz), 1.2-1.6 (76H), 0.89 (12H). ¹³C NMR (300 MHz, CD₂Cl₂, δ ppm): 159.1, 145.8, 142.8, 141.3, 137.8, 133.3, 131.9, 131.3, 129.5, 128.4, 128.3, 123.1, 116.3, 114.8, 114.4, 107.3, 68.3, 36.1, 32.2, 31.7, 30.0, 29.8, 29.7, 29.6, 29.5, 26.4, 23.0, 22.9, 14.2. HRMS (MALDI-TOF): calcd: 1132.8975 (M-I₂)⁺, found: 1132.9160.

5,9-Bis-(4-dodecyloxyphenyl)-3,11-dihexyldibenz[*a,j*]anthracene-6,8-dicarbaldehyde (4a): A 250 mL two-neck round-bottom flask containing **3a** (5.374 g, 4.41 mmol) and a magnetic stir-bar was evacuated and then placed under positive pressure of argon. Dry tetrahydrofuran (100 mL) was then added via syringe and the mixture was stirred to completely dissolve **3a**. The solution was subsequently cooled in a dry-ice/acetone bath at -78 °C, before 1.7 M *tert*-butyllithium in pentane (7.8 mL, 13.2 mmol) was added dropwise via syringe. This mixture was stirred at -78 °C for 1 hour, after which iron(0)pentacarbonyl (1.33 mL, 10.1 mmol) was added via syringe. After 10 minutes, the dry-ice/acetone bath was removed, and the mixture was allowed to warm up to room temperature. Stirring was continued overnight. The resulting mixture was then quenched with glacial acetic acid (4 mL), and stirred for 1 hour, before being diluted with dichloromethane and poured into a separatory funnel containing deionized water. The mixture was extracted with further portions of dichloromethane (3 x 70 mL) and the organic layer was separated out and dried over anhydrous magnesium sulfate. Removal of the solvent under rotary evaporation afforded a dark-colored crude mixture containing the target dialdehyde as well as monoaldehyde byproduct. This was purified by flash chromatography on a silica gel column (30% v/v dichloromethane/hexane to 65% dichloromethane/hexane, gentle gradient) to give **4a** as a yellow solid (1.102 g, 25%). Note: The first yellow band the elutes contains monoaldehyde, whilst the second yellow band contains the desired dialdehyde. ¹H NMR (300 MHz, CD₂Cl₂, δ ppm): 10.88 (1H, s), 10.10 (2H, s), 9.91 (1H, s), 8.90 (2H, d, *J* = 8.7 Hz), 7.66 (2H, d, *J* = 7.5 Hz), 7.47 (2H, s), 7.33 (4H, d, *J* = 8.4 Hz), 7.09 (4H, d, *J* = 8.4 Hz), 4.08 (4H, t, *J* = 6.6 Hz), 2.69 (4H, t, *J* = 7.8 Hz), 0.8-1.9 (68H). ¹³C NMR (300 MHz, CD₂Cl₂, δ ppm): 195.1, 159.6, 149.0, 142.7, 132.5, 131.9, 130.7, 130.6, 129.1, 128.7, 128.2, 128.0, 127.0, 124.7, 123.1, 115.7, 114.5, 68.5, 36.1,

32.2, 32.0, 31.6, 29.96, 29.93, 29.9, 29.7, 29.6, 29.6, 29.2, 26.4, 23.0, 22.9, 14.2, 14.1. HRMS (MALDI-TOF): calcd: 1022.7152 (M)⁺, found: 1022.8704.

5,9-Bis-(4-dodecyloxyphenyl)-3,11-didodecyldibenz[*a,j*]anthracene-6,8-dicarbaldehyde (4b)

4b was synthesized in a fashion analogous to **4a**, starting from **3b** (2.06 g, 1.49 mmol). The crude product was purified by column chromatography (25% dichloromethane/hexane to 70% dichloromethane/hexane, gentle gradient) to give pure **4b** (0.354 g, 20%). ¹H NMR (300 MHz, CD₂Cl₂, δ ppm): 10.87 (1H, s), 10.10 (2H, s), 9.88 (1H, s), 8.88 (2H, d, *J* = 8.4 Hz), 7.65 (2H, d, *J* = 7.8 Hz), 7.47 (2H, s), 7.34 (4H, d, *J* = 8.1 Hz), 7.10 (4H, d, *J* = 8.1 Hz), 4.09 (4H, t, *J* = 6.3 Hz), 2.68 (4H, t, *J* = 7.2 Hz), 0.8-1.9 (92H). ¹³C NMR (300 MHz, CD₂Cl₂, δ ppm): 195.0, 159.6, 149.0, 142.6, 132.5, 131.9, 130.7, 130.6, 129.1, 128.7, 128.2, 128.0, 127.0, 124.7, 123.1, 115.7, 114.5, 68.5, 36.1, 32.2, 31.6, 30.0, 29.9, 29.7, 29.65, 29.61, 29.5, 26.4, 23.0, 14.2. HRMS (MALDI-TOF): calcd: 1213.8928 (M + Na)⁺, found: 1212.7060.

5,9-Bis-(4-dodecyloxyphenyl)-6,8-diethynyl-3,11-dihexyldibenz[*a,j*]anthracene (5a): A 250 mL single-neck round-bottom flask containing a magnetic stir-bar was charged with triphenylphosphine (2.255 g, 8.6 mmol) and carbon tetrabromide (1.426 g, 4.3 mmol), and subsequently placed under argon atmosphere. The flask was immersed into an ice-water bath, and then dry dichloromethane (50 mL) was added via syringe, with simultaneous stirring to dissolve the reagents, giving a clear yellow solution. To this was added a solution of **4a** (1.102 g, 1.075 mmol) in dichloromethane (10 mL), and the mixture was allowed to slowly warm up to room temperature overnight. After the reaction was complete, dichloromethane was poured in to dilute the mixture, which was transferred into a separatory funnel and extracted with additional

portions of dichloromethane (3 x 60 mL). The combined organic extracts were dried over anhydrous magnesium sulfate, filtered through a fluted filter funnel and then the solvent was removed by rotary evaporation. The crude product could be quickly purified by flash chromatography through a short column/pad of silica gel. Concentrating the fractions affords the intermediate geminal dibromide (ca. 1.41 g, 1.06 mol), which should not be stored, but instead, used as soon as possible in the next step (i.e. conversion to alkyne). In a 100 mL one-neck, round-bottom flask containing a magnetic stir-bar and the purified geminal dibromide (ca. 1.41 g, 1.06 mol) under argon atmosphere, anhydrous tetrahydrofuran (30 mL) was added via syringe to give a clear solution. After cooling the solution down to -78 °C in a dry-ice/acetone bath, 1.6 M *n*-butyllithium in hexanes (3.3 mL, 5.28 mmol) was added dropwise by syringe. The reaction mixture was stirred for about 2 hours, after which an aqueous solution of ammonium chloride was introduced via syringe, and the mixture was allowed to warm to room temperature (at this point, the mixture should emit violet under a hand-held UV lamp). Diethyl ether was used to dilute the mixture, which was transferred into a separatory funnel and extracted with further portions of ether (3 x 50 mL). The combined organic extracts were dried over anhydrous magnesium sulfate, filtered, and then concentrated to near-dryness under rotary evaporation. The crude dialkyne was then purified by flash chromatography on a silica gel column (20% v/v dichloromethane/hexane) to give **5a** (0.70 g, 64%). ¹H NMR (300 MHz, CD₂Cl₂, δ ppm): 9.99 (1H, s), 9.62 (1H, s), 8.96 (2H, d, *J* = 8.7 Hz), 7.62 (2H, d, *J* = 8.1 Hz), 7.45 (2H, d), 7.44 (4H, d, *J* = 8.7 Hz), 7.08 (4H, d, *J* = 8.7 Hz), 4.08 (4H, t, *J* = 6.6 Hz), 3.53 (2H, s), 2.71 (4H, t, *J* = 7.8 Hz), 0.8-2.0 (68H). ¹³C NMR (300 MHz, CD₂Cl₂, δ ppm): 159.1, 144.2, 142.5, 131.8, 131.4, 129.9, 128.9, 128.7, 128.5, 127.6, 125.5, 123.0, 118.0, 116.0, 114.2, 85.8, 81.7, 68.3, 36.2, 34.8,

32.2, 31.9, 31.8, 31.7, 30.0, 29.9, 29.7, 29.6, 29.2, 26.4, 25.5, 23.0, 22.9, 14.2, 14.1. HRMS (MALDI-TOF): calcd: 1014.7254 (M)⁺, found: 1015.0544.

5,9-Bis-(4-dodecyloxyphenyl)-6,8-diethynyl-3,11-didodecyldibenz[*a,j*]anthracene (5b): **5b** was synthesized in a fashion analogous to **5a**. The geminal dibromide was purified in an identical way, and the crude dialkyne was also purified by column chromatography (25% v/v dichloromethane/hexane) to give pure **5b** (0.10 g, 86%). ¹H NMR (300 MHz, CD₂Cl₂, δ ppm): 10.01 (1H, s), 9.63 (1H, s), 8.98 (2H, d, *J* = 8.7 Hz), 7.63 (2H, d, *J* = 8.4 Hz), 7.46 (2H, s), 7.43 (4H, d, *J* = 8.7 Hz), 7.09 (4H, d, *J* = 8.7 Hz), 4.09 (4H, t, *J* = 6.6 Hz), 3.52 (2H, s), 2.71 (4H, t, *J* = 7.5 Hz), 0.8-1.9 (92H). ¹³C NMR (300 MHz, CD₂Cl₂, δ ppm): 159.1, 144.2, 142.5, 132.1, 131.8, 131.4, 129.9, 128.9, 128.7, 128.6, 127.7, 125.6, 123.0, 118.0, 114.2, 85.8, 81.6, 68.3, 36.1, 34.8, 32.2, 31.8, 31.7, 29.94, 29.9, 29.73, 29.71, 29.7, 29.6, 29.5, 29.3, 26.4, 25.4, 22.9, 22.89, 20.6, 14.1. HRMS (MALDI-TOF): calcd 1182.9132 (M)⁺, found: 1183.1765.

Macrocycle 6a: In a 500-mL single-neck round-bottom flask containing a magnetic stir-bar was added *tetrakis*-(triphenylphosphine)palladium(0) (0.080 g, 0.0069 mmol), 1,4-benzoquinone (0.067 g, 0.62 mmol), copper(I) iodide (0.020 g, 0.103 mmol), anhydrous diisopropylamine (25 mL), and anhydrous toluene (60 mL). The mixture was stirred at room temperature under argon atmosphere to effect complete dissolution. Then, a solution of **5a** (0.70 g, 0.689 mmol) in dry toluene (30 mL) was slowly added to the mixture via a glass syringe operated by a syringe-pump, with the addition rate set to 1.5 mL/h. After addition was complete, the mixture was allowed to stir for another 2 days at room temperature. Upon reaction completion, the solvents were removed by rotary evaporation to leave a yellow-brown residue. Dichloromethane was then

added to the residue and the solution was transferred into a separatory funnel, where it was washed several times with water. The organic layer was dried over anhydrous magnesium sulfate, filtered, and the solvent was removed to give a crude product. This was purified by flash chromatography on a silica gel column (30% v/v dichloromethane/hexane) to give **6a** as a lemon-yellow solid (0.29 g, 41 %). Occasionally, more than one round of column chromatography may be required to effect complete purification. ¹H NMR (300 MHz, CDCl₃, δ ppm): 9.87 (2H, s), 9.40 (2H, s), 8.85 (4H, d, *J* = 8.7 Hz), 7.50 (4H, d, *J* = 8.4 Hz), 7.43 (4H, s), 7.33 (8H, d, *J* = 8.4 Hz), 7.02 (8H, d, *J* = 8.7 Hz), 4.14 (8H, t, *J* = 6.3 Hz), 2.60 (8H, t, *J* = 7.8 Hz), 0.8-2.1 (136H). ¹³C NMR (300 MHz, CDCl₃, δ ppm): 159.0, 145.2, 142.1, 132.0, 130.7, 129.9, 129.1, 128.9, 128.4, 119.6, 118.1, 116.0, 115.1, 114.1, 113, 82.6, 81.2, 68.1, 32.1, 31.9, 31.6, 31.1, 30.8, 30.6, 30.3, 30.1, 29.9, 29.86, 29.8, 29.6, 29.1, 26.5, 22.9, 22.8, 18.0, 14.3. HRMS (MALDI-TOF): calcd: 2025.4195 (M)⁺, found: 2026.2059.

Macrocycle 6b: Macrocycle **6b** was synthesized in an analogous fashion to **6a**, starting from **5b** (0.10 g, 0.0845 mmol). It was purified by flash chromatography on a silica gel column (30% v/v dichloromethane/hexane), to afford **6b** as a lemon-yellow solid (47 mg, 47%). ¹H NMR (300 MHz, CDCl₃, δ ppm): 9.93 (2H, s), 9.47 (2H, s), 8.90 (4H, d, *J* = 8.4 Hz), 7.56 (4H, d, *J* = 8.4 Hz), 7.51 (4H, s), 7.42 (8H, d, *J* = 8.4 Hz), 7.10 (8H, d, *J* = 8.4 Hz), 4.23 (8H, t, *J* = 6.3 Hz), 2.68 (8H, t, *J* = 6.9 Hz), 1.98 (8H, m, *J* = 6.9 Hz), 0.8-1.7 (176H). ¹³C NMR (300 MHz, CDCl₃, δ ppm): 159.0, 145.2, 142.2, 132.1, 130.8, 130.0, 128.9, 128.4, 123.1, 118.2, 114.1, 82.7, 81.3, 68.2, 53.3, 36.2, 32.2, 31.8, 30.0, 29.96, 29.9, 29.8, 29.6, 26.6, 23.0. HRMS (MALDI-TOF): calcd: 2361.7951 (M)⁺, found: 2361.8767.

4',6'-Bis-(*p*-(dodecyloxy)phenylethynyl)-4,4''-dimethoxy-[1,1':3',1'']terphenyl (7): Terphenyl 7 was synthesized in an analogous manner to **2a** and **2b**, starting with **1** (3.0 g, 3.73 mmol) and 4-methoxyphenylboronic acid (1.70 g, 11.16 mmol). The crude product was purified by flash chromatography on a silica gel column (40% v/v dichloromethane/hexane), to give **7** as a white solid (2.56 g, 80%). ¹H NMR (300 MHz, CD₂Cl₂, δ ppm): 7.84 (1H, s), 7.70 (4H, d, *J* = 8.7 Hz), 7.46 (1H, s), 7.33 (2H, d, *J* = 8.7 Hz), 7.02 (4H, d, *J* = 8.7 Hz), 6.85 (4H, d, *J* = 8.7 Hz), 3.96 (4H, t, *J* = 6.6 Hz), 3.87 (6H, s), 0.8-1.8 (46H). ¹³C NMR (300 MHz, CD₂Cl₂, δ ppm): 159.7, 159.6, 133.0, 132.5, 130.6, 127.8, 120.3, 115.1, 114.7, 114.3, 113.6, 92.9, 87.5, 68.4, 55.5, 32.2, 29.9, 29.8, 29.6, 29.4, 26.2, 22.9, 14.1. HRMS (MALDI-TOF): calcd: 858.5587 (M)⁺, found: 858.2749.

Bis-spirocyclohexadienone 8: A 250-mL single-neck round-bottom flask containing **7** (2.14 g, 2.49 mmol) and a magnetic stir-bar was placed under argon atmosphere. Anhydrous dichloromethane (65 mL) was then added via syringe and the resulting mixture was stirred for 10 minutes. Upon complete dissolution of the solid, the flask was immersed into a dry-ice/acetone bath at -78 °C. After stirring at that temperature for 5 minutes, a 1.0 M solution of ICl in dichloromethane (6.0 mL, 6 mmol) was added slowly via syringe. After the dark-colored mixture was stirred for 1 hour at -78 °C, it was diluted with dichloromethane and then transferred into a separatory funnel containing aqueous sodium hydroxide (~0.5 M, 100 mL). The dark mixture was decolorized upon shaking with NaOH, and the organic layer was extracted several times with additional dichloromethane (3 x 80 mL). The combined organic extracts were dried over anhydrous magnesium sulfate, filtered, and the solvent removed by rotary evaporation. The residue was titrated with hexane (~25 mL) and the resulting suspension was filtered through a

fritted glass filter funnel. The off-white solid was washed with several portions of hexane, and then dried by air suction for 1-2 hours, giving an off-white powder (1.61 g, ca. 70%). This partially purified **8** can be used in the next step without further purification. (Notes: (i) compound **8** shows somewhat low solubility in many common organic solvents, making column chromatography impractical, (ii) storage of **8** is possible, but should be kept refrigerated. Immediate use in the next step is recommended.) ¹H NMR (300 MHz, CD₂Cl₂, δ ppm): 7.52 (1H, s), 7.36 (4H, d, *J* = 8.4 Hz), 6.87 (4H, d, *J* = 9.0 Hz), 6.84 (1H, s), 6.48 (4H, d, *J* = 10.2 Hz), 6.39 (4H, d, *J* = 9.9 Hz), 3.96 (4H, d, *J* = 6.9 Hz), 0.8-1.8 (46H). HRMS (MALDI-TOF): calcd: 858.5587 (M - I₂)⁺, found 858.2749.

5,9-Bis-(4-dodecyloxyphenyl)-3,11-didodecyloxy-6,8-diiododibenz[*a,j*]anthracene (9): To a 100-mL round-bottom flask containing a magnetic stir-bar was added **8** (1.0 g, ca. 0.923 mmol), dodecanol (5.0 g, 26.8 mmol), and dichloromethane (9 mL) (Schlenk techniques were unnecessary for this reaction). The mixture was stirred to give an off-white suspension. The flask was placed in an ice-water bath, after which concentrated sulfuric acid (~1.0 mL in total) was added dropwise to the rapidly stirring suspension using a glass dropper. Addition of acid was discontinued once the white suspension gave way to a brown solution. This solution was subsequently allowed to stir for 6 hours at room temperature. After carefully neutralizing the final mixture with aqueous NaOH or NaHCO₃, the mixture was diluted with dichloromethane and transferred into a separatory funnel containing concentrated brine solution. The mixture was extracted with dichloromethane (3 x 80 mL), and the combined organic extracts were dried over anhydrous magnesium sulfate. After filtration and subsequent removal of solvent by rotary evaporation, a residue of the crude product was obtained. This was purified by flash chromatography on a silica gel column (25% v/v dichloromethane/hexane) to afford pure **9**

(0.887 g, ca. 68%). ¹H NMR (300 MHz, CD₂Cl₂, δ ppm): 9.31 (1H, s), 9.27 (1H, s), 8.57 (2H, d, *J* = 9.3 Hz), 7.0-7.2 (10H), 6.74 (2H, s), 4.04 (4H, t, *J* = 5.7 Hz), 3.76 (4H, d, *J* = 5.7 Hz), 0.9-1.9 (92H). ¹³C NMR (300 MHz, CD₂Cl₂, δ ppm): 159.0, 158.5, 145.0, 141.3, 137.7, 134.5, 131.3, 130.7, 129.4, 124.6, 123.9, 116.7, 115.1, 114.4, 111.5, 107.9, 68.3, 68.2, 32.3, 30.0, 29.9, 29.8, 29.7, 29.5, 26.5, 26.4, 23.0, 14.3. HRMS (MALDI-TOF): calcd: 1164.8874 (M – I₂)⁺, found: 1165.0823.

5,9-Bis-(4-dodecyloxyphenyl)-3,11-didodecyloxydibenz[*a,j*]anthracene-6,8-dicarbaldehyde

(10): **10** was synthesized in a fashion analogous to **4a** and **4b**, starting from **9** (0.464 g, 0.327 mmol). The crude product was also purified by flash chromatography on a silica gel column (25% dichloromethane/hexane to 70% dichloromethane/hexane, gentle gradient) to give pure **10** (0.12 g, 30%). ¹H NMR (300 MHz, CD₂Cl₂, δ ppm): 10.73 (1H, s), 10.05 (2H, s), 9.54 (1H, s), 8.71 (2H, d, *J* = 9.0 Hz), 7.34 (2H, d, *J* = 2.4 Hz), 7.31 (4H, d, *J* = 8.4 Hz), 6.98 (4H, d, *J* = 2.4 Hz), 4.08 (4H, t, *J* = 6.3 Hz), 3.85 (4H, t, *J* = 6.0 Hz), 0.8-2.0 (92H). ¹³C NMR (300 MHz, CD₂Cl₂, δ ppm): 195.0, 159.6, 158.5, 148.0, 133.3, 132.4, 129.5, 128.7, 128.0, 126.3, 125.8, 124.6, 119.0, 114.5, 111.0, 68.5, 68.3, 32.2, 30.0, 29.94, 29.9, 29.8, 29.7, 29.6, 29.4, 26.4, 26.3, 23.0, 14.2. HRMS (MALDI-TOF): calcd: 1222.8928 (M)⁺, found: 1222.7428.

5,9-Bis-(4-dodecyloxyphenyl)-6,8-diethynyl-3,11-didodecyloxydibenz[*a,j*]anthracene (11):

11 was synthesized in a fashion analogous to **5a** and **5b**. The intermediate geminal dibromide was purified in an identical way, and the crude dialkyne was also purified by column chromatography (25% v/v dichloromethane/hexane) to give pure **11** (80 mg, 67%). ¹H NMR (300 MHz, CD₂Cl₂, δ ppm): 9.66 (1H, s), 9.53 (1H, s), 8.79 (2H, d, *J* = 8.7 Hz), 7.41 (4H, d, *J* =

7.5 Hz), 7.27 (2H, d, $J = 8.1$ Hz), 7.06 (4H, d, $J = 8.1$ Hz), 7.00 (2H, s), 4.05 (4H, t), 3.86 (4H, t), 3.51 (2H, s), 0.9-1.9 (92H). ^{13}C NMR (300 MHz, CD_2Cl_2 , δ ppm): 159.1, 158.4, 143.4, 133.5, 131.8, 131.4, 128.8, 128.7, 125.7, 124.6, 124.5, 118.5, 117.2, 114.9, 114.2, 110.6, 85.8, 81.7, 68.3, 32.2, 30.0, 29.95, 29.8, 29.76, 29.7, 29.5, 26.4, 26.3, 23.0, 14.2. HRMS (MALDI-TOF): calcd: 1214.9030 (M)⁺, found: 1214.9469.

Macrocycle 12: Macrocycle **12** was synthesized in an analogous fashion to **6a**, starting from **10** (80 mg, 0.066 mmol). It was purified by flash chromatography on a silica gel column (35% v/v dichloromethane/hexane), to afford **12** as a lemon-yellow solid (37 mg, 46%). ^1H NMR (300 MHz, CDCl_3 , δ ppm): 9.71 (2H, s), 9.22 (2H, s), 8.82 (4H, d, $J = 9.0$ Hz), 7.40 (4H, d, $J = 8.4$ Hz), 7.27 (4H, s), 7.22 (8H, d, $J = 9.0$ Hz), 7.09 (8H, d, $J = 8.1$ Hz), 4.22 (8H, t), 3.84 (8H, t), 1.98 (8H, m), 0.8-1.7 (176H). ^{13}C NMR (300 MHz, CDCl_3 , δ ppm): 158.9, 158.3, 144.4, 133.5, 132.0, 130.9, 128.9, 128.6, 124.8, 118.7, 114.2, 82.7, 81.3, 68.2, 32.2, 30.0, 29.95, 29.9, 29.8, 29.7, 29.5, 26.6, 26.4, 23.0, 14.4. HRMS (MALDI-TOF): calcd: 2427.6777 (M)⁺, found 2427.8788.

5,9-Bis-(4-dodecyloxyphenyl)-3,11-bis-(3,7,11-trimethyldodecyloxy)-6,8-diiododibenz[*a,j*]-anthracene (13): **13** was synthesized in an analogous fashion to **9**, starting with compound **8** (2.0 g, 1.85 mmol) and using 3,7,11-trimethyldodecanol (excess) as the alcohol instead. The crude product was purified by flash chromatography on a silica gel column (15% v/v dichloromethane/hexane) to afford pure **13** (2.4 g, ca. 44 %). ^1H NMR (300 MHz, CD_2Cl_2 , δ ppm): 9.45 (1H, s), 9.31 (1H, s), 8.69 (2H, d, $J = 9.3$ Hz), 7.25 (2H, d, $J = 8.7$ Hz), 7.18 (4H, d, $J = 8.4$ Hz), 7.06 (4H, d, $J = 8.4$ Hz), 6.79 (2H, s), 4.07 (4H, t, $J = 6.3$ Hz), 3.91 (4H, t, $J = 6.3$

Hz), 0.85-1.88 (104H). ^{13}C NMR (300 MHz, CD_2Cl_2 , δ ppm): 159.1, 158.5, 145.1, 141.4, 137.7, 134.6, 131.3, 130.8, 129.5, 124.7, 124.0, 116.9, 115.2, 114.5, 111.6, 107.9, 68.3, 67.7, 66.6, 39.6, 37.6, 37.5, 36.3, 33.1, 32.3, 30.1, 30.0, 29.9, 29.8, 29.7, 28.3, 26.4, 25.1, 24.6, 23.0, 22.8, 22.7, 19.8, 19.7, 19.6, 14.2. HRMS (MALDI-TOF): calcd: 1248.9813 ($\text{M} - \text{I}_2$)⁺, found: 1248.9209.

5,9-Bis-(4-dodecyloxyphenyl)-3,11-bis-(3,7,11-trimethyldodecyloxy)dibenz[*a,j*]anthracene-6-carbaldehyde (14): **14** was synthesized in a fashion analogous to **4a**, starting from **13** (2.40 g, 1.6 mmol), with the exception that the first yellow band instead of the second one was isolated during the purification stage of silica gel column chromatography (30% v/v dichloromethane/hexane) to give pure **14** (0.90 g, 44%). ^1H NMR (300 MHz, CD_2Cl_2 , δ ppm): 10.20 (1H, s), 10.05 (1H, s), 10.03 (1H, s), 9.58 (1H, s), 8.76 (2H, d), 7.72 (1H, s), 7.31 (4H, d, $J = 8.4$ Hz), 7.00-7.50 (18H), 6.80 (1H, s), 3.89-4.07 (8H, t), 0.87-1.86 (104H). ^{13}C NMR (300 MHz, CD_2Cl_2 , δ ppm): 159.6, 159.1, 159.0, 158.5, 158.2, 148.9, 148.4, 145.0, 138.3, 137.9, 133.5, 133.3, 133.0, 132.4, 131.3, 131.2, 130.1, 129.2, 128.8, 128.6, 128.1, 126.9, 126.2, 125.9, 125.2, 124.6, 114.5, 111.1, 108.8, 68.4, 39.6, 37.7, 37.5, 36.5, 36.3, 36.2, 33.1, 32.2, 30.1, 30.0, 29.8, 29.7, 29.6, 28.3, 26.4, 25.1, 24.6, 23.0, 22.8, 22.7, 19.8, 19.7, 19.6, 14.2. HRMS (MALDI-TOF): calcd: 1278.9918 (M)⁺, found 1278.7395.

5,9-Bis-(4-dodecyloxyphenyl)-6-ethynyl-3,11-bis-(3,7,11-trimethyldodecyloxy)dibenz[*a,j*]-anthracene (15): **15** was synthesized in a fashion analogous to **5a**, starting with **14** (0.90 g, 0.70 mmol). The intermediate geminal dibromide was purified in an identical way, and the crude alkyne was purified by column chromatography (20% v/v dichloromethane/hexane) to give pure **10** (0.74 g, 83% over two steps). ^1H NMR (300 MHz, CD_2Cl_2 , δ ppm): 9.69 (1H, s), 8.87 (2H, s),

7.77 (2H, s), 7.03-7.51 (13H), 3.93-4.03 (8H), 3.48 (1H, s), 0.9-1.9 (104H). ^{13}C NMR (300 MHz, CD_2Cl_2 , δ ppm): 159.1, 159.0, 158.4, 158.3, 143.2, 138.4, 133.5, 133.3, 133.1, 131.8, 131.5, 131.2, 129.7, 129.2, 128.5, 128.4, 128.3, 126.6, 124.8, 124.5, 118.2, 117.2, 116.3, 114.8, 114.6, 114.2, 110.7, 109.7, 85.8, 81.9, 68.3, 66.6, 39.6, 37.7, 37.6, 36.5, 36.4, 36.3, 33.1, 32.3, 30.1, 30.0, 29.8, 29.7, 28.3, 26.5, 26.4, 25.1, 24.6, 23.0, 22.8, 22.7, 19.8, 19.7, 19.6, 14.2. HRMS (MALDI-TOF): calcd: 1274.9969 (M)⁺, found 1274.8785.

Compound 16: Compound **16** was synthesized in an analogous fashion to **6a** (but without high dilution), starting from **15** (0.74 g, 0.58 mmol). It was purified by flash chromatography on a silica gel column (30% v/v dichloromethane/hexane), to afford **16** as a lemon-yellow solid (0.69 g, 47%). ^1H NMR (300 MHz, CD_2Cl_2 , δ ppm): 9.65 (2H, s), 8.86 (4H, s), 8.81 (2H, s), 7.70 (2H, s), 7.28-7.38 (12H), 6.87-7.02 (12H), 3.81-3.97 (16H, t), 0.86-1.75 (208H). ^{13}C NMR (300 MHz, CDCl_3 , δ ppm): 159.0, 158.6, 158.3, 158.1, 144.1, 137.9, 133.2, 133.0, 132.8, 131.8, 131.1, 130.7, 129.8, 129.0, 128.6, 128.1, 125.0, 124.7, 118.1, 114.6, 114.3, 82.7, 68.1, 67.9, 66.4, 54.3, 54.0, 53.6, 53.3, 52.9, 39.7, 37.8, 37.7, 37.6, 36.5, 33.1, 32.3, 30.2, 30.1, 30.0, 29.9, 29.8, 29.7, 28.3, 26.4, 26.3, 25.2, 24.7, 23.0, 22.8, 22.7, 19.8, 19.7, 14.3. HRMS (MALDI-TOF): calcd: 2547.9782 (M)⁺, found 2547.6915.

References and Notes

[1] a) Sakamoto, J.; Schlüter, A. D.; *Eur. J. Org. Chem.* **2007**, 2700-2712; b) Zhang, W.; Moore, J. S. *Angew. Chem. Int. Ed.* **2006**, *45*, 4416-4439; c) Kumar, S. *Chem. Soc. Rev.* **2006**, *35*, 83-109.

[2] Akiyama, S.; Misumi, S.; Nakagawa, M. *Bull. Chem. Soc. Jpn.* **1960**, *33*, 1293-1298.

- [3] a) Toyota, S.; Goichi, M.; Kotani, M. *Angew. Chem. Int. Ed.* **2004**, *43*, 2248-2251; b) Toyota, S.; Kurokawa, M.; Araki, M.; Nakamura, K.; Iwanaga, T. *Org. Lett.* **2007**, *9*, 3655-3658; c) Goichi, M.; Toyota, S. *Chem. Lett.* **2006**, *35*, 684-685; d) Goichi, M.; Segawa, K.; Suzuki, S.; Toyota, S. *Synthesis* **2005**, *13*, 2116-2118; e) Toyota, S.; Goichi, M.; Kotani, M.; Takezaki, M. *Bull. Chem. Soc. Jpn.* **2005**, *78*, 2214-2227; f) Toyota, S.; Suzuki, S.; Goichi, M. *Chem. Eur. J.* **2006**, *12*, 2482-2487.
- [4] a) Taylor, M. S.; Swager, T. M. *Angew. Chem. Int. Ed.* **2007**, *46*, 8480-8483; b) Bunz, U. H. F. *Chem. Rev.* **2000**, *100*, 1605-1644; c) Becker, K.; Lagoudakis, P. G.; Gaefke, G.; Höger, S.; Lupton, J. M. *Angew. Chem. Int. Ed.* **2007**, *46*, 1; d) Marsden, J. A.; Haley, M. M. *J. Org. Chem.* **2005**, *70*, 10213-10226.
- [5] a) Grimsdale, A. C.; Wu, J.; Müllen, K. *Chem. Commun.* **2005**, 2197-2204; b) Tyutyulkov, N.; Müllen, K.; Baumgarten, M.; Ivanova, A.; Tadjer, A. *Synth. Met.* **2003**, *139*, 99-107; c) Simpson, C. D.; Brand, J. D.; Berresheim, A. J.; Przybilla, L.; Rader, H. J.; Müllen, K. *Chem. Eur. J.* **2002**, *8*, 1424-1429; d) Ito, S.; Wehmeier, M.; Brand, J. D.; Kubel, C.; Epsch, R.; Rabe, J. P.; Müllen, K. *Chem. Eur. J.* **2000**, *6*, 4327-4342.
- [6] a) Zhang, X.; Larock, R. C. *J. Am. Chem. Soc.* **2005**, *127*, 12230-12231; b) Yao, T.; Campo, M. A.; Larock, R. C. *J. Org. Chem.* **2005**, *70*, 3511-3517.
- [7] a) Würthner, F. *Chem. Commun.* **2004**, 1564-1579; b) Würthner, F. *Pure Appl. Chem.* **2006**, *78*, 2341-2349.
- [8] a) Holzwarth, A. R., Schaffner, K. *Photosynth. Res.* **1994**, *41*, 225-233; b) McDermott, G., Prince, S. M., Freer, A. A., Hawthornthwaite-Lawless, A. M., Papiz, M. Z., Cogdell, R. J., Isaacs, N. W. *Nature* **1995**, *374*, 517-521; c) Pullerits, T., Sundström, V. *Acc. Chem. Res.*

- 1996, 29, 381-389; d) Balaban, T. S., Tamiaki, H., Holzwarth, A. R. *Top. Curr. Chem.* **2005**, 258, 1-38.
- [9] a) Takahashi, R., Kobuke, Y. *J. Am. Chem. Soc.* **2003**, 125, 2372-2373; b) Yamaguchi, T., Kimura, T., Matsuda, H., Aida, T. *Angew. Chem. Int. Ed.* **2004**, 43, 6350-6355; c) Elemans, J. A. A. W., van Hameren, R., Nolte, R. J. M., Rowan, A. E. *Adv. Mater.* **2006**, 18, 1251-1266; d) Wang, H., Kaiser, T. E., Uemura, S., Würthner, F. *Chem. Commun.* **2008**, 1181-1183.
- [10] a) Kaiser, T. E., Wang, H., Stepanenko, V., Würthner, F. *Angew. Chem. Int. Ed.* **2007**, 46, 5541-5544; b) Yagai, S., Seki, T., Karatsu, T., Kitamura, A., Würthner, F. *Angew. Chem. Int. Ed.* **2008**, 47, 3367-3371; c) Li, X.-Q., Zhang, X., Ghosh, S., Würthner, F. *Chem. Eur. J.* **2008**, 14, 8074-8078; d) Würthner, F., Bauer, C., Stepanenko, V., Yagai, S. *Adv. Mater.* **2008**, 20, 1695-1698.
- [11] a) Kobayashi, T., Ed. *J-Aggregates*; World Scientific: Singapore 1996. b) Möbius, D. *Adv. Mater.* **1995**, 7, 437-444.
- [12] Borsenberger, P. M., Chowdry, A., Hoesterey, D. C., Mey, W. *J. Appl. Phys.* **1978**, 44, 5555-5564.
- [13] Chatterjee, S., Davis, P. D., Gottschalk, P., Kurz, M. E., Sauerwein, B., Yang, X., Schuster, G. B. *J. Am. Chem. Soc.* **1990**, 112, 6329-6338.
- [14] a) Wang, Y. *Chem. Phys. Lett.* **1986**, 126, 209-214; b) Wang, Y. *J. Opt. Soc. Am. B.* **1991**, 8, 981-985; c) Kobayashi, S. *Mol. Cryst. Liq. Cryst.* **1992**, 217, 77-81.
- [15] Tischler, J. R., Bradley, M. S., Bulović, V. *Opt. Lett.* **2006**, 31, 2045-2047.

- [16] a) Tischler, J. R., Bradley, M. S., Bulović, V., Song, J. H., Nurmikko, A. *Phys. Rev. Lett.* **2005**, *95*, 036401; b) Tischler, J. R., Bradley, M. S., Zhang, Q., Atay, T., Nurmikko, A., Bulović, V. *Org. Electron.* **2007**, *8*, 94-113.
- [17] Goldfinger, M. B.; Crawford, K. B.; Swager, T. M. *J. Am. Chem. Soc.* **1997**, *119*, 4578-4593.
- [18] Goldfinger, M. B.; Khushrav, K. B.; Swager, T. M. *J. Org. Chem.* **1998**, *63*, 1676-1686.
- [19] a) Corey, E. J.; Fuchs, P. L. *Tetrahedron Lett.* **1972**, 3769-3772; b) Ramirez, F.; Desai, N. B.; McKelvie, N. *J. Am. Chem. Soc.* **1962**, *84*, 1745-1747.
- [20] Williams, V. E.; Swager, T. M. *J. Polym. Sci., Part A: Polym. Chem.* **2000**, *38*, 4669-4676.
- [21] Li, C.-W.; Wang, C.-I.; Liao, H.-Y.; Chaudhuri, R.; Liu, R.-S. *J. Org. Chem.* **2007**, *72*, 9203-9207.
- [22] a) Fowler, P. W.; Lillington, M.; Olson, L. P. *Pure Appl. Chem.* **2007**, *79*, 969-980; b) Boydston, A. J.; Haley, M. M.; Williams, R. V.; Armantrout, J. R. *J. Org. Chem.* **2002**, *67*, 8812-8819; c) Soncini, A.; Domene, C.; Engelberts, J. J.; Fowler, P. W.; Rassat, A.; van Lenthe, J. H.; Havenith, R. W. A.; Jennekens, L. W. *Chem. Eur. J.* **2005**, *11*, 1257-1266; d) Lepetit, C.; Godard, C.; Chauvin, R. *New J. Chem.* **2001**, *25*, 572-580.
- [23] a) Jelley, E. E. *Nature* **1936**, *138*, 1009. b) Scheibe, G. *Angew. Chem.* **1936**, *49*, 563.
- [24] Scheibe, G. *Optische Anregung organischer Systeme*, 2. Internationales Farbensymposium, Ed. Foerst, W., Verlag Chemie, Weinheim: 1966, p. 109.
- [25] Mascaro, D. J., Thompson, M. E., Smith, H. I., Bulović, V. *Org. Electron.* **2005**, *6*, 211-220.
- [26] Garbuzov, D. Z.; Bulović, V.; Burrows, P.E.; Forrest, S. R. *Chem. Phys. Lett.* **1996**, *249*, 433-437.

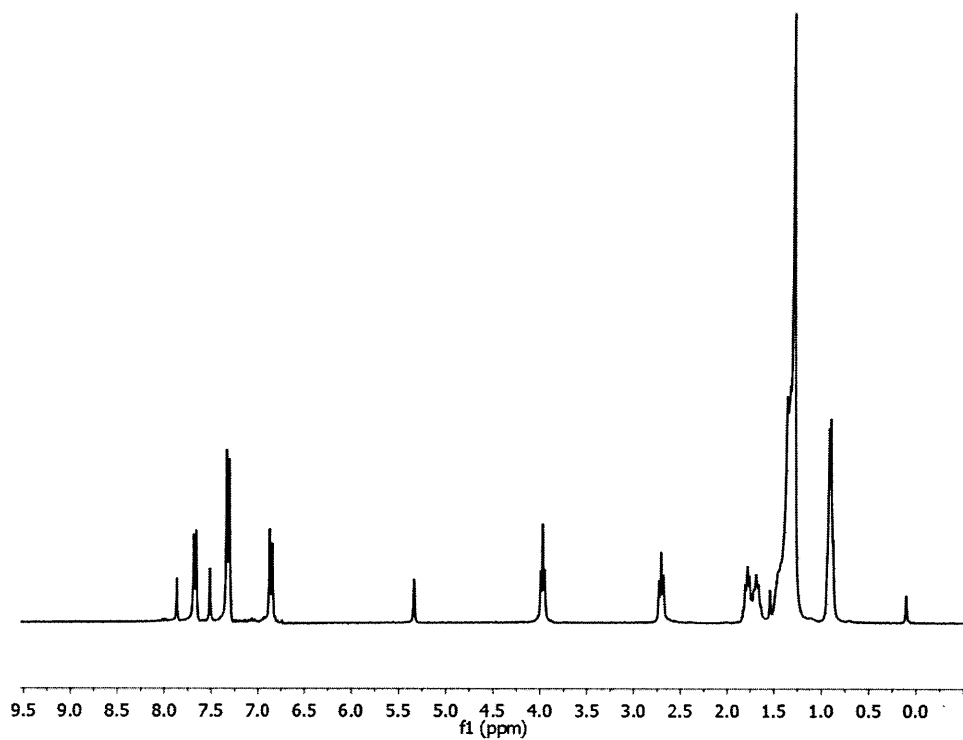
- [27] a) Kuhn, H. *J. Chem. Phys.* **1970**, *53*, 101-108; b) Kirstein, S.; Mohwald, H. *Adv. Mater.* **1995**, *7*, 460-463; c) Peyratout, C.; Daehne, L. *Phys. Chem. Chem. Phys.* **2002**, *4*, 3032-3039.
- [28] Spano, F. C.; Mukamel, S. *J. Chem. Phys.* **1989**, *91*, 683-700.
- [29] Potma, E.O.; Wiersma, D.A. *J. Chem. Phys.* **1998**, *108*, 4894-4903.
- [30] Vanburgel, M.; Wiersma, D.A.; Duppen, K. *J. Chem. Phys.* **1995**, *102*, 20-33.
- [31] a) Spano, F. C.; Kuklinski, J. R.; Mukamel, S. *Phys. Rev. Lett.* **1990**, *65*, 211-214; b) De Boer, S.; Wiersma, D. A. *Chem. Phys. Lett.* **1990**, *165*, 45-53. c) Spano, F. C.; Kuklinski, J. R.; Mukamel, S. *J. Chem. Phys.* **1991**, *94*, 7534-7544. d) Meinardi, F.; Cerminara, M., Sassella, A.; Bonifacio, R.; Tubino, R. *Phys. Rev. Lett.* **2003**, *91*, 247401.
- [32] Dicke, R. H. *Phys. Rev.* **1954**, *93*, 99-110.
- [33] Rousseau, E.; Van der Auweraer, M.; De Schryver, F. C. *Langmuir* **2000**, *16*, 8865-8870.
- [34] Knapp, E. W.; Scherer, P. O. J.; Fischer, S. F. *Chem. Phys. Lett.* **1984**, *111*, 481-486.
- [35] *Spartan '04 V1.0.0*; Wavefunction, Inc.: Irvine, CA; 2004.
- [36] a) Kena-Cohen, S.; Davanco, M.; Forrest, S. R. *Phys. Rev. Lett.* **2008**, *101*, 116401; b) Holmes, R. J.; Forrest, S. R. *Phys. Rev. Lett.* **2004**, *93*, 186404; c) Lidzey, D. G.; Bradley, D. D. C.; Skolnick, M. S.; Virgili, T.; Walker, S.; Whittaker, D. M. *Nature*, **1998**, *395*, 53-55.

Chapter 3 Appendix

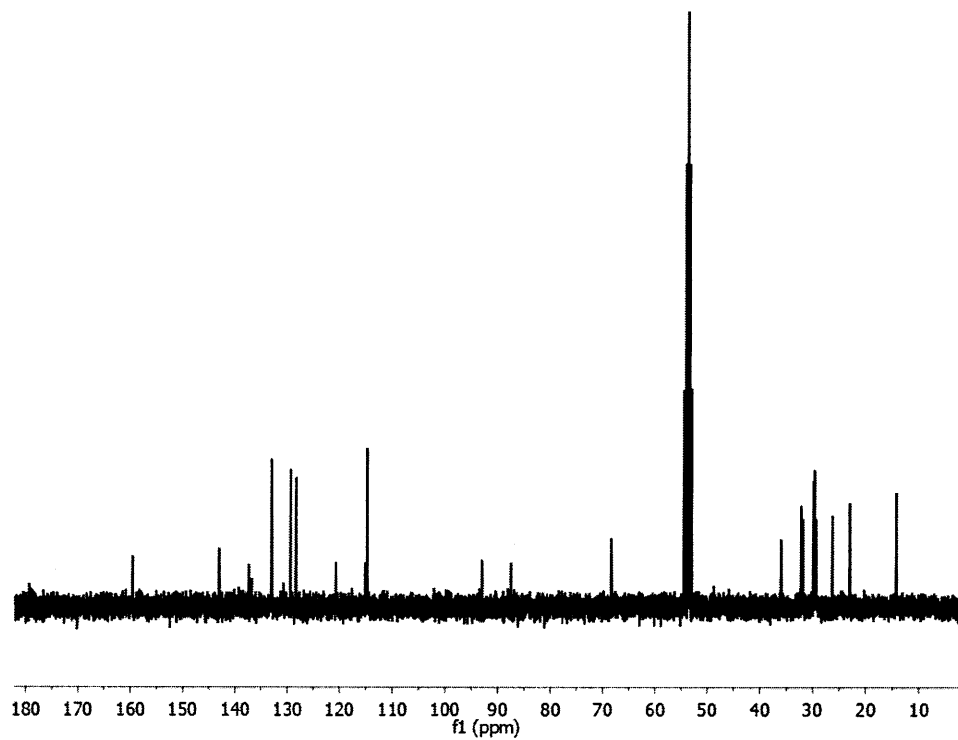
^1H -NMR and ^{13}C -NMR Spectra

Adapted and reproduced with permission from:

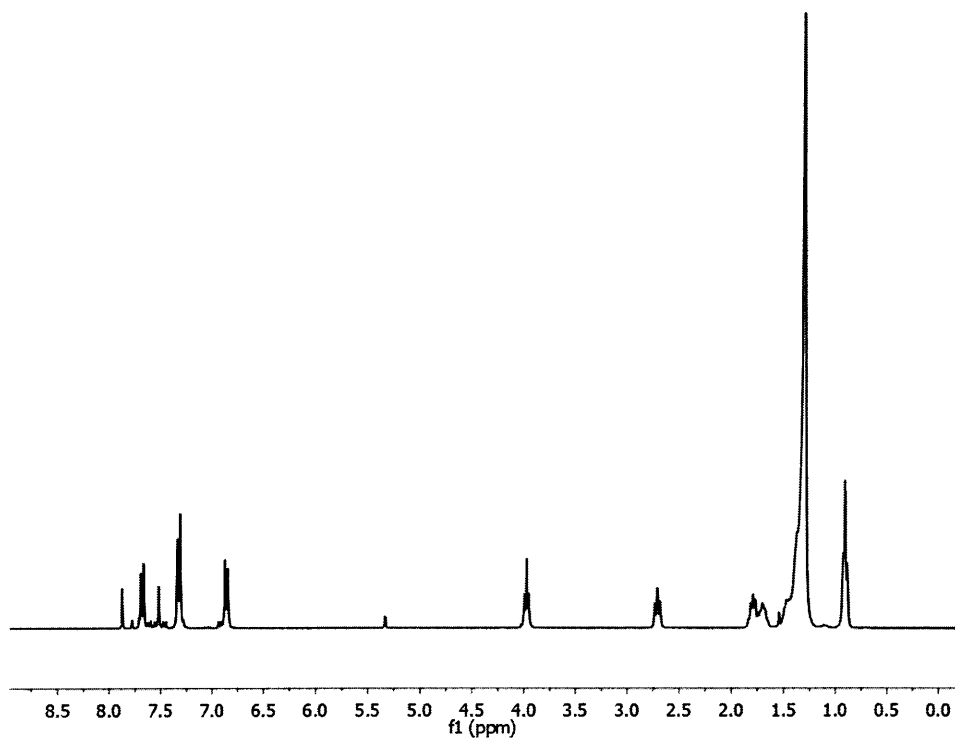
Chan, J. M. W., Tischler, J. R., Kooi, S. E., Bulović, V., Swager, T. M. *J. Am. Chem. Soc.* **2009**,
131, 5659-5666.



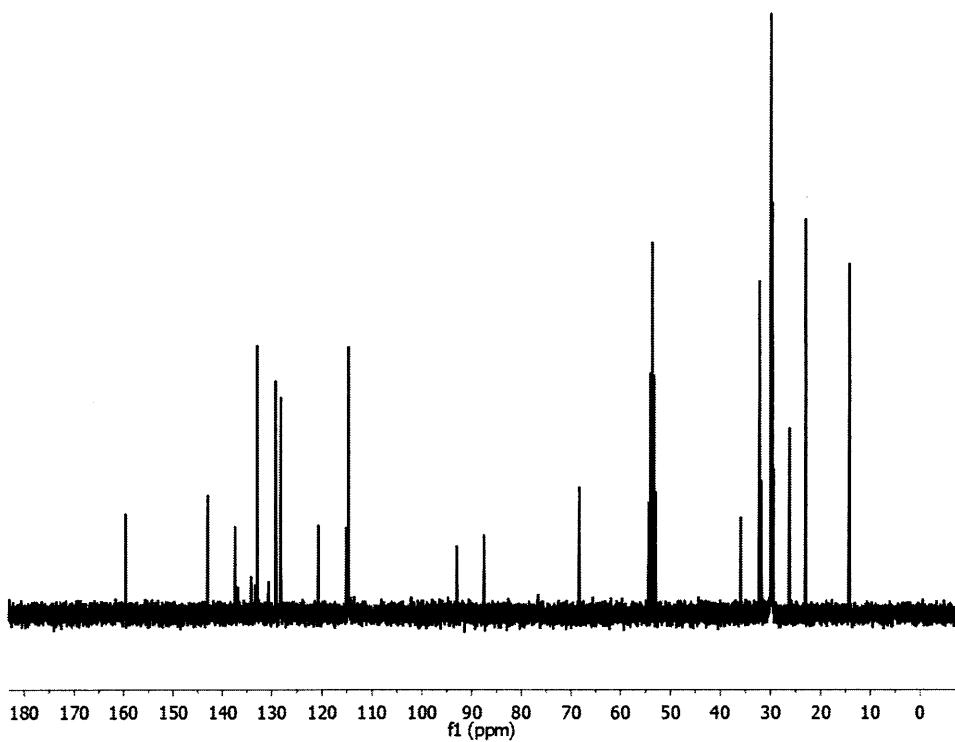
Spectrum 7. ¹H-NMR spectrum of **2a** (300 MHz, CD₂Cl₂).



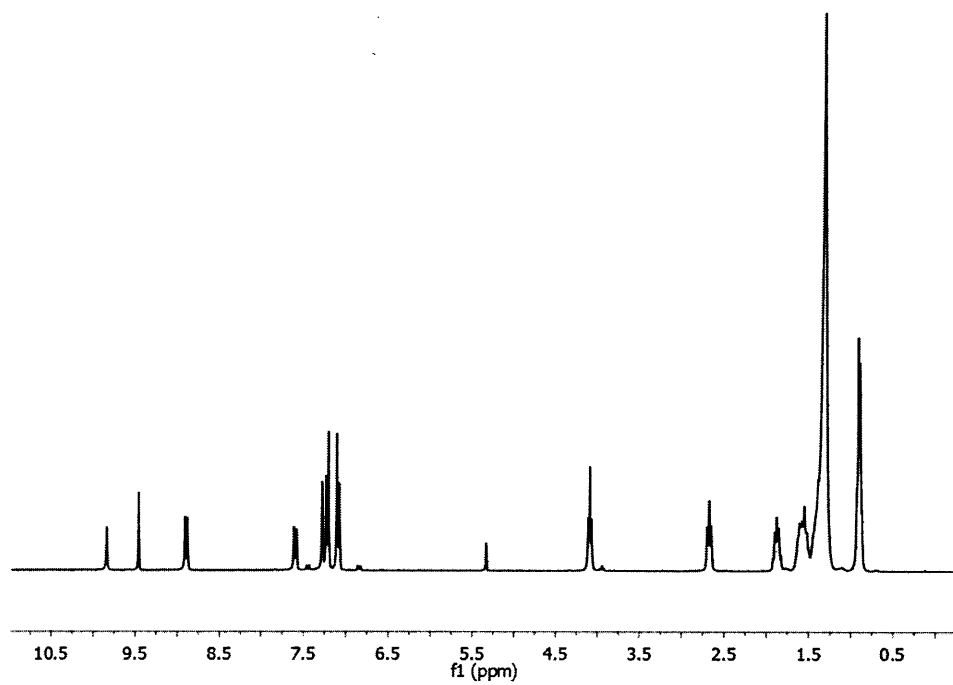
Spectrum 8. ¹³C-NMR spectrum of **2a** (300 MHz, CD₂Cl₂).



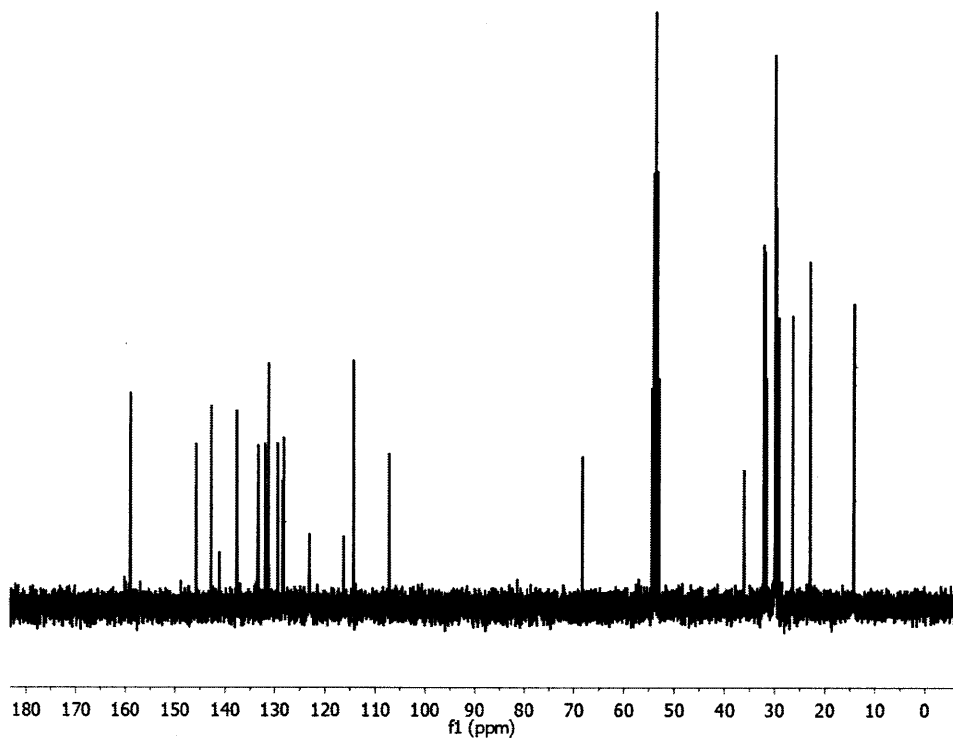
Spectrum 9. ^1H -NMR spectrum of **2b** (300 MHz, CD_2Cl_2).



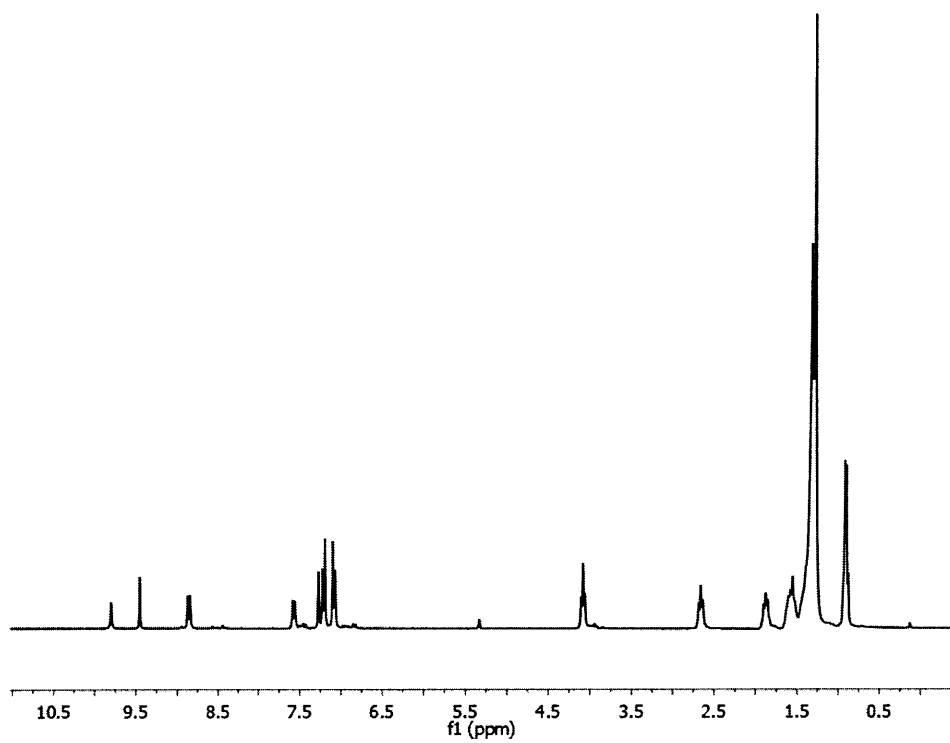
Spectrum 10. ^{13}C -NMR spectrum of **2b** (300 MHz, CD_2Cl_2).



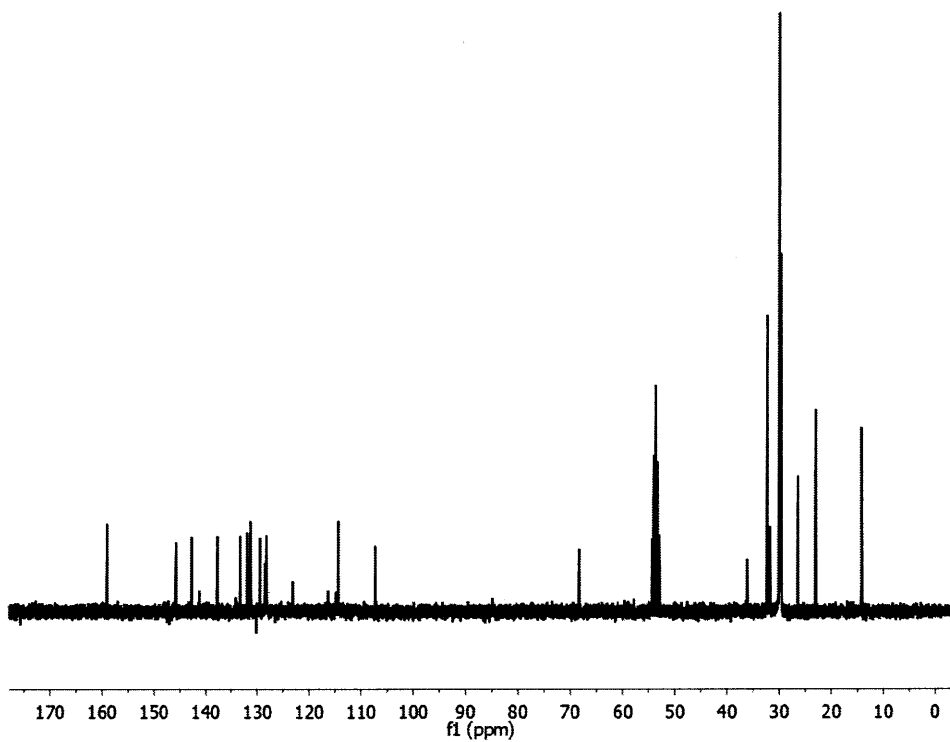
Spectrum 11. ¹H-NMR spectrum of **3a** (300 MHz, CD₂Cl₂).



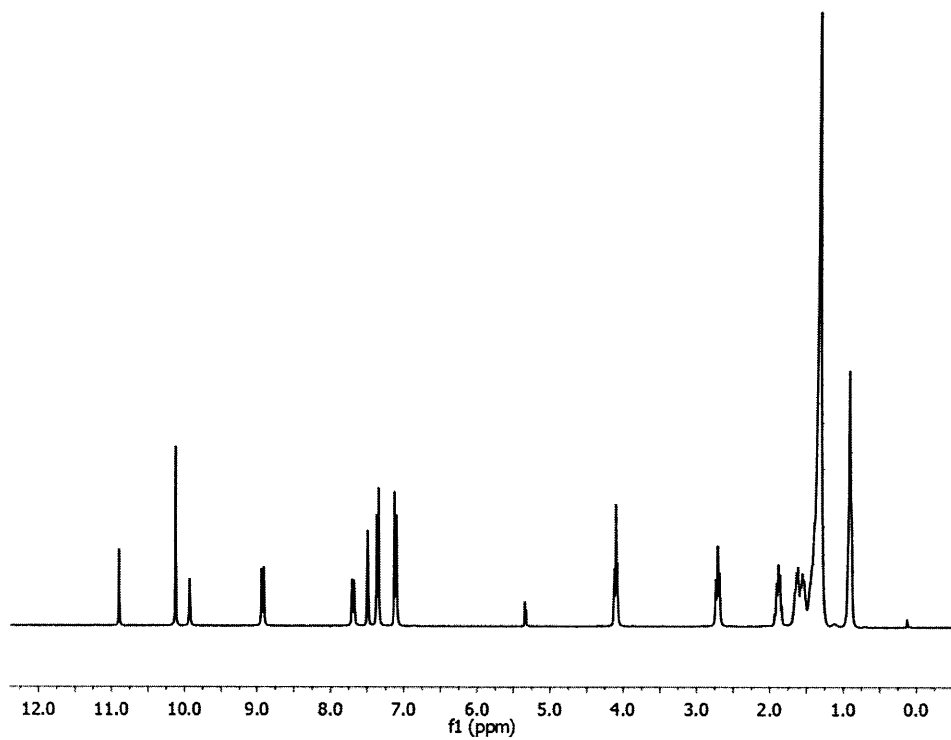
Spectrum 12. ¹³C-NMR spectrum of **3a** (300 MHz, CD₂Cl₂).



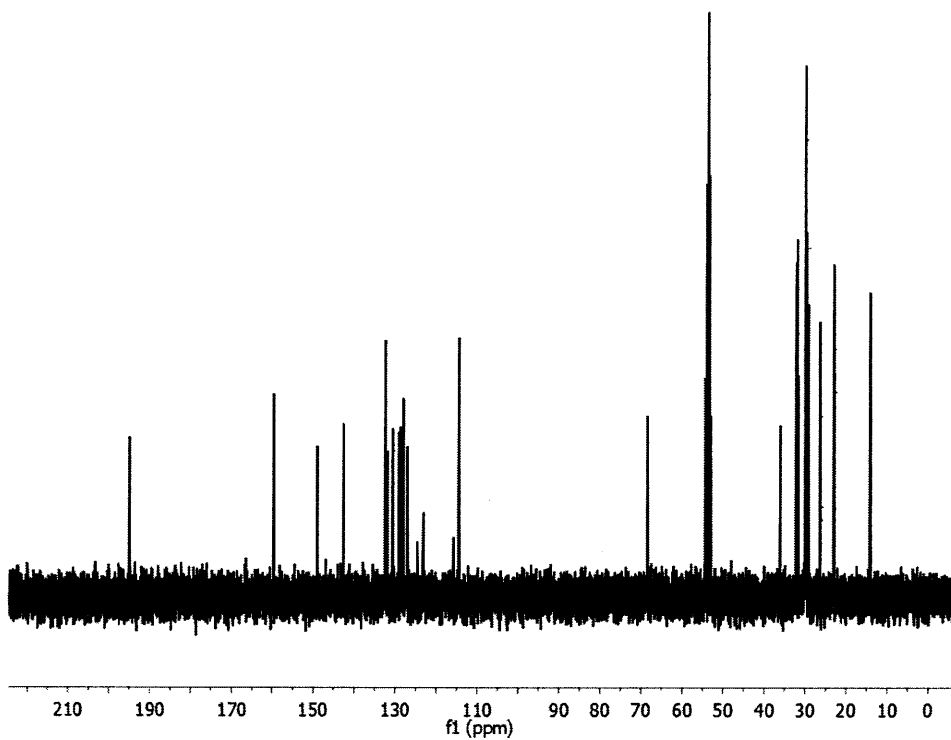
Spectrum 13. ^1H -NMR spectrum of **3b** (300 MHz, CD_2Cl_2).



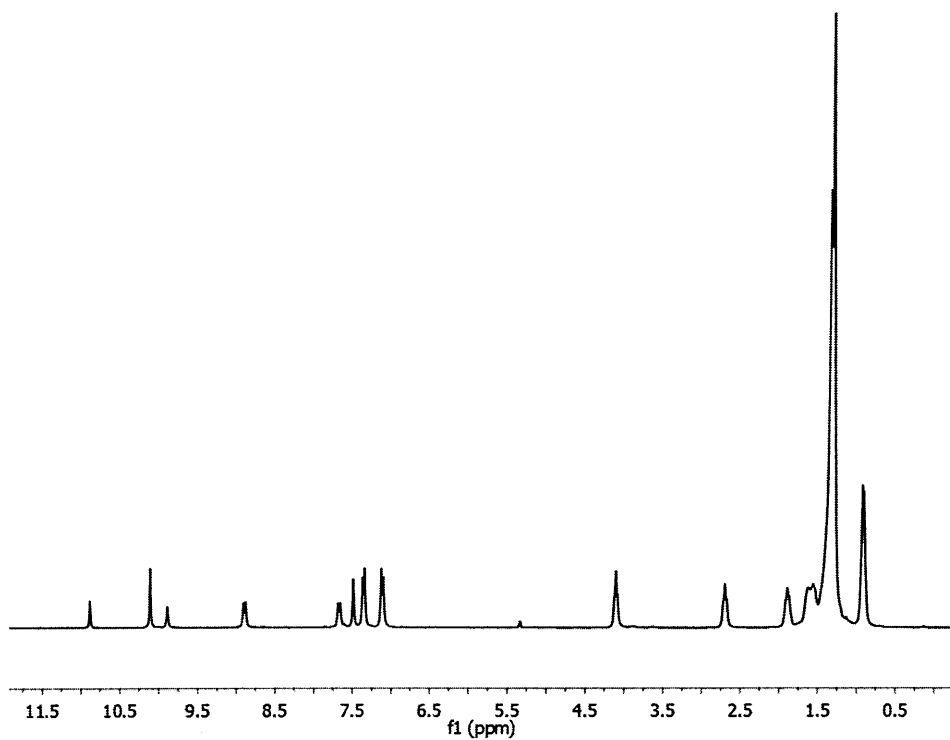
Spectrum 14. ^{13}C -NMR spectrum of **3b** (300 MHz, CD_2Cl_2).



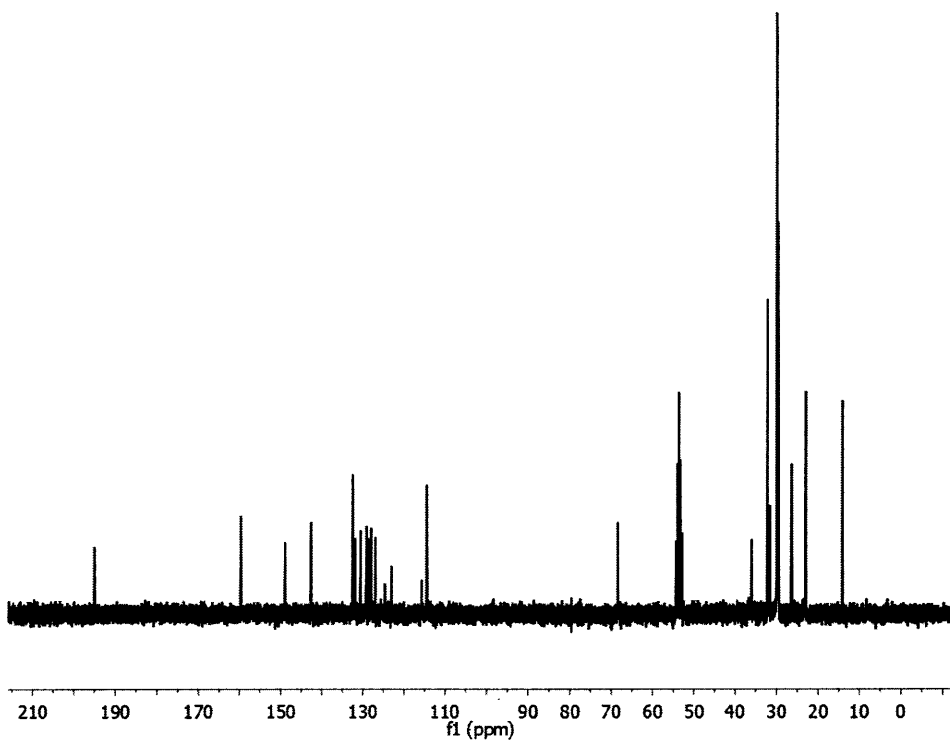
Spectrum 15. ^1H -NMR spectrum of **4a** (300 MHz, CD_2Cl_2).



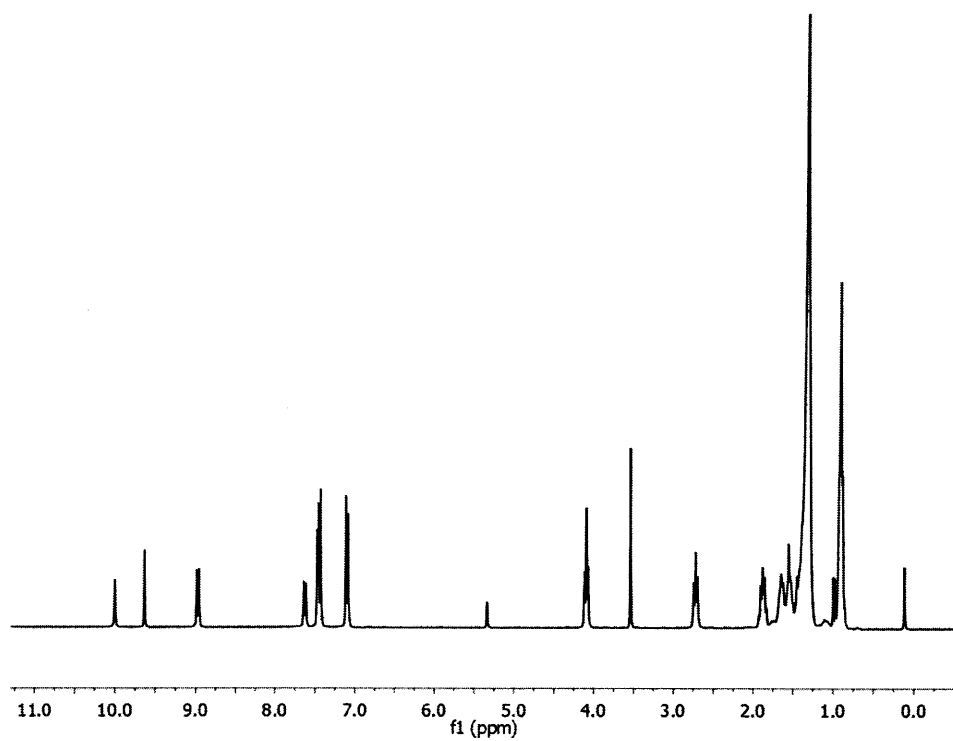
Spectrum 16. ^{13}C -NMR spectrum of **4a** (300 MHz, CD_2Cl_2).



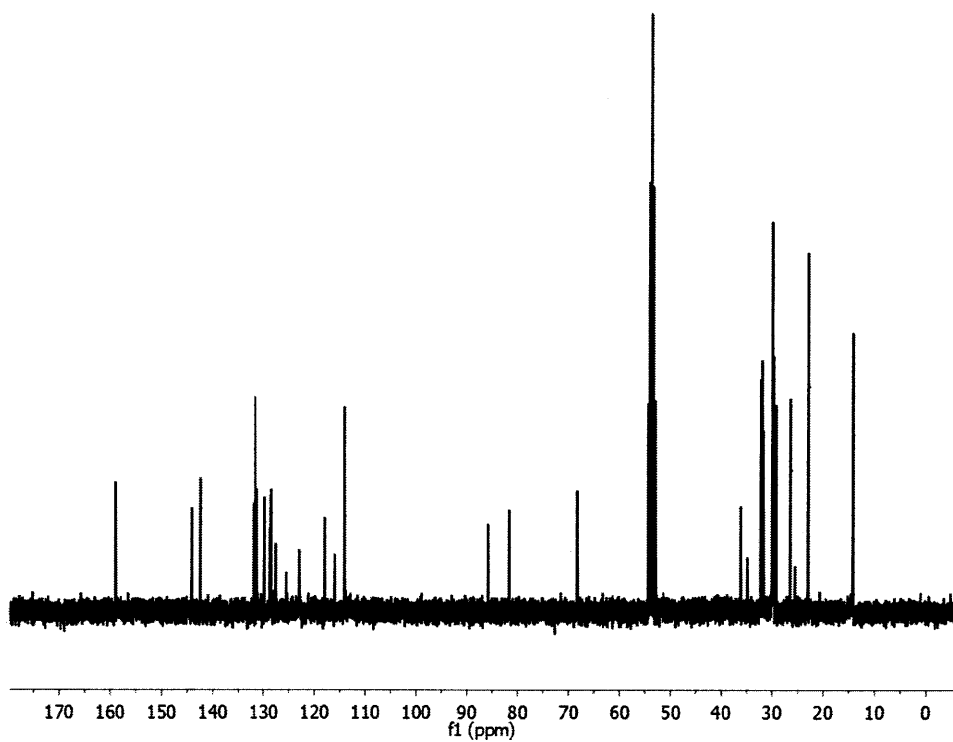
Spectrum 17. ^1H -NMR spectrum of **4b** (300 MHz, CD_2Cl_2).



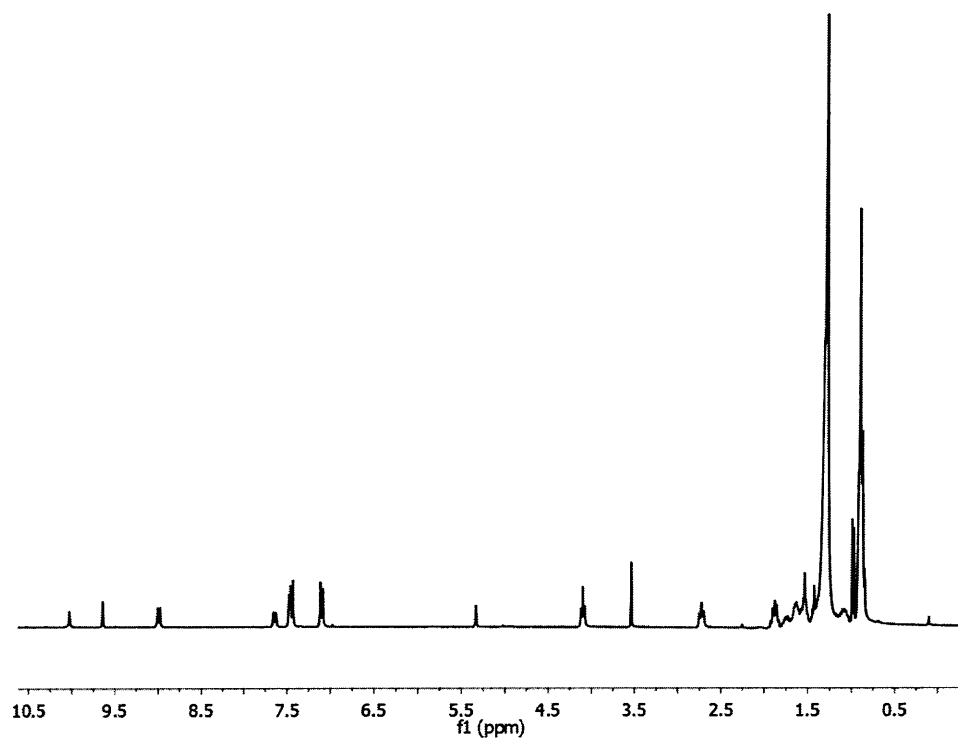
Spectrum 18. ^{13}C -NMR spectrum of **4b** (300 MHz, CD_2Cl_2).



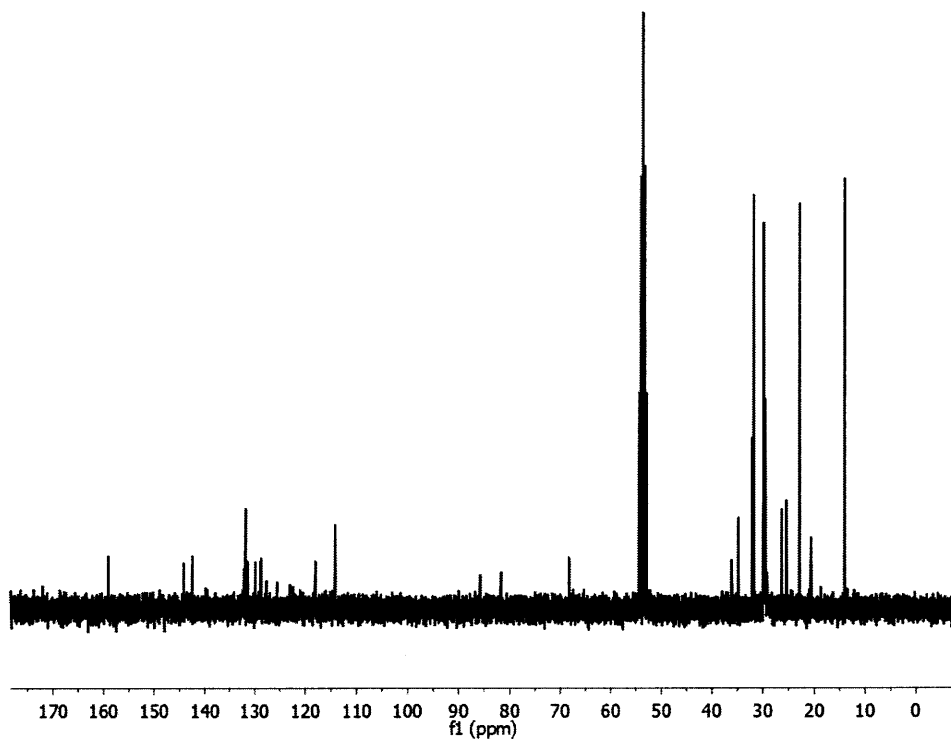
Spectrum 19. ¹H-NMR spectrum of **5a** (300 MHz, CD₂Cl₂).



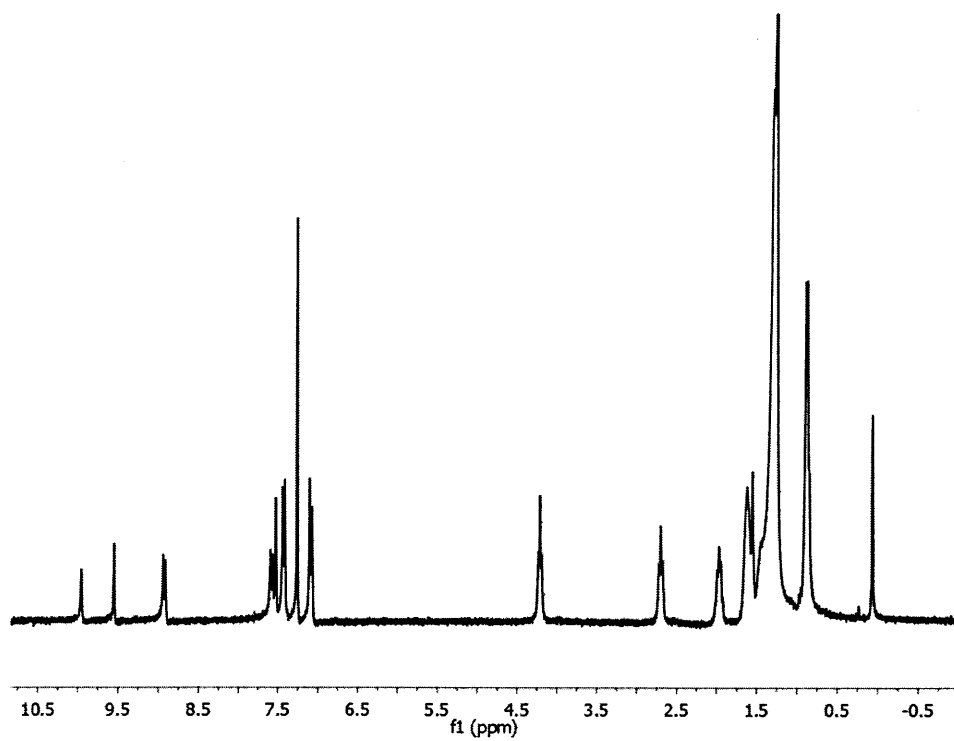
Spectrum 20. ¹³C-NMR spectrum of **5a** (300 MHz, CD₂Cl₂).



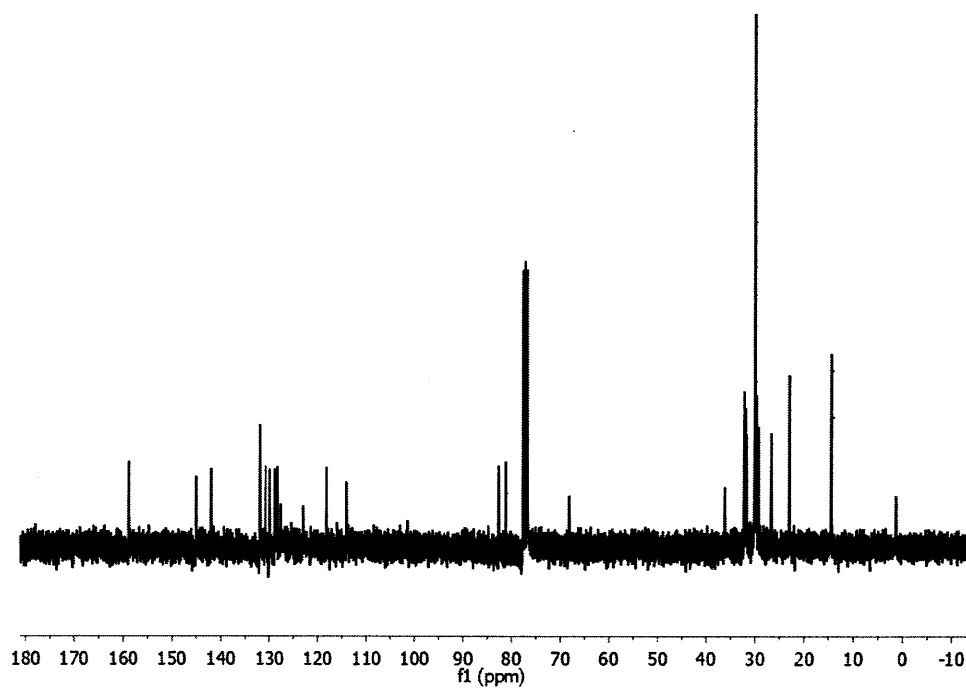
Spectrum 21. ¹H-NMR spectrum of **5b** (300 MHz, CD₂Cl₂).



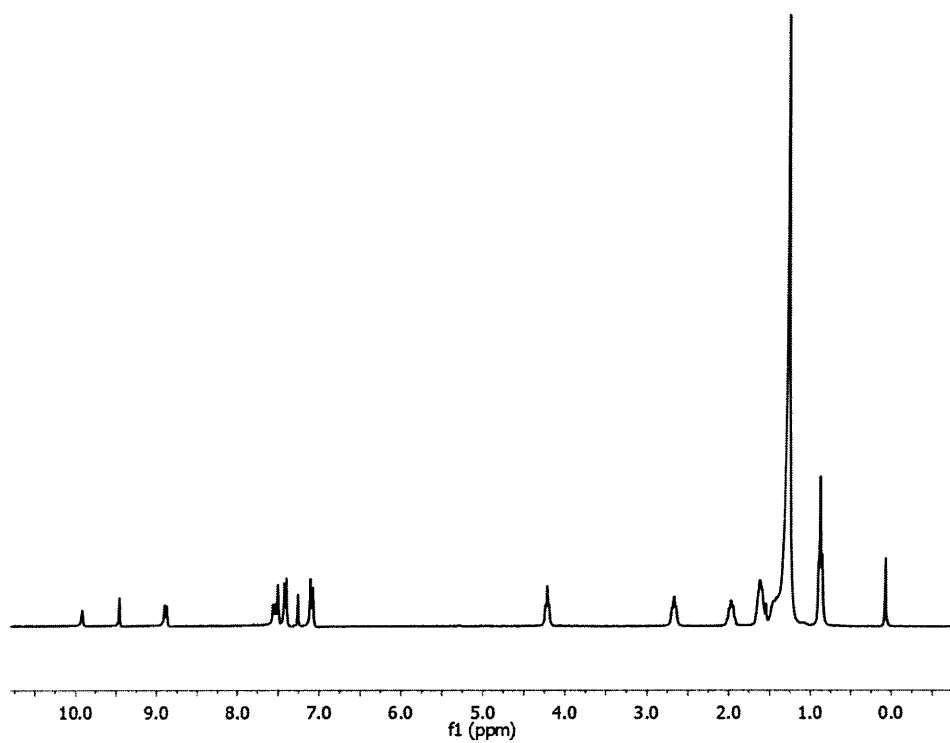
Spectrum 22. ¹³C-NMR spectrum of **5b** (300 MHz, CD₂Cl₂).



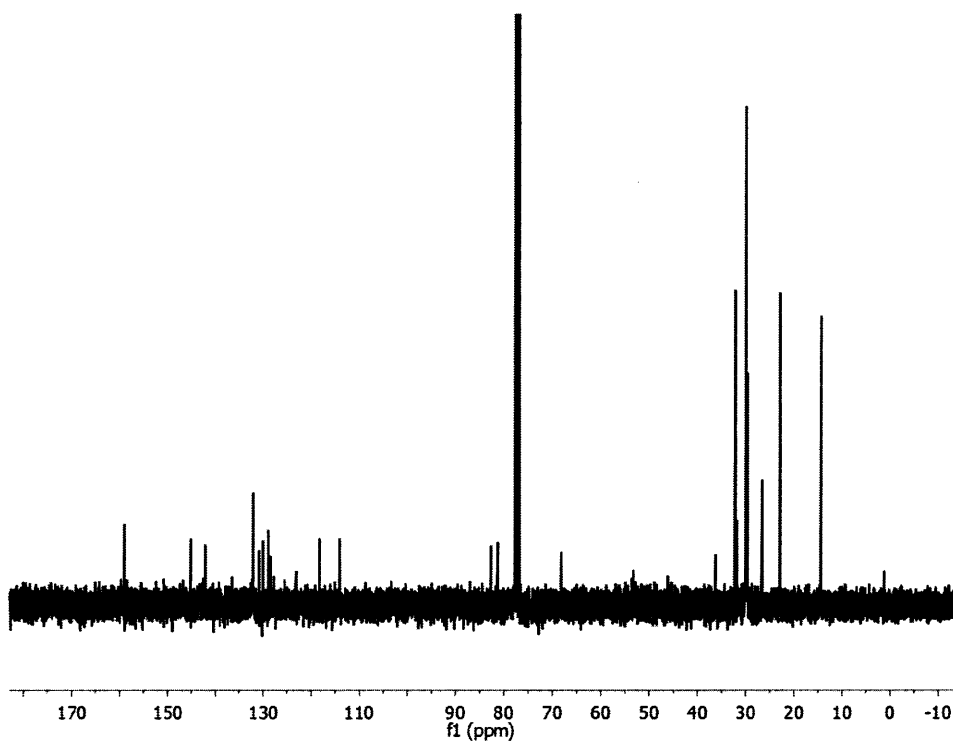
Spectrum 23. ^1H -NMR spectrum of **6a** (300 MHz, CDCl_3).



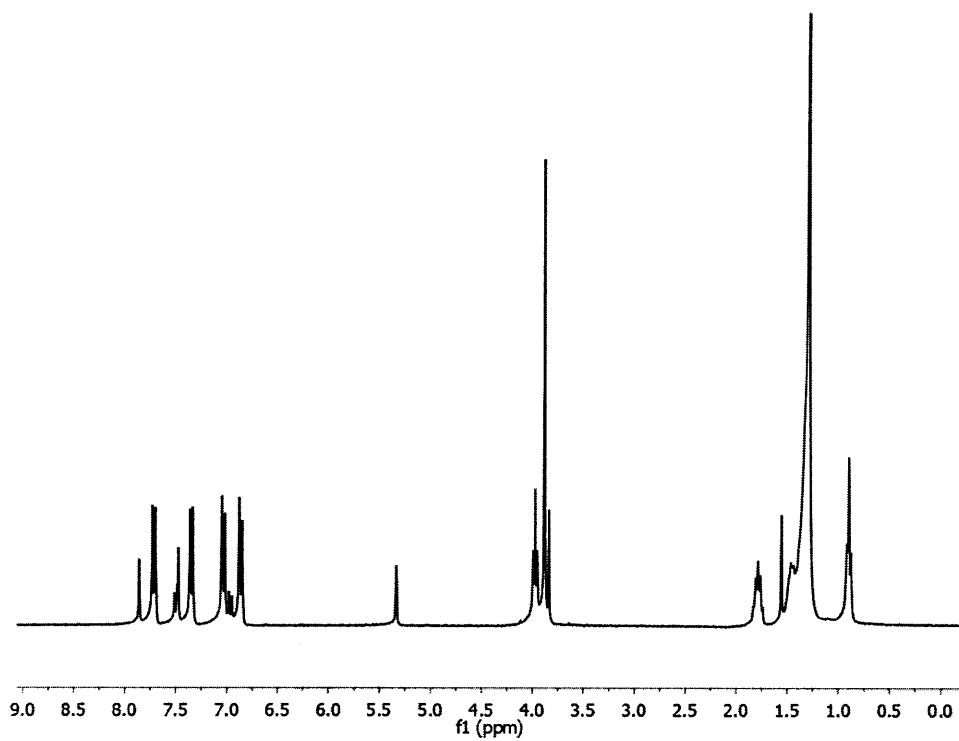
Spectrum 24. ^{13}C -NMR spectrum of **6a** (300 MHz, CDCl_3).



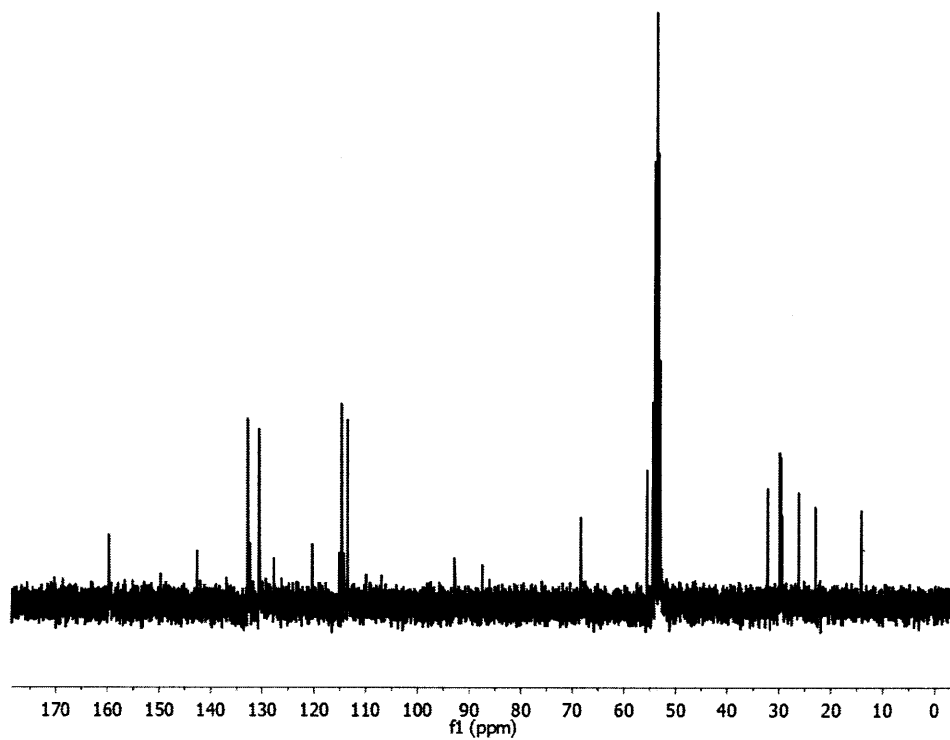
Spectrum 25. ^1H -NMR spectrum of **6b** (300 MHz, CDCl_3).



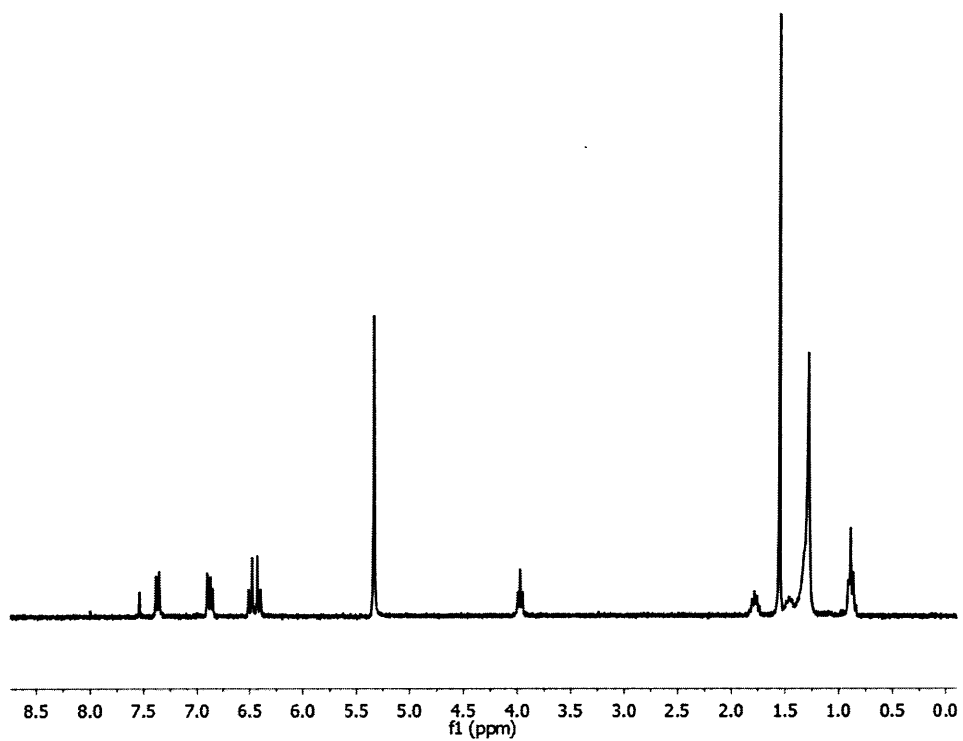
Spectrum 26. ^{13}C -NMR spectrum of **6b** (300 MHz, CDCl_3).



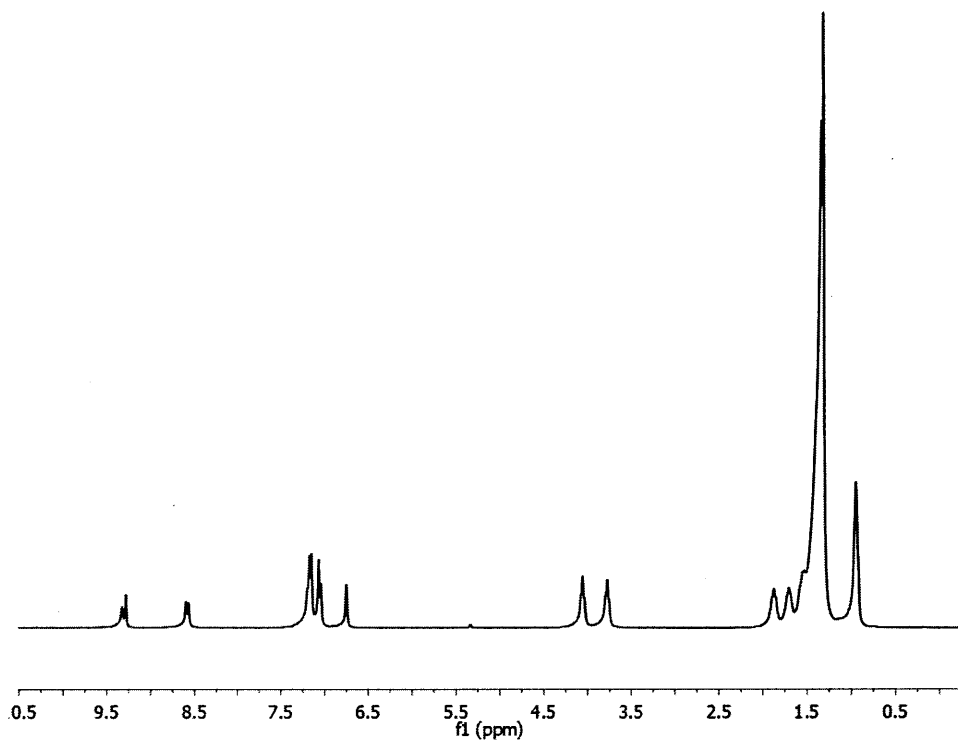
Spectrum 27. ^1H -NMR spectrum of **7** (300 MHz, CD_2Cl_2).



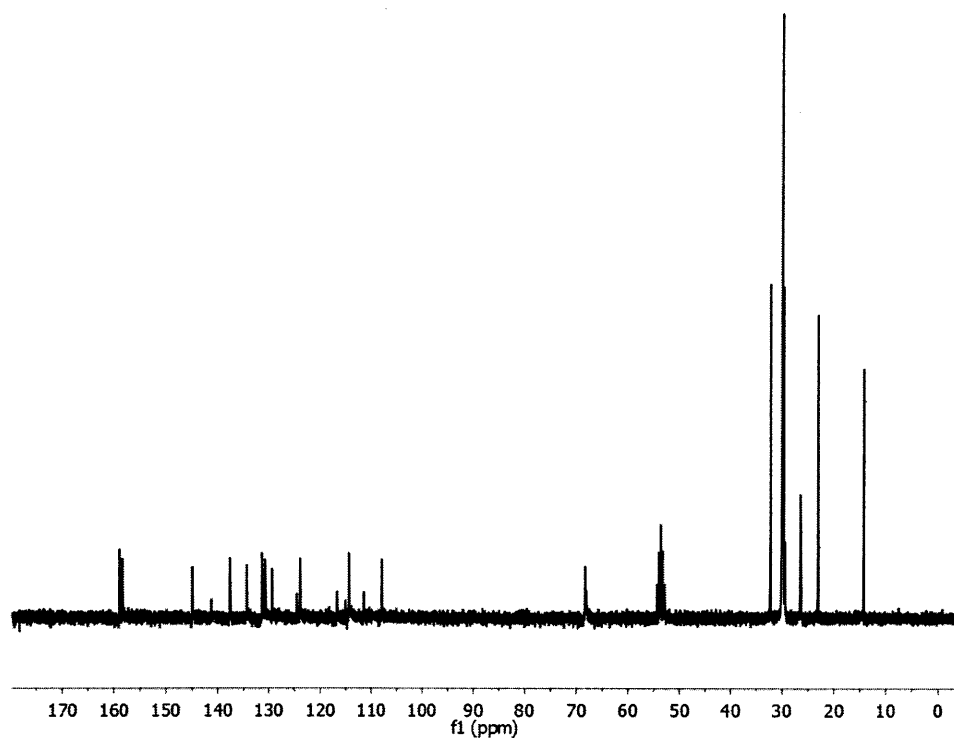
Spectrum 28. ^{13}C -NMR spectrum of **7** (300 MHz, CD_2Cl_2).



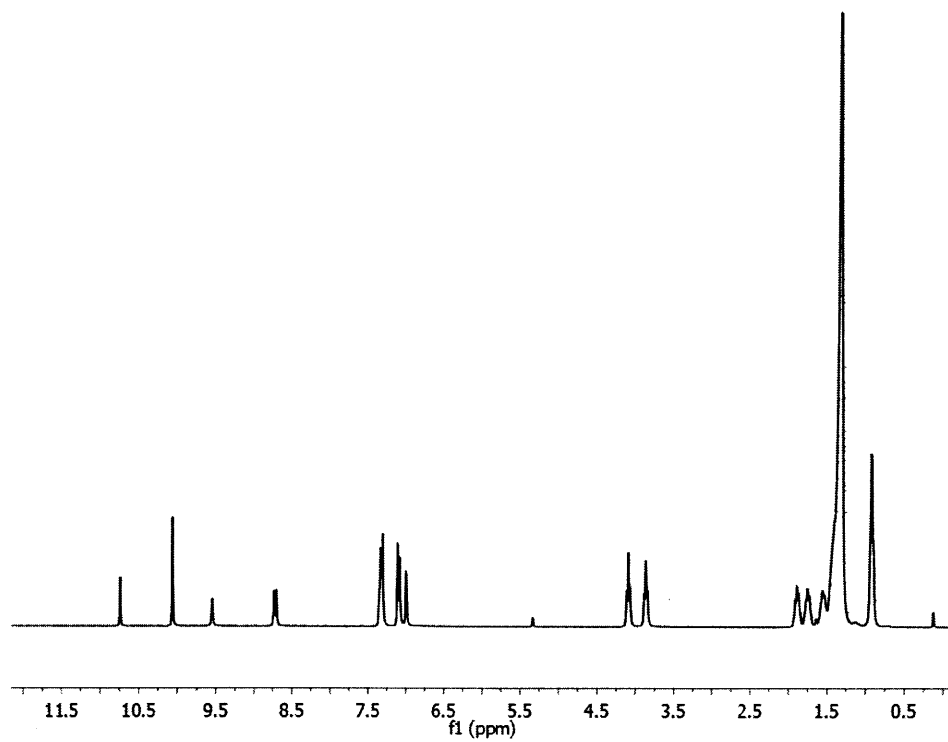
Spectrum 29. ^1H -NMR spectrum of **8** (300 MHz, CD_2Cl_2).



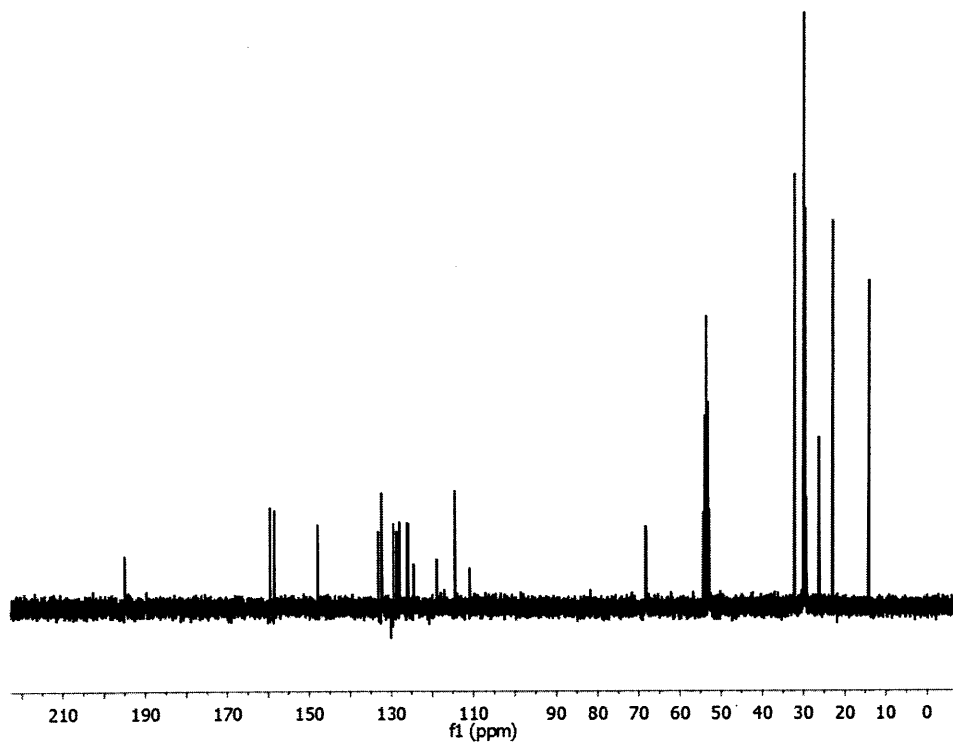
Spectrum 30. ^1H -NMR spectrum of **9** (300 MHz, CD_2Cl_2).



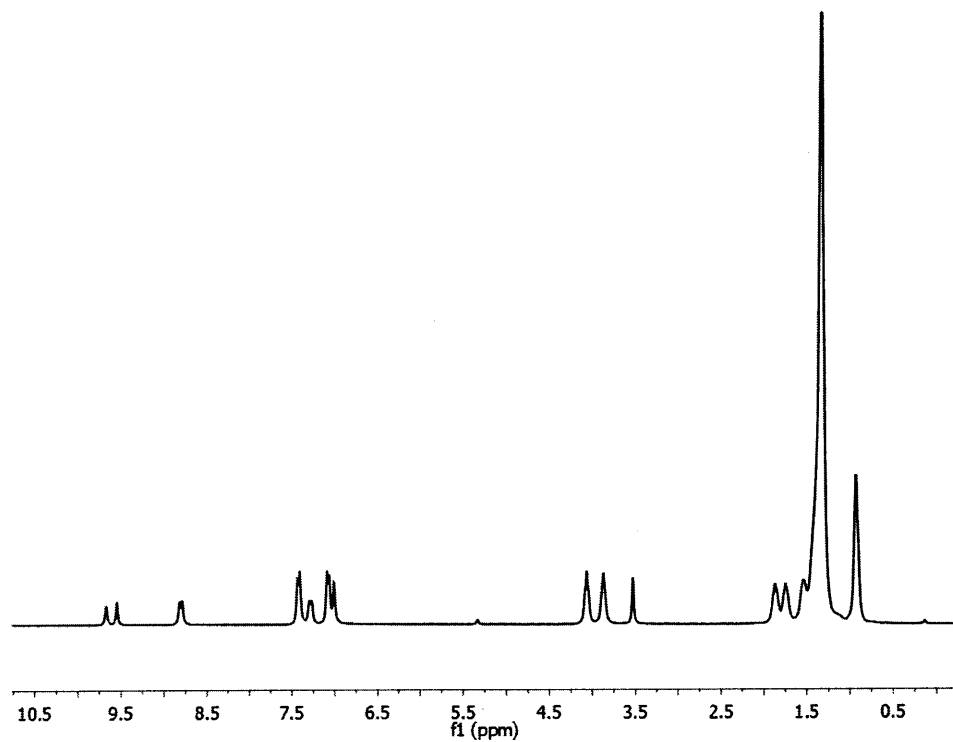
Spectrum 31. ^{13}C -NMR spectrum of **9** (300 MHz, CD_2Cl_2).



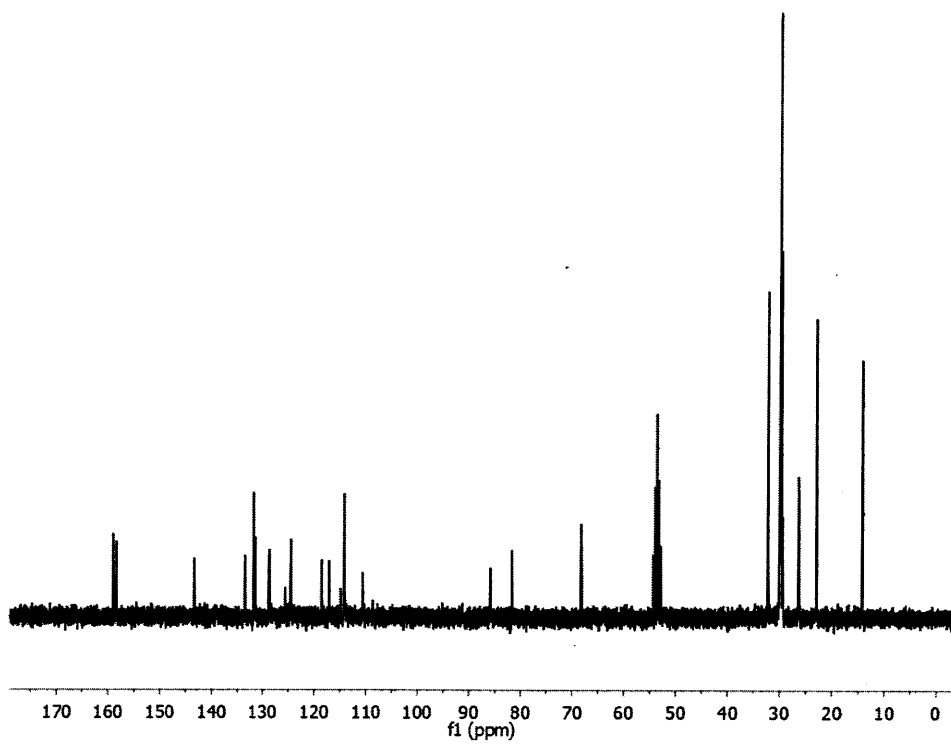
Spectrum 32. ^1H -NMR spectrum of **10** (300 MHz, CD_2Cl_2).



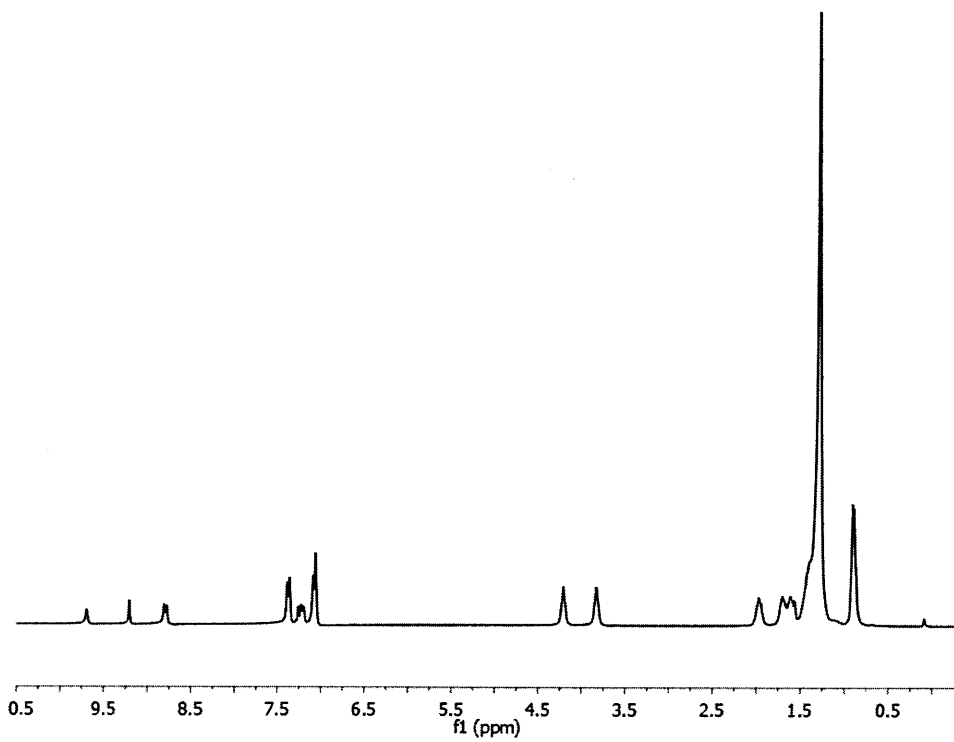
Spectrum 33. ^{13}C -NMR spectrum of **10** (300 MHz, CD_2Cl_2).



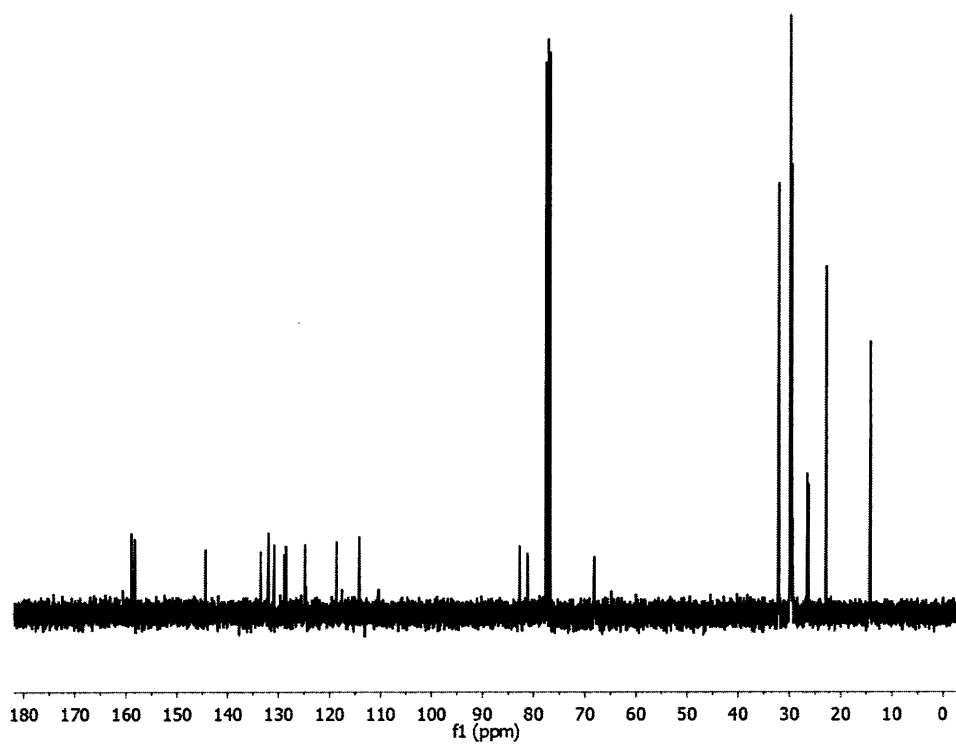
Spectrum 34. ^1H -NMR spectrum of **11** (300 MHz, CD_2Cl_2).



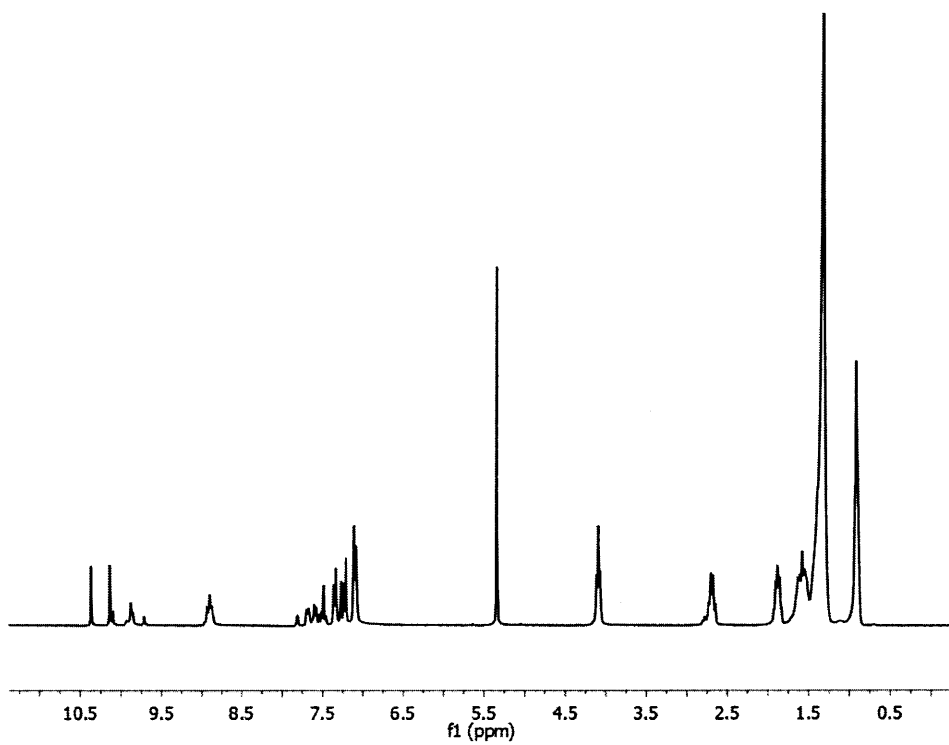
Spectrum 35. ^{13}C -NMR spectrum of **11** (300 MHz, CD_2Cl_2).



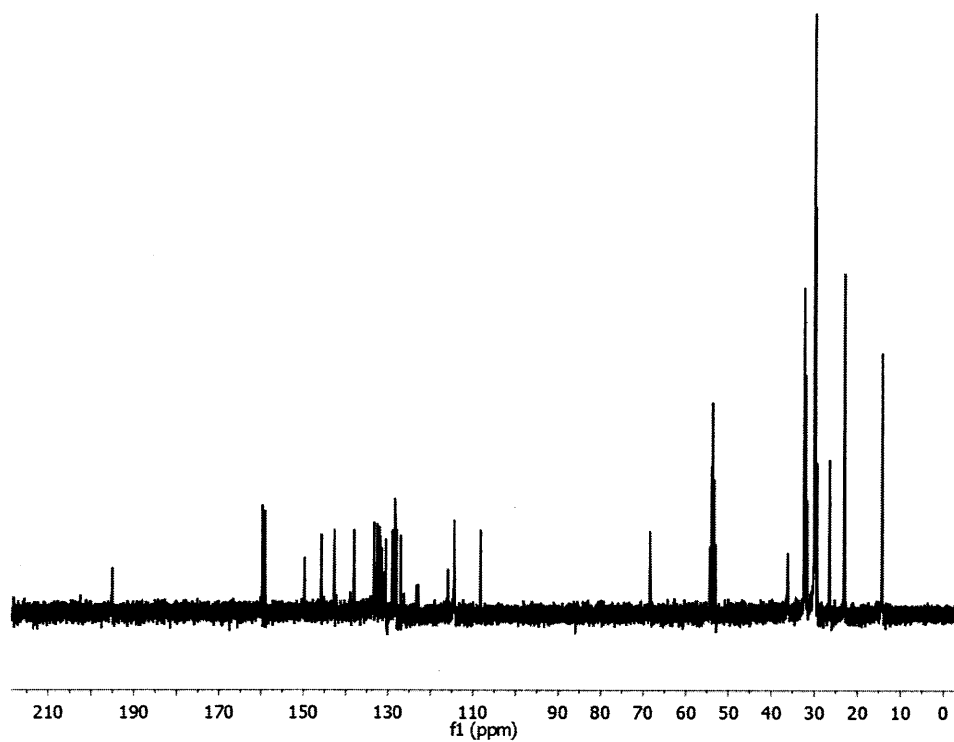
Spectrum 36. ^1H -NMR spectrum of **12** (300 MHz, CDCl_3).



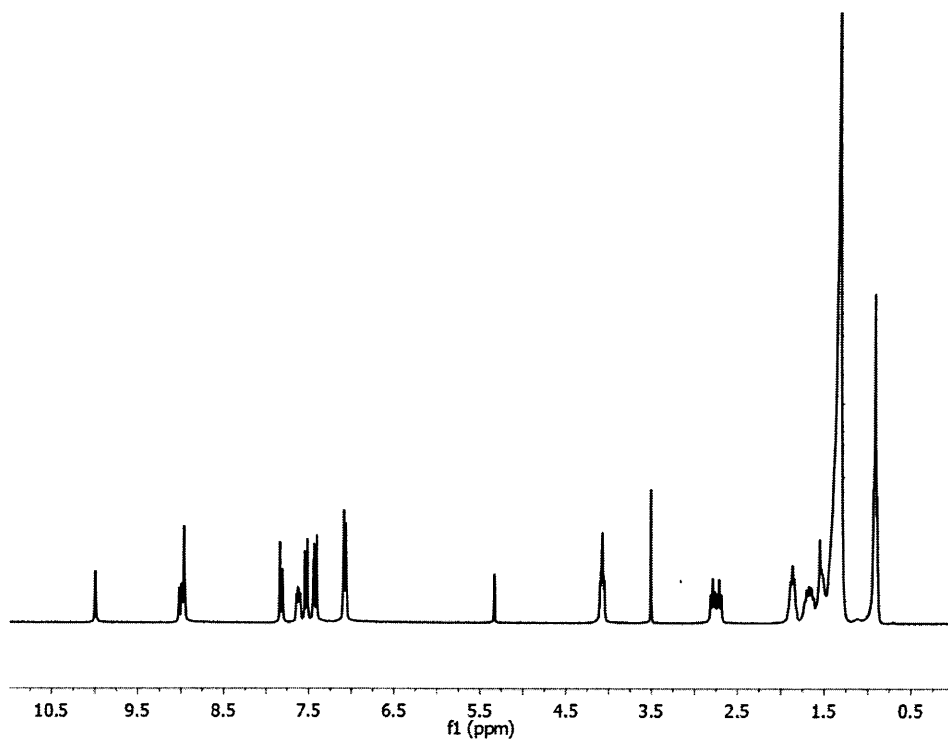
Spectrum 37. ^{13}C -NMR spectrum of **12** (300 MHz, CDCl_3).



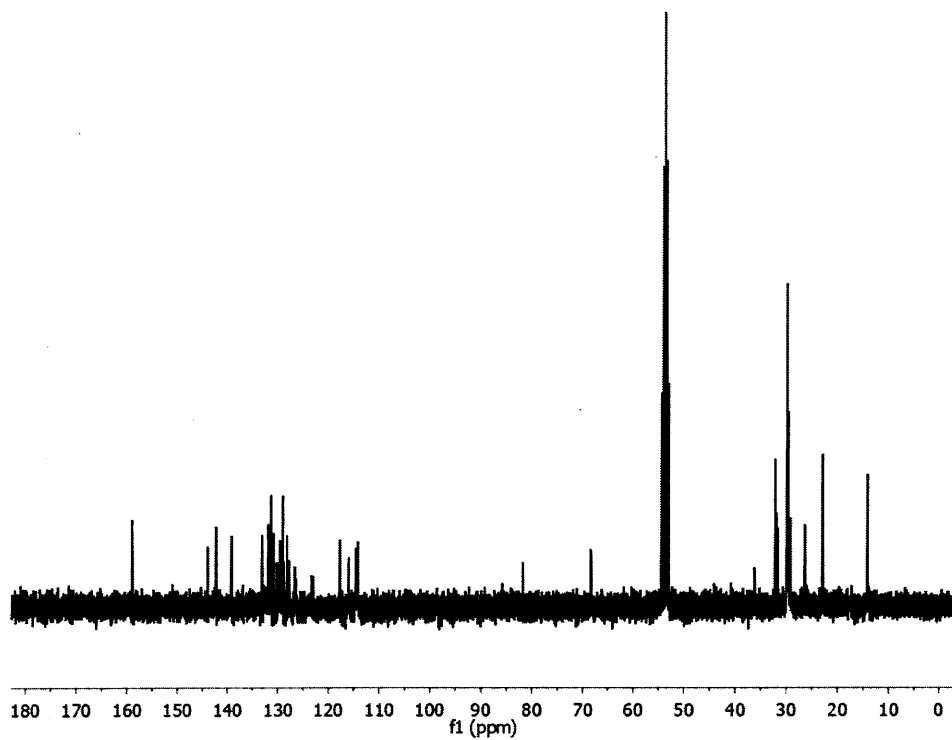
Spectrum 38. ^1H -NMR spectrum of **13** (300 MHz, CD_2Cl_2).



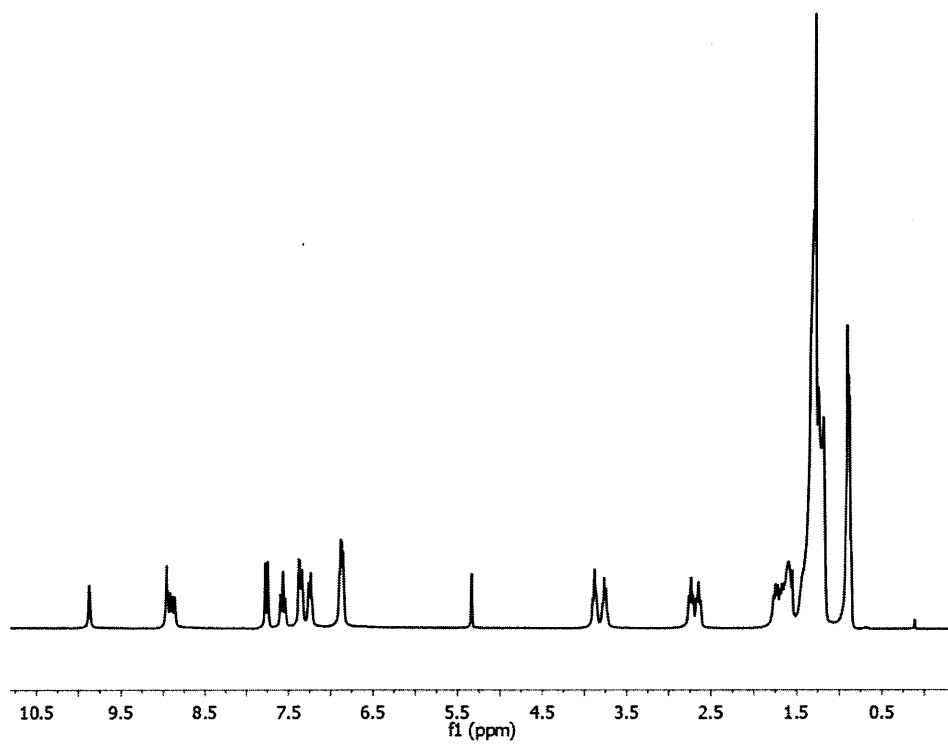
Spectrum 39. ^{13}C -NMR spectrum of **13** (300 MHz, CD_2Cl_2).



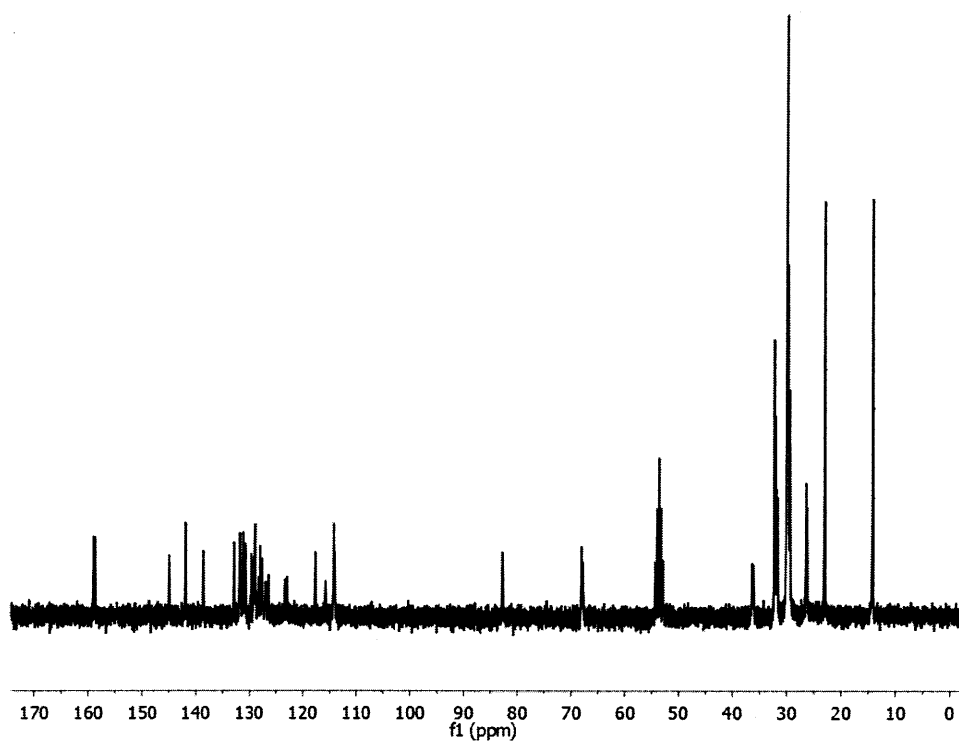
Spectrum 40. ^1H -NMR spectrum of **14** (300 MHz, CD_2Cl_2).



Spectrum 41. ^{13}C -NMR spectrum of **14** (300 MHz, CD_2Cl_2).



Spectrum 42. ^1H -NMR spectrum of **15** (300 MHz, CD_2Cl_2).



Spectrum 43. ^{13}C -NMR spectrum of **15** (300 MHz, CD_2Cl_2).

Chapter 4
Synthesis of Stair-stepped Polymers
Containing Dibenz[*a,h*]anthracene
Subunits

Adapted and reproduced with permission from:

Chan, J. M. W., Kooi, S. E., Swager, T. M. *Macromolecules* **2010**, *43*, 2789-2793.

4.1 Introduction

Poly(aryleneethynylene)s (PAEs)¹ represent a class of conjugated polymers that has received much attention over the past two decades due to their interesting electronic and photophysical properties. In general, PAEs are highly fluorescent and relatively photo-stable. These properties, along with their ease of synthesis, make PAEs a popular class of conjugated polymers that has found numerous technological applications, e.g. in the field of chemical sensors.² The general structure of a PAE, i.e. alternating aromatic blocks and carbon-carbon triple bonds, allows for great flexibility in the design and tunability of the polymer's physical properties. Harnessing the power and versatility of organic synthesis, it is possible to prepare diverse monomers containing virtually any degree of structural complexity, which could then be used to synthesize a range of polymers with varying properties. As a result of our recent work on dibenz[*a,j*]anthracene based J-aggregating macrocycles,³ we became interested in incorporating the isomeric dibenz[*a,h*]anthracene motif (Figure 4.1, center) into conjugated polymers.

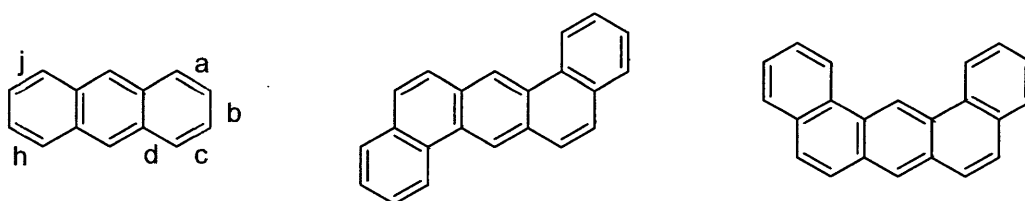


Figure 4.1. Anthracene (left), dibenz[*a,h*]anthracene (center), dibenz[*a,j*]anthracene (right).

Over the years, the aryl component of PAEs has seen a wide variety of different aromatic groups, with the simple benzene ring being the most common, i.e. poly(phenyleneethynylene)s (PPEs). Polycyclic aromatic moieties such as anthracene have also been used frequently,⁴ and previous work in our group has also employed more complex building blocks such as

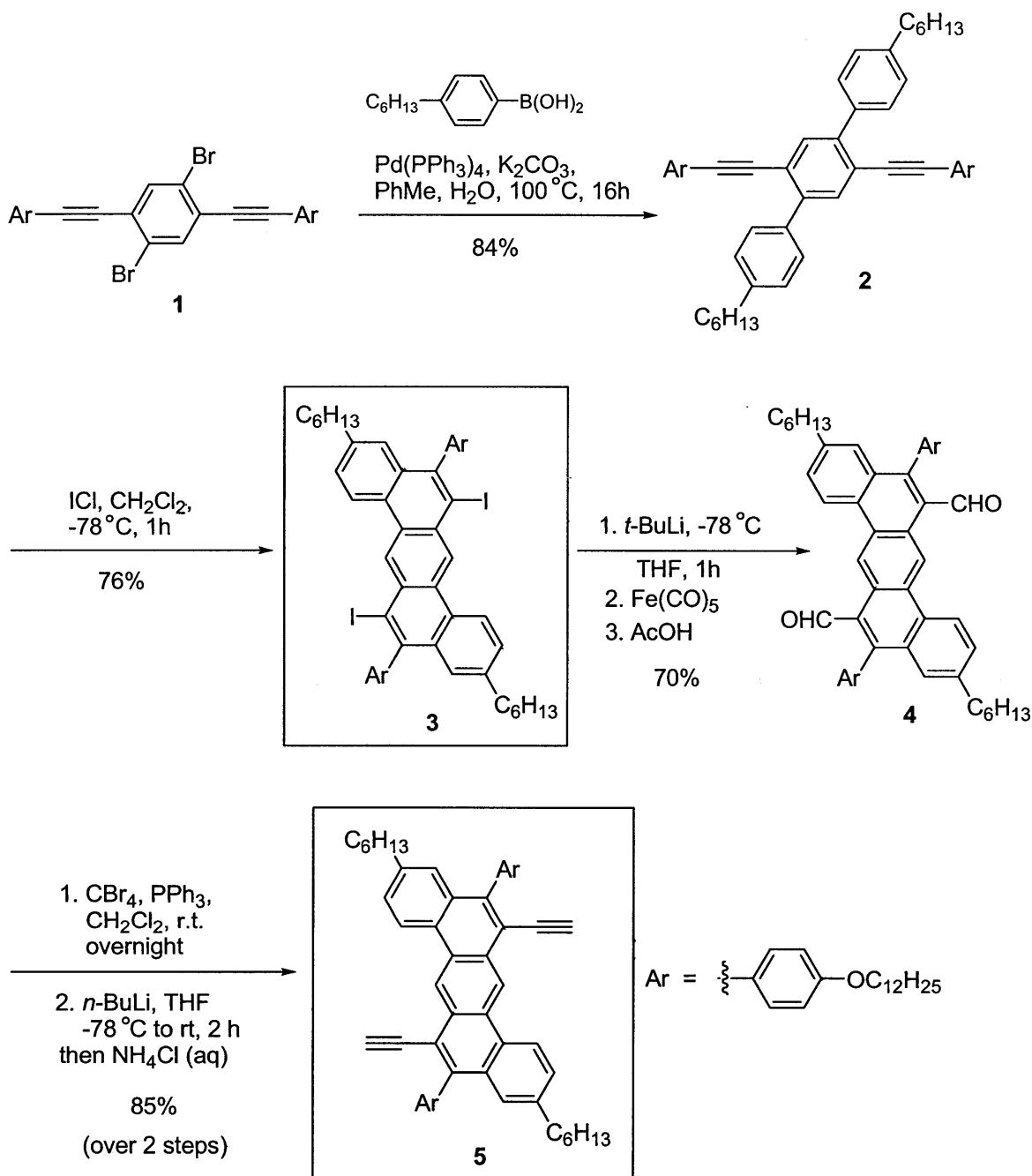
dibenzochrysenes⁵ and triphenylenes.⁶ In most of the aforementioned examples, the resulting polymers can be approximated to linear rigid rods, as a consequence of the *para*-substitution pattern between repeat units of the polymer backbone. With 6,13- and 5,12- linkage patterns on our dibenz[*a,h*]anthracene building block, the resulting polymers would adopt a ‘stair-stepped’ structure instead, and we were curious as to how this aromatic moiety, along with the unusual substitution patterns, would affect the physical properties of the resulting polymers.

Herein, we report the synthesis of new monomers containing dibenz[*a,h*]anthracene subunits and their successful incorporation into conjugated polymers.

4.2 Results and Discussion

The dibenz[*a,h*]anthracene-based monomers **3** and **5** were both synthesized in good yields from the dibromide starting material **1** over two and four steps respectively (Scheme 4.1). Subjecting dibromide **1** to double Suzuki coupling with two equivalents of 4-hexylphenylboronic acid under generic conditions led to the terphenyl derivative **2**, which was then converted to monomer **3** via a twofold electrophilic cyclization brought about by treatment with iodine monochloride at -78 °C. Diiodide **3** can be converted to monomer **5** over several steps, starting with the formation of dialdehyde **4** via a lithiation/formylation procedure, followed by a Corey-Fuchs homologation⁷ to establish two terminal alkynes. Straightforward conversion of diiodide **3** to dialkyne **5** via a Sonogashira coupling/deprotection protocol tends to be unsuccessful, as we have recently described elsewhere.³

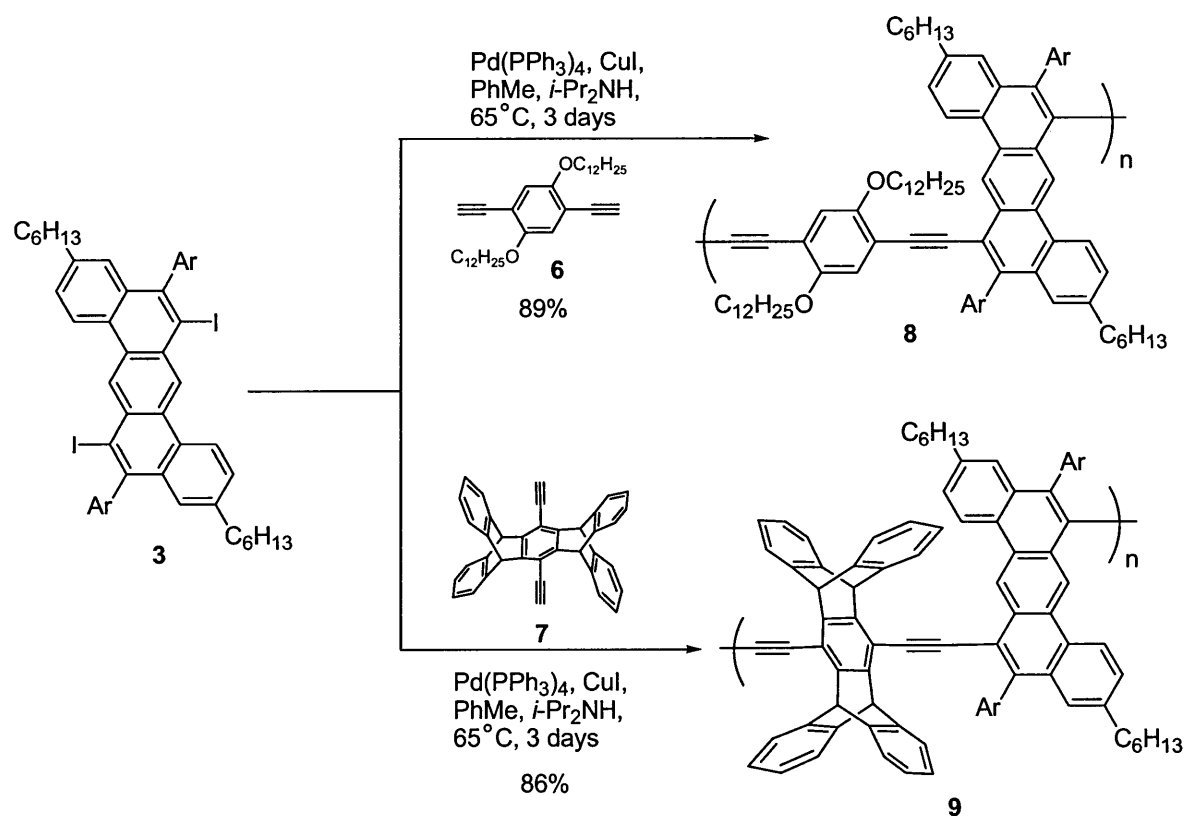
Scheme 4.1. Synthesis of monomers **3** and **5**.

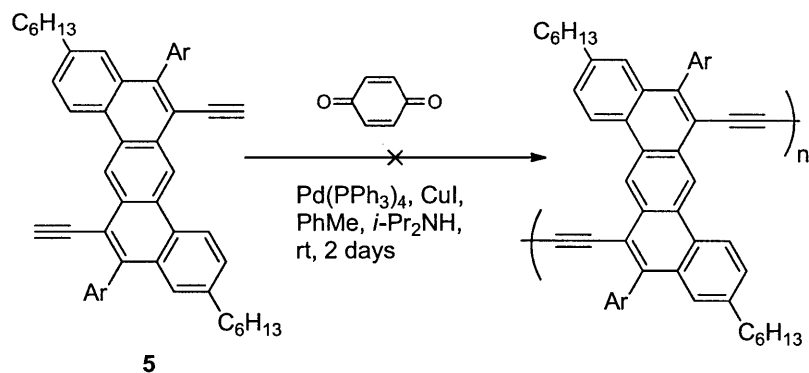


Diiodide monomer **3** was used in the preparation of polymers **8** and **9** via palladium-catalyzed Sonogashira polycondensation with comonomers **6** and **7** respectively (Scheme 4.2). We reacted the simple dialkyne **6** with the sterically hindered diiodide **3** in order to test the latter's viability in polymer formation. This turned out to be facile, giving the desired polymer in

89% yield. In the second reaction, the sterically bulky monomer **7** (6,13-diethynylpentiptycene), which had been previously used in the production of non-aggregating poly(arylene ethynylene)s,⁸ was successfully copolymerized with **3**. The successful reaction of these two hindered molecules attested to the reactivity and viability of diiodide **3** as a monomer. Gratifyingly, polymers were obtained in high yield in both cases, with **8** being isolated as an orange solid, and **9** as a lemon-yellow solid. We also attempted a homopolymerization of monomer **5** using modified Glaser-type coupling conditions with *p*-benzoquinone as the oxidant. Unfortunately, the yield in this case was much lower (*ca.* 60%), and the purification process also proved challenging.

Scheme 4.2. Synthesis of polymers **8** and **9**.



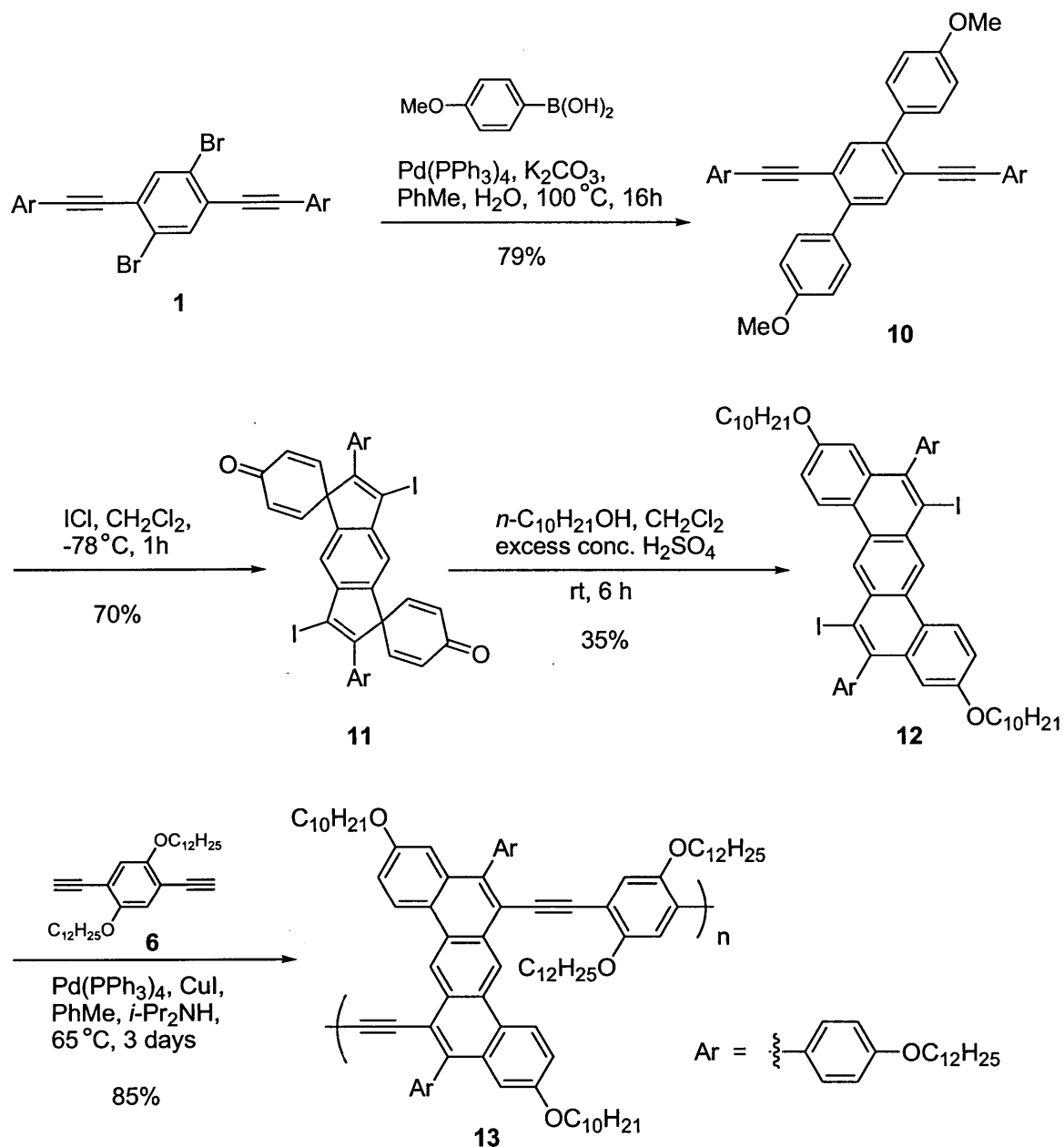


As a result, only a very minute quantity of the butadiyne-type polymer could be isolated, precluding the possibility of rigorous characterization. Furthermore, the polymer was found to have low solubility in various organic solvents. In conclusion, using dialkyne **5** to form a stair-stepped homopolymer appears to be unsuccessful. Based on the above findings, the adequately substituted dibenz[*a,h*]anthracene motif can easily be incorporated into poly(aryleneethynylene)s via Sonogashira polycondensation, but accessing butadiyne-type polymers using Glaser coupling proved to be more problematic.

To investigate the effects of alkoxy vs. alkyl substitution on the photophysical properties of the resulting polymers, the analogous monomer **12** was synthesized. This diiodide **12** can once again be prepared using a sequence of transformations (Scheme 4.3) similar to those used in the synthesis of our J-aggregating dibenz[*a,j*]anthracene-based macrocycles. Beginning with dibromide **1**, double Suzuki coupling with 4-methoxyphenylboronic acid affords terphenyl **10** in good yield. The terphenyl is subjected to iodine monochloride to produce the bis-spirocyclic compound **11**, which is partially purified and subsequently converted to the desired diiodide monomer via an acid-catalyzed rearrangement. Using Sonogashira conditions identical to those used in synthesizing polymer **8**, monomer **12** was copolymerized with dialkyne **6** over 3 days to

give poly(aryleneethynylene) **13**. The conversion occurred in high yield, and polymer **13** was isolated as a red solid.

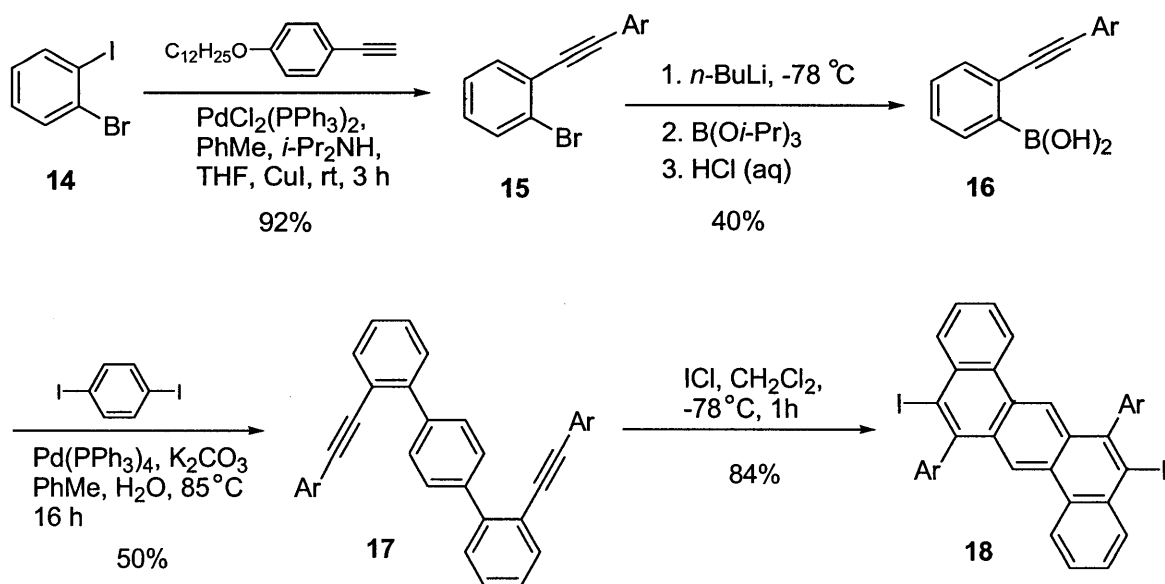
Scheme 4.3. Synthesis of polymer **13**.



Following the successful application of the dibenz[*a,h*]anthracene-based monomers **3** and **12** in Sonogashira polymerization, we then explored other dibenz[*a,h*]anthracenes bearing

different substitution patterns. This led to the synthesis of monomer **18**, in which iodine atoms are situated at carbons 5 and 12 of the polycyclic arene instead of carbons 6 and 13, which would produce a structurally different polymer backbone featuring ‘stair-steps’ of gentler gradient. The synthesis of polymer **19** (Scheme 4.4) begins with the commercially available 1-bromo-2-iodobenzene, which is subjected to an iodine-selective Sonogashira coupling to give compound **15**. For unknown reasons, attempts to prepare terphenyl **17** by Suzuki coupling two equivalents of **15** with benzene-1,4-diboronic acid were unsuccessful. However, when **15** was first converted to boronic acid **16**, followed by Suzuki coupling with half an equivalent of 1,4-diiodobenzene, the terphenyl derivative **17** could be obtained in reasonable yield. Subsequent double electrophilic cyclizations with iodine monochloride were carried out on **17** to give the target monomer **18**. The diiodide was then copolymerized with dialkyne **6** to afford polymer **19** (deep red solid) in high yield.

Scheme 4.4. Synthesis of polymer **19**.



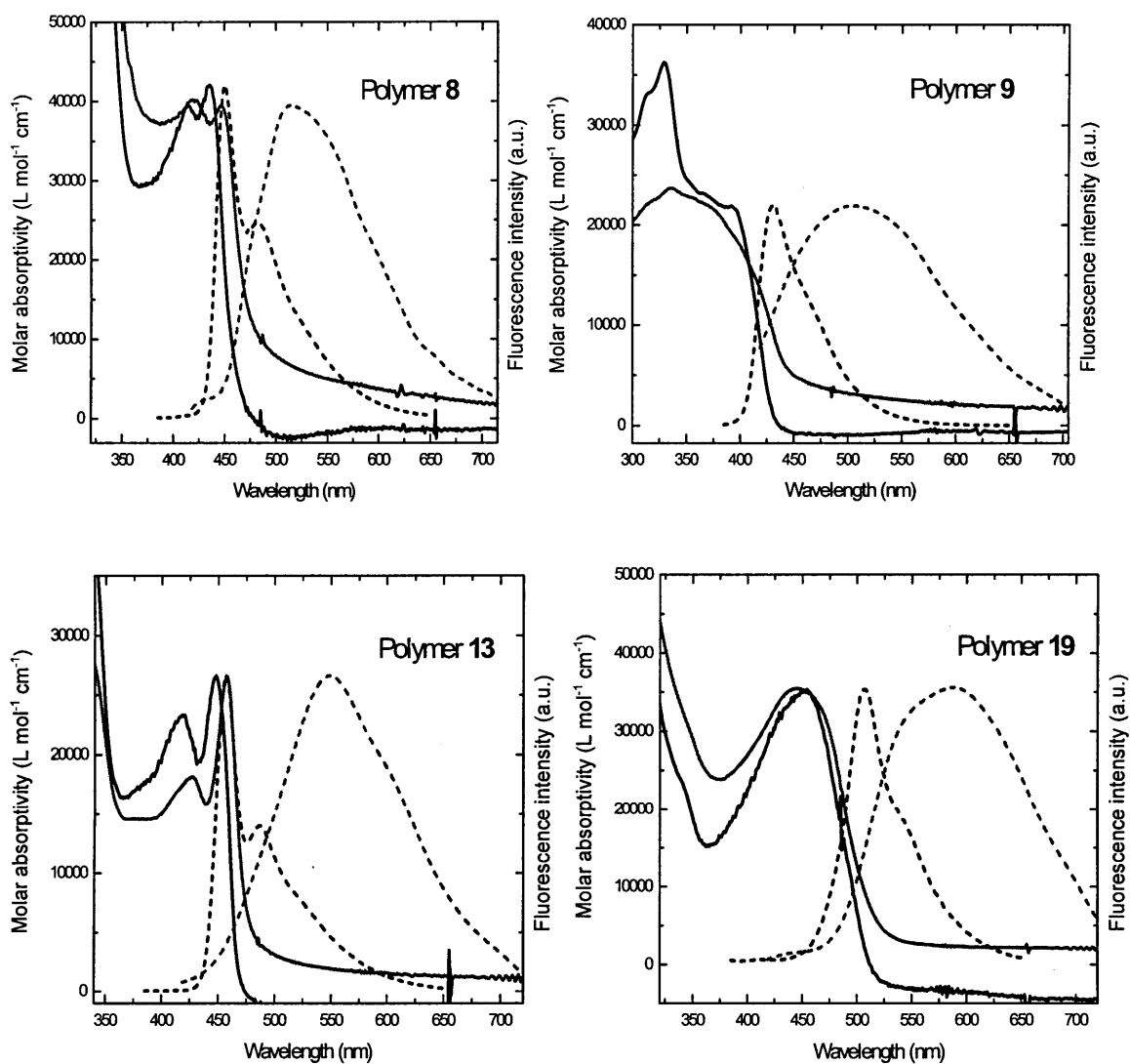
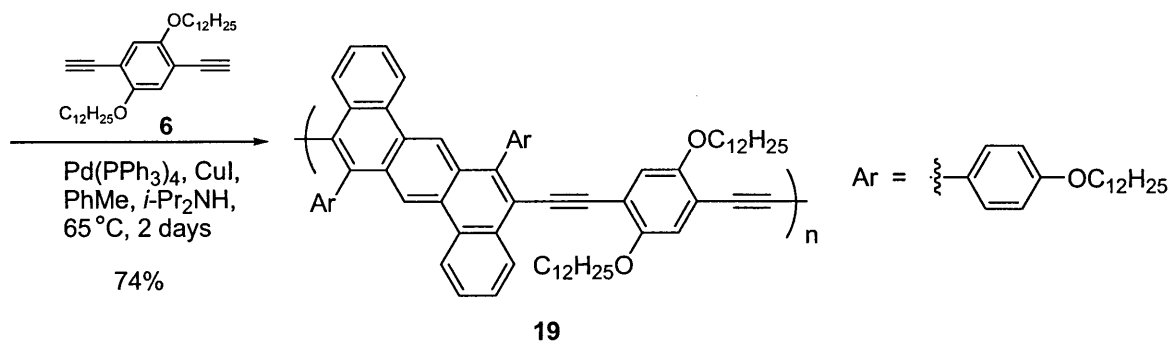


Figure 4.2. UV-vis (solid lines) and fluorescence (dashed lines) spectra of polymers 8, 9, 13, 19 in chloroform solution (black) and in thin films (red; normalized).

Table 4.1. Characterization and Spectroscopic Data for Polymers **8**, **9**, **13**, **19**

Polymer	M_n/M_w^a (10^3 g mol $^{-1}$)	λ_{\max} (nm)		λ_{em} (nm)		Φ_f	lifetimes (bimodal) (ns)	
		solution ($\epsilon/\text{L mol}^{-1}$ cm^{-1}) b	thin film	soln. (thin film)	solution c (thin film) d		soln.	thin film
8	21.5/50.2	436 (4200)	447	450 (509)	0.29 (0.050)	1.0 (94%) 2.7 (6%)	1.4 (98%) 5.1 (2%)	
9	10.6/25.7	392 (21900)	336	430 (505)	0.34 (0.049)	2.0 (93%) 6.0 (7%)	1.7 (97%) 6.7 (3%)	
13	19.0/72.0	448 (26600)	457	457 (550)	0.32 (0.070)	1.4 (97%) 3.5 (3%)	2.0 (95%) 7.4 (5%)	
19	10.4/17.4	454 (35300)	450	507 (579)	0.23 (0.018)	1.1 (92%) 2.6 (8%)	1.2 (98%) 4.2 (2%)	

a Determined by GPC using polystyrene standards. b Molar absorptivity based on the molecular weight of a repeating unit. c Against quinine sulfate in 0.1 M H_2SO_4 ($\Phi_f = 0.546$, $\lambda_{\text{ex}} = 366$ nm). 9 d Against perylene in PMMA ($\Phi_f = 0.87$, $\lambda_{\text{ex}} = 412$ nm). 10

Polymer **8** shows an absorption maximum (λ_{\max}) of 436 nm in solution, and is a blue-green emitter (Table 4.1, Figure 4.2). Its solution photoluminescence spectrum shows peak emission at 450 nm, with a secondary peak at 483 nm. Polymer **9**, which incorporates the bulky pentiptycene unit, displays blue-shifted absorption and emission relative to polymer **8**. The steric bulk of the pentiptycenes probably reduces overall conjugation along the polymer backbone by twisting the monomer subunits relative to one another. These factors lead to the observation of pure blue emission instead of blue-green. Another interesting feature of polymer **9** is that unlike the pentiptycene-containing PPEs previously synthesized in our group 11 , the presence of that bulky comonomer does not seem to prevent aggregation, as evidenced by the red shift and reduced fluorescence quantum yield of polymer **9** films compared to the corresponding solutions. We believe there are two reasons for this. First, unlike the pentiptycene-containing PPEs, polymer **9** incorporates rather large polycyclic aromatic dibenz[*a,h*]anthracene units. By contrast, the much smaller comonomers (single benzene ring) of our pentiptycene-containing PPEs are dwarfed by the larger pentiptycene units, resulting in polymers whose backbones are exceedingly

well-shielded sterically, thus preventing aggregation and self-quenching in concentrated solutions and thin films. With such large π -surface areas present in polymer **9**, the three-dimensional bulk of the pentiptycene units are unable to effectively shield the polymer backbone, and as a result, interchain π - π stacking between polycyclic aromatic units still occurs, producing bathochromic shifts and lowered quantum yields. Secondly, it must be noted the polymer **9** is structurally a stair-stepped polymer rather than a PPE, whereby the two flanking pentiptycene groups are connected to the dibenz[*a,h*]anthracene unit at different ‘levels’ of the ‘staircase’ (vs. *para* substitution in PPEs), resulting in further reduction of the pentiptycene shielding efficiency. As for polymer **13**, the replacement of alkyl chains with alkoxy groups (compare with polymer **8**) in the dibenz[*a,h*]anthracene subunits brought about a small red shift. Apart from this, the spectral profiles of the structurally similar **8** and **13** are nearly identical. Polymer **19**, which features 5,12-substituted dibenz[*a,h*]anthracene repeat units, experiences less intrachain steric repulsions between the monomer repeat units compared to polymer **8**. Thus, increased conjugation and a corresponding bathochromic shift in the absorption and fluorescence spectra were expected. This was indeed observed, making polymer **19** the most spectroscopically red-shifted polymer of the series, showing maximum absorption at 454 nm and green emission at 507 nm (with a shoulder at 541 nm).

4.3 Conclusions

Several new polycyclic aromatic monomers based on the dibenz[*a,h*]anthracene motif have been synthesized from readily available starting materials. These monomers are easily copolymerized with a variety of comonomers in cross-coupling polymerizations to give fluorescent stair-stepped poly(aryleneethynylene)s. These conjugated polymers exhibit high

solubilities as well as relatively blue-shifted absorption and emission maxima. We have found that the degree of blue-shifting can be tuned by employing comonomers of varying steric bulk, and also by changing the substitution pattern on the polycyclic aromatic component. These properties suggest potential applications as blue-to-green emitters in various optoelectronic devices.

4.4 Experimental Section

General Methods and Instrumentation: All reactions were performed under an argon atmosphere, using over-dried glassware and standard Schlenk techniques. *Tetrakis*-(triphenylphosphine)palladium(0) was purchased from Strem Chemicals, Inc. Diethynylpentiptycene (**7**) was purchased from Nomadics Inc. (Stillwater, OK, USA). All other reagents were obtained from Alfa Aesar and Aldrich Chemical Co., Inc., and used as received. Anhydrous toluene, tetrahydrofuran, and dichloromethane were obtained from a solvent purification system (Innovative Technologies). Silica gel (40-63 μm) was obtained from SiliCycle Inc. Dry diisopropylamine (DIPA) was obtained by distilling reagent-grade DIPA over sodium hydroxide pellets. Nuclear Magnetic Resonance (NMR) spectra were recorded on a Varian Mercury (300 MHz) NMR spectrometer located in the MIT Department of Chemistry Instrumentation Facility (DCIF). High-resolution mass spectra (HR-MS) were also obtained at the MIT DCIF using matrix-assisted laser desorption ionization time-of-flight (MALDI-TOF) or direct analysis in real time electrospray ionization (DART-ESI). Polymer molecular weights were determined in THF solutions on an Agilent 1100 series HPLC/GPC system with three PLgel columns in series (10^3 , 10^4 , 10^5 Å) against narrow polystyrene standards. Polymer thin films were spin-cast from ~ 2 mg/mL chloroform solutions on microscope glass coverslips using

an EC101DT photoresist spinner (Headway Research, Inc.) at a 1000 rpm rate for 1 minute. UV/Vis spectra were recorded on an Agilent 8453 diode-array spectrophotometer. Emission spectra and fluorescence quantum yield measurements were acquired on a SPEX Fluorolog fluorometer (model FL-321, 450 W xenon lamp) using either right-angle (solution measurements) or front-face detection (film measurements). Fluorescence quantum yields of all polymer solutions and films were estimated by comparison with standards of known quantum yields, in this case quinine sulfate in 0.1 M sulfuric acid (for solutions) and perylene in poly(methylmethacrylate) matrix (for films). Polymer solutions were excited at 366 nm, with their optical densities kept around 0.05. Quantum yield values were then calculated as per Lakowicz.¹ Fluorescence lifetime measurements were performed by exciting both thin film and solution samples with 160 fs pulses at 390 nm obtained by frequency doubling the output of a Coherent RegA Ti:Sapphire amplifier laser system. A Hamamatsu C4780 DynaSpect Picosecond Fluorescence Lifetime System operating in photon counting mode and triggered by an Agilent 81104A Pulse Pattern Generator was used to spectrally and temporally resolve the resulting fluorescence. The instrument response function of the fluorescence lifetime system was 40 ps. The fluorescence intensity for the thin film samples, used in the calculation of the quantum yield, was collected in the same fluorescence lifetime system. Each thin film sample was excited with the same laser fluence, spot size, and excitation and collection geometry.

3',6'-Bis-(*p*-(dodecyloxy)phenylethynyl)-4,4''-dihexyl-[1,1':4',1'']terphenyl (2): A 250 mL two-neck round-bottom flask containing a magnetic stir-bar was charged with the dibromide **1** (or 1,4-dibromo-2,5-bis-(4-dodecyloxyphenylethynyl)benzene) (1.539 g, 1.91 mmol), 4-hexylphenylboronic acid (0.947 g, 4.59 mmol), *tetrakis*-(triphenylphosphine)palladium(0) (0.066

g, 0.057 mmol), potassium carbonate (0.660 g, 4.78 mmol), toluene (25 mL), and water (3 mL) under an atmosphere of argon. The mixture was stirred and briefly sparged by bubbling argon through it for 5-10 minutes using a long needle. Following the degassing, the mixture was then stirred vigorously and heated at 100 °C for 16 hours. After allowing the reaction mixture to cool down to room temperature, it was diluted with diethyl ether and transferred into a separatory funnel, and extracted with additional portions of ether (3 x 40 mL). The combined organic extracts were dried over anhydrous magnesium sulfate, filtered through a piece of fluted filter paper into a 500 mL round-bottom flask, and then concentrated by rotary evaporate to give a residue of the crude product. This was purified by flash chromatography on a silica gel column (20% v/v dichloromethane/hexane) to afford **2** (1.55 g, 84%). ¹H NMR (300 MHz, CD₂Cl₂, δ ppm): 7.68 (2H, s), 7.66 (4H, d, *J* = 7.5 Hz), 7.32 (4H, d, *J* = 8.1 Hz), 7.29 (4H, d, *J* = 8.7 Hz), 6.83 (4H, d, *J* = 8.7 Hz), 3.95 (4H, t, *J* = 6.6 Hz), 2.71 (4H, t, *J* = 7.5 Hz), 1.3-1.8 (56H), 0.89-0.95 (12H). ¹³C NMR (300 MHz, CD₂Cl₂, δ ppm): 178.3, 159.7, 143.0, 142.0, 137.0, 133.6, 133.0, 129.4, 128.3, 121.8, 115.1, 114.7, 93.9, 88.2, 68.3, 35.9, 32.2, 32.0, 31.8, 29.9, 29.8, 29.6, 29.4, 29.3, 26.2, 22.9, 14.2, 14.1. HRMS (MALDI-TOF): calcd: 966.7254 (M)⁺, found: 966.4072.

5,12-Bis-(4'-dodecyloxyphenyl)-3,10-dihexyl-6,13-diiododibenz[*a,h*]anthracene (3): A 25-mL two-neck round-bottom flask containing **2** (0.100 g, 0.104 mmol) and a magnetic stir-bar was placed under argon atmosphere. Anhydrous dichloromethane (9 mL) was then added via syringe and the resulting mixture was stirred for 5 minutes. Upon complete dissolution of the solid, the flask was immersed into a dry-ice/acetone bath at -78 °C. After stirring at that temperature for 5 minutes, a 1.0 M solution of ICl in dichloromethane (0.25 mL, 0.25 mmol) was

added slowly via syringe. After the dark-colored mixture was stirred for 1 hour at -78 °C, it was diluted with dichloromethane and then transferred into a separatory funnel containing aqueous sodium hydroxide (~0.5 M, 20 mL). The dark mixture was decolorized upon shaking with NaOH, and extracted several times with additional dichloromethane (3 x 20 mL). The combined organic extracts were dried over anhydrous magnesium sulfate, filtered, and the solvent removed by rotary evaporation, leaving behind a crude product that was subsequently purified by flash chromatography on a silica gel column (18% v/v dichloromethane/hexane). The relevant fractions were combined and the solvent was removed, affording **3** (0.096 g, 76%) as a white solid. ¹H NMR (300 MHz, CDCl₃, δ ppm): 9.74 (2H, s), 8.88 (2H, d, *J* = 8.1 Hz), 7.60 (2H, d, *J* = 6.9 Hz), 7.24 (4H, d, *J* = 8.7 Hz), 7.09 (4H, d, *J* = 8.7 Hz), 4.10 (4H, t, *J* = 6.3 Hz), 2.67 (4H, t, *J* = 7.2 Hz), 0.8-1.9 (68H). ¹³C NMR (300 MHz, CDCl₃, δ ppm): 159.0, 146.2, 142.6, 138.0, 133.2, 131.4, 131.3, 129.8, 129.0, 128.6, 128.5, 123.3, 114.5, 109.9, 107.5, 68.3, 36.2, 32.2, 31.9, 31.7, 30.0, 29.9, 29.8, 29.7, 29.6, 29.1, 26.5, 23.0, 22.9, 14.4. HRMS (MALDI-TOF): calcd: 964.7097 (M-I₂)⁺, found: 967.8396 (M-I₂)⁺, 1092.8617 (M-I)⁺.

5,12-Bis-(4'-dodecyloxyphenyl)-3,10-dihexyldibenz[*a,h*]anthracene-6,13-dicarbaldehyde (4)

A 25 mL two-neck round-bottom flask containing **3** (0.034 g, 0.028 mmol) and a magnetic stir-bar was evacuated and then placed under positive pressure of argon. Dry tetrahydrofuran (5 mL) was then added via syringe and the mixture was stirred to completely dissolve **3**. The solution was subsequently cooled in a dry-ice/acetone bath at -78 °C, before 1.7 M *tert*-butyllithium in pentane (0.05 mL, 0.0837 mmol) was added via syringe. This mixture was stirred at -78 °C for 1 hour, after which iron(0)pentacarbonyl (0.015 mL, 0.11 mmol) was added via syringe. After 10 minutes, the dry-ice/acetone bath was removed, and the mixture was allowed to warm up to

room temperature. Stirring was continued overnight. The resulting mixture was then quenched with glacial acetic acid (1.0 mL), and stirred for 1 hour, before being diluted with dichloromethane and poured into a separatory funnel containing deionized water. The mixture was extracted with further portions of dichloromethane (3 x 20 mL) and the organic layer was separated out and dried over anhydrous magnesium sulfate. Removal of the solvent under rotary evaporation afforded a dark-colored crude mixture containing the target dialdehyde as well as monoaldehyde byproduct. This was purified by flash chromatography on a silica gel column (40% v/v dichloromethane/hexane, gentle gradient) to give **4** as a yellow solid (0.020 g, 70%).

Notes: a) The first yellow band that elutes contains monoaldehyde byproduct, whilst the second yellow band contains the desired dialdehyde **4**; b) we have subsequently found that dry DMF may be used in place of the more hazardous iron pentacarbonyl reagent, giving comparable yields and easier workup. ¹H NMR (300 MHz, CD₂Cl₂, δ ppm): 10.77 (2H, s), 10.19 (2H, s), 8.92 (2H, d, *J* = 8.4 Hz), 7.70 (2H, d, *J* = 8.1 Hz), 7.48 (2H, s), 7.39 (4H, d, *J* = 8.4 Hz), 7.11 (4H, d, *J* = 8.4 Hz), 4.10 (4H, t, *J* = 6.6 Hz), 2.71 (4H, t, *J* = 7.5 Hz), 0.8-1.9 (68H). ¹³C NMR (300 MHz, CD₂Cl₂, δ ppm): 195.7, 159.6, 150.7, 142.6, 132.5, 131.7, 131.2, 129.7, 128.2, 128.1, 126.5, 123.7, 120.2, 114.4, 68.5, 36.0, 32.2, 31.9, 31.6, 29.9, 29.7, 29.6, 29.1, 26.3, 23.0, 22.9, 14.1. HRMS (MALDI-TOF): calcd: 1022.7152 (M)⁺, found: 1022.8704.

5,12-Bis-(4'-dodecyloxyphenyl)-6,13-diethynyl-3,10-dihexyldibenz[*a,h*]anthracene (5): A 25 mL single-neck round-bottom flask containing a magnetic stir-bar was charged with triphenylphosphine (0.041 g, 0.156 mmol) and carbon tetrabromide (0.026 g, 0.078 mmol), and subsequently placed under argon atmosphere. The flask was immersed into an ice-water bath, and then dry dichloromethane (3 mL) was added via syringe, with simultaneous stirring to

dissolve the reagents, giving a clear yellow solution. To this was added a solution of **4** (0.020 g, 0.195 mmol) in dichloromethane (1 mL), and the mixture was allowed to slowly warm up to room temperature overnight. After the reaction was complete, dichloromethane was poured in to dilute the mixture, which was transferred into a separatory funnel and extracted with additional portions of dichloromethane (3 x 20 mL). The combined organic extracts were dried over anhydrous magnesium sulfate, filtered through a fluted filter funnel and then the solvent was removed by rotary evaporation. The crude product was quickly purified by flash chromatography through a short column/pad of silica gel. Concentrating the fractions affords the intermediate geminal dibromide (ca. 16 mg), which should not be stored, but instead, used as soon as possible in the next step (i.e. conversion to alkyne). In a 25 mL one-neck, round-bottom flask containing a magnetic stir-bar and the partially purified geminal dibromide (ca. 16 mg, 0.012 mmol) under argon atmosphere, anhydrous tetrahydrofuran (2.0 mL) was added via syringe to give a clear solution. After cooling the solution down to -78 °C in a dry-ice/acetone bath, 1.6 M *n*-butyllithium in hexanes (0.04 mL, 0.064 mmol) was added by syringe. The reaction mixture was stirred for about 2 hours, after which an aqueous solution of ammonium chloride (2-3 mL) was introduced via syringe, and the mixture was allowed to warm to room temperature (at this point, the mixture should show violet emission under a hand-held UV lamp). Diethyl ether was used to dilute the mixture, which was transferred into a separatory funnel and extracted with further portions of ether (3 x 25 mL). The combined organic extracts were dried over anhydrous magnesium sulfate, filtered, and then concentrated under rotary evaporation. The crude dialkyne was then purified by flash chromatography on a silica gel column (20% v/v dichloromethane/hexane) to give **5** (10 mg with respect to dialdehyde, 85% over two steps). ¹H NMR (300 MHz, CD₂Cl₂, δ ppm): 9.81 (2H, s), 8.85 (2H, d, *J* = 8.7 Hz), 7.57 (2H, d, *J* = 8.4

Hz), 7.43 (2H, s), 7.43 (4H, d, $J = 8.4$ Hz), 7.08 (4H, d, $J = 8.7$ Hz), 4.08 (4H, t, $J = 6.6$ Hz), 3.61 (2H, s), 2.68 (4H, t, $J = 7.5$ Hz), 0.8-1.9 (68H). ^{13}C NMR (300 MHz, CD_2Cl_2 , δ ppm): 159.1, 144.5, 142.5, 131.9, 131.8, 131.4, 129.6, 128.9, 128.7, 127.5, 123.2, 120.9, 118.0, 114.2, 86.1, 81.8, 68.3, 36.1, 32.2, 31.9, 31.7, 30.0, 29.9, 29.7, 29.6, 29.2, 26.4, 23.0, 22.9, 14.2, 14.1. HRMS (MALDI-TOF): calcd: 1014.7254 (M)⁺, found: 1014.6481.

3',6'-Bis-(*p*-dodecyloxy)phenylethynyl)-4,4''-dimethoxy[1,1':4',1'']terphenyl (10):

Terphenyl **10** was synthesized in an analogous manner to **2**, starting with **1** (0.5 g, 0.62 mmol) and 4-methoxyphenylboronic acid (0.30 g, 1.97 mmol). The crude product was purified by flash chromatography on a silica gel column (35% v/v dichloromethane/hexane), to give **7** as a white solid (0.42 g, 79%). ^1H NMR (300 MHz, CD_2Cl_2 , δ ppm): 7.70 (4H, d, $J = 8.7$ Hz), 7.65 (2H, s), 7.31 (4H, d, $J = 9.0$ Hz), 7.03 (4H, d, $J = 8.7$ Hz), 6.84 (4H, d, $J = 8.7$ Hz), 3.95 (4H, t, $J = 6.6$ Hz), 3.88 (6H, s), 1.2-1.8 (40H), 0.88 (6H, t, $J = 6.9$ Hz). ^{13}C NMR (300 MHz, CD_2Cl_2 , δ ppm): 159.7, 141.4, 133.6, 133.0, 132.1, 130.6, 130.1, 121.6, 115.1, 114.7, 113.6, 93.8, 88.2, 68.3, 55.5, 32.2, 29.9, 29.8, 29.6, 29.4, 26.2, 22.9, 14.1. HRMS (MALDI-TOF): calcd: 858.5587 (M)⁺, found: 858.2730.

Bis-spirocyclohexadienone 11: A 250-mL single-neck round-bottom flask containing **10** (0.42 g, 0.49 mmol) and a magnetic stir-bar was placed under argon atmosphere. Anhydrous dichloromethane (20 mL) was then added via syringe and the resulting mixture was stirred for 10 minutes. Upon complete dissolution of the solid, the flask was immersed into a dry-ice/acetone bath at -78 °C. After stirring at that temperature for 5 minutes, a 1.0 M solution of ICl in dichloromethane (1.2 mL, 1.2 mmol) was added slowly via syringe. After the dark-colored

mixture was stirred for 1 hour at $-78\text{ }^{\circ}\text{C}$, it was diluted with dichloromethane and then transferred into a separatory funnel containing aqueous sodium hydroxide ($\sim 0.5\text{ M}$, 40 mL). The dark mixture was decolorized upon shaking with NaOH, and extracted several times with additional dichloromethane ($3 \times 30\text{ mL}$). The combined organic extracts were dried over anhydrous magnesium sulfate, filtered, and the solvent removed by rotary evaporation. The residue was titrated with hexane ($\sim 20\text{ mL}$) and the resulting suspension was filtered through a fritted glass filter funnel. The off-white solid was washed with several portions of hexane, and then dried by air suction for 1-2 hours, giving an off-white powder (0.37 g , ca. 70%). This partially purified **11** can be used in the next step without further purification. (Notes: (i) compound **11** shows very low solubility in many common organic solvents, making column chromatography impossible, (ii) storage of **8** is possible, but should be kept refrigerated. Immediate use in the next step is recommended.) $^1\text{H NMR}$ (300 MHz , CD_2Cl_2 , $\delta\text{ ppm}$): 7.33 (4H, d, $J = 9.0\text{ Hz}$), 7.15 (2H, s), 6.86 (4H, d, $J = 9.0\text{ Hz}$), 6.49-6.51 (8H), 3.94 (4H, t, $J = 6.9\text{ Hz}$), 0.8-1.8 (46H). HRMS (MALDI-TOF): calcd: $828.5118\text{ (M - I}_2\text{)}^+$, found 830.0553 .

5,12-Bis-(4'-dodecyloxyphenyl)-3,10-didodecyloxy-6,13-diiododibenz[*a,h*]anthracene (12):

To a 100-mL round-bottom flask containing a magnetic stir-bar was added **11** (0.061 g , ca. 0.056 mmol), excess decanol (2 mL), and dichloromethane (3 mL) (Schlenk techniques are unnecessary for this reaction). The mixture was stirred to give an off-white suspension. The flask was placed in an ice-water bath, after which concentrated sulfuric acid ($\sim 1.0\text{ mL}$ in total) was added dropwise to the rapidly stirring suspension using a glass dropper. Addition of acid was discontinued once the white suspension gave way to a brown solution. This solution was

subsequently allowed to stir for 6 hours at room temperature. The mixture was diluted with dichloromethane and transferred into a separatory funnel where it was neutralized carefully with aqueous NaOH. The mixture was extracted with dichloromethane (3 x 40 mL), and the combined organic extracts were dried over anhydrous magnesium sulfate. After filtration and subsequent removal of solvent by rotary evaporation, a residue of the crude product was obtained. This was purified by flash chromatography on a silica gel column (25% v/v dichloromethane/hexane) to afford pure **12** (27 mg, ca. 35%). ¹H NMR (300 MHz, CDCl₃, δ ppm): 9.58 (2H, s), 8.81 (2H, d, *J* = 9.3 Hz), 7.31 (2H, d, *J* = 9.0 Hz), 7.25 (4H, d, *J* = 8.7 Hz), 7.09 (4H, d, *J* = 8.7 Hz), 6.85 (2H, s), 4.09 (4H, t, *J* = 6.6 Hz), 3.85 (4H, d, *J* = 6.6 Hz), 0.8-1.9 (62H). ¹³C NMR (300 MHz, CDCl₃, δ ppm): 180.2, 159.0, 145.8, 138.0, 134.3, 131.2, 130.9, 129.3, 128.5, 124.7, 124.5, 117.2, 114.6, 111.7, 108.1, 68.3, 32.2, 30.0, 29.9, 29.8, 29.7, 29.6, 29.4, 26.4, 26.3, 23.0, 14.4. HRMS (MALDI-TOF): calcd: 1108.8248 (M - I₂)⁺, 1235.7292 (M - I)⁺, found: 1108.4958, 1236.1852.

1-bromo-2-(*p*-(dodecyloxy)phenylethynyl)benzene (15): A 100 mL round-bottom flask equipped with a magnetic stir bar was charged with 1-bromo-2-iodobenzene (0.91 mL, 7 mmol), PdCl₂(PPh₃)₂ (0.098 g, 0.14 mmol), CuI (0.14 g, 0.735 mmol), and placed under an inert argon atmosphere. Anhydrous tetrahydrofuran (10 mL), toluene (15 mL), and diisopropylamine (15 mL) were then introduced via syringe, and the mixture was stirred briefly before a solution of 4-dodecyloxyethynylbenzene (2.13 g, 7.4 mmol) in tetrahydrofuran (5 mL) was added dropwise using a syringe. The reaction mixture was stirred at room temperature for 3 hours. Upon completion, the mixture was rotary evaporated to remove all the solvents. The residue was diluted with hexanes and dichloromethane and subsequently extracted in a separatory funnel with

additional dichloromethane (3 x 40 mL). The organic extracts were combined, dried over anhydrous MgSO₄, and then concentrated *in vacuo*. The crude product was purified by flash chromatography on a silica gel column (13% v/v dichloromethane/hexane) to afford pure **15** as a white solid (2.85 g, 92%). ¹H NMR (300 MHz, CD₂Cl₂, δ ppm): 7.63 (1H, d, *J* = 8.1 Hz), 7.55 (1H, d, *J* = 7.5 Hz), 7.51 (2H, d, *J* = 6.6 Hz), 7.31 (1H, t, *J* = 7.5 Hz), 7.20 (1H, t, *J* = 7.8 Hz), 6.89 (2H, d, *J* = 6.9 Hz), 3.98 (2H, t, *J* = 6.6 Hz), 1.78 (2H, m, *J* = 6.9 Hz), 1.3-1.8 (20H), 0.89 (3H, t, *J* = 6.9 Hz). ¹³C NMR (300 MHz, CD₂Cl₂, δ ppm): 178.3, 160.0, 133.3, 133.2, 132.6, 129.4, 127.4, 125.8, 125.4, 114.8, 114.6, 94.3, 86.8, 68.4, 32.2, 29.9, 29.8, 29.6, 29.4, 26.2, 22.9, 14.1. HRMS (DART-ESI): calcd: 441.1788 (M+H)⁺, found: 441.1789.

2-(*p*-(dodecyloxy)phenylethynyl)benzeneboronic acid (16): A 100 mL round-bottom flask equipped with a magnetic stir bar was charged with **15** (1.064 g, 2.41 mmol) and placed under argon. Anhydrous THF (20 mL) was added via syringe, and the mixture was stirred to dissolve the solid. The solution was cooled down to -78 °C in an acetone/dry ice bath. Then, 1.6 M *n*-butyllithium in hexanes (2.1 mL, 3.37 mmol) was added slowly via syringe. The mixture was allowed to stir at -78 °C for about 90 minutes, after which triisopropylborate (1.6 mL, 6.72 mmol) was added via syringe. After 20 minutes, the cooling bath was removed and the mixture was allowed to warm up to room temperature overnight. During the workup, deionized water (15 mL) was added, and the mixture was stirred for 1 hour. After rotary evaporation to remove most of the solvents, the residue was extracted with diethyl ether (3 x 50 mL) in a separatory funnel. The combined organic extracts were dried over anhydrous MgSO₄, and then concentrated *in vacuo*. The crude product was purified by flash chromatography on a silica gel column (50% v/v dichloromethane/hexane, then pure dichloromethane) to afford pure **16** as a white solid (0.39 g,

40%). ¹H NMR (300 MHz, CD₂Cl₂, δ ppm): 7.98 (1H, d, *J* = 7.5 Hz), 7.58 (1H, d, *J* = 7.5 Hz), 7.36-7.50 (4H), 6.91 (2H, d, *J* = 9.0 Hz), 6.04 (2H, s), 3.98 (2H, t, *J* = 6.6 Hz), 1.79 (2H, m, *J* = 6.9 Hz), 1.3-1.5 (20H), 0.89 (3H, t, *J* = 6.9 Hz). ¹³C NMR (300 MHz, CD₂Cl₂, δ ppm): 160.2, 135.7, 133.2, 132.5, 131.0, 128.2, 127.3, 115.0, 113.7, 93.9, 88.6, 68.4, 32.2, 29.9, 29.8, 29.6, 29.4, 26.2, 22.9, 14.1. HRMS (DART-ESI): calcd: 407.2768 (M+H)⁺, found: 407.2766.

2, 2''-Bis-(*p*-(dodecyloxy)phenylethynyl)-[1,1':4',1'']terphenyl (17): A 25 mL two-neck round-bottom flask equipped with a magnetic stir bar was charged with **16** (0.20 g, 0.492 mmol), 1,4-diiodobenzene (0.0738 g, 0.224 mmol), Pd(PPh₃)₄ (7.8 mg, 0.0067 mmol), potassium carbonate (0.0773 g, 0.56 mmol) and placed under inert argon. Toluene (4 mL) and water (0.8 mL) were added, and the mixture was stirred at 85 °C for 16 hours. Upon completion, the mixture was diluted with dichloromethane and transferred into a separatory funnel containing brine solution. Extraction was performed (3 x 30 mL dichloromethane) and the combined organic extracts were dried over anhydrous MgSO₄, and then concentrated *in vacuo*. The crude product was purified by flash chromatography on a silica gel column (25% v/v dichloromethane/hexane) to afford **17** (89 mg, 50%). Traces of yellow color in the product were removed by washing with small quantities of cold pentane. ¹H NMR (300 MHz, CD₂Cl₂, δ ppm): 7.82 (4H, s), 7.66 (2H, d, *J* = 7.5 Hz), 7.52 (2H, d, *J* = 7.5 Hz), 7.3-7.5 (4H), 7.27 (4H, d, *J* = 9.0 Hz), 6.75 (4H, d, *J* = 8.7 Hz), 3.89 (4H, t, *J* = 6.6 Hz), 1.74 (4H, m, *J* = 6.9 Hz), 1.2-1.6 (40H), 0.89 (6H, t, *J* = 6.9 Hz). ¹³C NMR (300 MHz, CD₂Cl₂, δ ppm): 159.5, 143.2, 140.0, 133.0, 132.9, 129.8, 129.1, 128.5, 127.4, 122.1, 115.1, 114.7, 92.8, 88.1, 68.3, 32.2, 29.9, 29.8, 29.6, 29.4, 26.2, 22.9, 14.1. HRMS (DART-ESI): calcd: 799.5449 (M+H)⁺, found: 799.5423.

6,13-Bis-(4'-dodecyloxyphenyl)-5,12-diiododibenz[*a,h*]anthracene (18): A 25-mL single-neck round-bottom flask containing **17** (0.030 g, 0.0375 mmol) and a magnetic stir-bar was placed under argon atmosphere. Anhydrous dichloromethane (5 mL) was then added via syringe and the resulting mixture was stirred for 5 minutes. Upon complete dissolution of the solid, the flask was immersed into a dry-ice/acetone bath at -78 °C. After stirring at that temperature for 5 minutes, a 1.0 M solution of ICl in dichloromethane (0.09 mL, 0.09 mmol) was added slowly via syringe. After the dark-colored mixture was stirred for 1 hour at -78 °C, it was diluted with dichloromethane and then transferred into a separatory funnel containing aqueous sodium hydroxide (~0.5 M, 40 mL). The dark mixture was decolorized upon shaking with NaOH, and extracted several times with additional dichloromethane (3 x 25 mL). The combined organic extracts were dried over anhydrous magnesium sulfate, filtered, and the solvent removed by rotary evaporation. The crude product was purified by flash chromatography on a silica gel column (23% v/v dichloromethane/hexane) to afford **18** (33 mg, 84%). Remaining discoloration in the product was removed by washing with small quantities of cold pentane. ¹H NMR (300 MHz, CD₂Cl₂, δ ppm): 8.69 (2H, s), 8.58 (2H, m), 8.34 (2H, m), 7.67 (4H, m), 6.3-6.7 (8H), 3.94 (4H, t, *J* = 6.6 Hz), 1.78 (4H, m, *J* = 7.5 Hz), 1.3-1.8 (40H), 0.89 (6H, t, *J* = 6.6 Hz). ¹³C NMR (300 MHz, CD₂Cl₂, δ ppm): 158.8, 144.7, 136.6, 135.3, 135.0, 131.5, 130.9, 129.5, 127.9, 127.6, 123.0, 122.3, 112.0, 106.1, 68.2, 32.2, 30.0, 29.9, 29.7, 29.6, 29.5, 26.3, 23.0, 14.2. HRMS (MALDI-TOF): calcd: 796.5219 (M - I₂)⁺, 923.4264 (M - I)⁺, found: 796.4190, 923.2850.

Polymer 8: A 25 mL Schlenk tube equipped with a magnetic stirrer was charged with a diiodide monomer **3** (0.041 g, 0.0336 mmol), diyne monomer **6** (0.0171 g, 0.0346 mmol), tetrakis(triphenylphosphine)palladium(0) (1.95 mg, 0.0017 mmol), and copper(I) iodide (0.32

mg, 0.0017 mmol). The tube was evacuated and back-filled with argon several times, after which anhydrous toluene (2 mL) and diisopropylamine (0.7 mL) were introduced via syringe. The mixture is sparged with argon for 10 minutes at room temperature, followed by stirring at 65 °C for 48 hours, and an additional 24 hours at 75 °C. Upon cooling to room temperature, the mixture was precipitated in rapidly stirring methanol and isolated by centrifugation. The polymer was redissolved in a minimum volume of chloroform, and the precipitation / centrifugation process was repeated several times in methanol, acetone, and pentane. Finally, polymer **8** was dried under reduced pressure to give an orange-red solid (45 mg, 89%). ¹H NMR (300 MHz, CDCl₃, δ ppm): 10.05 (2H, m), 9.79 (2H, m), 8.93 (2H, m), 6.54-7.58 (14H, m), 4.11 (8H, m), 2.70 (4H, m), 0.30-1.90 (114H, m). GPC (THF, vs. PS): M_n = 21500, M_w = 50200.

Polymer 9: A 25 mL Schlenk tube equipped with a magnetic stirrer was charged with a diiodide monomer **3** (0.029 g, 0.0238 mmol), diyne monomer **7** (0.0117 g, 0.0245 mmol), tetrakis(triphenylphosphine)palladium(0) (1.38 mg, 0.0012 mmol), and copper(I) iodide (0.23 mg, 0.0012 mmol). The tube was evacuated and back-filled with argon several times, after which anhydrous toluene (1.5 mL) and diisopropylamine (0.5 mL) were introduced via syringe. The mixture is sparged with argon for 10 minutes at room temperature, followed by stirring at 65 °C for 48 hours, and an additional 24 hours at 75 °C. Upon cooling to room temperature, the mixture was precipitated in rapidly stirring methanol and isolated by centrifugation. The polymer was redissolved in a minimum volume of chloroform, and the precipitation / centrifugation process was repeated several times in methanol, acetone, and pentane. Finally, polymer **9** was dried under reduced pressure to give a yellow solid (30 mg, 86%). ¹H NMR (300 MHz, CDCl₃, δ

ppm): 9.00 (2H, m), 5.95-7.80 (28H, m), 4.01 (8H, m), 2.71 (4H, m), 1.70-2.30 (114H, m). GPC (THF, vs. PS): $M_n = 10600$, $M_w = 25700$.

Polymer 13: A 25 mL Schlenk tube equipped with a magnetic stirrer was charged with a diiodide monomer **12** (0.027 g, 0.020 mmol), diyne monomer **6** (0.010 g, 0.020 mmol), tetrakis(triphenylphosphine)palladium(0) (1.1 mg, 0.00093 mmol), and copper(I) iodide (0.18 mg, 0.00093 mmol). The tube was evacuated and back-filled with argon several times, after which anhydrous toluene (1.5 mL) and diisopropylamine (0.5 mL) were introduced via syringe. The mixture is sparged with argon for 10 minutes at room temperature, followed by stirring at 65 °C for 48 hours, and an additional 24 hours at 75 °C. Upon cooling to room temperature, the mixture was precipitated in rapidly stirring methanol and isolated by centrifugation. The polymer was redissolved in a minimum volume of chloroform, and the precipitation / centrifugation process was repeated several times in methanol, acetone, and pentane. Finally, polymer **13** was dried under reduced pressure to give a red solid (62 mg, 85%). ¹H NMR (300 MHz, CDCl₃, δ ppm): 9.94 (2H, m), 9.00 (2H, m), 6.60-7.58 (14H, m), 3.96-4.10 (12H, m), 0.85-1.28 (130H, m). GPC (THF, vs. PS): $M_n = 19000$, $M_w = 72000$.

Polymer 19: A 25 mL Schlenk tube equipped with a magnetic stirrer was charged with a diiodide monomer **18** (0.033 g, 0.0314 mmol), diyne monomer **6** (0.016 g, 0.0323 mmol), tetrakis(triphenylphosphine)palladium(0) (1.81 mg, 0.0016 mmol), and copper(I) iodide (0.3 mg, 0.0016 mmol). The tube was evacuated and back-filled with argon several times, after which anhydrous toluene (2 mL) and diisopropylamine (0.6 mL) were introduced via syringe. The mixture is sparged with argon for 10 minutes at room temperature, followed by stirring at 65 °C

for 48 hours, and an additional 24 hours at 75 °C. Upon cooling to room temperature, the mixture was precipitated in rapidly stirring methanol and isolated by centrifugation. The polymer was redissolved in a minimum volume of chloroform, and the precipitation / centrifugation process was repeated several times in methanol, acetone, and pentane. Finally, polymer **19** was dried under reduced pressure to give a deep red solid (30 mg, 74%). ¹H NMR (300 MHz, CDCl₃, δ ppm): 8.78 (2H, m), 8.72 (2H, m), 8.40 (2H, m), 7.70 (4H, m), 6.25-6.96 (10H, m), 3.95 (8H, m), 0.85-2.00 (92H, m). GPC (THF, vs. PS): Mn = 10400, Mw = 17400.

References and Notes

- [1] a) Bunz, U. H. F. *Macromol. Rapid. Commun.* **2009**, *30*, 772-805; b) Bunz, U. H. F. *Chem. Rev.* **2000**, *100*, 1605-1644.
- [2] a) Burnworth, M.; Rowan, S. J.; Weder, C. *Chem. Eur. J.* **2007**, *13*, 7828-7836; b) Knapton, D.; Burnworth, M.; Rowan, S. J.; Weder, C. *Angew. Chem.* **2006**, *45*, 5825-5829; c) Zhang, S. W.; Swager, T. M. *J. Am. Chem. Soc.* **2003**, *125*, 3420-3421.
- [3] Chan, J. M. W.; Tischler, J. R.; Kooi, S. E.; Bulović, V.; Swager, T. M. *J. Am. Chem. Soc.* **2009**, *131*, 5659-5666.
- [4] a) Taylor, M. S.; Swager, T. M. *Angew. Chem. Int. Ed.* **2007**, *46*, 8480-8483; b) Anthony, J. E. *Chem. Rev.* **2006**, *106*, 5028-5048; c) Baumgarten, M.; Müller, U.; Bohnen, A.; Müllen, K. *Angew. Chem.* **1992**, *104*, 482-485; *Angew. Chem. Int. Ed. Engl.* **1992**, *31*, 448-451; d) Weitzel, H.-P.; Bohnen, A.; Müllen, K. *Makromol. Chem.* **1990**, *191*, 2815-2835; e) Weitzel, H.-P.; Müllen, K. *Makromol. Chem.* **1990**, *191*, 2837-2851; f) Heun, S.; Bässler, H.; Müller,

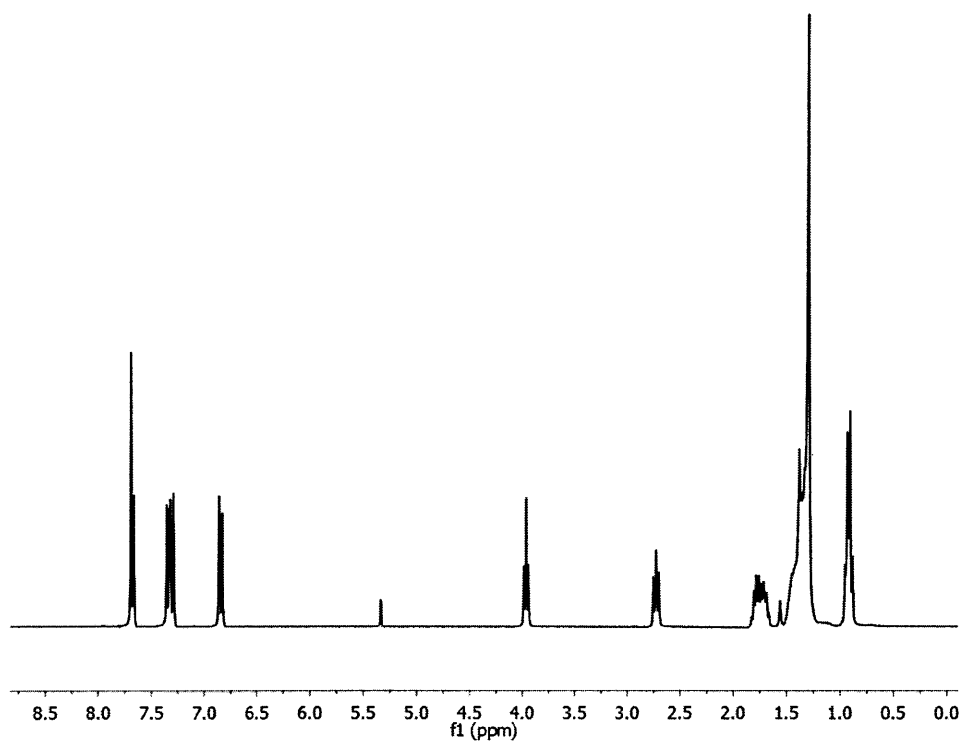
- U.; Müllen, K. *J. Phys. Chem.* **1994**, *98*, 7355-7358; g) Ishow, E.; Bouffard, J.; Kim, Y.; Swager, T. M. *Macromolecules*, **2006**, *39*, 7854-7858; h) Egbe, D. A. M.; Cornelia, B.; Nowotny, J.; Günther, W.; Klemm, E. *Macromolecules*, **2003**, *36*, 5459-5469; i) Kaneko, T.; Matsubara, T.; Aoki, T. *Chem. Mater.* **2002**, *14*, 3898-3906; j) Moroni, M.; Le Moigne, J.; Pham, T. A.; Bigot, J.-Y. *Macromolecules*, **1997**, *30*, 1964-1972; k) Swager, T. M.; Gil, C. J.; Wrighton, M. S. *J. Phys. Chem.* **1995**, *99*, 4886-4893. l) Yang, C.; Jacob, J.; Müllen, K. *Macromolecules*, **2006**, *39*, 5696-5704.
- [5] Yamaguchi, S.; Swager, T. M. *J. Am. Chem. Soc.* **2001**, *123*, 12087-12088.
- [6] Rose, A.; Lugmair, C. G.; Swager, T. M. *J. Am. Chem. Soc.* **2001**, *123*, 11298-11299.
- [7] Corey, E. J.; Fuchs, P. L. *Tetrahedron Lett.* **1972**, 3769-3772.
- [8] a) Zhu, Z.; Swager, T. M. *Org. Lett.* **2001**, *3*, 3471-3474; b) Zhao, D.; Swager, T. M. *Macromolecules* **2005**, *38*, 9377-9384.
- [9] a) Olmsted, J., III *J. Phys. Chem.* **1979**, *83*, 2581-2584; b) Demas, J. N.; Crosby, G. A. *J. Phys. Chem.* **1971**, *75*, 991-1024; c) Melhuish, W. H. *J. Phys. Chem.* **1961**, *65*, 229-235; d) Dawson, W. R.; Windsor, M. W. *J. Phys. Chem.* **1968**, *72*, 3251-3260.
- [10] Melhuish, W. H. *J. Opt. Soc. Am.* **1964**, *52*, 183-186.
- [11] a) Yang, J.-S.; Swager, T. M. *J. Am. Chem. Soc.* **1998**, *120*, 5321-5322; b) Yang, J.-S.; Swager, T. M. *J. Am. Chem. Soc.* **1998**, *120*, 11864-11873; c) Bouffard, J.; Swager, T. M. *Macromolecules* **2008**, *41*, 5559-5562.
- [12] Lakowicz, J. R., *Principles of Fluorescence Spectroscopy 3rd Ed.*; Springer: Singapore 2006.

Chapter 4 Appendix

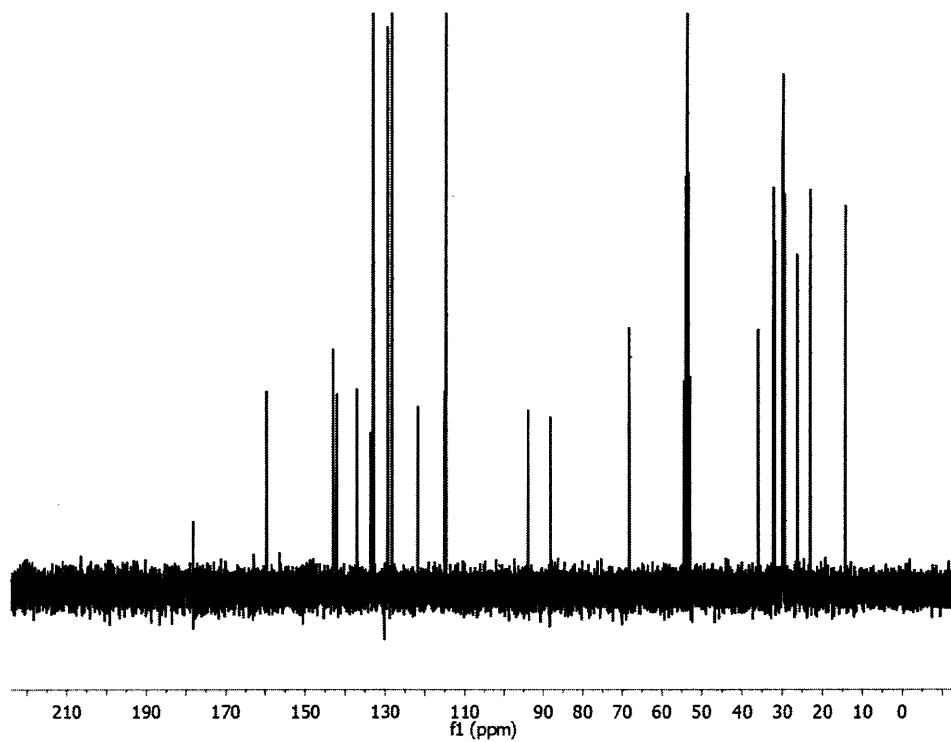
^1H -NMR and ^{13}C -NMR Spectra

Adapted and reproduced with permission from:

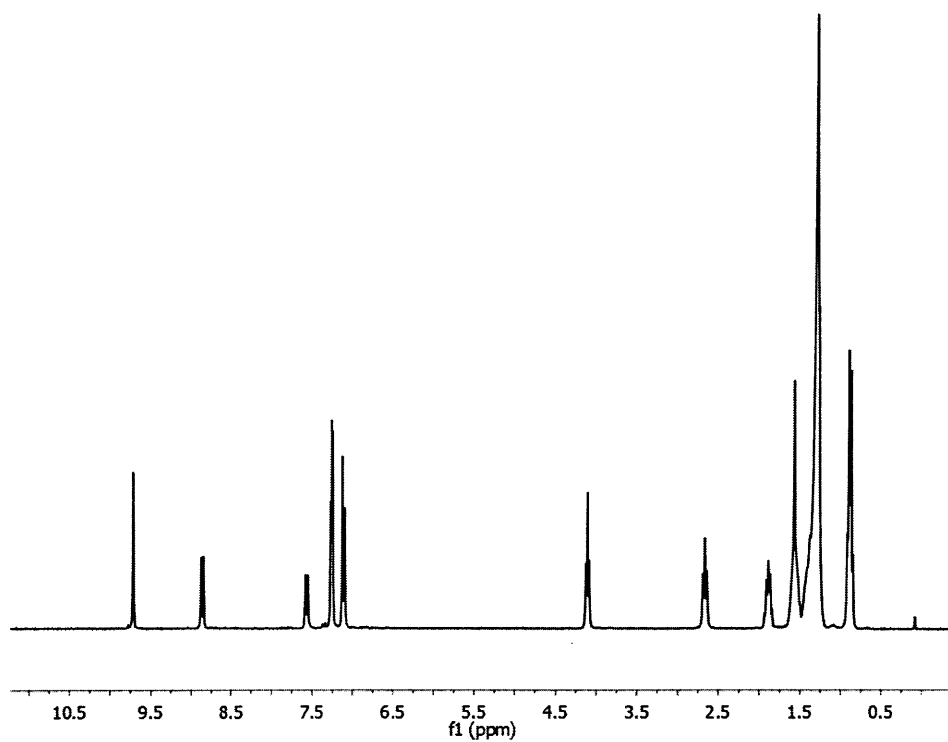
Chan, J. M. W., Kooi, S. E., Swager, T. M. *Macromolecules* **2010**, *43*, 2789-2793.



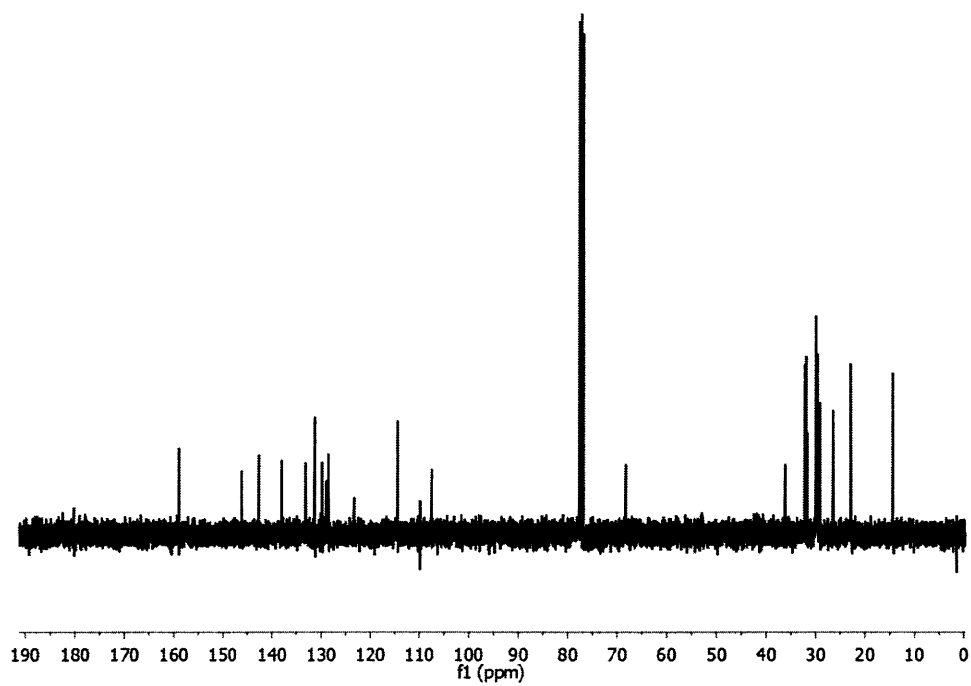
Spectrum 44. ^1H -NMR spectrum of **2** (300 MHz, CD_2Cl_2).



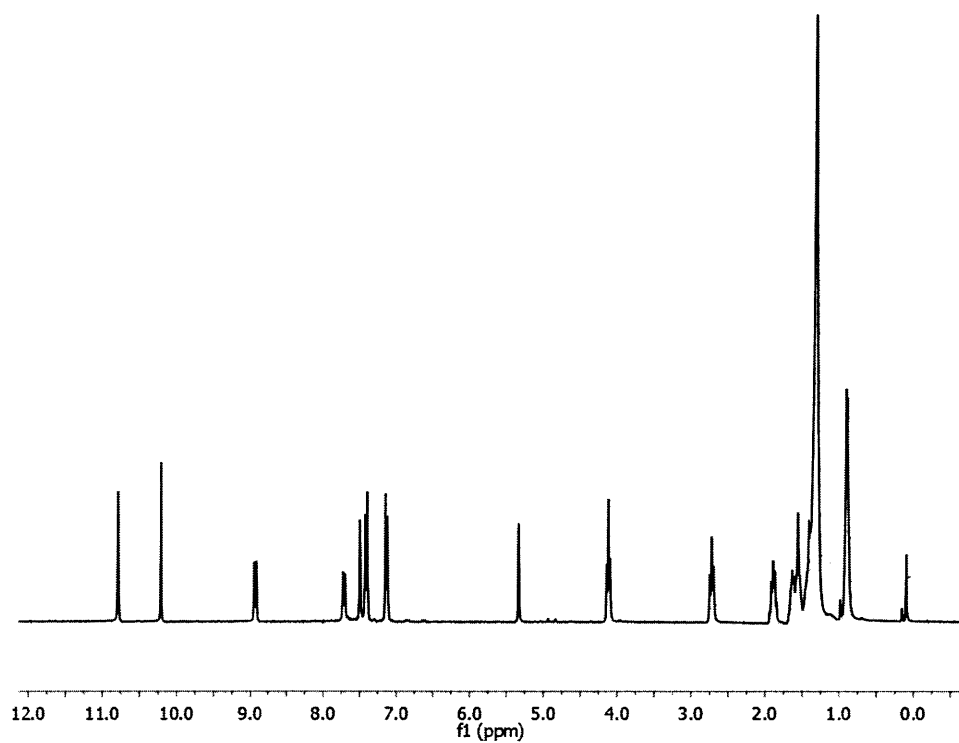
Spectrum 45. ^{13}C -NMR spectrum of **2** (300 MHz, CD_2Cl_2).



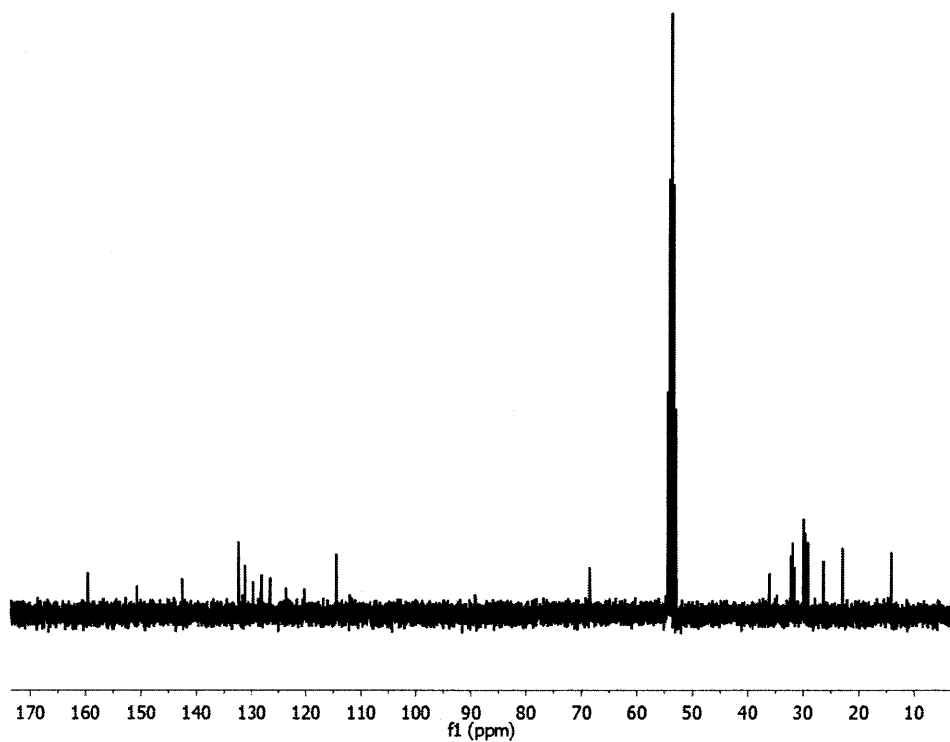
Spectrum 46. ^1H -NMR spectrum of **3** (300 MHz, CDCl_3).



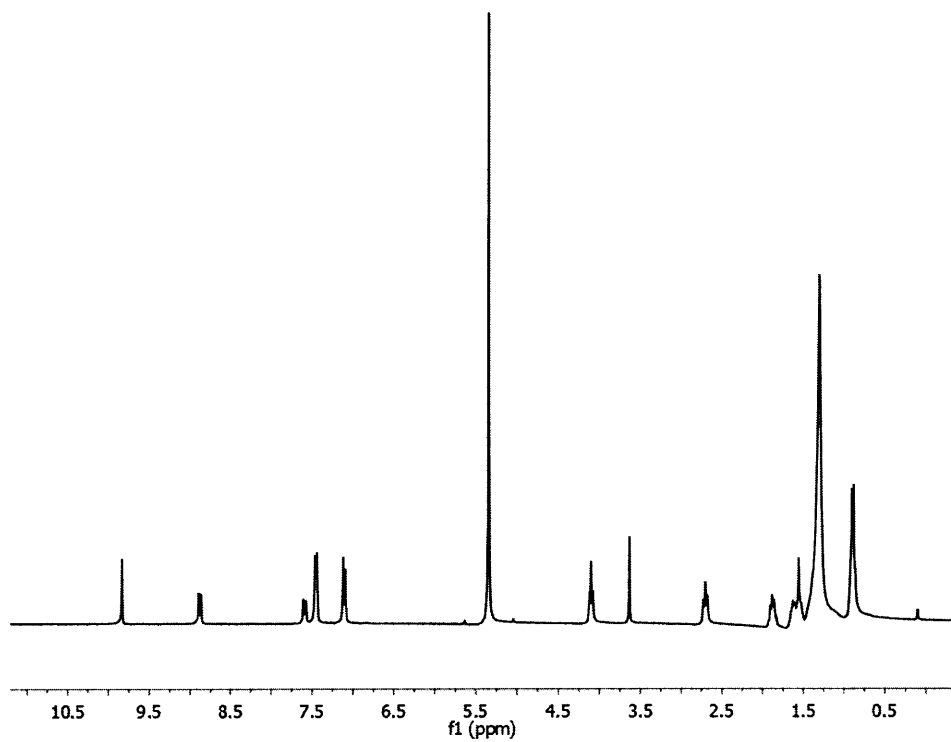
Spectrum 47. ^{13}C -NMR spectrum of **3** (300 MHz, CDCl_3).



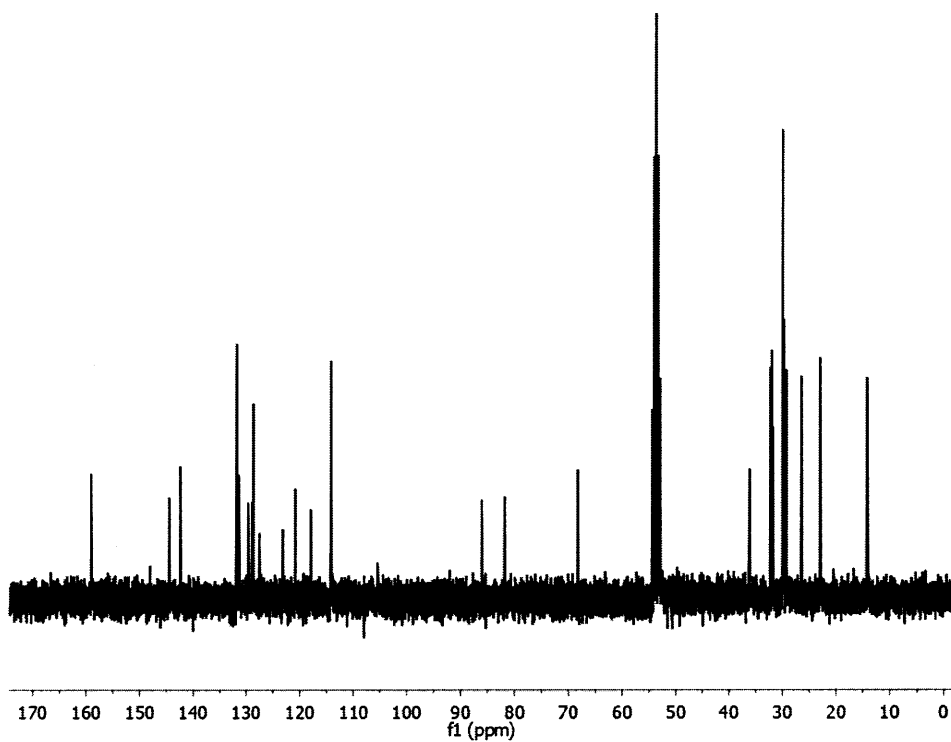
Spectrum 48. ^1H -NMR spectrum of **4** (300 MHz, CD_2Cl_2).



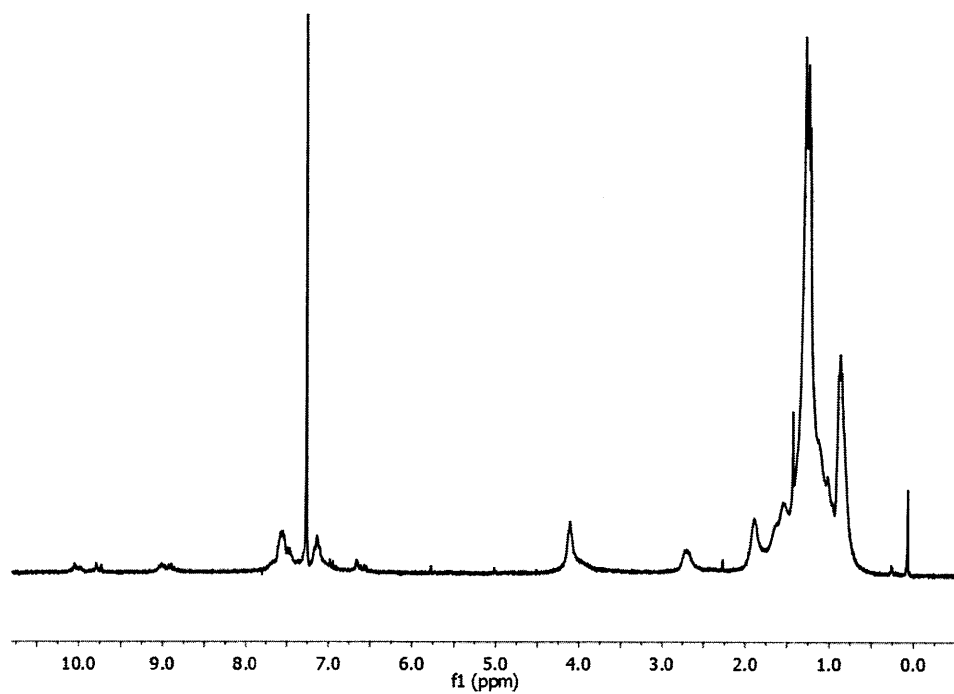
Spectrum 49. ^{13}C -NMR spectrum of **4** (300 MHz, CD_2Cl_2).



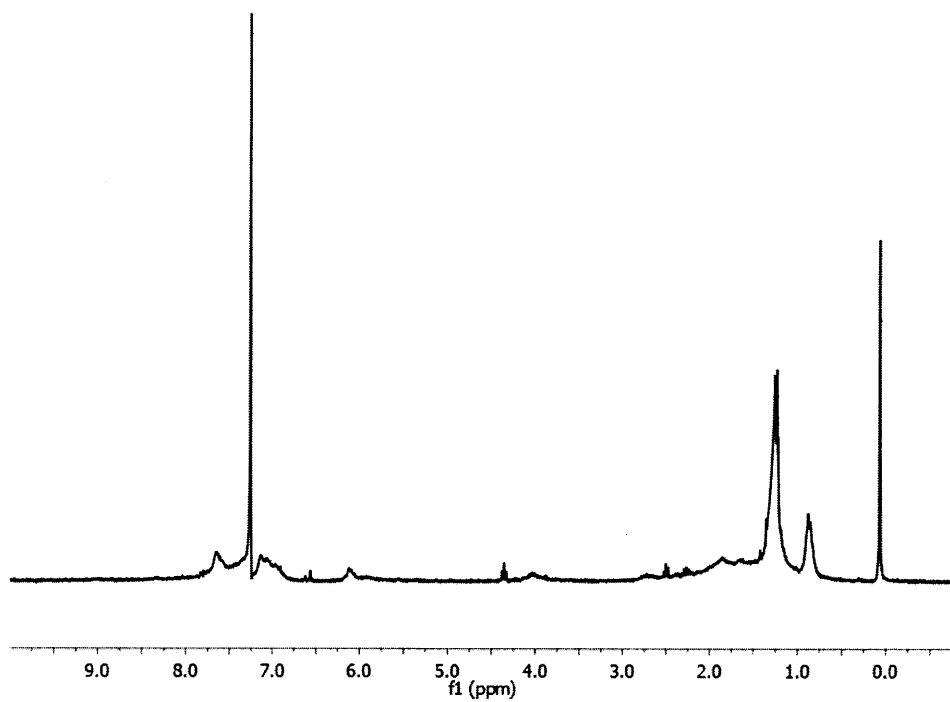
Spectrum 50. ^1H -NMR spectrum of **5** (300 MHz, CD_2Cl_2).



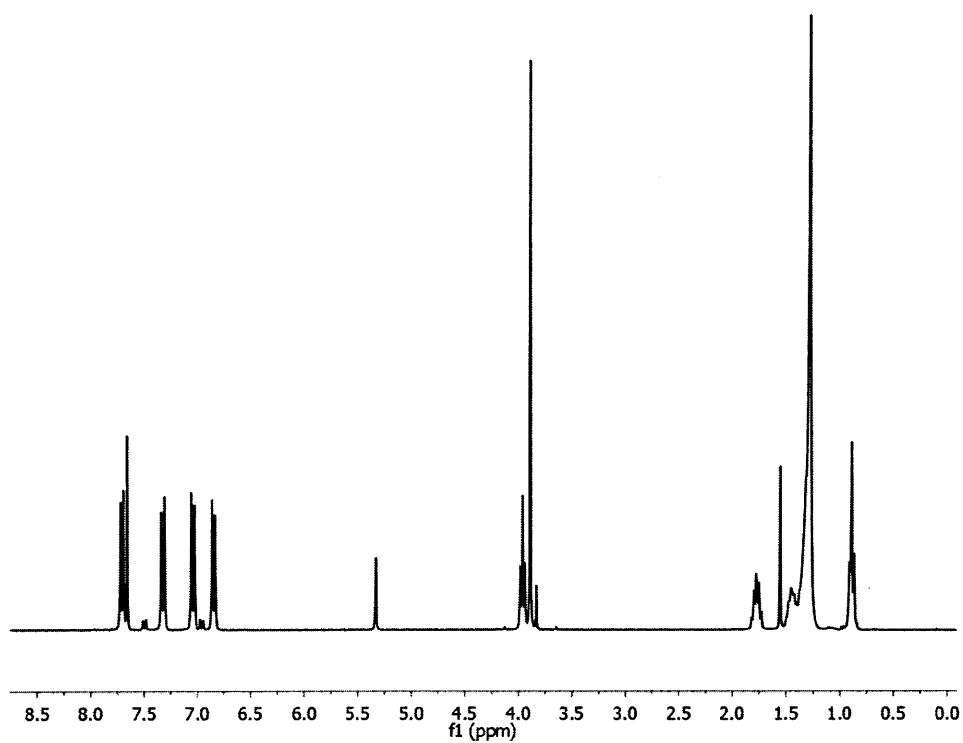
Spectrum 51. ^{13}C -NMR spectrum of **5** (300 MHz, CD_2Cl_2).



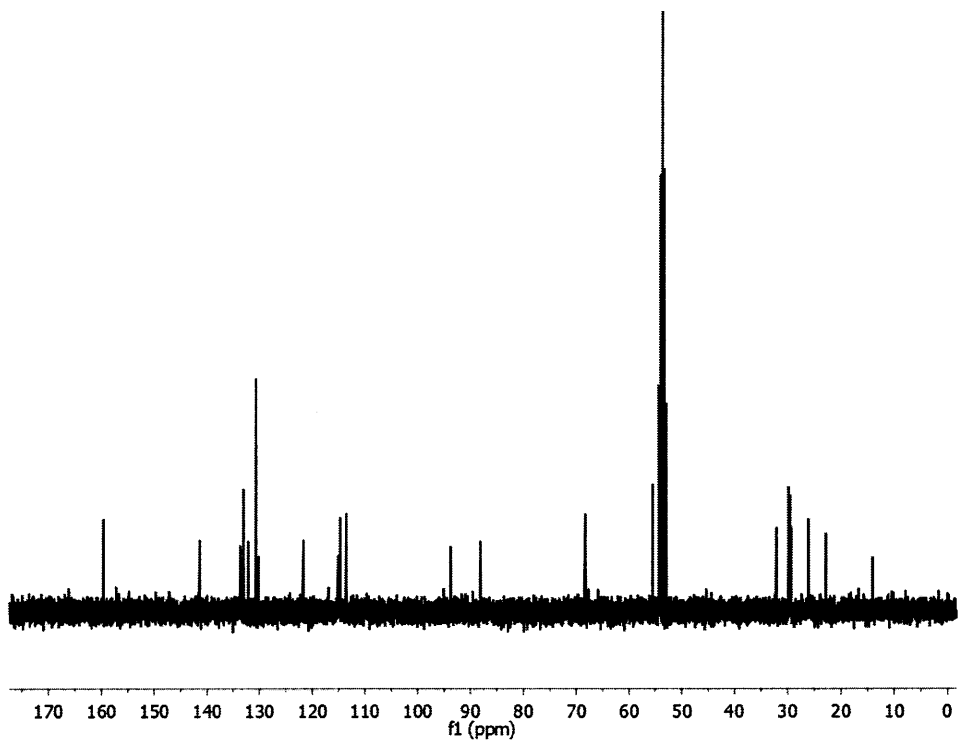
Spectrum 52. ¹H-NMR spectrum of **5** (300 MHz, CDCl₃).



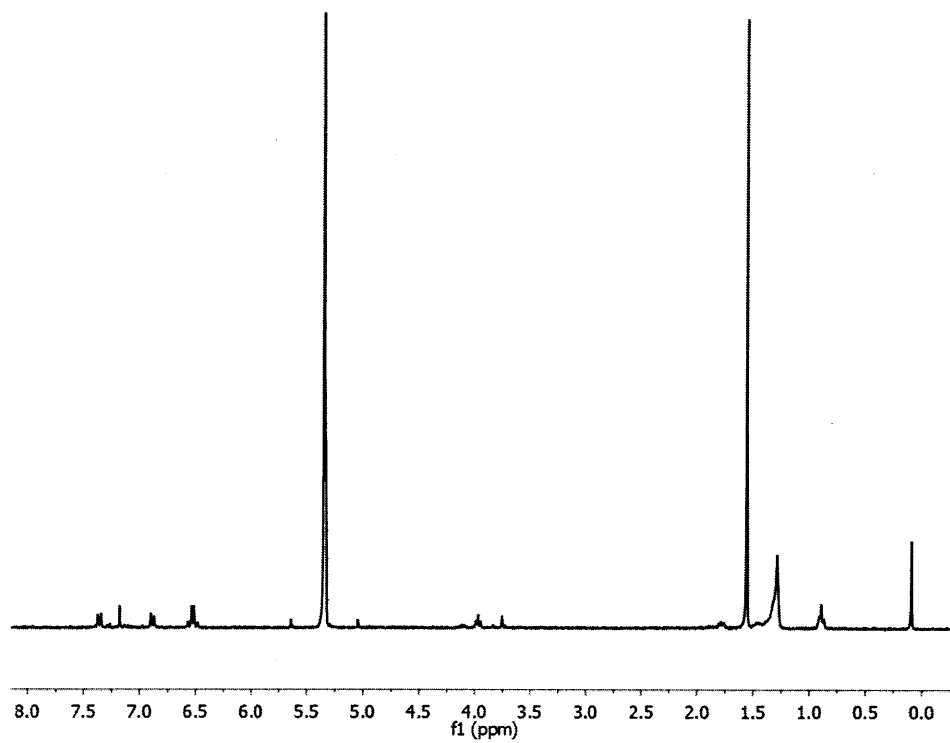
Spectrum 53. ¹H-NMR spectrum of **9** (300 MHz, CDCl₃).



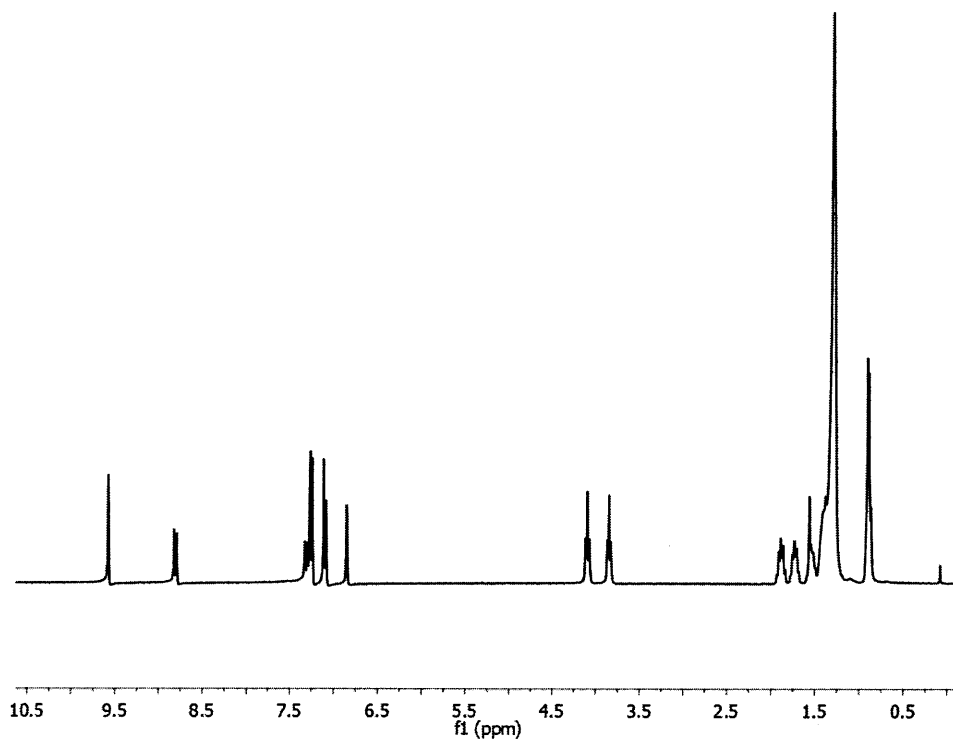
Spectrum 54. ^1H -NMR spectrum of **10** (300 MHz, CD_2Cl_2).



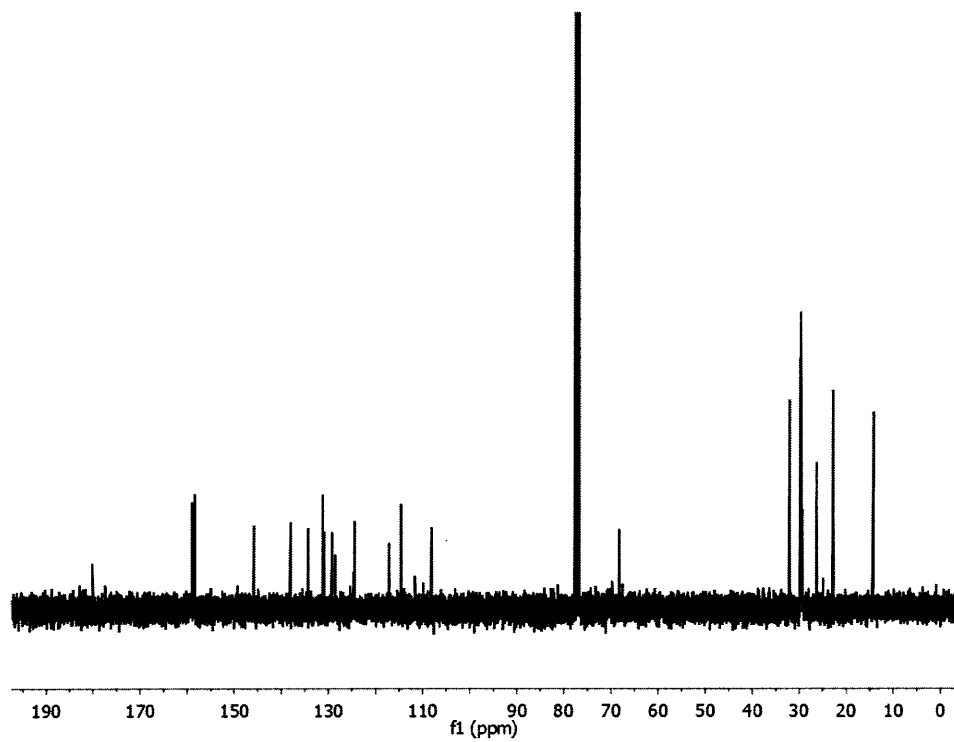
Spectrum 55. ^{13}C -NMR spectrum of **10** (300 MHz, CD_2Cl_2).



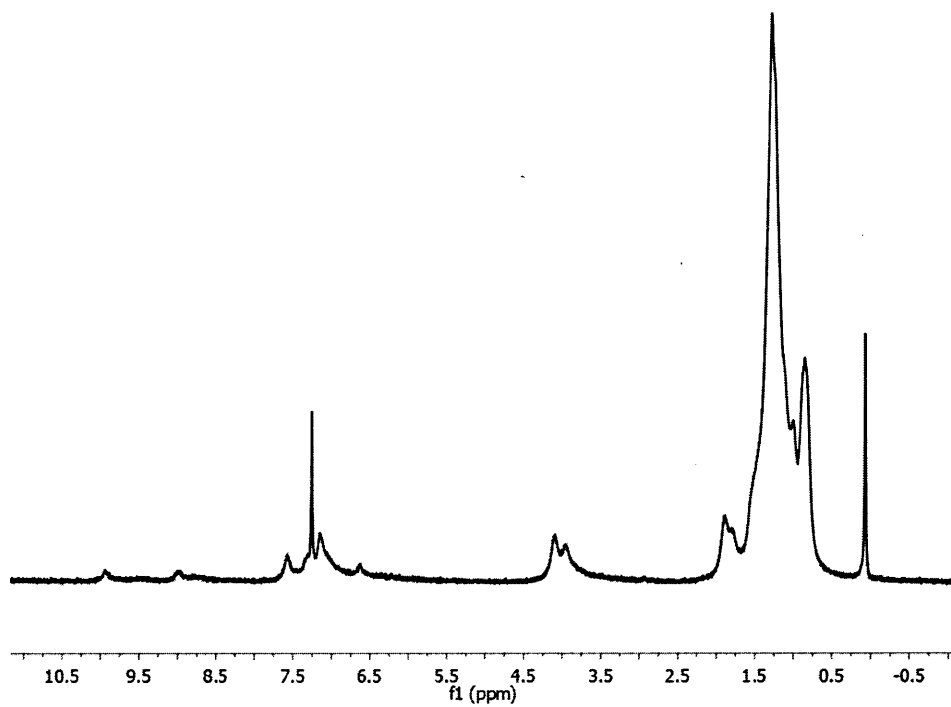
Spectrum 55. ^1H -NMR spectrum of **11** (300 MHz, CD_2Cl_2).



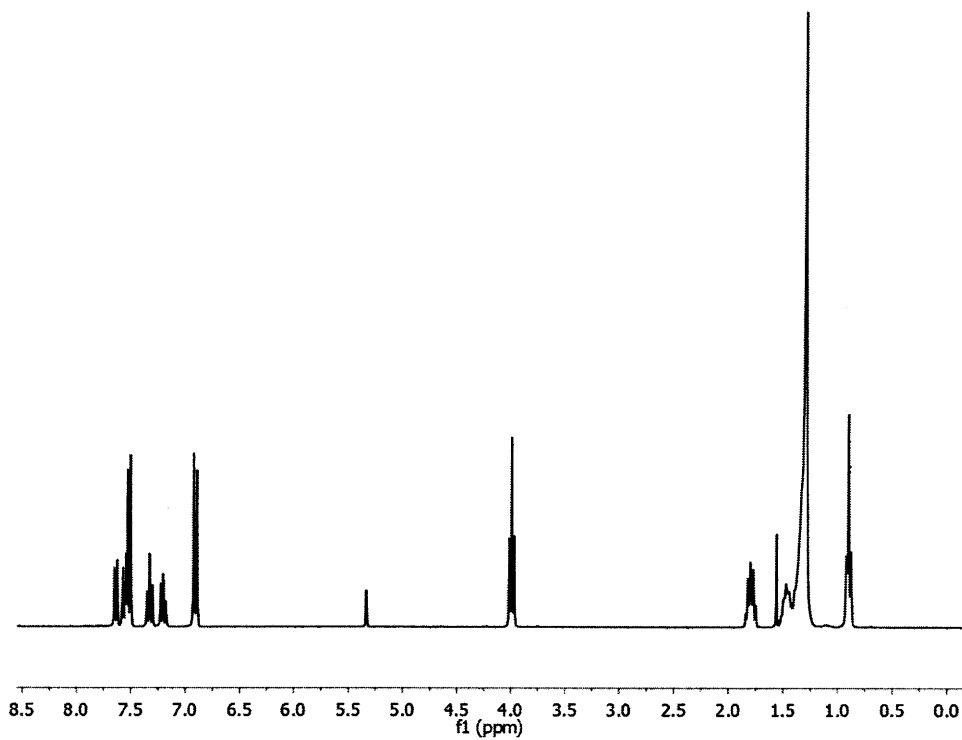
Spectrum 56. ^1H -NMR spectrum of **12** (300 MHz, CDCl_3).



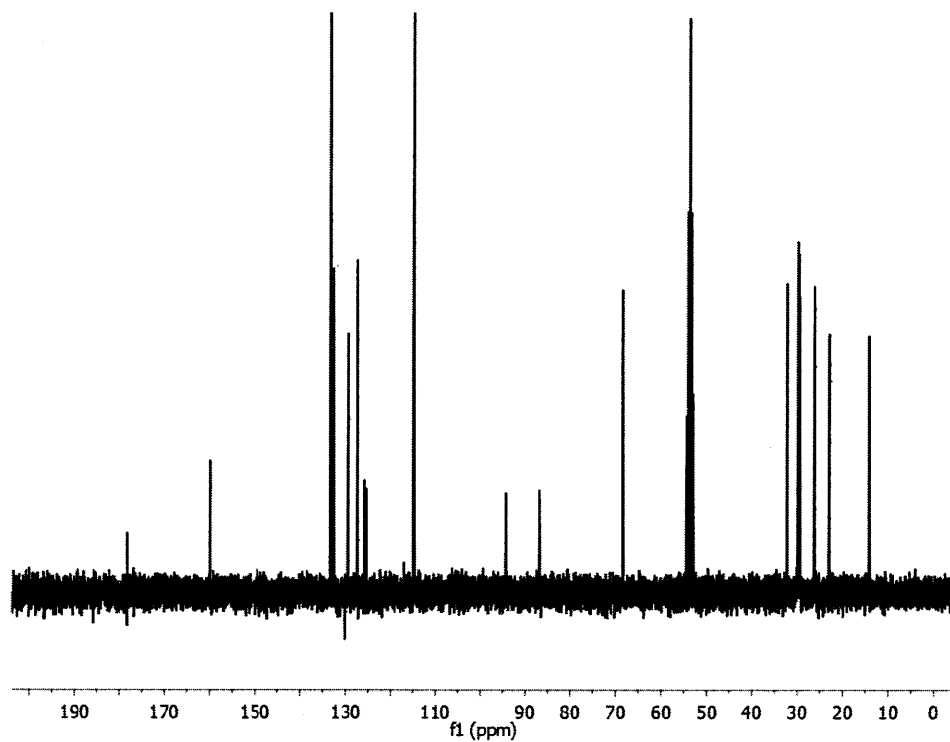
Spectrum 57. ^{13}C -NMR spectrum of **12** (300 MHz, CDCl_3).



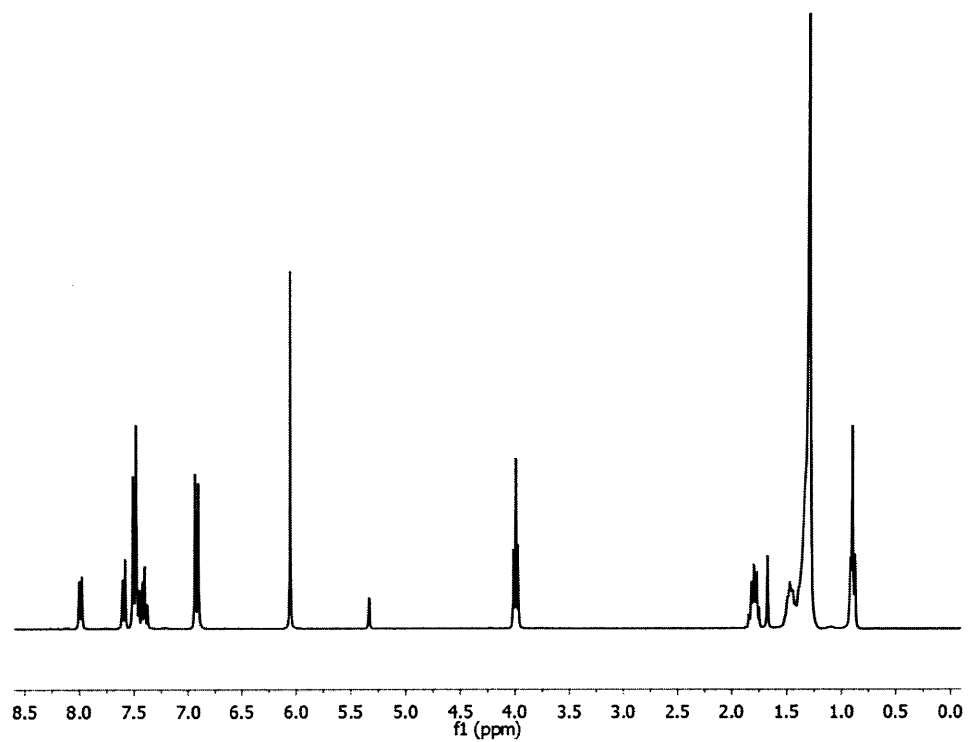
Spectrum 58. ^1H -NMR spectrum of **13** (300 MHz, CDCl_3).



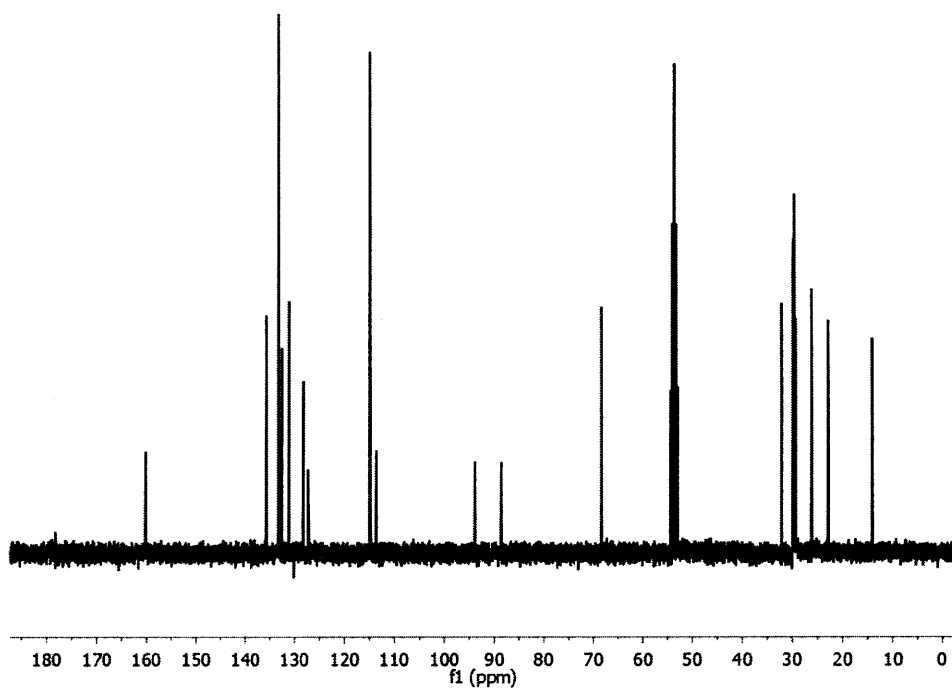
Spectrum 59. ^1H -NMR spectrum of **15** (300 MHz, CD_2Cl_2).



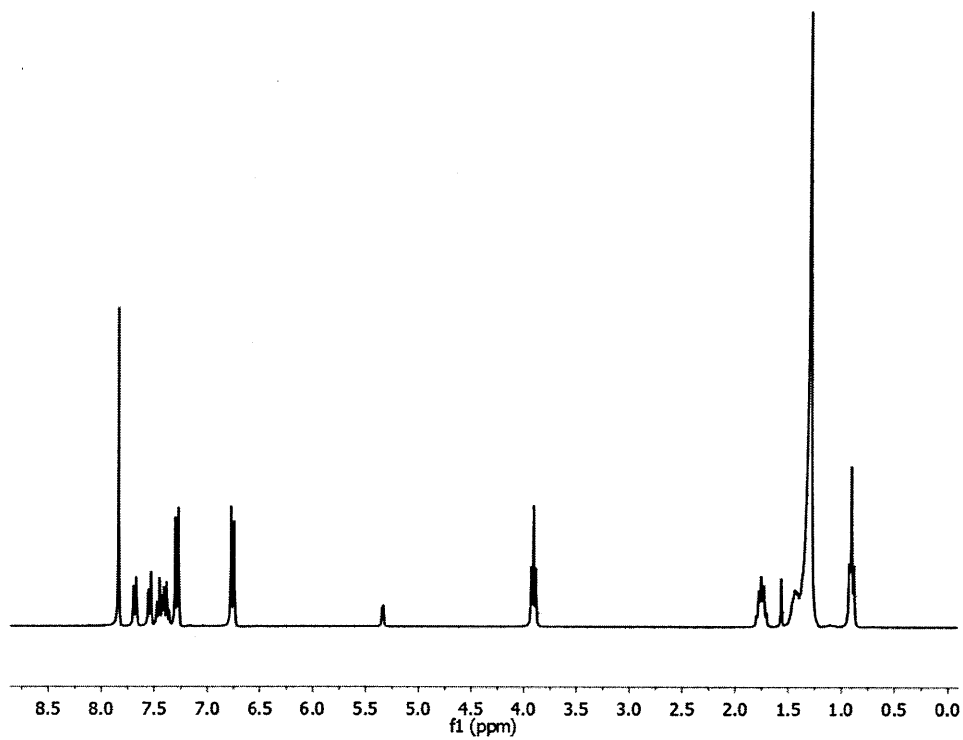
Spectrum 60. ^{13}C -NMR spectrum of **15** (300 MHz, CD_2Cl_2).



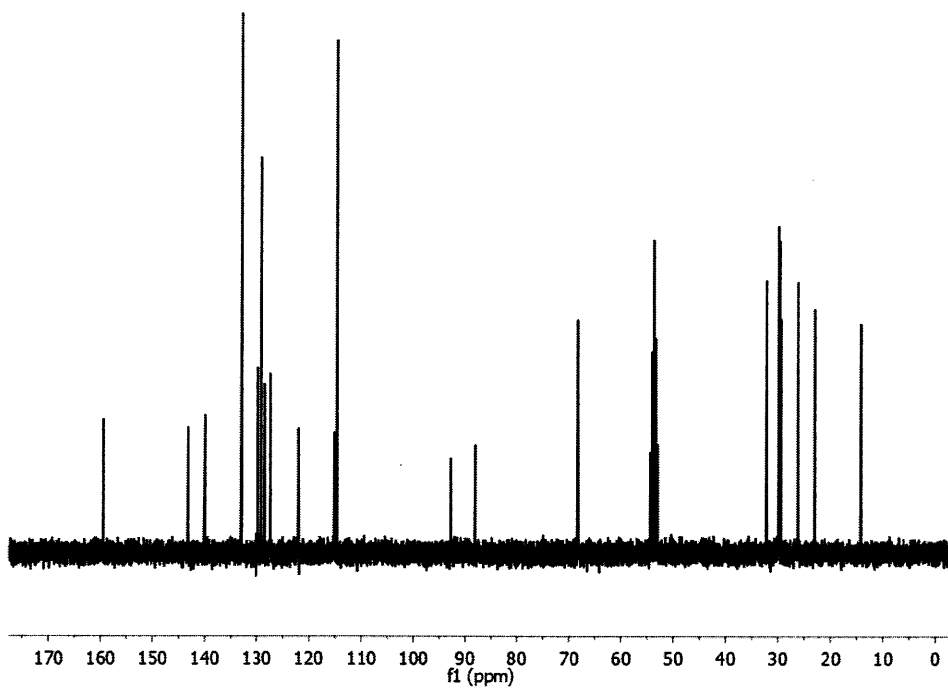
Spectrum 61. ^1H -NMR spectrum of **16** (300 MHz, CD_2Cl_2).



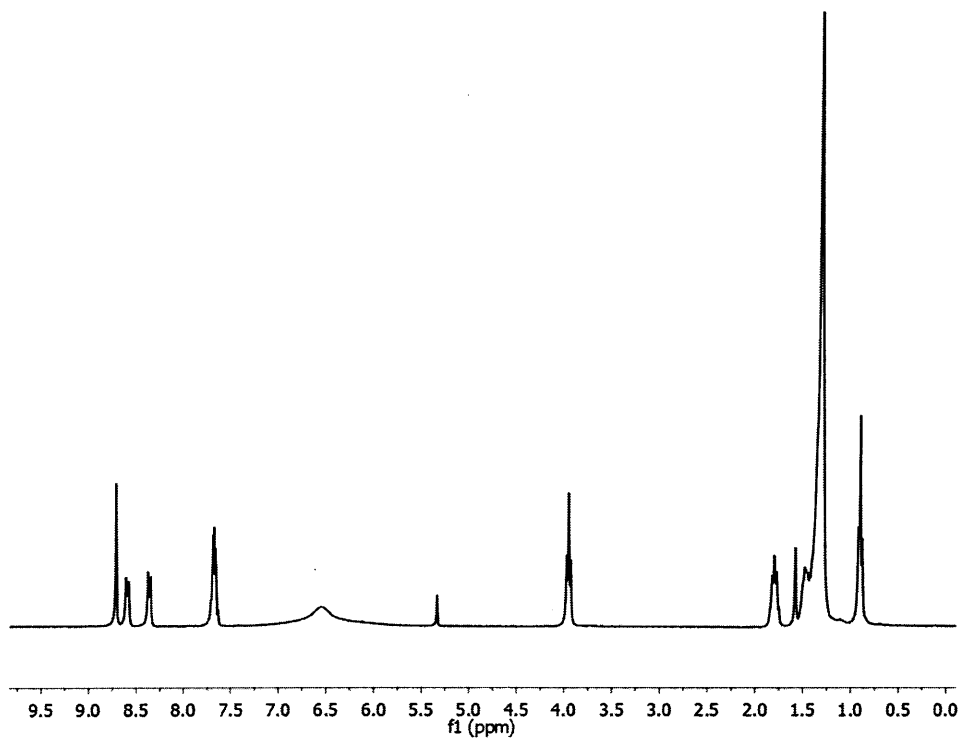
Spectrum 62. ^{13}C -NMR spectrum of **16** (300 MHz, CD_2Cl_2).



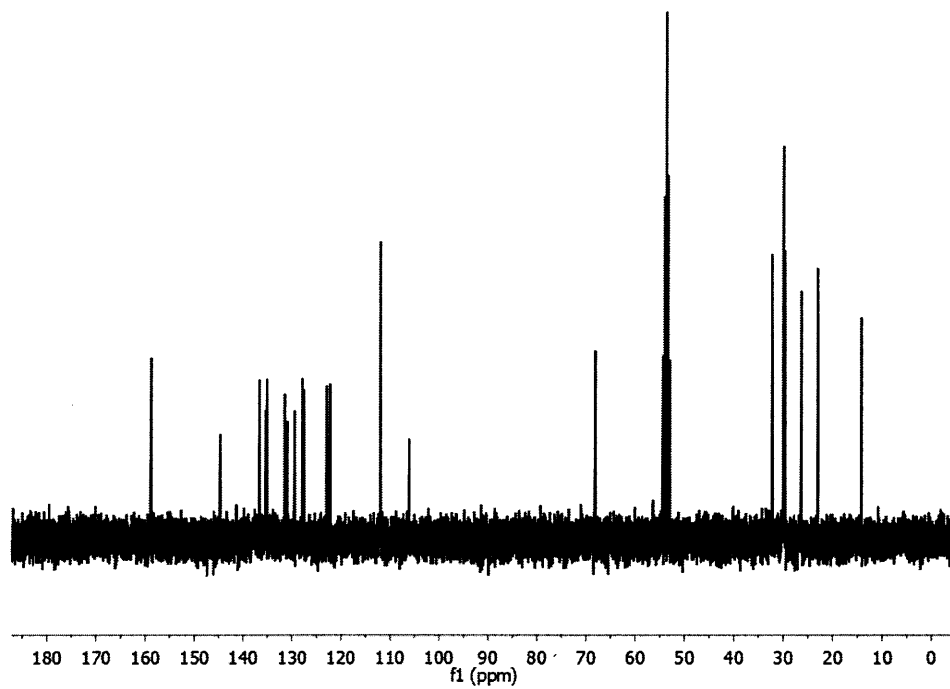
Spectrum 63. ^1H -NMR spectrum of **17** (300 MHz, CD_2Cl_2).



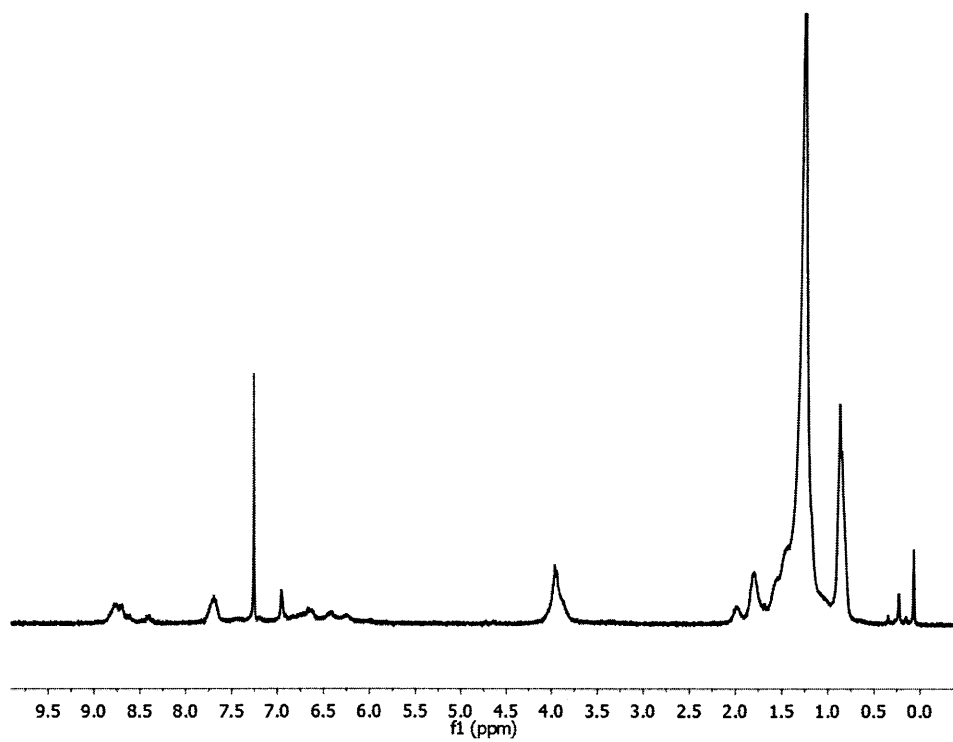
Spectrum 64. ^{13}C -NMR spectrum of **17** (300 MHz, CD_2Cl_2).



Spectrum 65. ^1H -NMR spectrum of **18** (300 MHz, CD_2Cl_2).



Spectrum 66. ^{13}C -NMR spectrum of **18** (300 MHz, CD_2Cl_2).



Spectrum 67. ^1H -NMR spectrum of **19** (300 MHz, CDCl_3).

Chapter 5
Towards Novel J-aggregating
Structures

5.1 Introduction

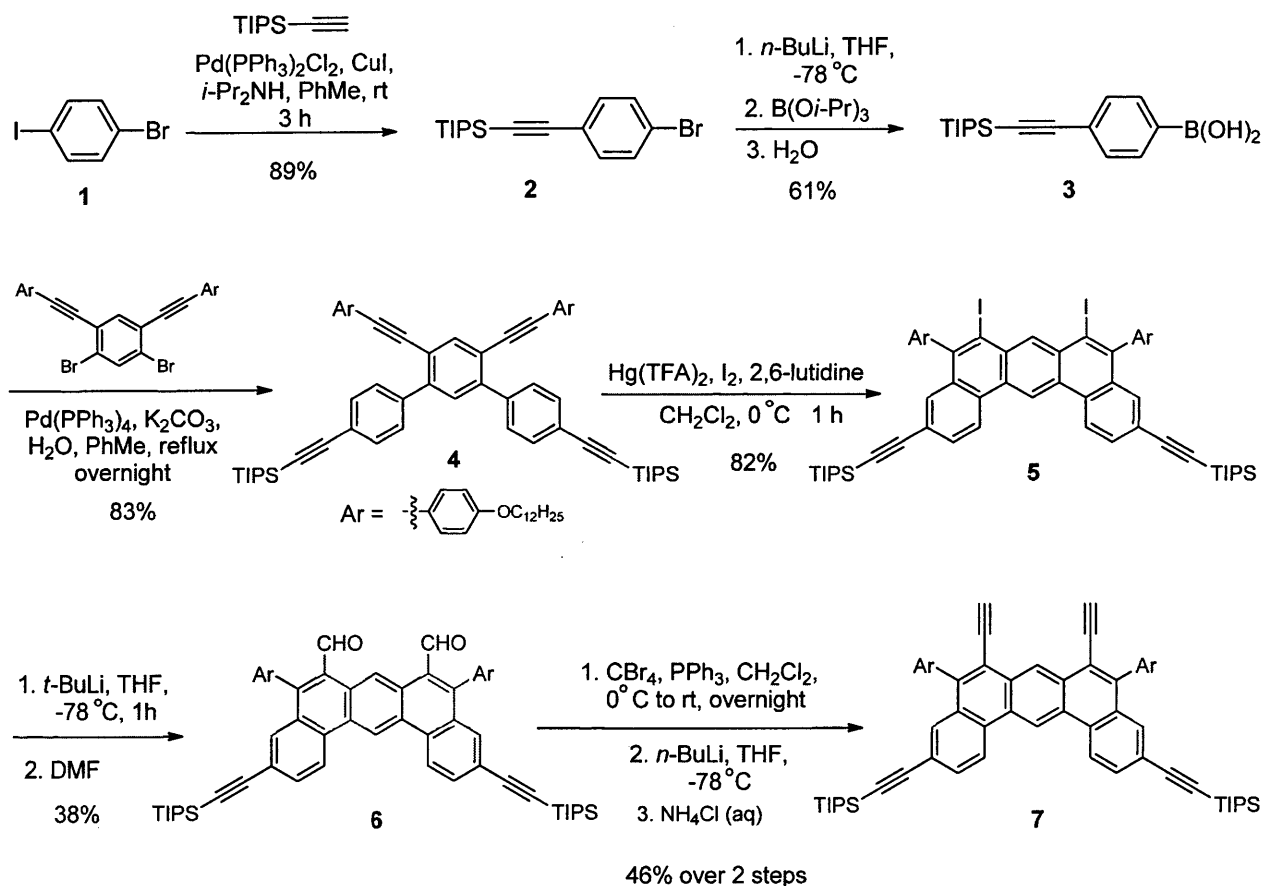
Following the success in designing and synthesizing the novel dibenz[*a,j*]anthracene-based J-aggregates described in Chapter 3, we envisioned a variety of new candidate structures based on the same design principles that had proven effective in producing J-aggregation in the abovementioned compounds. In particular, this follow-up work was an attempt to find J-aggregation in specially designed twisted polymers and small molecules. On one hand, a polymer would allow for band-gap tuning, enhanced stability, as well as increased processability compared to small molecules. However, with a polymer, one would also have to contend with the presence of unavoidable defects within the backbone, as well as morphologies and solid-state packing modes that are difficult to predict and even harder to control. Conversely, a small molecule candidate often allows for greater control of its structure-property relationship, but it is usually more challenging to produce uniform thin-films of small molecules as opposed to a soluble polymer. This translates into practical issues should the need for incorporation into devices arise. In any case, we decided to explore both small molecules and polymeric structures that possessed a slight internal twist, based on the observation that many common cyanine dye J-aggregates¹, as well as our dibenz[*a,j*]anthracene J-aggregates², are twisted out of planarity by virtue of intramolecular steric repulsions. By designing moderately twisted candidate structures with small dihedral angles, we had hoped to induce slip-stacked structures within the solid-state to bring about J-aggregation, not unlike the slipped arrangements seen in natural and artificial light-harvesting systems.³ The efforts detailed herein may be categorized into three parts. In the first attempt to create a J-aggregating polymer, the dimeric dibenz[*a,j*]anthracene motif was synthetically incorporated into a network polymer. The second approach was to design, *de novo*, a slip-inducing repeat unit that could easily be incorporated into a linear polymer structure. The

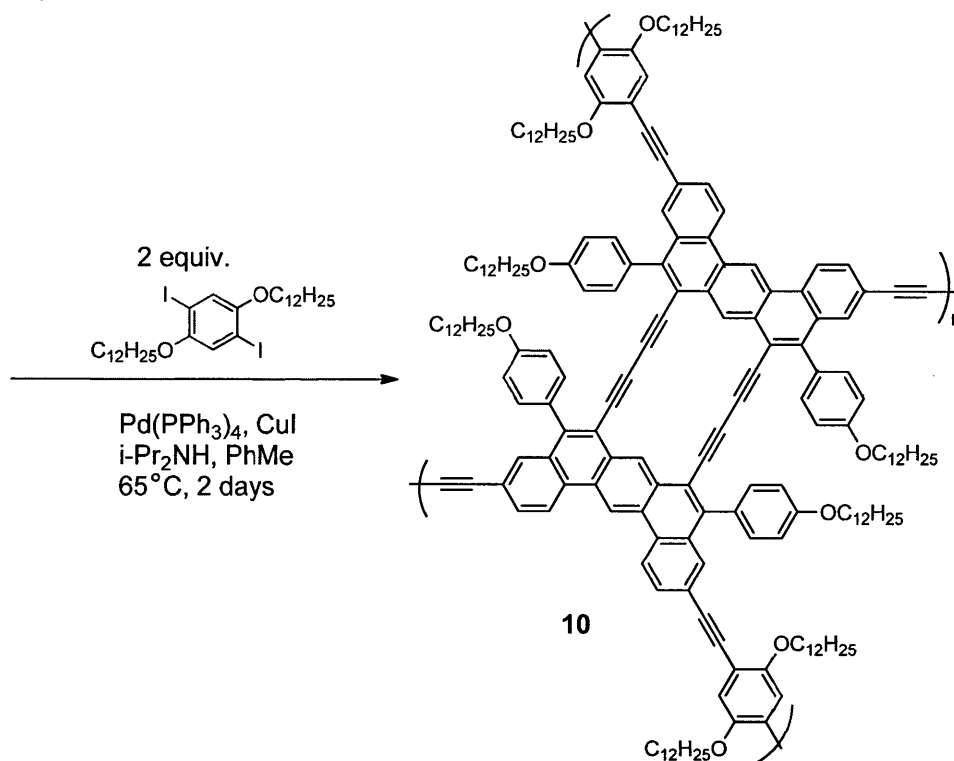
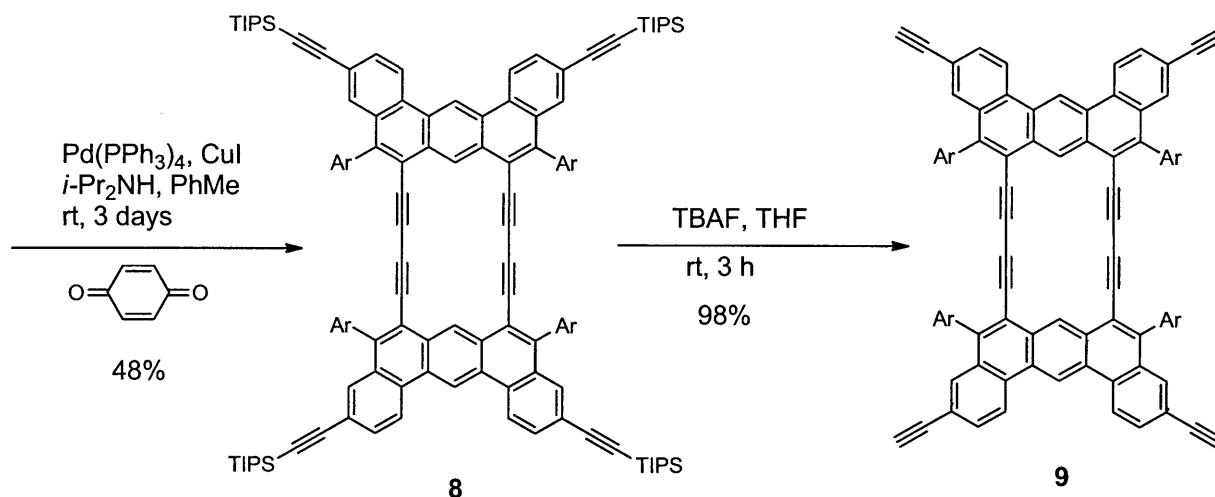
third and final approach involved the use of a class of polycyclic aromatic small molecules known as the dibenz[*a,m*]rubicenes, which are moderately twisted aromatic species that would otherwise be flat if not for the existence of internal steric repulsions.

5.2 Extension of the dibenz[*a,j*]anthracene dimer motif

Following the observation of J-aggregation in dibenz[*a,j*]anthracene-based macrocycles, it was interesting to determine whether this physical property would be retained in a polymer containing the same structural motif. In order to do this, monomer **9** was synthesized over eight steps from the commercially available 1-bromo-4-iodobenzene (Scheme 5.1).

Scheme 5.1. Synthesis of a network polymer containing dibenz[*a,j*]anthracene repeat units





The strategy for the synthesis of **9** is the same as that employed in the preparation of the dibenz[*a,j*]anthracene J-aggregates, namely, macrocycle formation via the annulation between two identical dibenz[*a,j*]anthracene subunits. In this case however, terminal alkynes instead of long alkyl chains are located on the polycyclic aromatic moieties, serving as synthetic handles for the subsequent polymerization. It should also be noted that in the lithiation/formylation step

going from **5** to **6**, the usual $\text{Fe}(\text{CO})_5$ followed by acetic acid workup could not be used, due to an apparent incompatibility with the protected alkynes. However, substituting the iron-based formylating reagent with anhydrous *N,N*-dimethylformamide gave good results. Following the macrocyclization step, the triisopropylsilyl-protected tetraalkyne **8** was tested spectroscopically. The solution absorption and emission maxima were found to be 447 nm and 462 nm respectively (Figure 5.1a), values which are nearly identical to those observed with the dibenz[*a,j*]anthracene J-aggregates. The significant difference however, is that compound **8** did not appear to J-aggregate in thin films, as evidenced by the complete absence of any intense J-band in the film-state UV-vis spectrum (Figure 5.1b). The lack of J-aggregation here is not surprising, given that the four bulky triisopropylsilyl groups would be expected to interfere with the π - π self-assembly process.

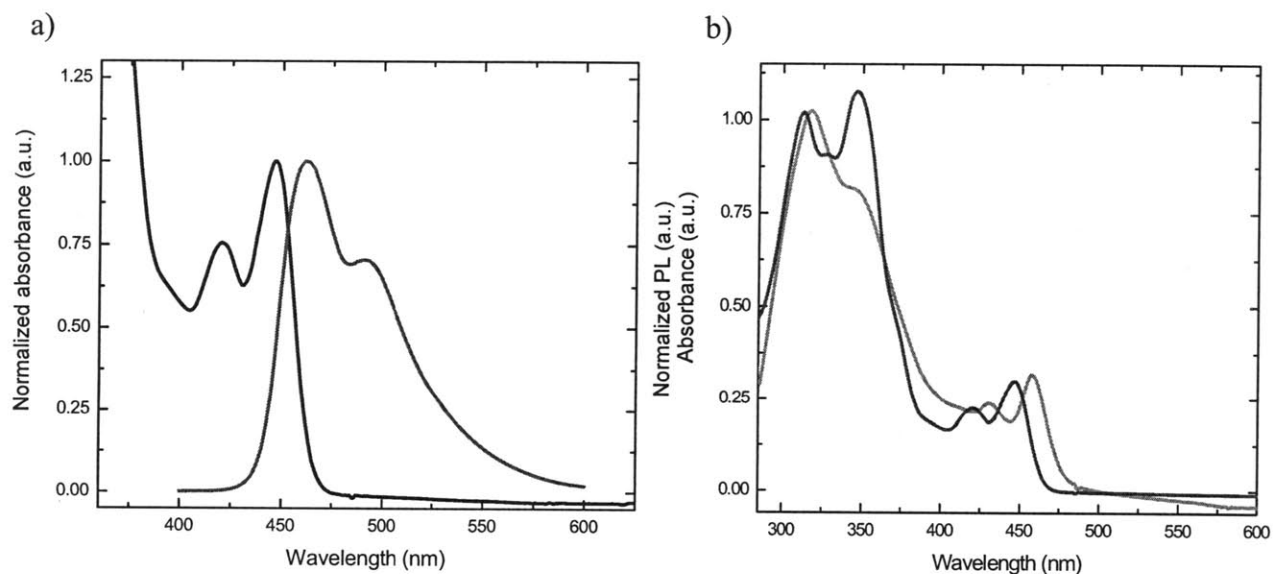


Figure 5.1 a) Absorption and emission spectra of **8** in chloroform. b) UV-vis absorption spectra of **8** (film vs. solution).

Upon deprotection, the resulting tetraalkyne **9** was also tested for photophysical properties. The solution absorption and emission maxima were found to be 445 nm and 459 nm respectively (Figure 5.2a), with little change in the values compared to the silyl-protected form.

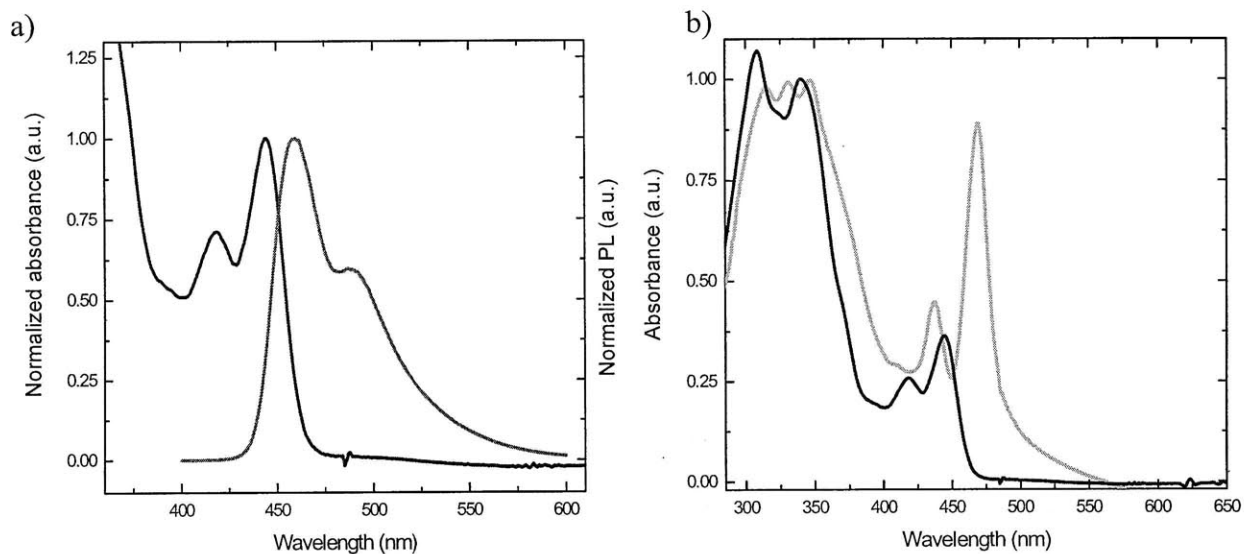


Figure 5.2 a) Absorption and emission spectra of **9** in chloroform. b) UV-vis absorption spectra of **9** (film vs. solution), with a sharp J-band observed in the film spectrum.

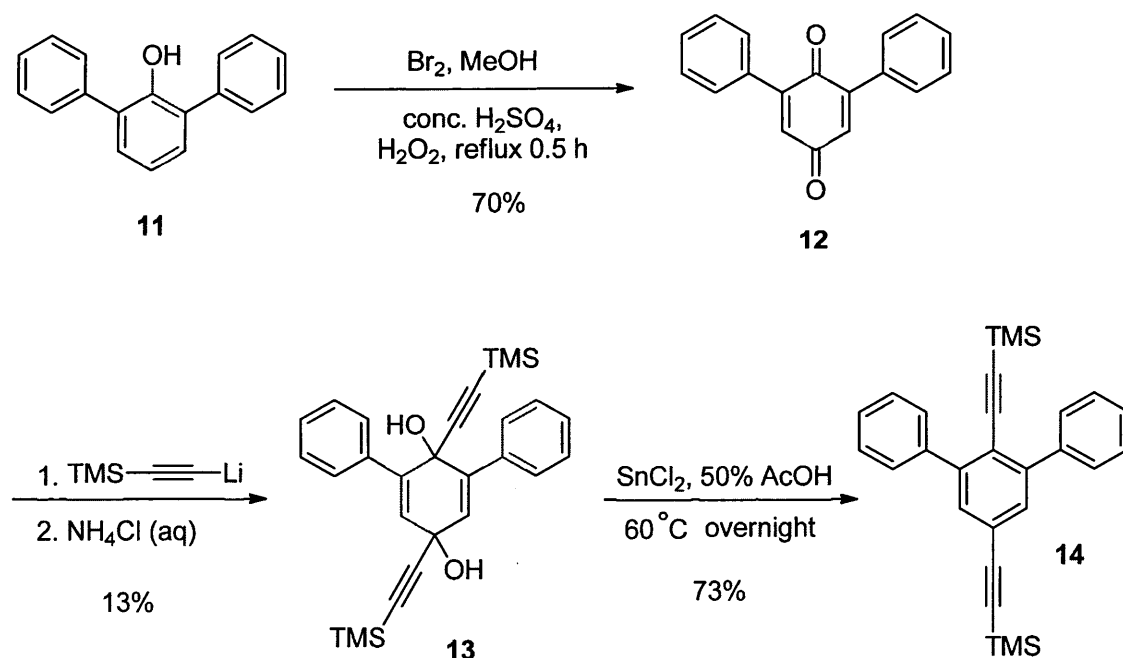
With the removal of the bulky protecting groups however, J-aggregation was now observed in the spin-coated thin films, as evidenced by the appearance of a sharp J-band at 486 nm that was absent in the solution phase UV-vis spectrum (Figure 5.2b). When **9** was subjected to a Sonogashira polycondensation with two equivalents of a simple diiodide coupling partner, the network polymer **10** was formed as a dense gel after two days. Subsequent washing, precipitation and drying of this polymer gave a yellow-green solid that was highly insoluble in all solvents, precluding the possibility of any photophysical studies. In any case, the solid also did not appear to display any photoluminescence upon irradiation with UV light. In the light of these findings, polymer **10** must be a very high molecular weight network polymer containing significant defects within its structure, accounting for its lack of solubility and fluorescence. In summary, the dimeric dibenz[*a,j*]anthryl macrocyclic motif has proven itself to be a reliable J-aggregating structure that it relatively tolerant of the nature of its substituents. However, it was not possible to achieve J-aggregation in a polymer by simply incorporating this motif as a repeat unit. While

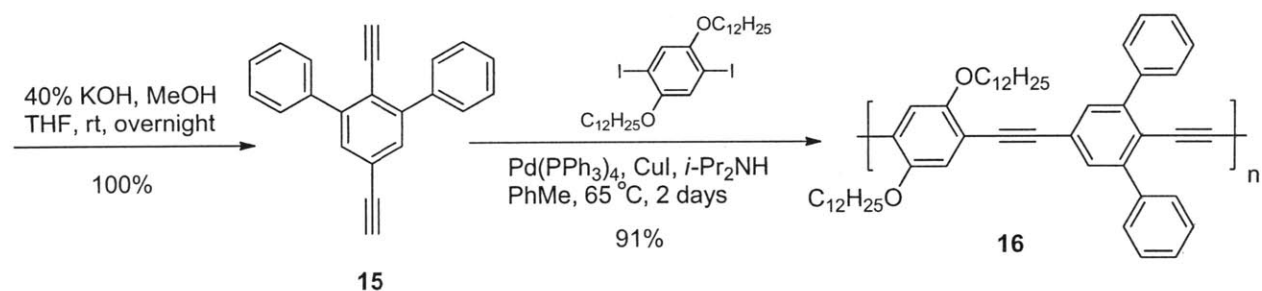
the precursor building block itself did display J-aggregation, its incorporation into a polymeric structure resulted in the loss of that property. This prompted the investigation of new candidate motifs in the search for potential J-aggregating polymers.

5.3 Polymer prototype and model studies

In our efforts to design a slip-inducing motif for potential J-aggregating polymers, a bis-*ortho* aryl-substituted benzenoid structure was tried. In contrast to a typical repeat unit in which the aryl substituents are *para* to each other, this motif possesses lower symmetry and it was hoped that the non-symmetrical distribution of steric bulk along the polymer backbone would lead to slip-stacking arrangements between polymer chains. In order to put this to the test, the simple 2,6-diphenyl substituted monomer **15** was first prepared over four steps (Scheme 5.2).

Scheme 5.2. Synthesis of polymer **16**





In the first step, the commercially available 2,6-diphenylphenol is oxidized to the quinone **12** using a published procedure⁴. Reaction of **12** with two equivalents of lithium trimethylsilylacetylide gives the diol **13** in 13% yield. The low yield is attributed to a spontaneous transannular dehydration reaction that converts a large portion of the desired diol to a stable ether. Finally, reduction with stannous chloride and subsequent deprotection gave the required dialkyne monomer **15**, which was subsequently copolymerized with a simple diiodide coupling partner to give polymer **16**. Spectroscopic measurements on the polymer were performed as part of a standard characterization routine.

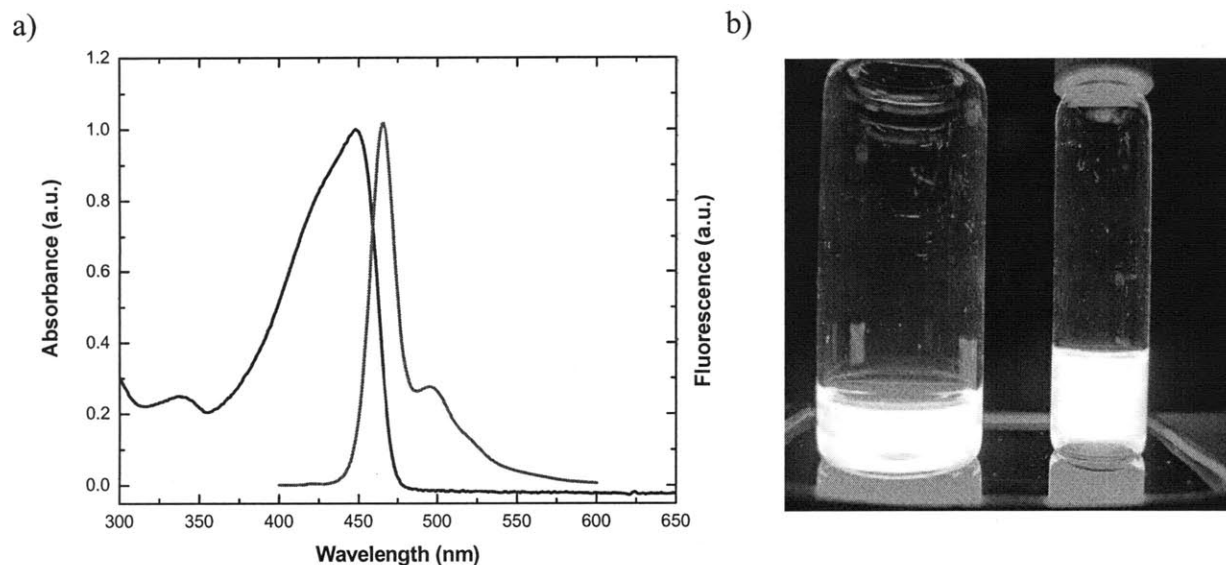
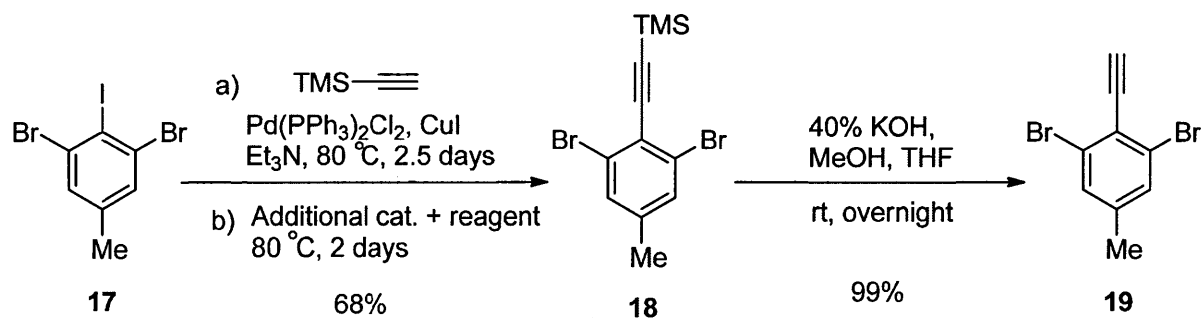
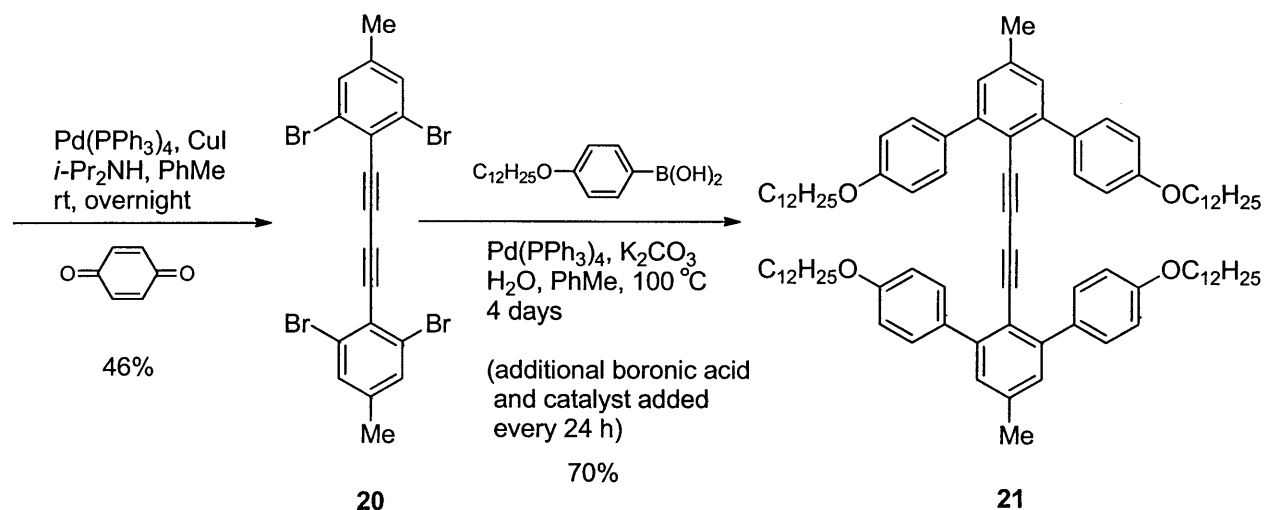


Figure 5.3 a) Absorption and emission spectra of polymer **12** in chloroform. b) Solutions of **12** under ultraviolet irradiation.

In solution phase, the absorption and emission maxima of polymer **16** were found to be 448 nm and 465 nm respectively (Figure 5.3a), with a relative fluorescence quantum yield of 85%. Thin films of the polymer were also spin-coated on to glass cover-slips and then annealed under toluene vapor prior to conducting photophysical studies. However, spectroscopic measurements did not reveal any special properties. No J-band was observed and the fluorescence of the polymer film was perceptibly lower compared to that of the solution. Failure to obtain J-aggregate properties in **16** was hypothesized to be either due to the randomness of the head/tail configuration within the polymer backbone (a result of the inherent limitation of the chosen synthetic route), and/or the fact that the 2,6-diarylbenzene design feature itself was not capable of producing J-aggregation. This then prompted the synthesis of the model compound **21**, which attempts to simulate part of a polymer with two 2,6-diarylbenzene segments connected in a head-to-tail fashion. This model study was performed as a prelude to any actual polymer preparation, since the synthesis of such a polymer containing exclusively head-to-head arrangements would be rather lengthy. In contrast, model compound **21** could be synthesized in only four steps (Scheme 5.3), in quantities that were more than sufficient for basic spectroscopic studies.

Scheme 5.3. Synthesis of model compound **21**





To prepare **21**, the commercially available trihalide **17** was subjected to a chemoselective Sonogashira coupling to replace the iodine with a TMS-protected alkyne. The conditions required to effect this transformation were much harsher than usual, probably due to the steric hindrance conferred by the two flanking bromine atoms. To obtain reasonable yields, 4.5 days of reaction time were required, with fresh palladium catalyst and trimethylsilylacetylene being added at the two-day mark. After facile basic deprotection of **18** and subsequent oxidative dimerization, the tetrabromide **20** was obtained. The final step involved a quadruple Suzuki coupling to replace all the bromines with alkoxyphenyl substituents. Once again, long reaction times were required for satisfactory results, possibly due to steric reasons. A total of 4 days were required for this reaction, with additional portions of boronic acid and fresh catalyst having to be introduced every 24 hours. Model compound **21** was ultimately obtained in 22% overall yield (4 steps). Surprisingly, the highly conjugated **21** was found to be completely non-emissive in both solution phase and in the solid state, thus casting doubts on the suitability of this design feature for J-aggregation. Unlike in the macrocyclic dibenz[*a,j*]anthracene-based J-aggregates, there exist no constraints to the degree of twisting that is possible in **21**. Thus, it is likely that steric repulsions between the four alkoxyphenyl groups cause the molecule to twist into an orthogonal

configuration in which the pair of terphenyl fragments are at/near 90° relative to each other. This breaks the conjugation within the molecule, accounting for the lack of photoluminescence. The orthogonal nature of the molecule, as well as the absence of any large, extended π -electron systems, probably makes π - π stacking difficult, which in turn renders J-aggregation a remote possibility.

5.4 Dibenz[*a,m*]rubicenes

Following the lack of success in achieving J-aggregation in polymers, attention was then turned to the polycyclic aromatic dibenz[*a,m*]rubicenes. These appeared to be promising candidates for J-aggregation since they not only had large π - π stacking surface areas, but also had slightly twisted topologies resulting from internal steric repulsions (Figure 5.4).

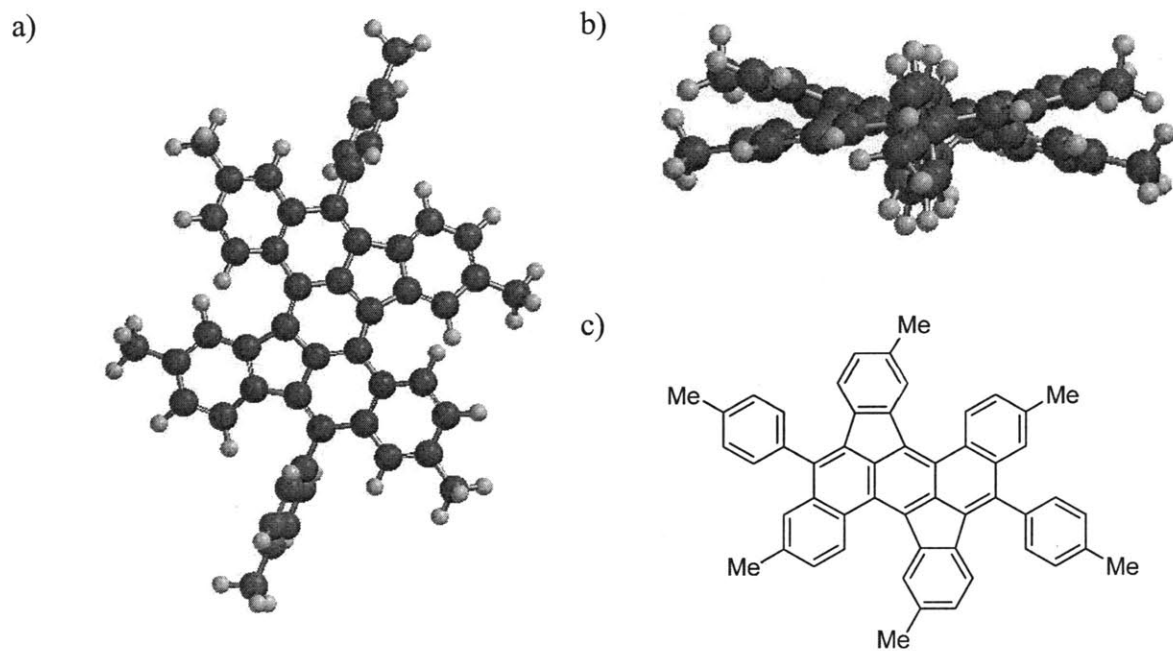
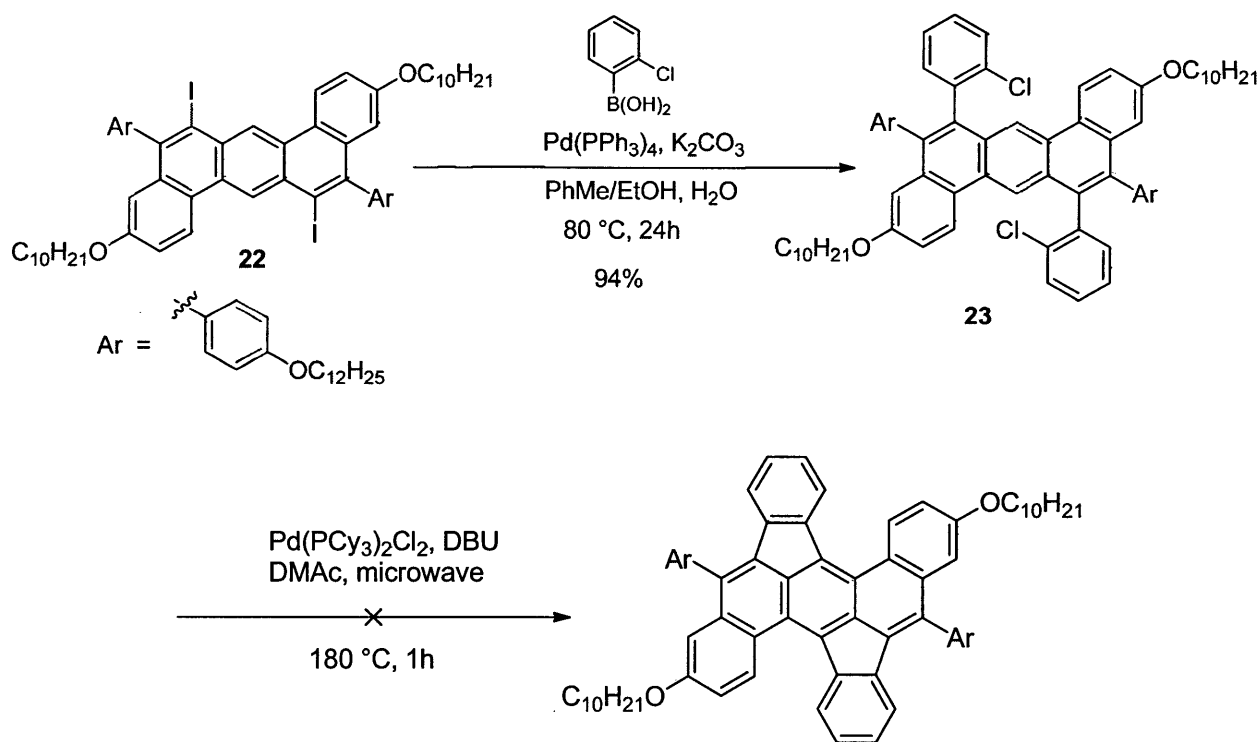


Figure 5.4 a) Spartan model of a substituted dibenz[*a,m*]rubicene (from top), b) Side-on view showing a dihedral angle of 16.6° , c) Two-dimensional representation of the molecule.

The specific substituted dibenz[*a,m*]rubicenes under consideration were predicted (Spartan '08, PM3) to have small dihedral angles of about 16.6°, similar in value to the calculated angles (22°) of the dibenz[*a,j*]anthracene-based J-aggregates. Preliminary synthetic investigations began with compound **22**, which had served as a monomer in our previous studies on stair-stepped conjugated polymers (Chapter 4). The strategy was to start with a dibenz[*a,h*]anthracene building block and then bridge the pair of *peri*-positions with *ortho*-phenylene units to arrive at a dibenz[*a,m*]rubicene framework. Literature precedents of such indenoannulations include the recent work of Lawrence Scott and co-workers, where microwave-facilitated intramolecular Heck reactions were used to bring about the desired transformation.⁵

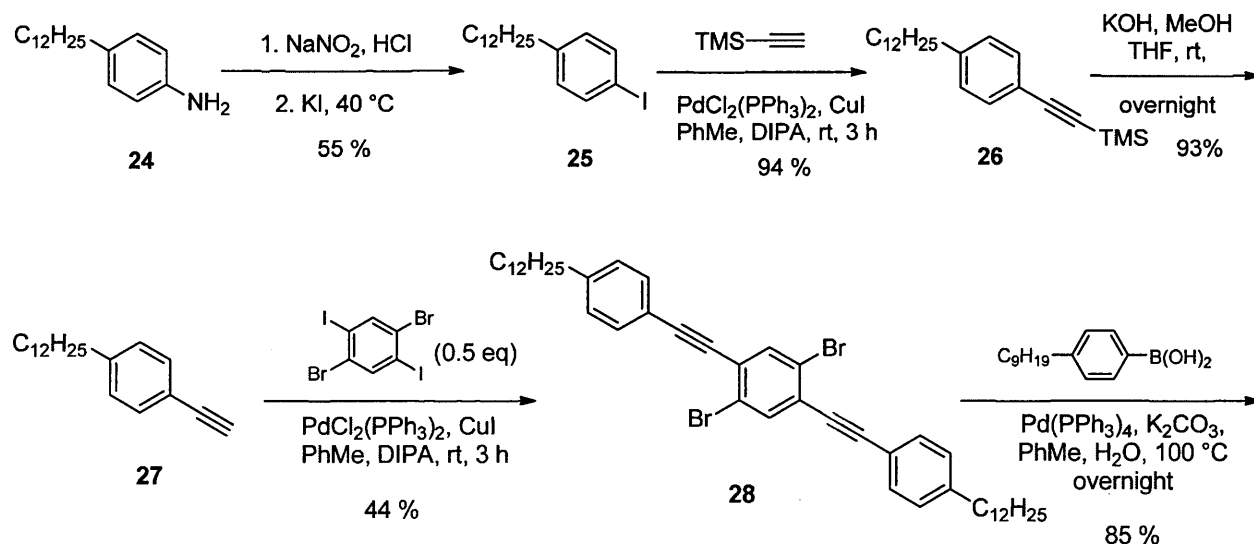
Scheme 5.4. Attempted synthesis of a substituted dibenz[*a,m*]rubicene

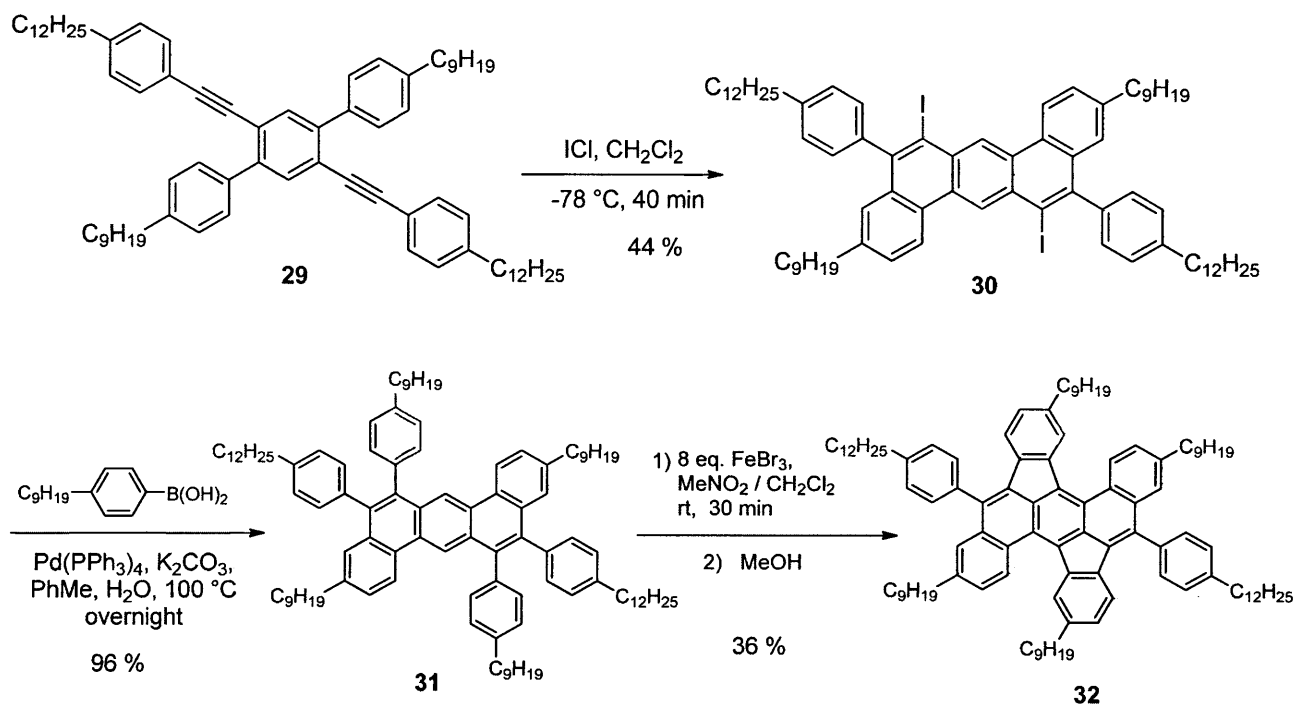


Following the literature procedure devised by Scott and co-workers, **22** was first subjected to a double Suzuki coupling reaction with 2-chlorophenylboronic acid to give **23** in

very high yield (Scheme 5.4). Then, a double intramolecular Heck reaction was attempted on **23** using the Scott conditions. However, despite trying out a multitude of microwave irradiation powers, reaction times, and palladium catalyst loadings, satisfactory results could not be obtained. Each run resulted in an inseparable mixture of unchanged starting material, monocyclized product, and the desired dibenz[*a,m*]rubicene. Unfortunately, subjecting these mixtures to further reaction (with fresh catalyst added) did not alter the relative amounts of the components. Just as this Heck reaction-based strategy was being abandoned, a reliable synthetic route to dibenz[*a,m*]rubicenes appeared in the literature. The strategy employed by Hseuh *et. al.* made use of an oxidative cyclization (Scholl reaction) instead of a palladium-catalyzed coupling for the crucial final step.⁶ In adopting the Hseuh strategy to prepare a dibenz[*a,m*]rubicene J-aggregate candidate, several modifications had to be made to **22** since it had alkoxy groups which could potentially complicate the Scholl reaction. Accordingly, the all-alkyl **30** was prepared instead (Scheme 5.5).

Scheme 5.5. Synthesis of dibenz[*a,m*]rubicene **32**





The known alkyne **27** was prepared over three steps starting from 4-dodecylaniline, and then taken up in a double Sonogashira coupling to afford **28**. Following this, the terphenyl derivative **29** was obtained via a double Suzuki coupling between **28** and 4-nonylphenylboronic acid, after which it was cyclized with iodine monochloride to diiodide **30**. After another double Suzuki coupling with 4-nonylphenylboronic acid, the oxidative cyclization substrate **31** was obtained in high yield. Treatment of **31** with iron(III) chloride under strictly anhydrous conditions gave the highly substituted dibenz[*a,m*]rubicene **32** as an orange-red solid upon methanol workup and subsequent purification. Compound **32** was then tested for J-aggregate properties.

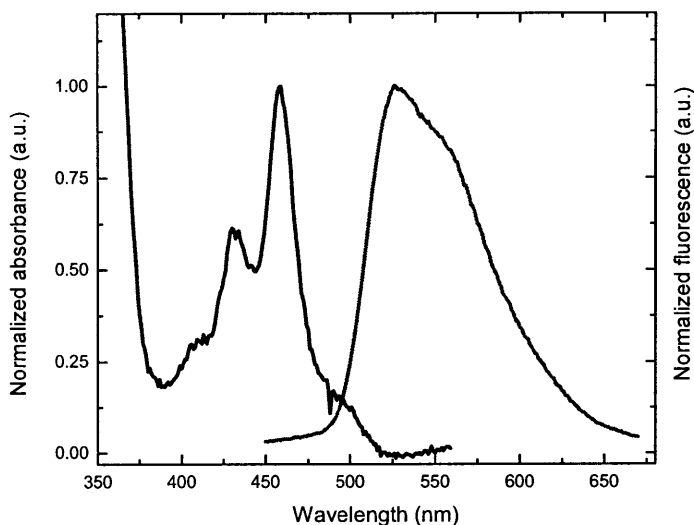


Figure 5.5 Absorption and emission spectra of **32** in chloroform solution

The absorption and emission maxima of **32** in solution phase were 459 nm and 527 nm respectively (Figure 5.5), with a surprisingly low fluorescence quantum yield of 10%. Thin films of the material were also spin-coated on to glass cover-slips and then annealed under toluene vapor prior to conducting photophysical measurements. J-aggregation was not observed with this dibenz[*a,m*]rubicene, and its fluorescence was also markedly diminished in the film state, to a point where it was impossible to obtain spectra with satisfactory signals. It remains unclear why **32** showed such a low fluorescence quantum yield. One possibility could be that the twisted molecule is fluxional, with low inversion/twisting energy barriers, thus presenting additional pathways for non-radiative decay from the first excited state. Even though J-aggregation was not seen with this particular dibenz[*a,m*]rubicene, abandoning the quest for J-aggregation in this class of molecules would be rather premature at this moment, keeping in mind the structural and topological similarities dibenz[*a,m*]rubicenes share with the dibenz[*a,j*]anthracene-based macrocycles are substantial. It may yet be possible to fine-tune the molecular structure/topology as well as the photophysical properties with the right set of substituents.

5.5 Conclusion

Several approaches towards novel J-aggregating structures were investigated, namely: a) the extension of a known dibenz[*a,j*]anthracene-based macrocyclic motif to polymers, b) synthesizing conjugated polymers with slip-inducing structural features, and c) highly substituted dibenz[*a,m*]rubicenes. The outcome of these studies proved to be disappointing. However, these investigations have not only resulted in the synthesis of numerous new compounds, but more importantly, provided insight as to what factors may be important in governing J-aggregation or the lack thereof, considering the fact that reliable structure-property relationships in rational J-aggregate design has not yet been thoroughly established. In particular, we think the dihedral angle of the twisted aromatic molecule, as well as the availability of π - π stacking surface area, are important in determining whether it can J-aggregate. With regards to these structural attributes, dibenz[*a,m*]rubicenes still appear to be promising, despite the failure to achieve J-aggregation in compound **32**. If a small library of dibenz[*a,m*]rubicenes possessing a wide variety of substituents could be synthesized, it may yet be possible to identify a lead compound that displays this special and somewhat elusive spectroscopic property.

5.6 Experimental Section

General Methods and Instrumentation: All reactions were performed under an argon atmosphere, using over-dried glassware and standard Schlenk techniques. Tetrakis-(triphenylphosphine)palladium(0) was purchased from Strem Chemicals, Inc. All other reagents were obtained from Aldrich Chemical Co., Inc., and used as received. Anhydrous toluene, tetrahydrofuran, and dichloromethane were obtained from a solvent purification system (Innovative Technologies). Dry diisopropylamine (DIPA) was obtained by distilling reagent-

grade DIPA over sodium hydroxide pellets. Nuclear Magnetic Resonance (NMR) spectra were recorded on a Varian Mercury (300 MHz) NMR spectrometer located in the MIT Department of Chemistry Instrumentation Facility (DCIF). Mass spectra were obtained on a Bruker Omnix MALDI-TOF instrument. UV/Vis spectra were recorded on an Agilent 8453 diode-array spectrophotometer. Emission spectra were acquired on a SPEX Fluorolog fluorometer (model FL-321, 450 W xenon lamp) using either right-angle detection (solution measurements) or front-face detection (thin film measurements).

4',6'-Bis-(*p*-(dodecyloxy)phenylethynyl)-4,4''-bis-(triisopropylsilylethynyl)[1,1':3',1'']-

terphenyl (4): A 500 mL two-neck round-bottom flask containing a magnetic stir-bar was charged with 1,5-dibromo-2,4-bis-(4-dodecyloxyphenylethynyl)benzene) (0.10 g, 0.124 mmol), 4-triisopropylsilylethynylphenylboronic acid (0.1 g, 0.311 mmol), *tetrakis*(triphenylphosphine)-palladium(0) (7.2 mg, 0.0062 mmol), potassium carbonate (0.070 g, 0.5 mmol), toluene (7 mL), and water (2 mL) under an atmosphere of argon. The mixture was stirred and briefly sparged by bubbling argon through it for 5-10 minutes using a long needle. Following the degassing, the mixture was then stirred vigorously and heated at 100 °C for 16 hours. After allowing the reaction mixture to cool down to room temperature, it was diluted with diethyl ether and transferred into a separatory funnel, and extracted with additional portions of ether (3 x 40 mL). The combined organic extracts were dried over anhydrous magnesium sulfate, filtered through a piece of fluted filter paper into a 500 mL round-bottom flask, and then concentrated by rotary evaporate to give a residue of the crude product. This was partially purified by flash chromatography on a silica gel column (15% v/v dichloromethane/hexane) to afford **4** (0.12 g, ca. 83 %). The discolored, partially purified **4** could be telescoped to the next step without any

detrimental effects, and the subsequent product there, **5**, could be completely purified. HRMS (MALDI-TOF): calcd: 1158.8044 (M)⁺, found: 1159.7964 (M+H)⁺.

5,9-Bis-(4-dodecyloxyphenyl)-3,11-bis-(triisopropylsilylethynyl)-6,8-diiododibenz[*a,j*]-

anthracene (5): A 250 mL two-neck round-bottom flask containing a magnetic stir-bar was charged with mercury (II) trifluoroacetate (0.102 g, 0.238 mmol) and iodine (0.21 g, 0.827 mmol). The flask was placed under an argon atmosphere, after which 7 mL of dry dichloromethane was introduced via syringe. The contents were stirred for about 15 minutes to dissolve as much of the solid reagents as possible. Then, the purple mixture was cooled down in an ice-water bath and stirred for an additional 5-10 minutes before 2,6-lutidine (28 μ L, 0.234 mmol) was added to the stirred mixture via a syringe. Upon stirring for an additional 5 minutes, a solution of **4** (0.12 g, 0.103 mmol) in dichloromethane (3 mL) was added slowly via syringe, and the resulting mixture was allowed to stir at a temperature 0 to 5 °C for 1 hour. Upon completion of the reaction, the mixture was diluted with dichloromethane, and then transferred into a 500 mL separatory funnel. The organic layer was shaken with aqueous sodium hydroxide, with its color changing from purple to yellow in the process. After the organic phase was collected in a clean 250 mL Erlenmeyer flask, the remaining aqueous layer was further extracted with additional dichloromethane (2 x 60 mL). The combined organic phases were dried over anhydrous magnesium sulfate and then filtered through a piece of fluted filter paper. The clear yellow filtrate was collected in a 500 mL round-bottom flask, and the solvent was removed by rotary evaporation, leaving behind a crude product that was subsequently purified by flash chromatography on a silica gel column (15% v/v dichloromethane/hexane). The relevant fractions were combined and the solvent was removed, affording **5** (0.12 g, 82%) as an off-white

solid. ^1H NMR (300 MHz, CD_2Cl_2 , δ ppm): 9.69 (1H, s), 9.41 (1H, s), 8.83 (2H, d, $J = 8.7$ Hz), 7.83 (2H, d, $J = 8.4$ Hz), 7.58 (2H, s), 7.18 (4H, d, $J = 8.7$ Hz), 7.09 (4H, d, $J = 8.7$ Hz), 4.08 (4H, t, $J = 6.6$ Hz), 0.8-1.9 (88H). ^{13}C NMR (300 MHz, CD_2Cl_2 , δ ppm): 159.3, 145.7, 141.7, 137.0, 132.9, 132.8, 132.5, 131.3, 130.9, 129.9, 128.9, 123.4, 122.9, 114.6, 108.2, 107.2, 93.0, 68.3, 32.2, 30.0, 29.9, 29.7, 29.6, 26.4, 23.0, 18.7, 14.2, 11.6. HRMS (MALDI-TOF): calcd: 1156.7888 (M-I_2)⁺, found: 1157.3200.

5,9-Bis-(4-dodecyloxyphenyl)-3,11-bis-(triisopropylsilylethynyl)dibenz[*a,j*]anthracene-6,8-dicarbaldehyde (6): A 250 mL two-neck round-bottom flask containing **5** (0.367 g, 0.26 mmol) and a magnetic stir-bar was evacuated and then placed under positive pressure of argon. Dry tetrahydrofuran (100 mL) was then added via syringe and the mixture was stirred to completely dissolve **5**. The solution was subsequently cooled in a dry-ice/acetone bath at -78 °C, before 1.6 M *tert*-butyllithium in pentane (0.49 mL, 0.78 mmol) was added dropwise via syringe. This mixture was stirred at -78 °C for 1 hour, after which anhydrous DMF (0.15 mL) was added via syringe. After 10 minutes, the dry-ice/acetone bath was removed, and the mixture was allowed to warm up to room temperature. Stirring was continued overnight. The resulting mixture was then diluted with dichloromethane and poured into a separatory funnel containing deionized water. The mixture was extracted with further portions of dichloromethane (3 x 30 mL) was the organic layer was separated out and dried over anhydrous magnesium sulfate. Removal of the solvent under rotary evaporation afforded a mixture containing the target dialdehyde as well as monoaldehyde byproduct. This was purified by flash chromatography on a silica gel column (30% v/v dichloromethane/hexane) to give **6** as a yellow solid (0.120 g, 38%). ^1H NMR (300 MHz, CD_2Cl_2 , δ ppm): 10.78 (1H, s), 10.07 (2H, s), 9.81 (1H, s), 8.88 (2H, d, $J = 8.7$ Hz), 7.90

(2H, d, $J = 7.8$ Hz), 7.81 (2H, s), 7.33 (4H, d, $J = 8.7$ Hz), 7.13 (4H, d, $J = 8.4$ Hz), 4.11 (4H, t, $J = 6.6$ Hz), 0.8-2.0 (88H). ^{13}C NMR (300 MHz, CD_2Cl_2 , δ ppm): 194.7, 159.9, 148.3, 132.8, 132.5, 132.3, 132.0, 131.8, 129.6, 128.2, 127.8, 127.0, 124.8, 123.3, 122.8, 117.0, 114.7, 106.9, 93.3, 68.5, 32.2, 31.8, 30.0, 29.9, 29.7, 29.6, 29.5, 26.3, 23.0, 22.9, 21.0, 18.7, 14.2, 11.6. HRMS (MALDI-TOF): calcd: 1214.7943 (M) $^+$, found: 1215.7375 ($\text{M}+\text{H}$) $^+$.

5,9-Bis-(4-dodecyloxyphenyl)-6,8-diethynyl-3,11-bis-(triisopropylsilylethynyl)dibenz[*a,j*]-

anthracene (7): A 250 mL single-neck round-bottom flask containing a magnetic stir-bar was charged with triphenylphosphine (0.42 g, 1.6 mmol) and carbon tetrabromide (0.267 g, 0.8 mmol), and subsequently placed under argon atmosphere. The flask was immersed into an ice-water bath, and then dry dichloromethane (15 mL) was added via syringe, with simultaneous stirring to dissolve the reagents, giving a clear yellow solution. To this was added a solution of **6** (0.1224 g, 0.1 mmol) in dichloromethane (5 mL), and the mixture was allowed to slowly warm up to room temperature overnight. After the reaction was complete, dichloromethane was poured in to dilute the mixture, which was transferred into a separatory funnel and extracted with additional portions of dichloromethane (3 x 30 mL). The combined organic extracts were dried over anhydrous magnesium sulfate, filtered through a fluted filter funnel and then the solvent was removed by rotary evaporation. The crude product could be quickly purified by flash chromatography through a short column/pad of silica gel. Concentrating the fractions affords the intermediate 170erminal dibromide (ca. 88 mg), which was not stored, but instead, used as soon as possible in the next step (i.e. conversion to alkyne). In a 100 mL one-neck, round-bottom flask containing a magnetic stir-bar and the purified 170erminal dibromide (ca. 88 mg) under argon atmosphere, anhydrous tetrahydrofuran (8 mL) was added via syringe to give a clear solution.

After cooling the solution down to -78 °C in a dry-ice/acetone bath, 1.6 M *n*-butyllithium in hexanes (0.31 mL, 0.5 mmol) was added dropwise by syringe. The reaction mixture was stirred for about 2 hours, after which an aqueous solution of ammonium chloride was introduced via syringe, and the mixture was allowed to warm to room temperature. Diethyl ether was used to dilute the mixture, which was transferred into a separatory funnel and extracted with further portions of ether (3 x 35 mL). The combined organic extracts were dried over anhydrous magnesium sulfate, filtered, and then concentrated to near-dryness under rotary evaporation. The crude dialkyne was then purified by flash chromatography on a silica gel column (30% v/v dichloromethane/hexane) to give **7** (55 mg, 46% over 2 steps). ¹H NMR (300 MHz, CD₂Cl₂, δ ppm): 9.93 (1H, s), 9.61 (1H, s), 8.95 (2H, d, *J* = 8.7 Hz), 7.84 (2H, d, *J* = 8.7 Hz), 7.78 (2H, s), 7.43 (4H, d, *J* = 8.7 Hz), 7.09 (4H, d, *J* = 8.7 Hz), 4.09 (4H, t, *J* = 6.6 Hz), 3.54 (2H, s), 0.8-1.9 (88H). ¹³C NMR (300 MHz, CD₂Cl₂, δ ppm): 159.3, 144.0, 131.9, 131.8, 131.7, 131.2, 130.7, 130.6, 130.3, 130.1, 128.1, 125.9, 123.2, 122.6, 118.9, 114.3, 107.2, 92.8, 81.1, 68.3, 32.2, 30.0, 29.9, 29.7, 29.6, 26.4, 22.9, 18.7, 14.2, 11.6. HRMS (MALDI-TOF): calcd: 1206.8044 (M)⁺, found: 1207.3715.

Macrocycle 8: In a 500-mL single-neck round-bottom flask containing a magnetic stir-bar was added *tetrakis*-(triphenylphosphine)palladium(0) (5.3 mg, 0.0046 mmol), *p*-benzoquinone (4.4 mg, 0.041 mmol), copper(I) iodide (1.3 mg, 0.0068 mmol), anhydrous diisopropylamine (20 mL), and anhydrous toluene (25 mL). The mixture was stirred at room temperature under argon atmosphere to effect complete dissolution. Then, a solution of **7** (0.055 g, 0.046 mmol) in dry toluene (20 mL) was slowly added to the mixture via a glass syringe operated by a syringe-pump, with the addition rate set to 1.5 mL/h. After addition was complete, the mixture was

allowed to stir for another 2 days at room temperature. Upon reaction completion, the solvents were removed by rotary evaporation to leave a yellow-brown residue. Dichloromethane was then added to the residue and the solution was transferred into a separatory funnel, where it was washed several times with water. The organic layer was dried over anhydrous magnesium sulfate, filtered, and the solvent was removed to give a crude product. This was purified by flash chromatography on a silica gel column (25% v/v dichloromethane/hexane) to give **8** as a lemon-yellow solid (39.9 mg, 48 %). Occasionally, more than one round of column chromatography may be required to effect complete purification. ¹H NMR (300 MHz, CD₂Cl₂, δ ppm): 9.95 (2H, s), 9.20 (2H, s), 8.90 (4H, d, *J* = 8.4 Hz), 7.78 (4H, s), 7.74 (4H, d, *J* = 8.4 Hz), 7.36 (8H, d, *J* = 8.4 Hz), 7.12 (8H, d, *J* = 8.7 Hz), 4.26 (8H, t, *J* = 6.3 Hz), 0.8-2.0 (176H). ¹³C NMR (300 MHz, CD₂Cl₂, δ ppm): 159.4, 145.5, 131.9, 131.3, 130.7, 130.5, 130.1, 129.9, 128.1, 122.5, 118.5, 114.4, 107.2, 92.7, 82.6, 81.1, 68.4, 32.2, 30.0, 29.9, 29.7, 26.6, 23.0, 18.7, 14.1, 11.6. HRMS (MALDI-TOF): calcd: 2409.5776 (M)⁺, found: 2410.6978 (M+H)⁺.

Macrocycle 9: A 50-mL round-bottomed flask containing a magnetic stir-bar was charged with **8** (0.040 g, 0.0165 mmol) and anhydrous THF (6 mL). A solution of 1.0 M tetra-*n*-butylammonium fluoride in THF (0.1 mL, 0.099 mmol) was then added via syringe, and the mixture was stirred at room temperature under argon for 3 hours. After 3 hours, the mixture was diluted with dichloromethane and transferred into a separatory funnel containing water, and extracted several times with additional portions of dichloromethane (3 x 25 mL). The organic layer was dried over anhydrous magnesium sulfate, filtered, and the solvent was removed to give the crude product. This was purified by flash chromatography on a silica gel column (40% v/v dichloromethane/hexane) to give **8** as a yellow solid (29 mg, 98%). ¹H NMR (300 MHz, CDCl₃,

δ ppm): 10.05 (2H, s), 9.08 (2H, s), 8.99 (4H, d, $J = 8.7$ Hz), 8.00 (4H, s), 7.79 (4H, d, $J = 8.4$ Hz), 7.51 (8H, d, $J = 8.4$ Hz), 7.34 (8H, d, $J = 8.7$ Hz), 4.47 (8H, t, $J = 6.3$ Hz), 3.27 (4H, s), 1.0-2.3 (92H). ^{13}C NMR (300 MHz, CDCl_3 , δ ppm): 159.1, 151.3, 145.0, 138.9, 136.3, 132.5, 131.8, 130.8, 130.6, 129.9, 127.8, 120.8, 118.6, 82.8, 80.8, 68.3, 32.2, 30.6, 30.0, 29.7, 26.6, 23.0, 14.4. HRMS (MALDI-TOF): calcd: 1785.0439 (M)⁺, found: 1785.4458.

Polymer 10: A 25 mL Schlenk tube equipped with a magnetic stirrer was charged with 2,5-didodecyloxy-1,4-diiodobenzene (0.0141 g, 0.0202 mmol), tetrayne monomer **9** (0.018 g, 0.0101 mmol), tetrakis(triphenylphosphine)palladium(0) (0.7 mg, 0.0006 mmol), and copper(I) iodide (0.12 mg, 0.0006 mmol). The tube was evacuated and back-filled with argon several times, after which anhydrous toluene (2.5 mL) and diisopropylamine (1 mL) were introduced via syringe. The mixture was sparged with argon for 10 minutes at room temperature, followed by stirring at 65 °C for 48 hours. Upon cooling to room temperature, the gel-like mixture was precipitated in rapidly stirring methanol and isolated by centrifugation. Finally, polymer **10** was dried under reduced pressure to give an insoluble yellow-green solid.

2',5'-bis-(trimethylsilylethynyl)-2',5'-dihydro[1,1':3',1''-terphenyl]-2',5'-diol (13): A 100-mL round-bottomed flask containing a magnetic stir-bar was charged with trimethylsilylacetylene (0.34 mL, 2.4 mmol) and anhydrous THF (8 mL). The stirred mixture was cooled down to -78 °C in a dry-ice/acetone bath before 1.6 M *n*-butyllithium (1.5 mL, 2.4 mmol) was added via syringe. After the mixture was stirred for 15 minutes, a solution of 2,6-diphenyl-1,4-benzoquinone (0.25 g, 0.96 mmol) in THF (3 mL) was introduced via syringe and the reaction mixture was stirred for 2 hours as it gradually warmed up from -78 °C to room

temperature. Upon completion, the mixture was diluted with ether and transferred into a separatory funnel containing water and ether. This was extracted several times with additional portions of ether (3 x 35 mL). The combined organic layers were dried over anhydrous magnesium sulfate, filtered, and the solvent was removed to give the crude product. This was purified by flash chromatography on a silica gel column (from 50% v/v dichloromethane/hexane to pure dichloromethane) to give **13** as a white powder (49 mg, 11%). ¹H NMR (300 MHz, CD₂Cl₂, δ ppm): 7.70 (4H, m), 7.38 (6H, m), 6.10 (2H, s), 2.48 (2H, s), 0.21 (9H, s), 0.07 (9H, s). ¹³C NMR (300 MHz, CD₂Cl₂, δ ppm): 141.4, 138.0, 129.6, 128.3, 128.1, 105.7, 105.4, 93.9, 90.5, 66.2, 63.3, -0.32, -0.75.

2,6-diphenyl-1,4-bis-(trimethylsilylethynyl)benzene (14): A 50-mL round-bottomed flask containing a magnetic stir-bar was charged with **13** (0.049 g, 0.11 mmol), tin(II) chloride (0.041 g, 0.22 mmol), ethanol (8 mL) and 50% aqueous acetic acid (1 mL). The mixture was stirred at 60 °C overnight, after which it was diluted with ether and transferred into a separatory funnel containing water and ether. This was extracted several times with additional portions of ether (3 x 35 mL). The combined organic layers were dried over anhydrous magnesium sulfate, filtered, and the solvent was removed to give the crude product. This was purified by flash chromatography on a silica gel column (from 20% v/v dichloromethane/hexane) to give **14** as a white powder (49 mg, 11%). ¹H NMR (300 MHz, CD₂Cl₂, δ ppm): 7.61 (4H, m), 7.42 (8H, m), 0.26 (9H, s), -0.02 (9H, s). ¹³C NMR (300 MHz, CD₂Cl₂, δ ppm): 145.7, 140.2, 131.7, 129.7, 128.0, 127.9, 123.2, 120.4, 104.5, 104.0, 103.4, 96.7, -0.23, -0.81.

2,6-diphenyl-1,4-bis-diethynylbenzene (15): A 25-mL round-bottomed flask containing a magnetic stir-bar was charged with **14** (0.033 g, 0.078 mmol), THF (3.0 mL) and methanol (1.5 mL). Then, 40% aqueous KOH (0.013 mL, 0.16 mmol) was added to the stirred solution via syringe, and the mixture was left to stir overnight at room temperature, after which it was diluted with ether and transferred into a separatory funnel containing water and ether. This was extracted several times with additional portions of ether (3 x 20 mL). The combined organic layers were dried over anhydrous magnesium sulfate, filtered, and the solvent was removed to give the crude product. This was purified by flash chromatography on a silica gel column (25% v/v dichloromethane/hexane) to give **15** as a white powder (26 mg, 99%). ¹H NMR (300 MHz, CD₂Cl₂, δ ppm): 7.40-7.61 (12H), 3.27 (1H, s), 3.07 (1H, s). ¹³C NMR (300 MHz, CD₂Cl₂, δ ppm): 146.2, 140.1, 132.2, 129.6, 128.2, 128.1, 122.5, 119.8, 85.8, 82.9, 81.8, 79.3.

Polymer 16: A 25 mL Schlenk tube equipped with a magnetic stirrer was charged with 2,5-didodecyloxy-1,4-diiodobenzene (0.064 g, 0.091 mmol), monomer **15** (0.026 g, 0.094 mmol), tetrakis(triphenylphosphine)-palladium(0) (5.3 mg, 0.0046 mmol), and copper(I) iodide (0.9 mg, 0.0046 mmol). The tube was evacuated and back-filled with argon several times, after which anhydrous toluene (4 mL) and diisopropylamine (1 mL) were introduced via syringe. The mixture was sparged with argon for 10 minutes at room temperature, followed by stirring at 65 °C for 48 hours and at 75 °C for another 24 hours. Upon cooling to room temperature, the mixture was precipitated in rapidly stirring methanol and isolated by centrifugation. The polymer was redissolved in a minimal volume of dichloromethane and the process of precipitation was repeated several times. Finally, polymer **16** was dried under reduced pressure to give a yellow

solid (60 mg, 91%). ^1H NMR (500 MHz, CDCl_3 , δ ppm): 7.50-7.70 (14H, br), 3.50-4.01 (4H, br), 0.90-2.13 (40H, br), 0.09 (6H, br).

2,6-dibromo-4-methyl-1-(trimethylsilylethynyl)benzene (18): A 50-mL Schlenk tube containing a magnetic stir-bar was charged with **17** (0.5 g, 1.33 mmol), dichlorobis(triphenylphosphine)palladium(II) (0.047 g, 0.067 mmol), copper(I) iodide (0.025 g, 0.133 mmol), and anhydrous triethylamine (2 mL). Then, trimethylsilylacetylene (0.21 mL, 1.46 mmol) was added via syringe and the reaction mixture was stirred at 80 °C under argon for 4.5 days, with additional trimethylsilylacetylene (0.053 mL), dichlorobis(triphenylphosphine)-palladium(II) (0.013 g), and copper(I) iodide (7 mg) being introduced into the mixture at the 2.5-day mark. After the reaction was complete, ether was added and the mixture was transferred into a separatory funnel containing water and ether. This was extracted several times with additional portions of ether (3 x 20 mL). The combined organic layers were dried over anhydrous magnesium sulfate, filtered, and the solvent was removed to give the crude product. This was purified by flash chromatography on a silica gel column (hexanes) to give **18** in good yield (0.312 g, 68%). ^1H NMR (300 MHz, CD_2Cl_2 , δ ppm): 7.37 (2H, s), 2.30 (3H, s), 0.30 (9H, s). ^{13}C NMR (300 MHz, CD_2Cl_2 , δ ppm): 141.4, 132.2, 126.1, 124.0, 104.2, 102.0, 20.9, 0.08, -0.30.

2,6-dibromo-4-methyl-1-ethynylbenzene (19): A 25-mL round-bottomed flask containing a magnetic stir-bar was charged with **18** (0.095 g, 0.273 mmol), THF (1.5 mL) and methanol (1.0 mL). Then, 1 drop of 40% aqueous KOH was added to the stirred solution via syringe, and the mixture was left to stir overnight at room temperature, after which it was diluted with ether and transferred into a separatory funnel containing water and ether. This was extracted several times

with additional portions of ether (3 x 20 mL). The combined organic layers were dried over anhydrous magnesium sulfate, filtered, and the solvent was removed to give the crude product. This was purified by flash chromatography on a silica gel column (hexanes) to give **19** almost quantitatively (74 mg, 99%). ¹H NMR (300 MHz, CD₂Cl₂, δ ppm): 7.41 (2H, s), 3.67 (1H, s), 2.31 (3H, s). ¹³C NMR (300 MHz, CD₂Cl₂, δ ppm): 142.1, 132.4, 126.3, 85.8, 81.0, 31.8, 22.9, 20.9, 14.1.

1,4-bis(2,6-dibromo-4-methylphenyl)buta-1,3-diyne (20): A 25-mL round-bottomed flask containing a magnetic stir-bar was charged with **19** (0.13 g, 0.48 mmol), tetrakis(triphenylphosphine)palladium(0) (0.027 g, 0.024 mmol), copper(I) iodide (0.014 g, 0.0713 mmol), 1,4-benzoquinone (0.046 g, 0.428 mmol), toluene (9.0 mL) and diisopropylamine (4 mL), and the mixture was stirred overnight at room temperature. Upon completion of reaction, the mixture was diluted with hexane and dichloromethane, and transferred into a separatory funnel containing water and dichloromethane. This was extracted several times with additional portions of dichloromethane (3 x 20 mL). The combined organic layers were dried over anhydrous magnesium sulfate, filtered, and the solvent was removed to give the crude product. This was purified by flash chromatography on a silica gel column (hexanes) to give **20** (59 mg, 46%). ¹H NMR (300 MHz, CD₂Cl₂, δ ppm): 7.43 (4H, s), 2.34 (6H, s). ¹³C NMR (300 MHz, CD₂Cl₂, δ ppm): 142.8, 132.5, 127.0, 81.5, 21.1.

1,4-bis(4,4''-didodecyloxy-5'-methyl-[1,1':3',1''-terphenyl]-2'-yl)buta-1,3-diyne (21): A 25-mL round-bottomed flask containing a magnetic stir-bar was charged with **20** (0.0594 g, 0.11 mmol), 4-dodecyloxyphenylboronic acid (0.20 g, 0.653 mmol), tetrakis-

(triphenylphosphine)palladium(0) (0.013 g, 0.011 mmol), potassium carbonate (0.075 g, 0.545 mmol), toluene (8 mL) and water (0.5 mL). The mixture was heated at 100 °C for 4 days, with additional 4-dodecyloxyphenylboronic acid (0.035 g) and tetrakis(triphenylphosphine)-palladium(0) (0.010 g) being introduced after 2.5 days had elapsed. Upon completion, the mixture was cooled to room temperature, diluted with ether, and then transferred into a separatory funnel containing water and ether. This was extracted several times with additional portions of ether (3 x 20 mL), and the combined organic layers were dried over anhydrous magnesium sulfate, filtered, and the solvent was removed to give the crude product. This was purified by flash chromatography on a silica gel column (20% v/v dichloromethane/hexane) to give **21** (0.097 mg, 70%). ¹H NMR (300 MHz, CD₂Cl₂, δ ppm): 7.49 (8H, d, *J* = 8.7 Hz), 7.13 (4H, s), 6.94 (8H, d, *J* = 8.7 Hz), 4.04 (8H, t, *J* = 6.6 Hz), 2.41 (6H, s), 1.85 (8H, m, *J* = 7.8 Hz), 1.31-1.53 (72H), 0.92 (12H, t, *J* = 6.9 Hz). ¹³C NMR (300 MHz, CD₂Cl₂, δ ppm): 159.2, 146.2, 139.4, 132.8, 130.7, 129.2, 115.7, 113.9, 82.1, 79.6, 68.2, 32.2, 30.0, 29.8, 29.7, 26.4, 23.0, 21.6, 14.2. HRMS (MALDI-TOF): calcd: 1270.9656 (M)⁺, found: 1288.9982 (M + NH₄)⁺.

6,13-bis(2-chlorophenyl)-3,10-bis(decyloxy)-5,12-bis(4-(dodecyloxy)phenyl)benzo[k]tetraphene (23): A 25-mL round-bottomed flask containing a magnetic stir-bar was charged with diiodide **22** (0.0338 g, 0.025 mmol), 2-chlorophenylboronic acid (9 mg, 0.057 mmol), tetrakis(triphenylphosphine)palladium(0) (2.2 mg, 0.0019 mmol), potassium carbonate (0.014 g, 0.099 mmol), toluene (2 mL), ethanol (2 mL), and water (0.15 mL). The mixture was heated at 80 °C for 24 hours under argon, after which it was cooled to room temperature, diluted with ether, and then transferred into a separatory funnel containing water and ether. This was extracted several times with additional portions of ether (3 x 20 mL), and the combined organic

layers were dried over anhydrous magnesium sulfate, filtered, and the solvent was removed to give the crude product. This was purified by flash chromatography on a silica gel column (20% v/v dichloromethane/hexane) to give **23** as a white solid (31.1 mg, 94%). ¹H NMR (300 MHz, CD₂Cl₂, δ ppm): 8.55 (2H, s), 8.25 (2H, d, *J* = 9.3 Hz), 6.7-7.5 (20H), 3.93 (4H, t, *J* = 6.3 Hz), 3.86 (4H, t, *J* = 6.3 Hz), 1.2-1.8 (72H), 0.88 (12H, t, *J* = 6.6 Hz). ¹³C NMR (300 MHz, CDCl₃, δ ppm): 158.1, 139.2, 138.6, 137.5, 135.6, 134.9, 134.1, 133.3, 131.8, 131.6, 130.9, 129.5, 129.1, 128.8, 128.4, 126.7, 124.7, 124.3, 120.2, 116.3, 113.9, 110.9, 68.2, 32.2, 30.0, 29.9, 29.8, 29.7, 29.6, 29.4, 26.4, 26.3, 23.0, 22.9, 14.4. HRMS (MALDI-TOF): calcd: 1330.8251 (M)⁺, found: 1330.3632.

2,5-dibromo-1,4-bis(4'-dodecylphenylethynyl)benzene (28): A 50-mL round-bottomed flask containing a magnetic stir-bar was charged with 1,4-dibromo-2,5-diiodobenzene (1.58 g, 3.24 mmol), tetrakis(triphenylphosphine)palladium(0) (0.075 g, 0.065 mmol), copper(I) iodide (0.024 g, 0.126 mmol) and anhydrous triethylamine (11 mL). The mixture was stirred as a solution of 4-dodecylphenylacetylene (2.1 g, 7.76 mmol) in THF (3 mL) was introduced slowly via syringe. Stirring was continued for another 3 hours at room temperature, after which all the solvent was removed by rotary evaporation. Ether (40 mL) was added to the residue and then the mixture was transferred into a separatory funnel containing water. This was extracted several times with additional portions of ether (3 x 30 mL), and the combined organic layers were dried over anhydrous magnesium sulfate, filtered, and the solvent was removed to give the crude product. This was purified by flash chromatography on a silica gel column (10% v/v dichloromethane/hexane) to give **28** as a white solid (1.1 g, 44%). ¹H NMR (300 MHz, CDCl₃, δ ppm): 7.76 (2H, s), 7.49 (4H, d, *J* = 8.1 Hz), 7.18 (4H, d, *J* = 8.4 Hz), 2.62 (4H, t, *J* = 7.8 Hz),

1.61 (4H, m, $J = 6.9$ Hz), 1.25-1.30 (40H), 0.88 (6H, t, $J = 6.9$ Hz). ^{13}C NMR (300 MHz, CDCl_3 , δ ppm): 144.7, 136.1, 131.4, 128.8, 126.6, 123.9, 119.7, 97.2, 86.6, 36.2, 32.2, 31.5, 29.9, 29.8, 29.7, 29.6, 29.5, 23.0, 14.4. HRMS (EI): calcd: 770.3062 (M)⁺, found: 772.29 ($\text{M}+\text{H}$)⁺.

2',5'-bis((4-dodecylphenyl)ethynyl)-4,4''-dinonyl-1,1':4',1''-terphenyl (29): A 100-mL round-bottomed flask containing a magnetic stir-bar was charged with **28** (1.031 g, 1.01 mmol), 4-nonylphenylboronic acid (0.672 g, 2.53 mmol), tetrakis(triphenylphosphine)-palladium(0) (0.07 g, 0.061 mmol), potassium carbonate (0.70 g, 5.05 mmol), toluene (30 mL), ethanol (1.5 mL), and water (1.5 mL). The mixture was heated at 100 °C overnight under argon, after which it was cooled to room temperature, diluted with ether, and then transferred into a separatory funnel containing water. The mixture was extracted several times with additional portions of ether (3 x 40 mL), and the combined organic layers were dried over anhydrous magnesium sulfate, filtered, and the solvent was removed to give the crude product. This was purified by flash chromatography on a silica gel column (15% v/v dichloromethane/hexane) to give **29** (0.874 g, 85%). ^1H NMR (300 MHz, CD_2Cl_2 , δ ppm): 7.71 (2H, s), 7.68 (4H, d, $J = 8.1$ Hz), 7.34 (4H, d, $J = 8.4$ Hz), 7.29 (4H, d, $J = 8.1$ Hz), 7.15 (4H, d, $J = 8.4$ Hz), 2.72 (4H, t, $J = 7.8$ Hz), 2.61 (4H, t, $J = 8.1$ Hz), 1.60-1.75 (8H), 1.28-1.40 (68H), 0.90 (12H, t, $J = 6.9$ Hz). ^{13}C NMR (300 MHz, CD_2Cl_2 , δ ppm): 144.1, 143.0, 142.3, 136.9, 133.8, 131.4, 130.2, 129.3, 128.7, 128.3, 121.8, 120.4, 94.0, 88.9, 36.1, 35.9, 32.2, 31.8, 31.5, 29.9, 29.8, 29.7, 29.6, 29.5, 23.0, 22.9, 14.2, 14.1. HRMS (MALDI-TOF): calcd: 1018.8295 (M)⁺, found: 1018.5169.

5,12-bis(4-dodecylphenyl)-6,13-diiodo-3,10-dinonylbenzo[k]tetraphene (30): A 100-mL round-bottomed flask containing a magnetic stir-bar was charged with **29** (0.874 g, 0.857 mmol)

and anhydrous dichloromethane (6.0 mL). The stirred mixture was cooled down to -78 °C in a dry-ice/acetone bath, and a solution of 1.0 M iodine monochloride (2.14 mL, 2.14 mmol) in dichloromethane was added slowly via syringe. The mixture was allowed to stir for 1 hour at -78 °C, after which it was diluted with dichloromethane and transferred into a separatory funnel containing an aqueous solution of potassium hydroxide. The mixture was extracted several times with additional portions of dichloromethane (3 x 40 mL), and the combined organic layers were dried over anhydrous magnesium sulfate, filtered, and the solvent was removed to give the crude product. This was purified by flash chromatography on a silica gel column (10% v/v dichloromethane/hexane) to give **30** (0.48 g, 44%). ¹H NMR (300 MHz, CDCl₃, δ ppm): 9.73 (2H, s), 8.87 (2H, d, *J* = 8.4 Hz), 7.57 (2H, d, *J* = 8.4 Hz), 7.40 (4H, d, *J* = 7.8 Hz), 7.23 (4H, d, *J* = 9.3 Hz), 2.80 (4H, t, *J* = 7.8 Hz), 2.67 (4H, t, *J* = 7.5 Hz), 1.2-1.8 (76H), 0.88 (4H, t, *J* = 6.3 Hz). ¹³C NMR (300 MHz, CDCl₃, δ ppm): 146.5, 143.0, 142.8, 142.5, 133.0, 131.4, 129.9, 129.8, 129.0, 128.7, 128.6, 128.5, 128.4, 123.3, 106.8, 36.2, 36.1, 32.2, 31.7, 31.5, 30.0, 29.9, 29.8, 29.7, 29.6, 29.4, 23.0, 14.4. HRMS (MALDI-TOF): calcd: 1016.8138 (M-I₂)⁺, found: 1017.0534.

5,12-bis(4-dodecylphenyl)-3,10-dinonyl-6,13-bis(4-nonylphenyl)benzo[k]tetraphene (31):

A 100-mL round-bottomed flask containing a magnetic stir-bar was charged with **30** (0.48 g, 0.378 mmol), 4-nonylphenylboronic acid (0.281 g, 1.13 mmol), tetrakis(triphenylphosphine)-palladium(0) (0.026 g, 0.0227 mmol), potassium carbonate (0.261 g, 1.89 mmol), toluene (15 mL), ethanol (5 mL), and water (1 mL). The mixture was heated at 100 °C overnight under argon, after which it was cooled to room temperature, diluted with ether, and then transferred into a separatory funnel containing water. The mixture was extracted several times with

additional portions of ether (3 x 35 mL), and the combined organic layers were dried over anhydrous magnesium sulfate, filtered, and the solvent was removed to give the crude product. This was purified by flash chromatography on a silica gel column (10% v/v dichloromethane/hexane) to give **31** (0.518 g, 96%). ¹H NMR (300 MHz, CD₂Cl₂, δ ppm): 8.88 (2H, s), 8.26 (2H, d, *J* = 8.7 Hz), 7.35 (2H, d, *J* = 8.4 Hz), 7.31 (2H, s), 7.08-7.21 (16H), 2.50-2.70 (12H), 1.20-1.60 (96H), 0.84-0.90 (18H). ¹³C NMR (300 MHz, CD₂Cl₂, δ ppm): 141.7, 141.3, 141.2, 137.5, 137.3, 132.6, 131.4, 131.1, 130.7, 128.5, 128.2, 128.0, 127.7, 127.5, 127.3, 122.6, 121.3, 36.1, 35.8, 32.3, 32.2, 32.1, 31.7, 31.6, 30.0, 29.9, 29.8, 29.7, 29.6, 29.5, 29.4, 23.0, 22.9, 14.2, 14.1. HRMS (MALDI-TOF): calcd: 1423.1737 (M)⁺, found: 1423.4473.

5,14-bis(4-dodecylphenyl)-3,8,12,17-tetranonyldibenz[*a,m*]rubicene (32): A 25-mL round-bottomed flask containing a magnetic stir-bar was charged with **31** (0.060 g, 0.042 mmol) and anhydrous dichloromethane (2 mL). Then, a solution of anhydrous iron(III) bromide (0.124 g, 0.421 mmol) in dry nitromethane (1 mL) was added via syringe. The mixture was allowed to stir for 30 minutes at room temperature, after which the reaction was quenched with anhydrous methanol (3.5 mL). This was then transferred into a separatory funnel containing water and dichloromethane. The mixture was extracted several times with additional portions of dichloromethane (3 x 25 mL), and the combined organic layers were dried over anhydrous magnesium sulfate, filtered, and the solvent was removed to give the crude product. This was purified by flash chromatography on a silica gel column (10-15% v/v dichloromethane/hexane) to give **32** as a red-orange solid (21.2 mg, 36%). ¹H NMR (300 MHz, CD₂Cl₂, δ ppm): 9.23 (2H, d, *J* = 8.1 Hz), 8.50 (2H, s), 7.40-7.60 (8H), 7.19 (2H, d, *J* = 6.0 Hz), 7.09 (2H, d, *J* = 7.2 Hz), 6.86 (2H, d, *J* = 8.1 Hz), 6.59 (2H, d, *J* = 7.8 Hz), 2.86 (4H, t, *J* = 7.2 Hz), 2.74 (4H, t, *J* = 7.5

Hz), 2.67 (4H, t, $J = 7.2$ Hz), 0.85-2.05 (102H). ^{13}C NMR (300 MHz, CD_2Cl_2 , δ ppm): 143.2, 142.65, 141.6, 135.7, 132.0, 129.9, 129.3, 127.2, 124.1, 36.1, 32.2, 31.8, 30.0, 29.9, 29.7, 29.6, 22.9, 14.1. HRMS (MALDI-TOF): calcd: 1419.1425 (M)⁺, found: 1419.3226.

References and Notes

- [1] (a) Möbius, D. *Adv. Mater.* **1995**, *7*, 437–444. (b) Kobayashi, T., Ed. *J-Aggregates*; World Science: Singapore, 1996.
- [2] Chan, J. M. W., Tischler, J. R., Kooi, S. E., Bulović, V., Swager, T. M. *J. Am. Chem. Soc.* **2009**, *131*, 5659-5666.
- [3] (a) Hoeben, F. J. M.; Jonkheim, P.; Meijer, E. W.; Schenning, A. P. H. *J. Chem. Rev.* **2005**, *105*, 1491–1546 (b) Wasielewski, M. R. *J. Org. Chem.* **2006**, *71*, 5051–5066 (c) Yamamoto, Y.; Fukushima, T.; Suna, Y.; Ishii, N.; Saeki, A.; Seki, S.; Tagawa, S.; Taniguchi, M.; Kawai, T.; Aida, T. *Science* **2006**, *314*, 1761–1764 (d) Miller, R. A.; Presley, A. D.; Francis, M. B. *J. Am. Chem. Soc.* **2007**, *129*, 3104–3109 (e) *Photosynthetic Light-Harvesting Systems: Organization and Function*; Scheer, H.; Schneider, S., Eds.; de Gruyter: Berlin, 1988. (f) Prokhorenko, V. I.; Steensgard, D. B.; Holzwarth, A. R. *Biophys. J.* **2000**, *79*, 2105–2120 (g) Takahashi, R.; Kobuke, Y. *J. Am. Chem. Soc.* **2003**, *125*, 2372–2373 (h) Yamaguchi, T.; Kimura, T.; Matsuda, H.; Aida, T. *Angew. Chem. Int. Ed.* **2004**, *43*, 6350–6355 (i) Elemans, J. A. A. W.; van Hameren, R.; Nolte, R. J. M.; Rowan, A. E. *Adv. Mater.* **2006**, *18*, 1251–1266.
- [4] Minisci, F.; Citterio, A.; Vismara, E.; Fontana, F.; De Bernardinis, S.; Correale, M. *J. Org. Chem.* **1989**, *54*, 728-731.

[5] Steinberg, B. D.; Jackson, E. A.; Filatov, A. S.; Wakamiya, A.; Petrukhina, M. A.; Scott, L. T. *J. Am. Chem. Soc.* **2009**, *131*, 10537-10545.

[6] Hseuh, H.; Hsu, M.; Wu, T.; Liu, R. *J. Org. Chem.* **2009**, *74*, 8448-8451.

Chapter 5 Appendix
 ^1H -NMR and ^{13}C -NMR Spectra

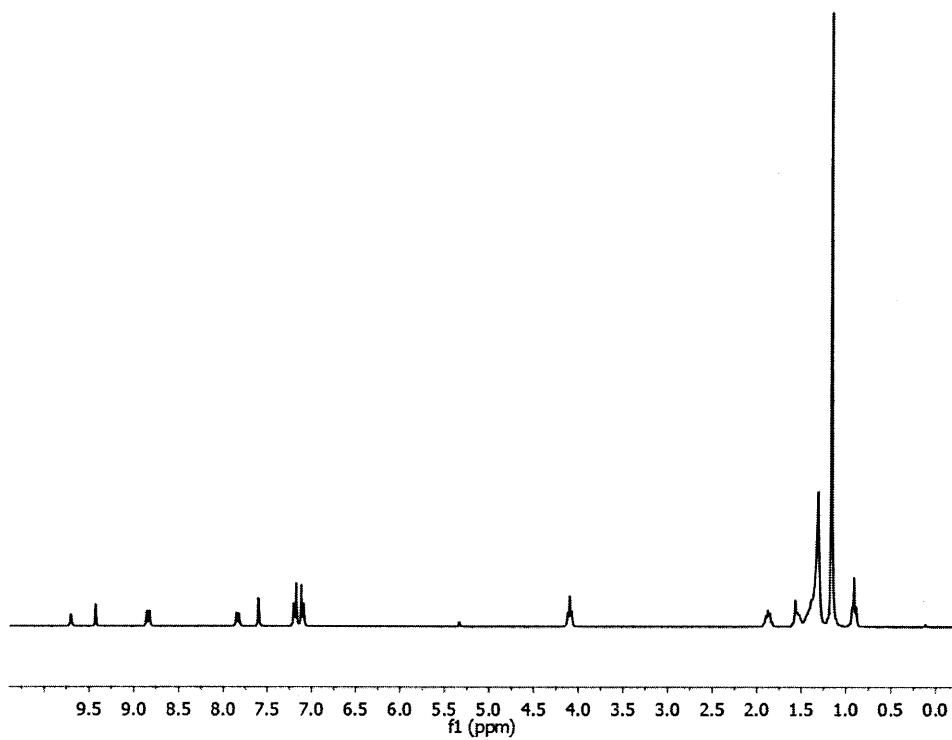


Figure 5.A.1. ^1H -NMR spectrum of **5** (300 MHz, CD_2Cl_2).

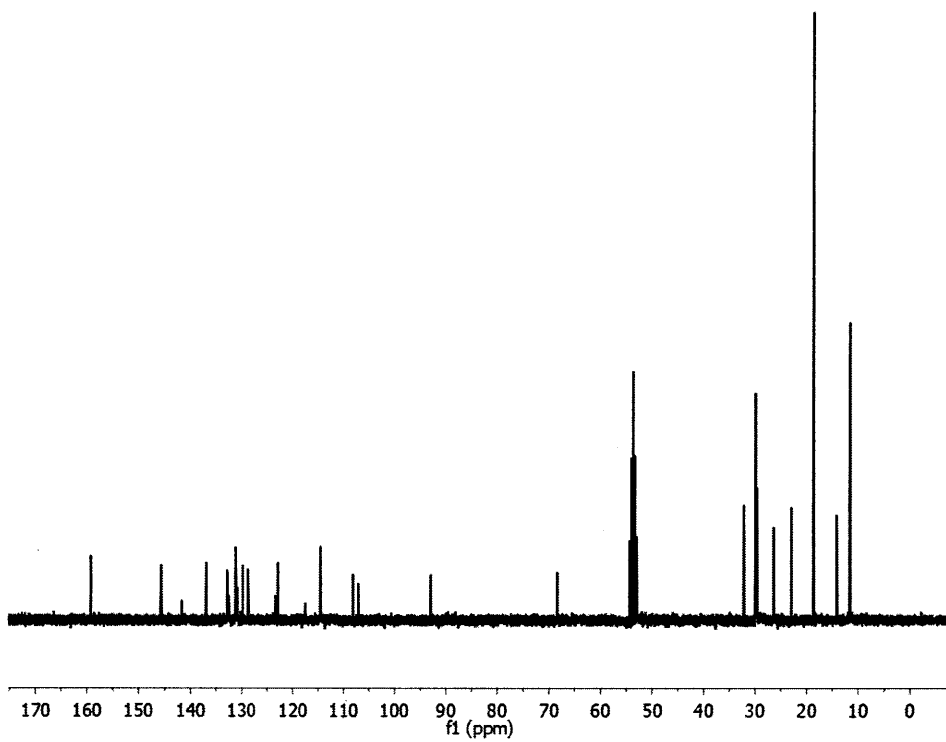


Figure 5.A.2. ^{13}C -NMR spectrum of **5** (300 MHz, CD_2Cl_2).

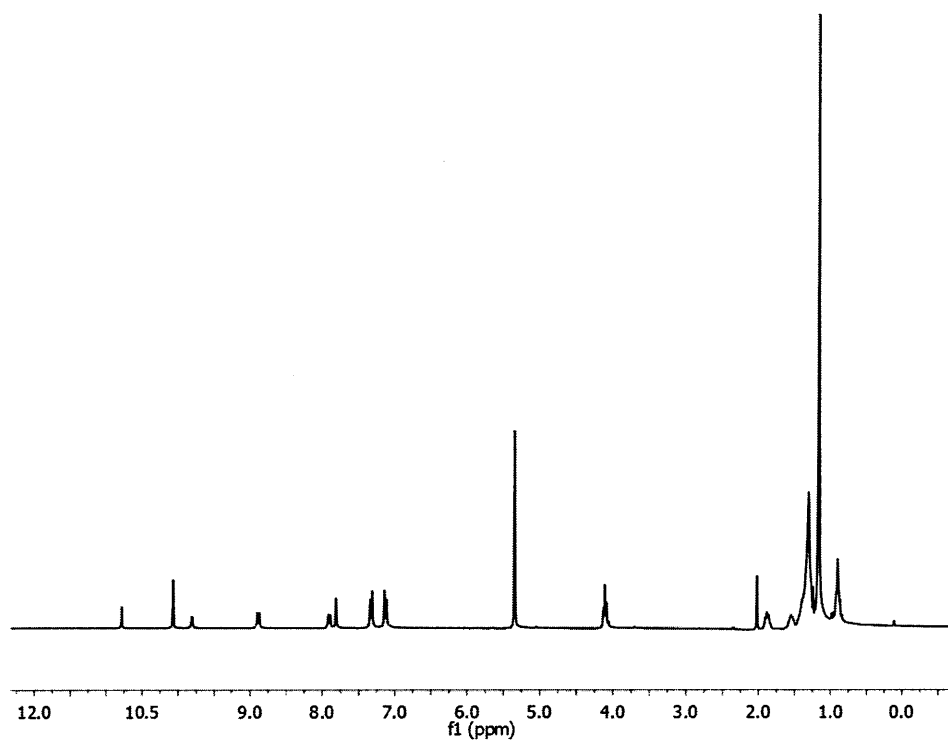


Figure 5.A.3. ^1H -NMR spectrum of **6** (300 MHz, CD_2Cl_2).

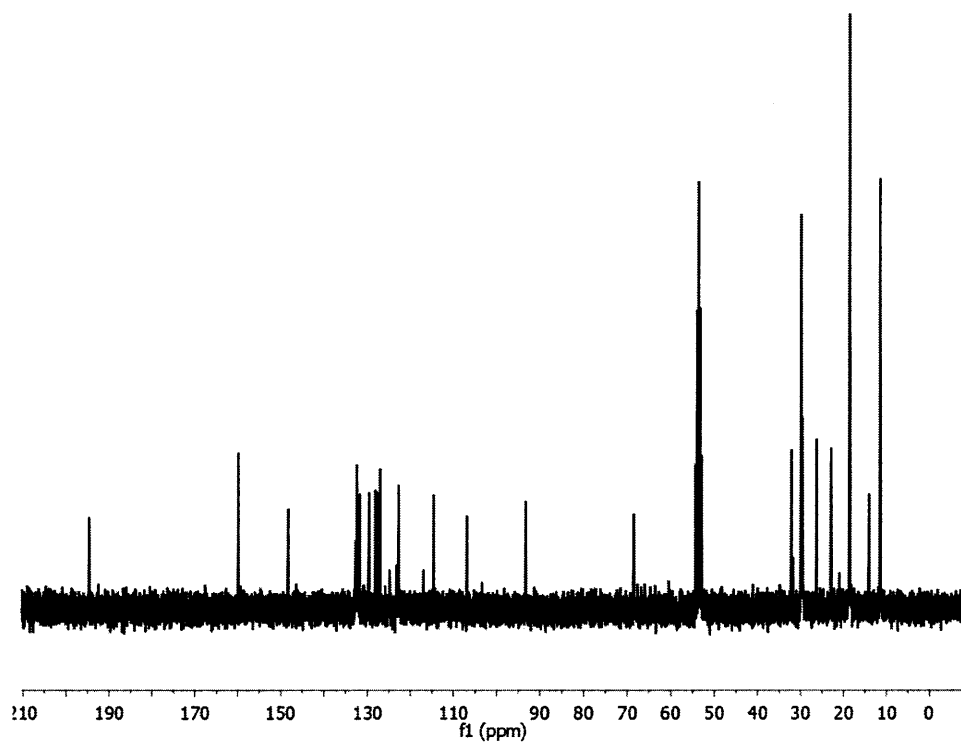


Figure 5.A.4. ^{13}C -NMR spectrum of **6** (300 MHz, CD_2Cl_2).

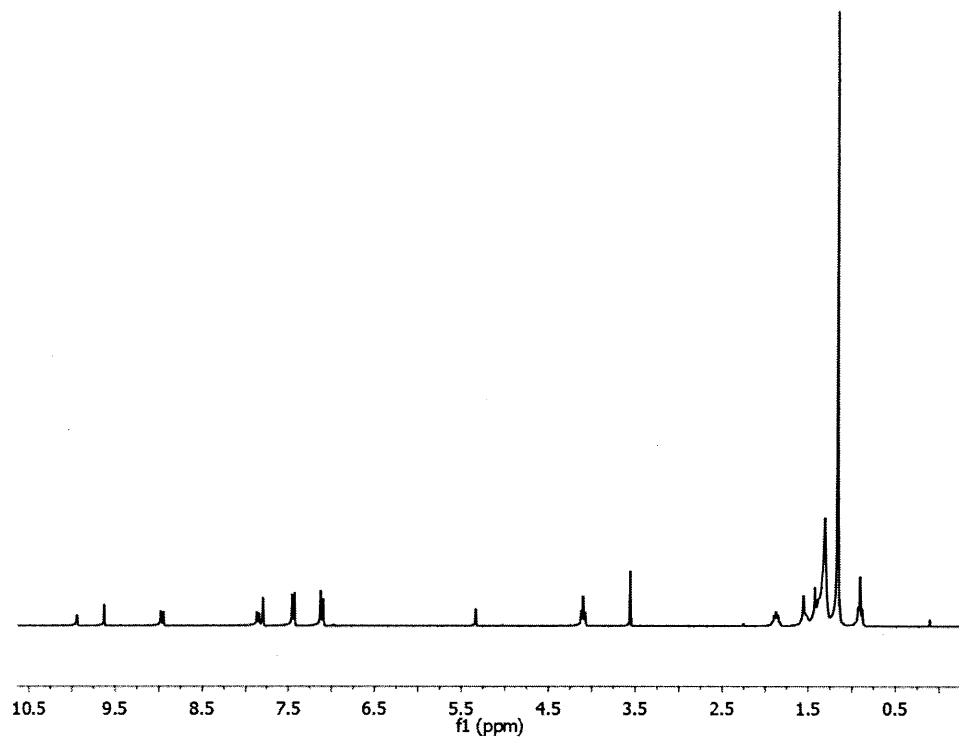


Figure 5.A.5. ^1H -NMR spectrum of 7 (300 MHz, CD_2Cl_2).

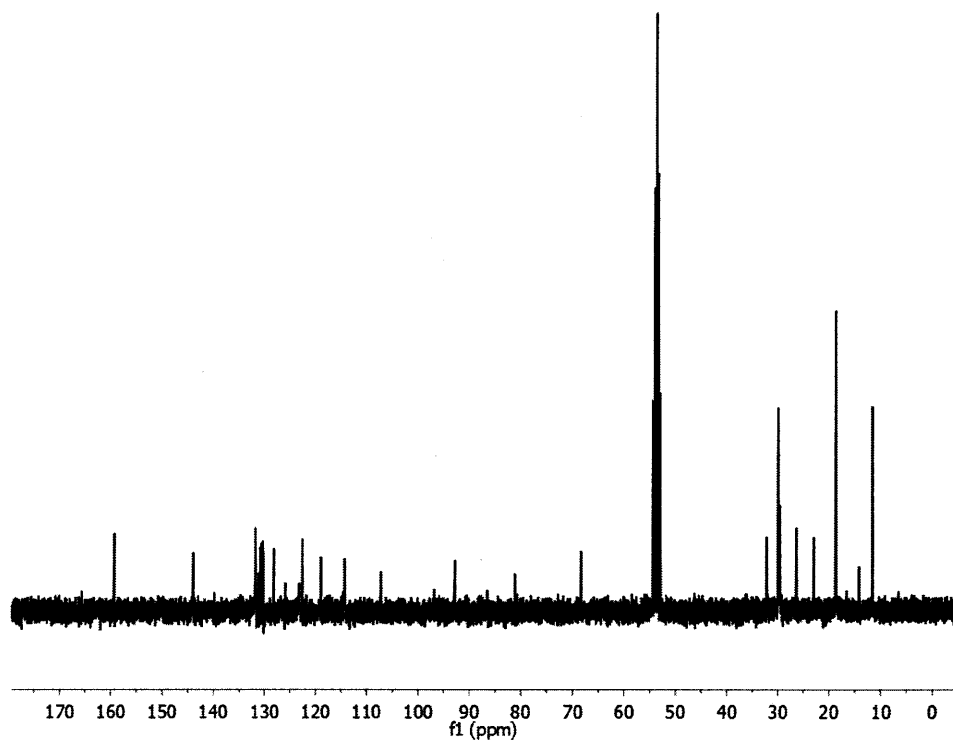


Figure 5.A.6. ^{13}C -NMR spectrum of 7 (300 MHz, CD_2Cl_2).

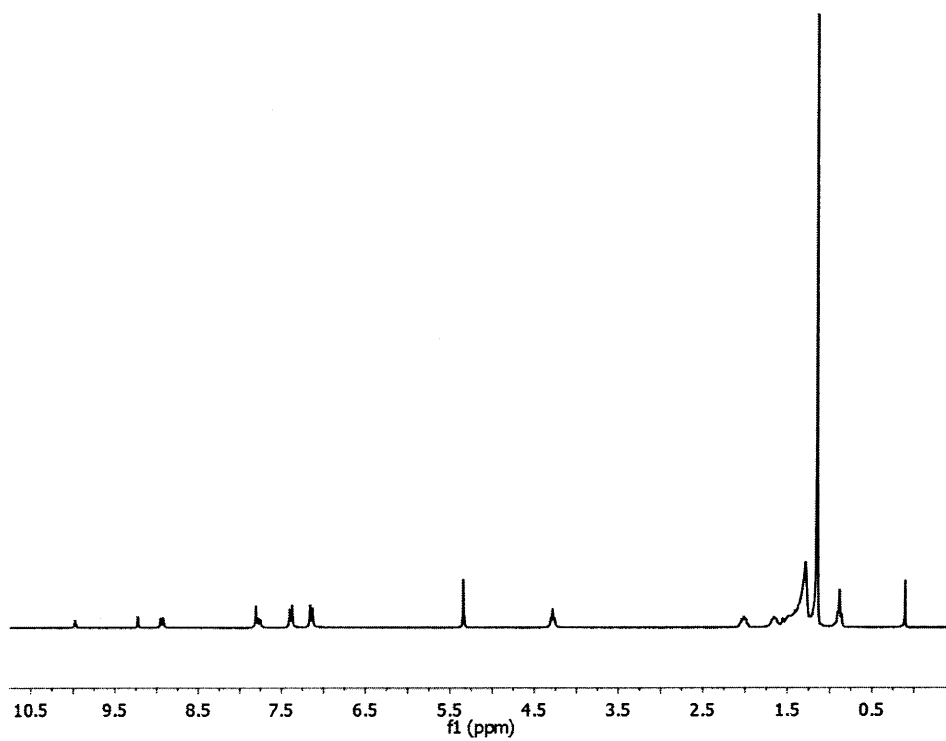


Figure 5.A.7. ^1H -NMR spectrum of **8** (300 MHz, CD_2Cl_2).

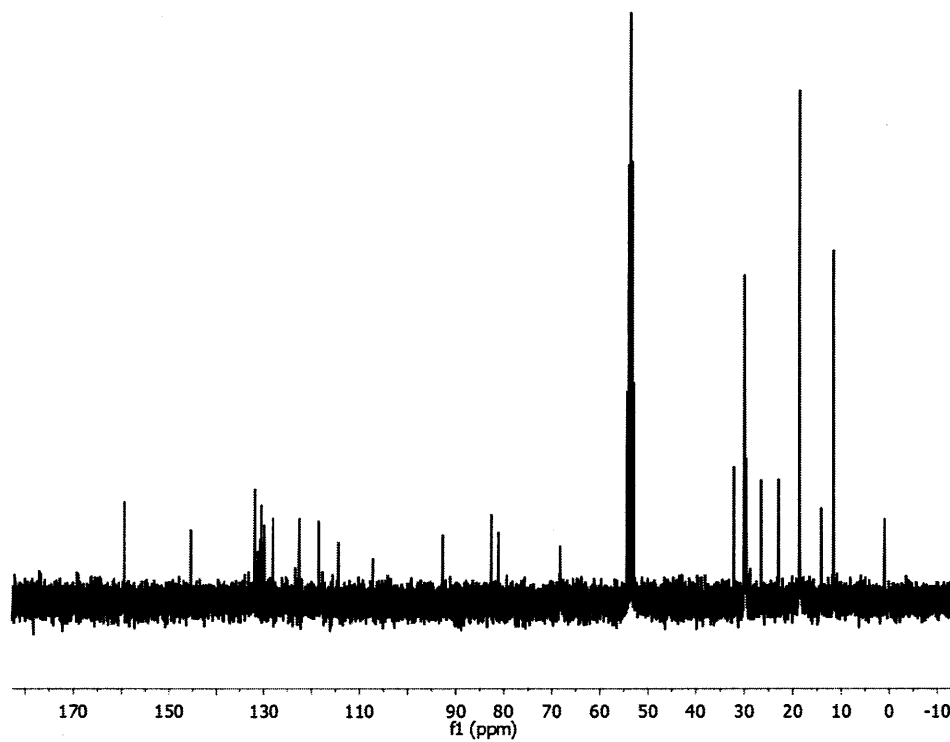


Figure 5.A.8. ^{13}C -NMR spectrum of **8** (300 MHz, CD_2Cl_2).

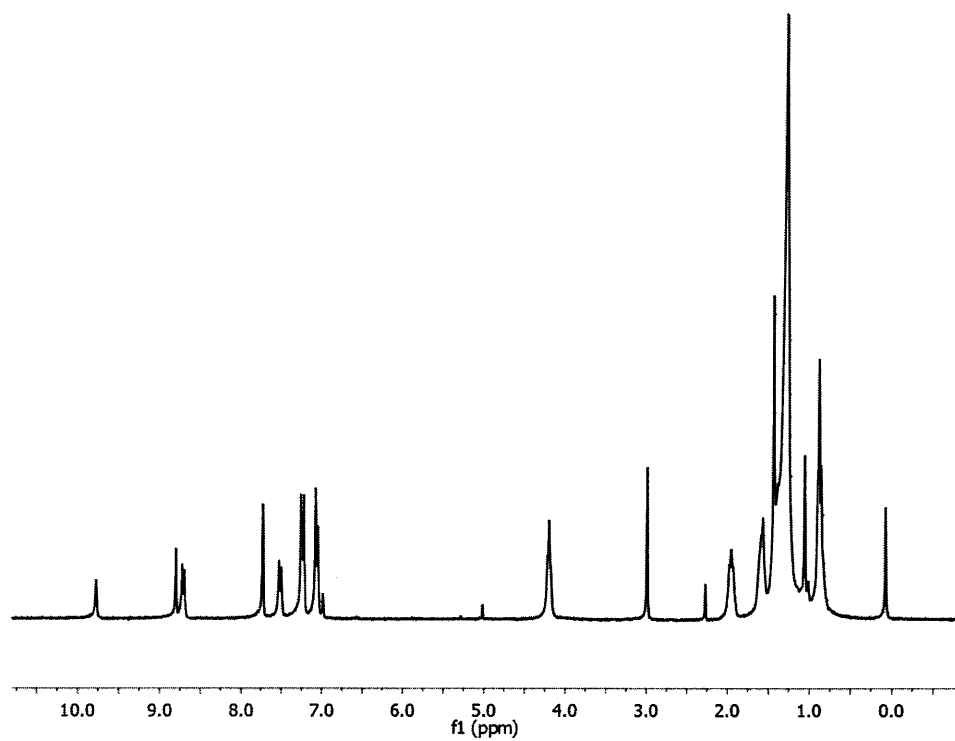


Figure 5.A.9. ^1H -NMR spectrum of **9** (300 MHz, CDCl_3).

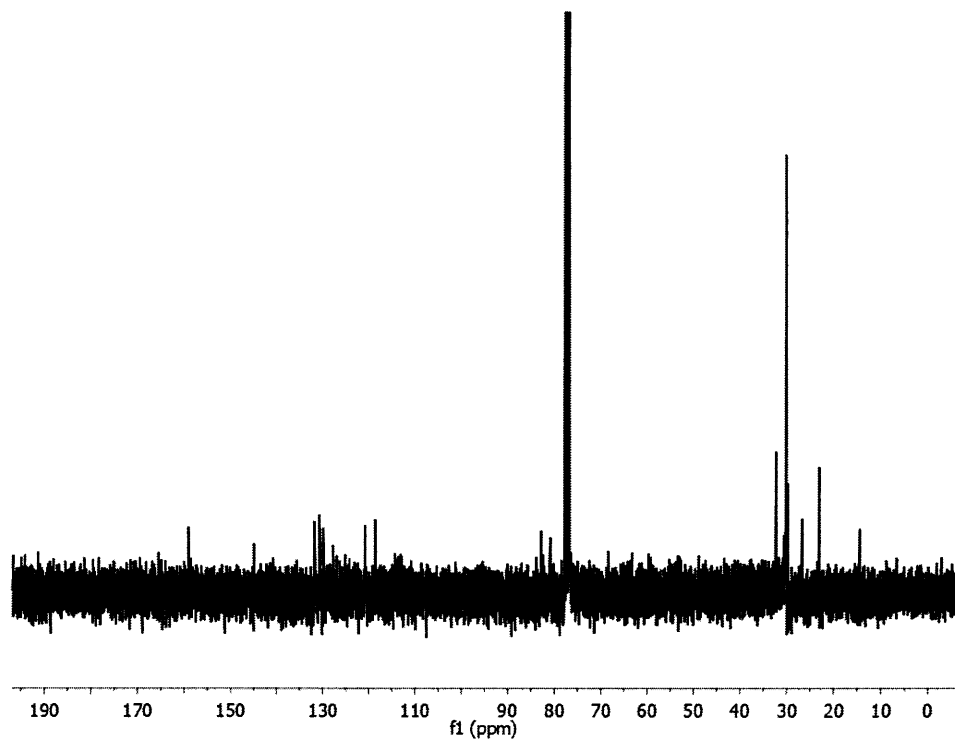


Figure 5.A.10. ^{13}C -NMR spectrum of **9** (300 MHz, CDCl_3).

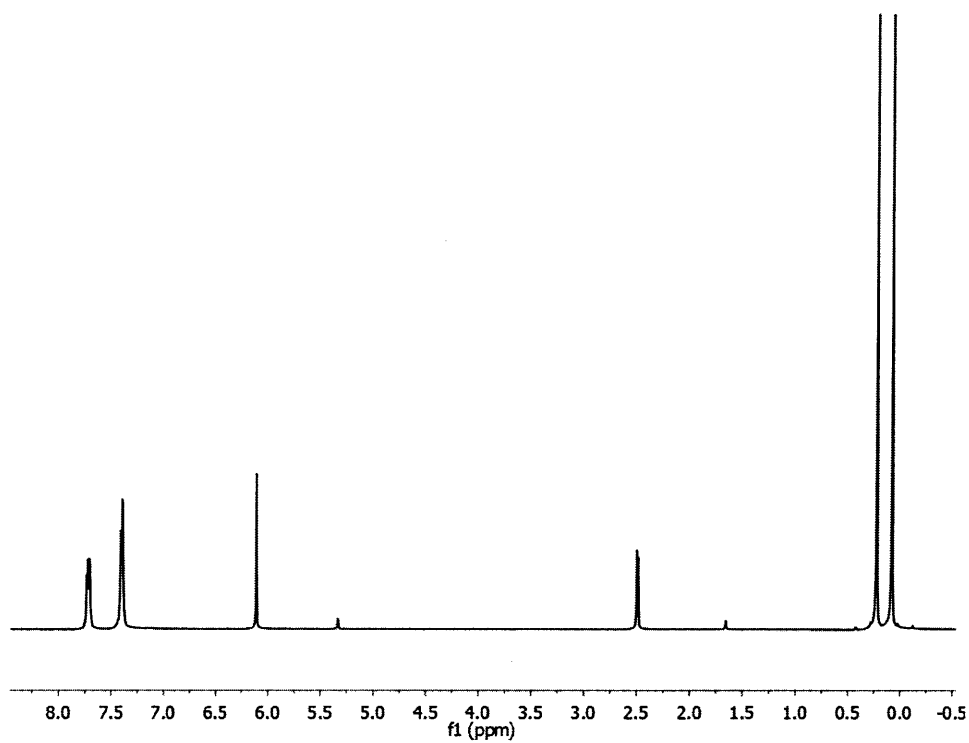


Figure 5.A.11. ^1H -NMR spectrum of **13** (300 MHz, CD_2Cl_2).

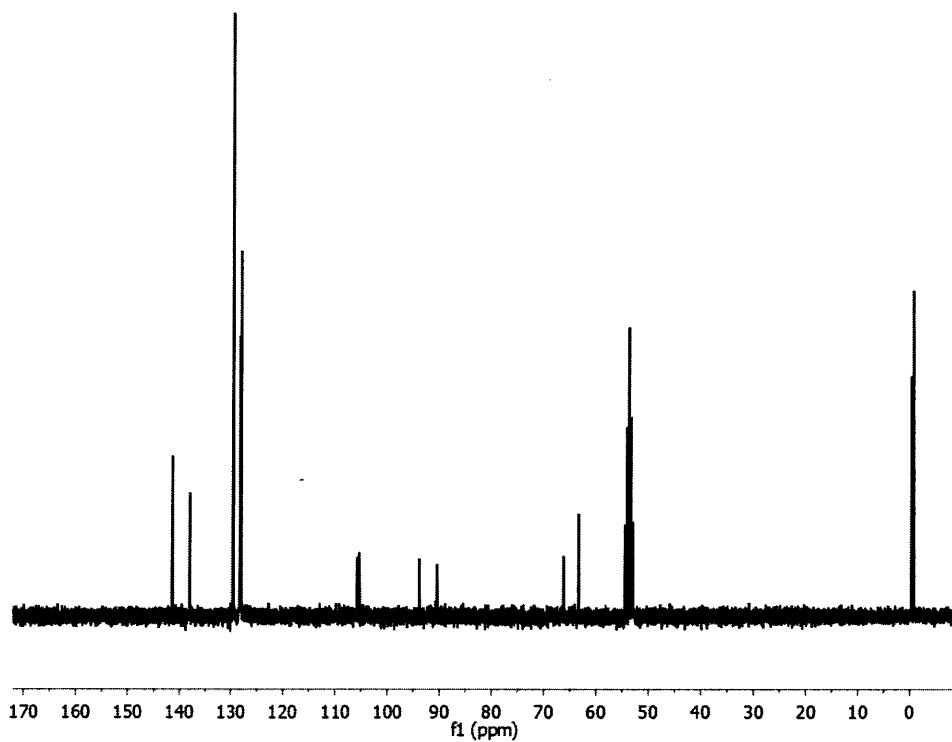


Figure 5.A.12. ^{13}C -NMR spectrum of **13** (300 MHz, CD_2Cl_2).

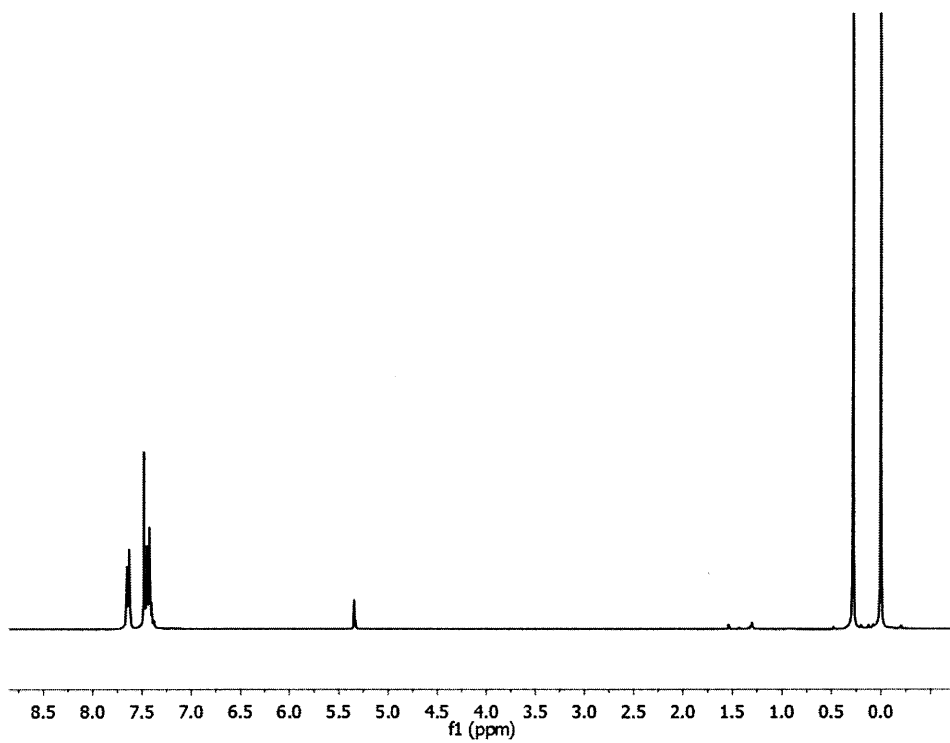


Figure 5.A.13. ^1H -NMR spectrum of **14** (300 MHz, CD_2Cl_2).

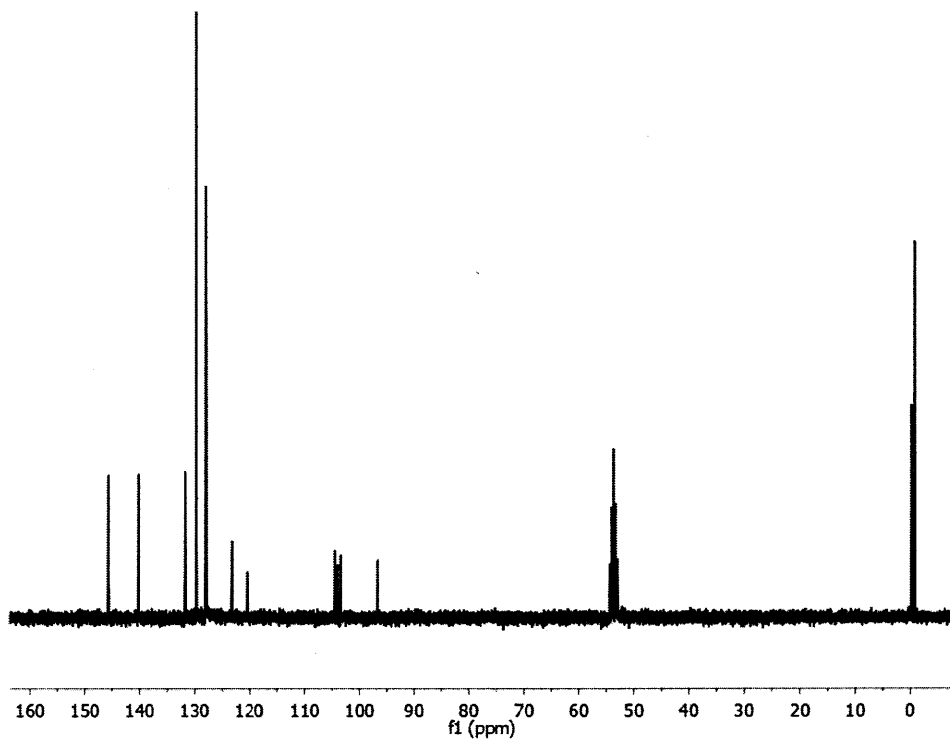


Figure 5.A.14. ^{13}C -NMR spectrum of **14** (300 MHz, CD_2Cl_2).

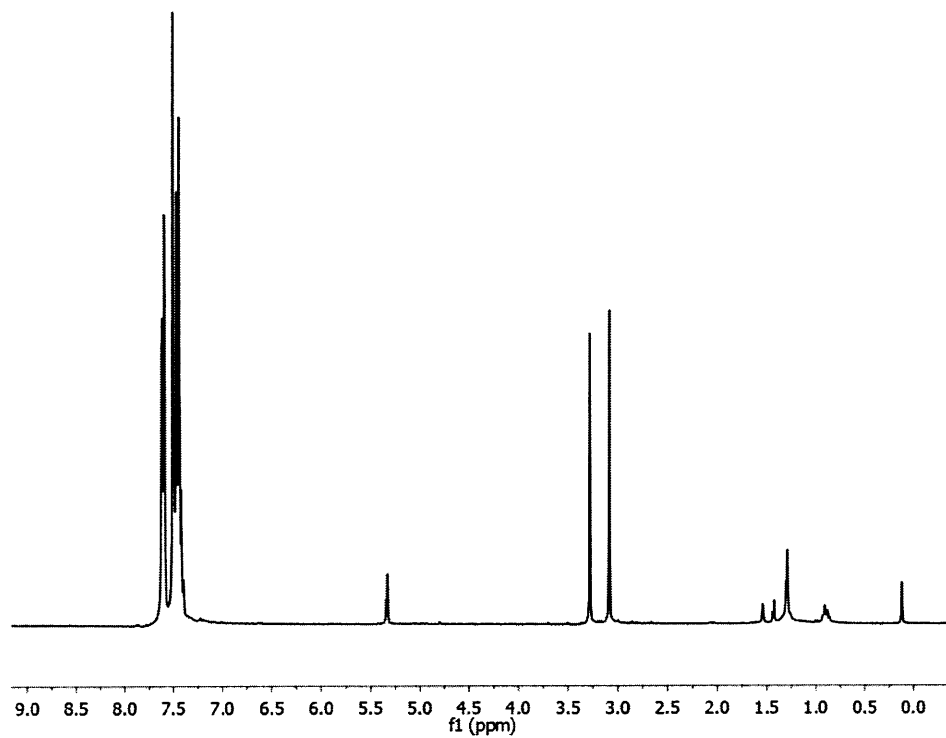


Figure 5.A.15. ^1H -NMR spectrum of **15** (300 MHz, CD_2Cl_2).

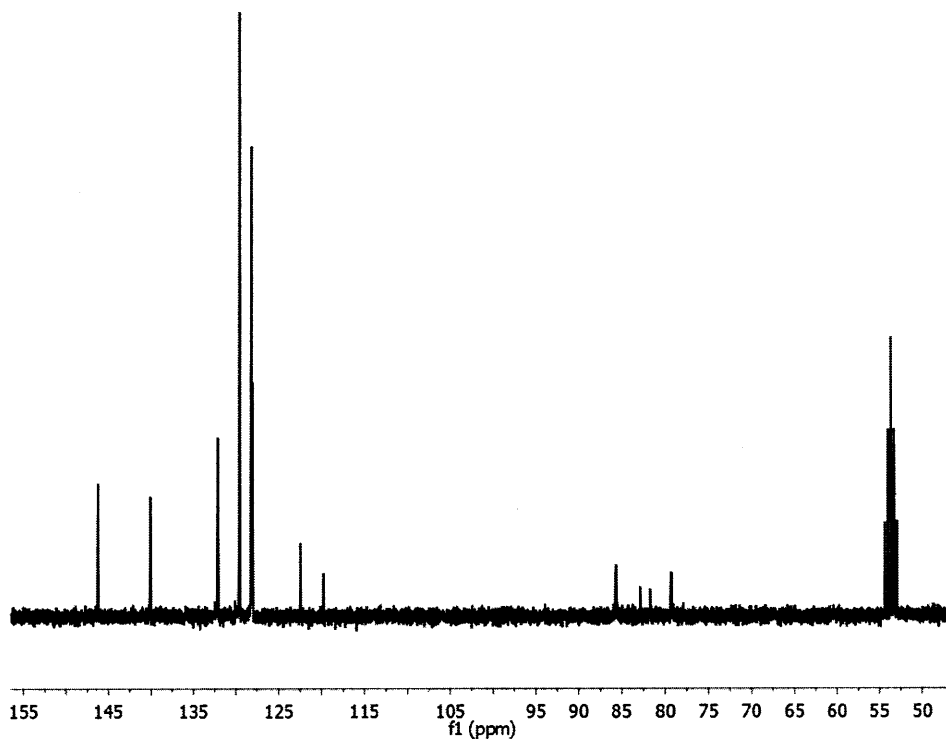


Figure 5.A.16. ^{13}C -NMR spectrum of **15** (300 MHz, CD_2Cl_2).

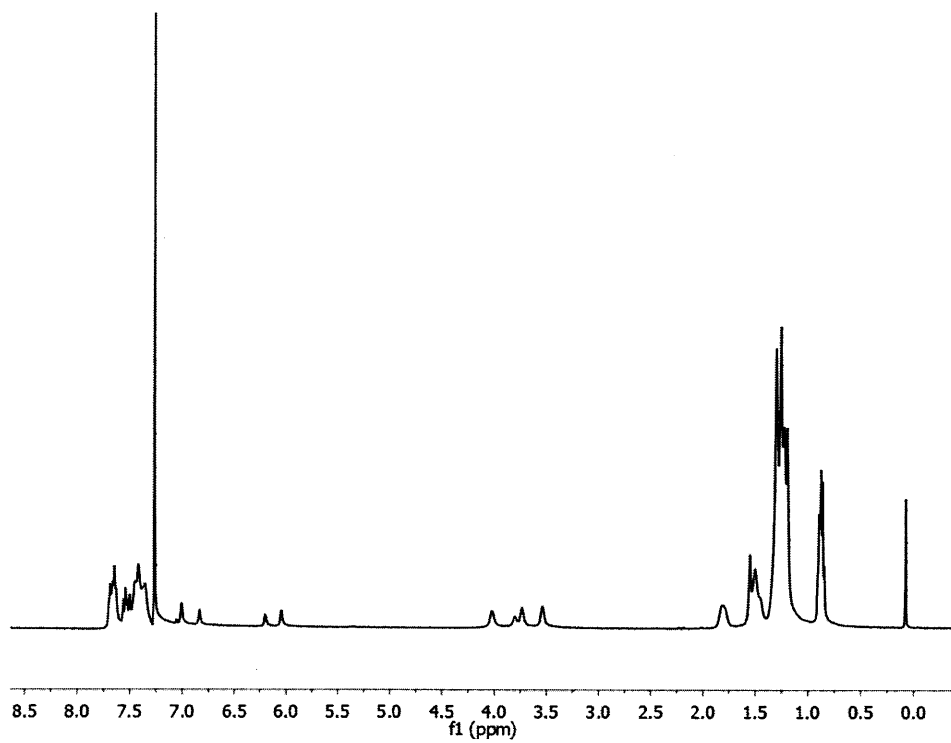


Figure 5.A.17. ^1H -NMR spectrum of polymer **16** (500 MHz, CDCl_3).

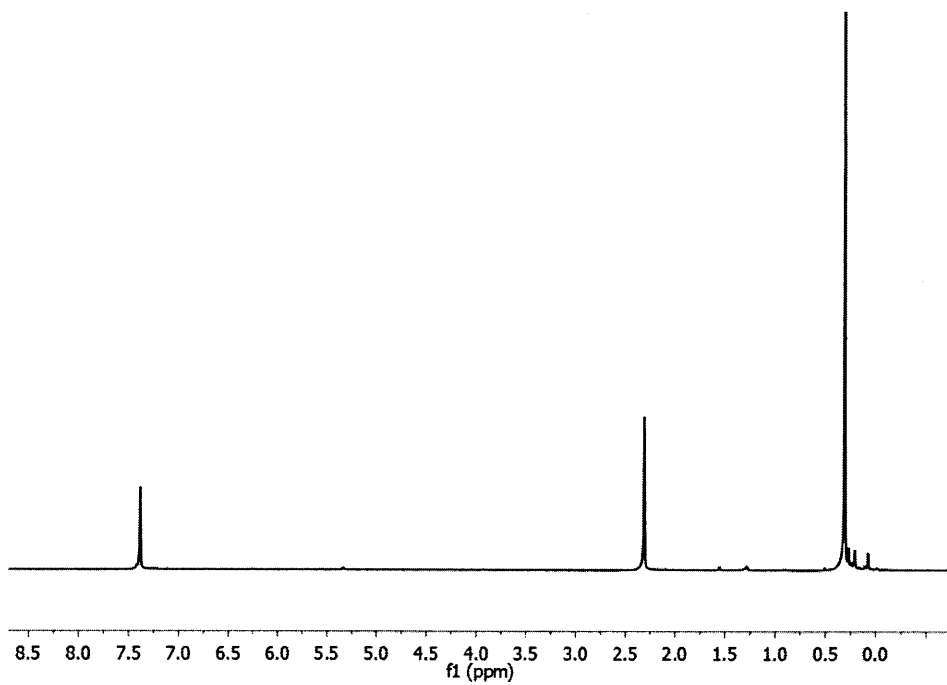


Figure 5.A.18. ^1H -NMR spectrum of **18** (300 MHz, CD_2Cl_2).

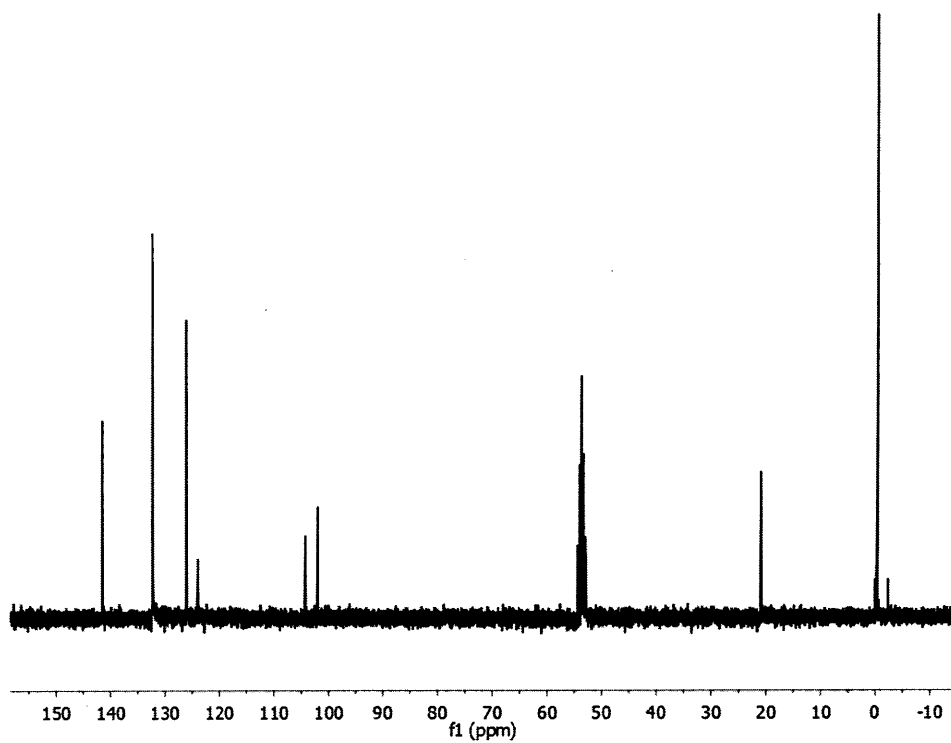


Figure 5.A.19. ^{13}C -NMR spectrum of **18** (300 MHz, CD_2Cl_2).

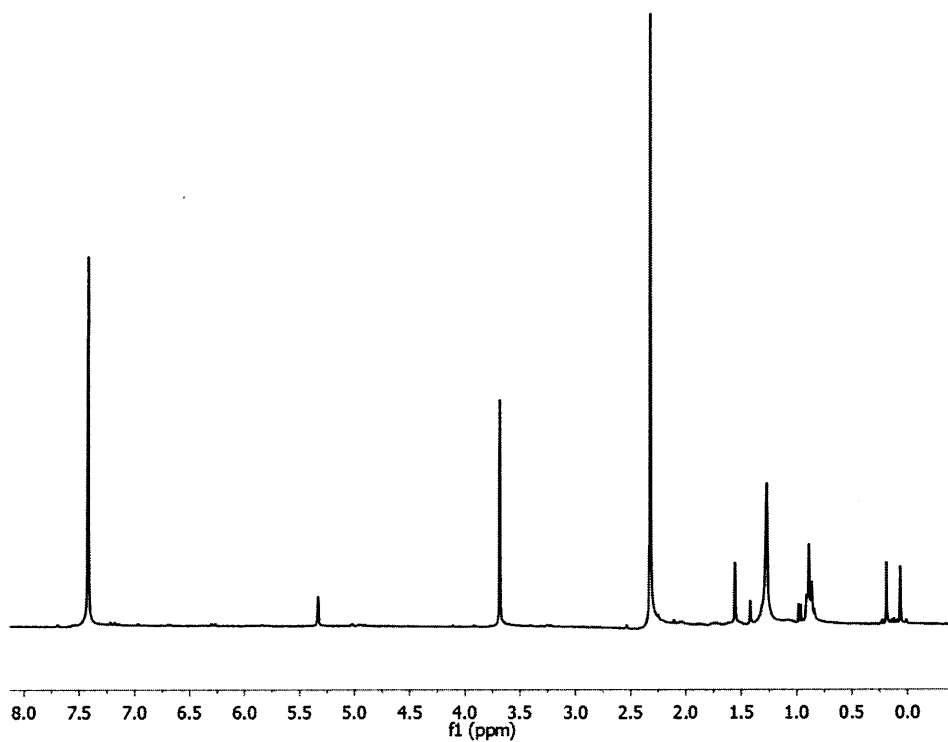


Figure 5.A.20. ^1H -NMR spectrum of **19** (300 MHz, CD_2Cl_2).

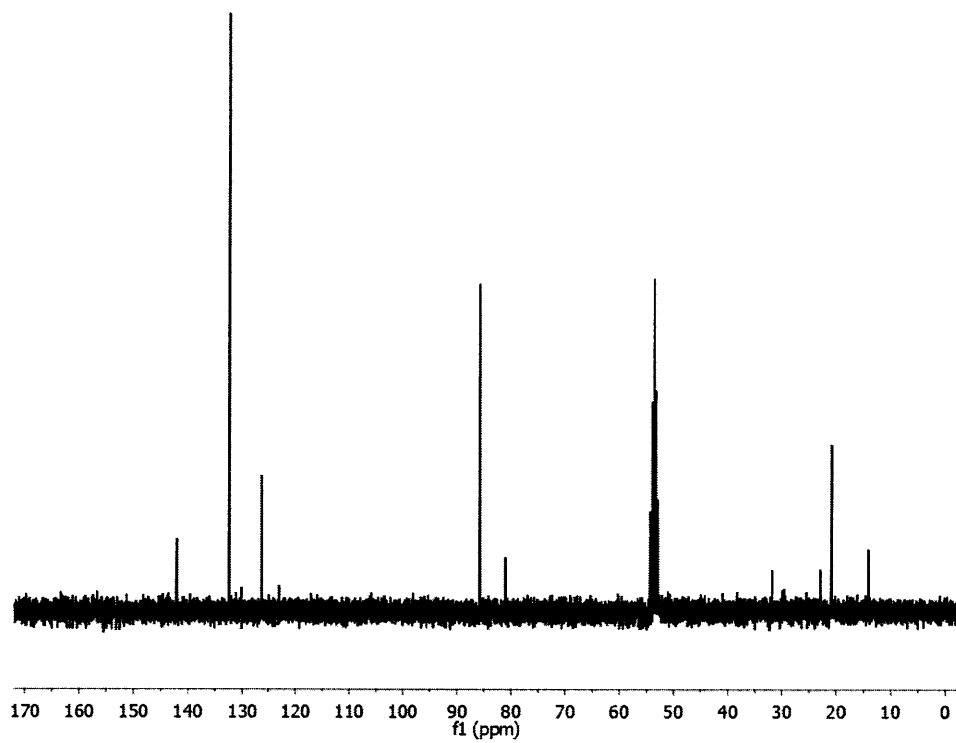


Figure 5.A.21. ^{13}C -NMR spectrum of **19** (300 MHz, CD_2Cl_2).

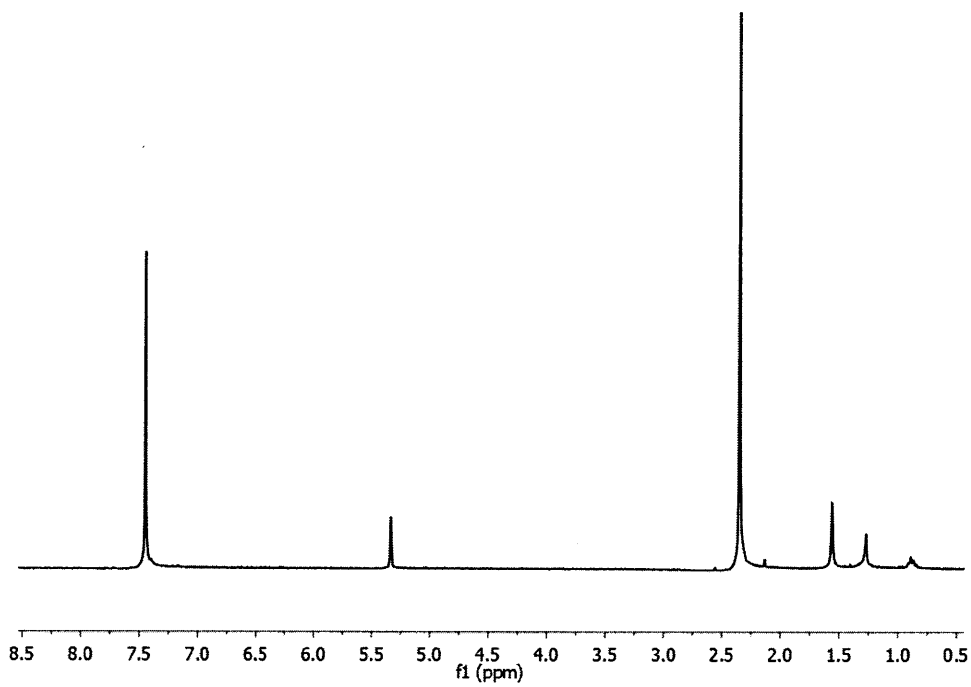


Figure 5.A.22. ^1H -NMR spectrum of **20** (300 MHz, CD_2Cl_2).

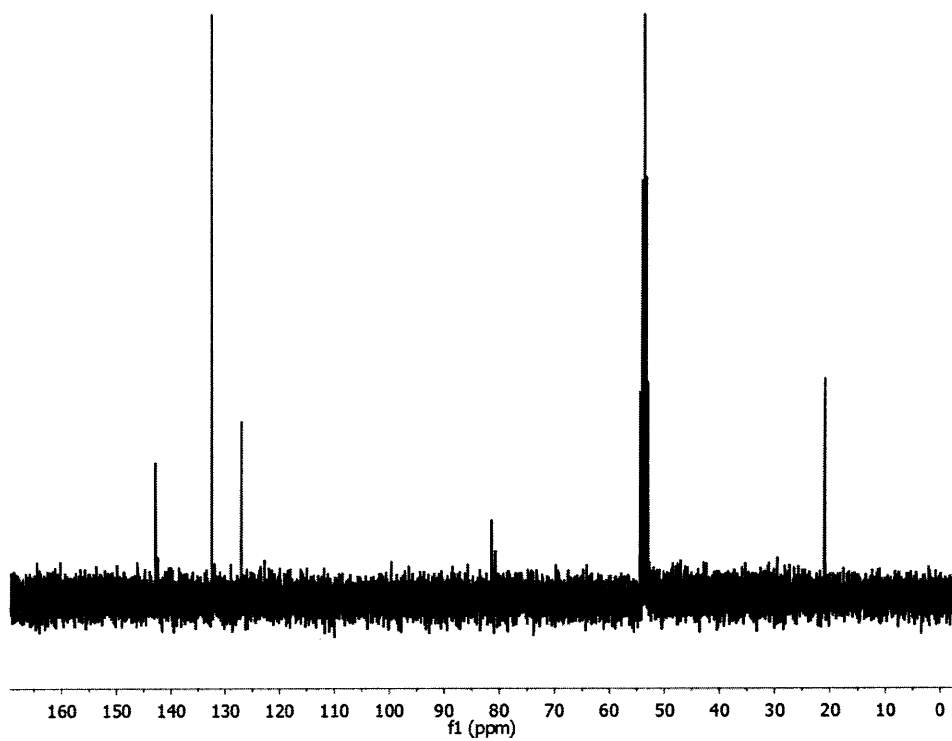


Figure 5.A.23. ^{13}C -NMR spectrum of **20** (300 MHz, CD_2Cl_2).

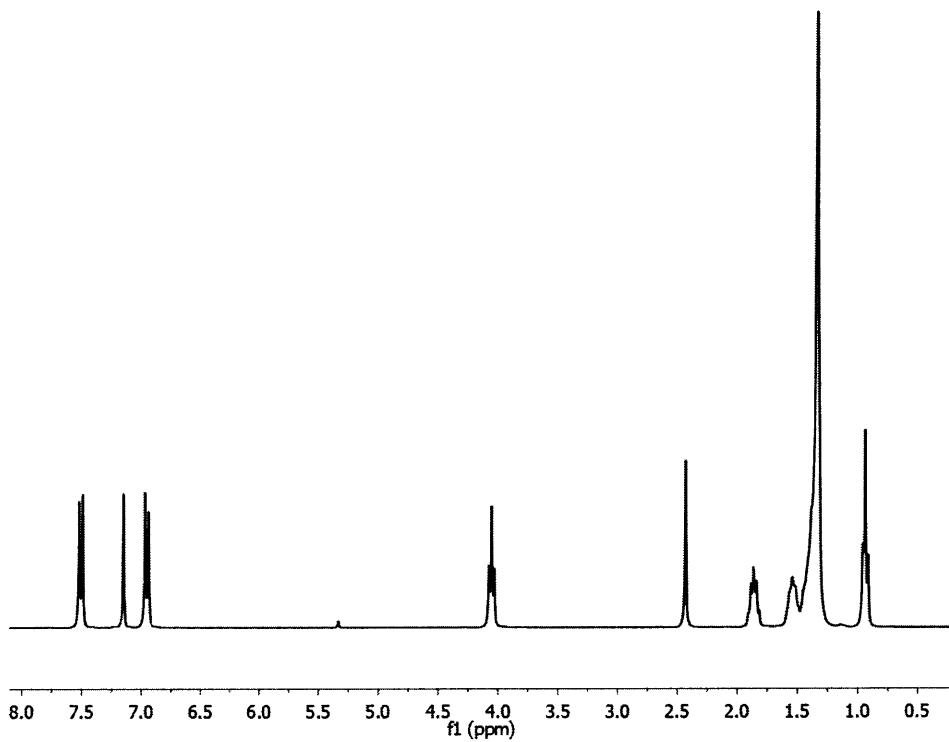


Figure 5.A.24. ^1H -NMR spectrum of **21** (300 MHz, CD_2Cl_2).

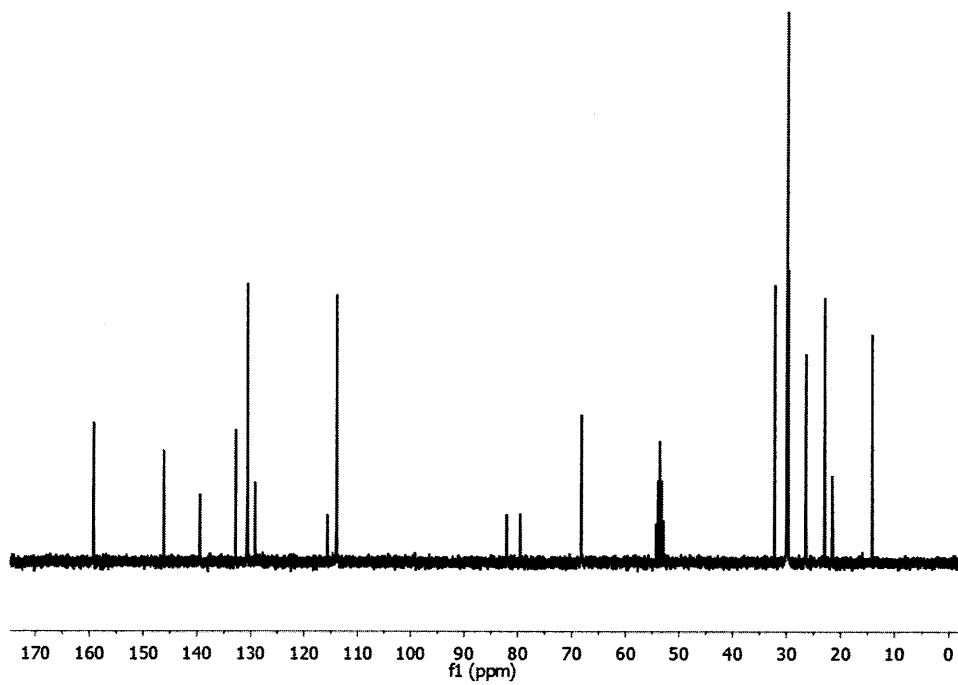


Figure 5.A.25. ^{13}C -NMR spectrum of **21** (300 MHz, CD_2Cl_2).

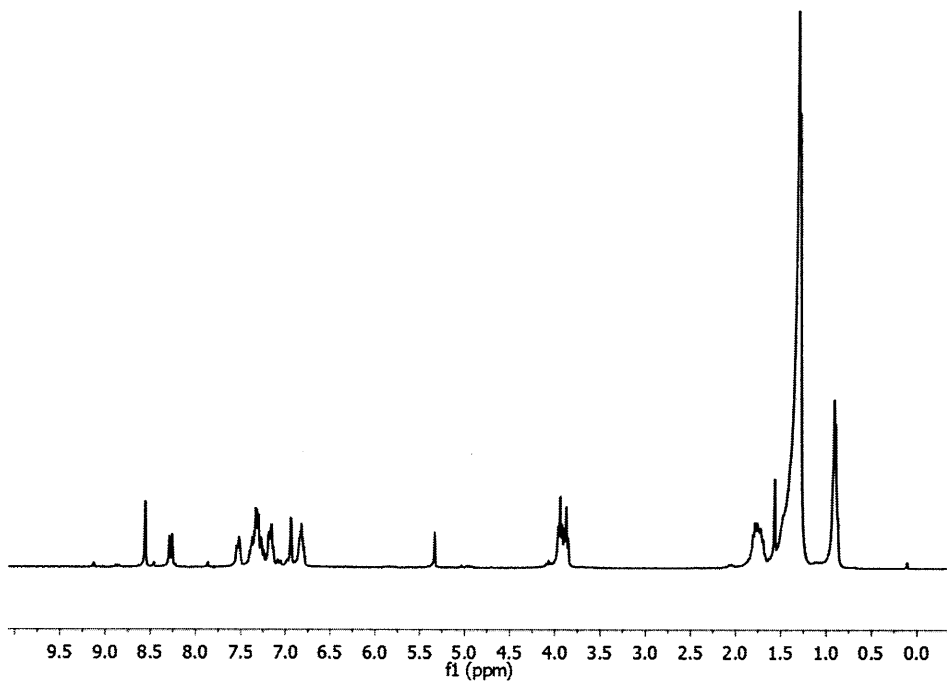


Figure 5.A.26. ^1H -NMR spectrum of **23** (300 MHz, CD_2Cl_2).

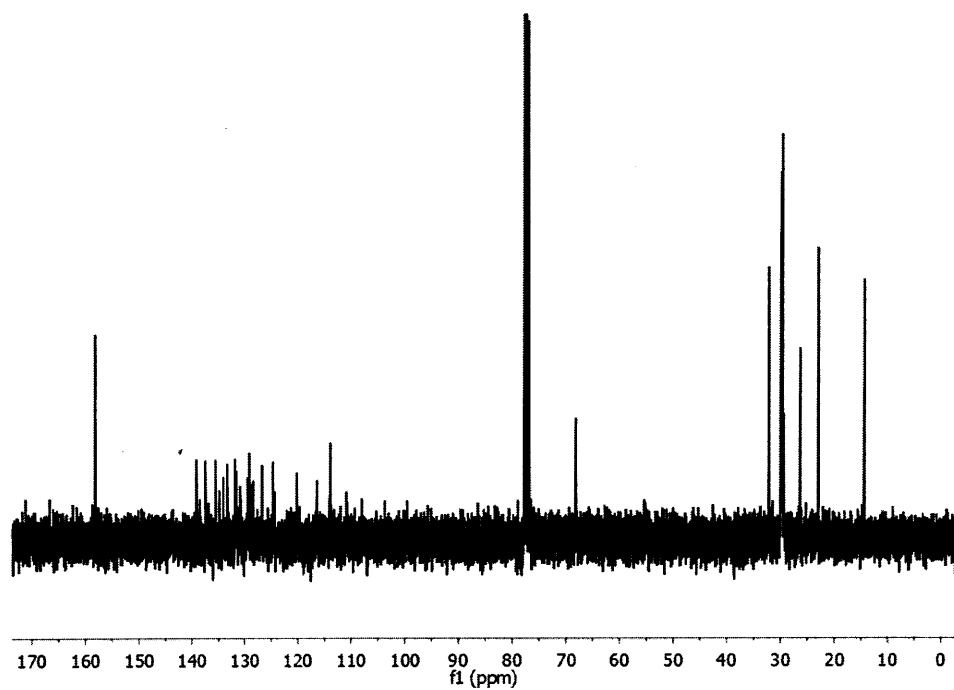


Figure 5.A.27. ^{13}C -NMR spectrum of **23** (300 MHz, CDCl_3).

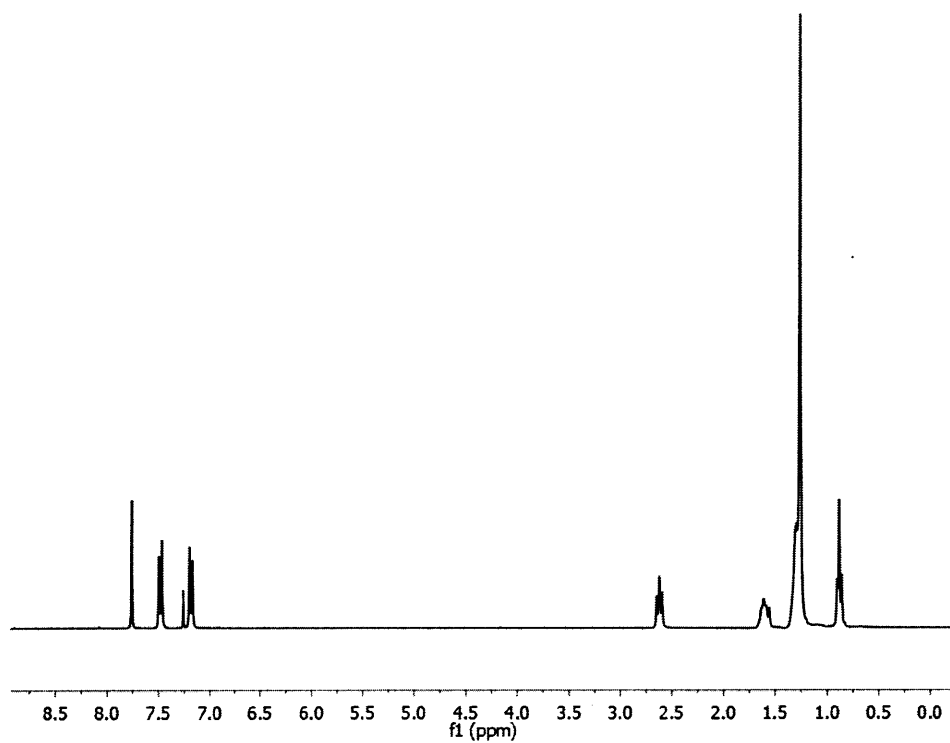


Figure 5.A.28. ^1H -NMR spectrum of **28** (300 MHz, CDCl_3).

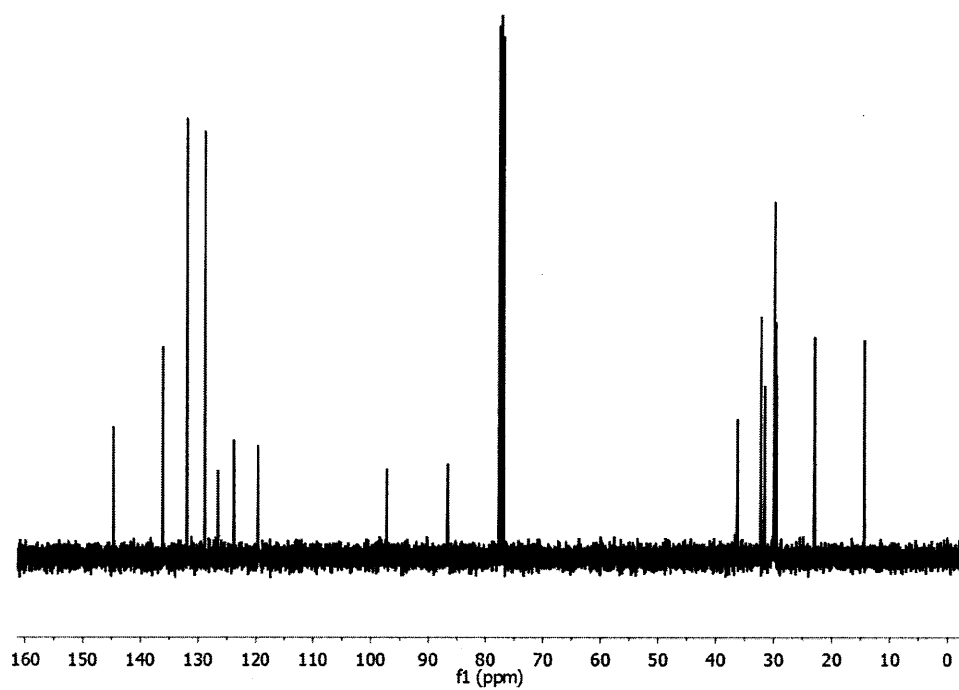


Figure 5.A.29. ^{13}C -NMR spectrum of **28** (300 MHz, CDCl_3).

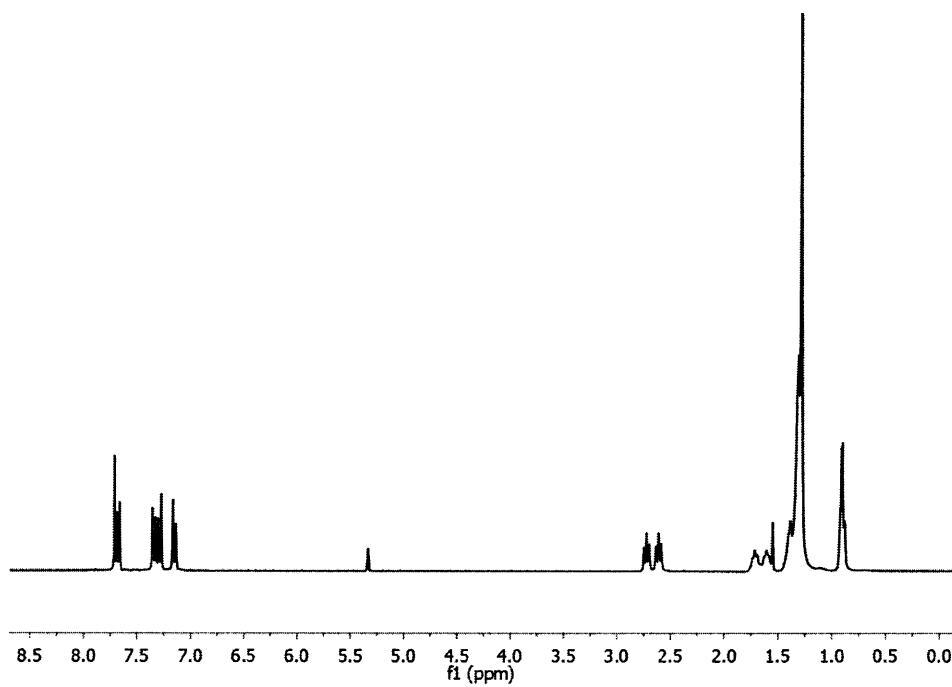


Figure 5.A.30. ^1H -NMR spectrum of **29** (300 MHz, CD_2Cl_2).

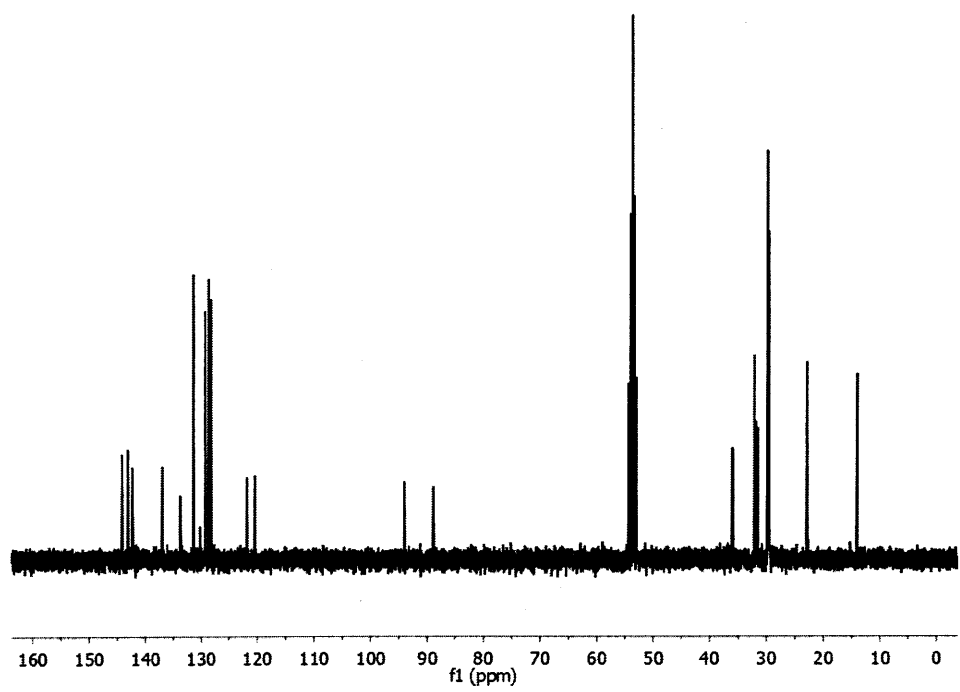


Figure 5.A.31. ^{13}C -NMR spectrum of **29** (300 MHz, CD_2Cl_2).

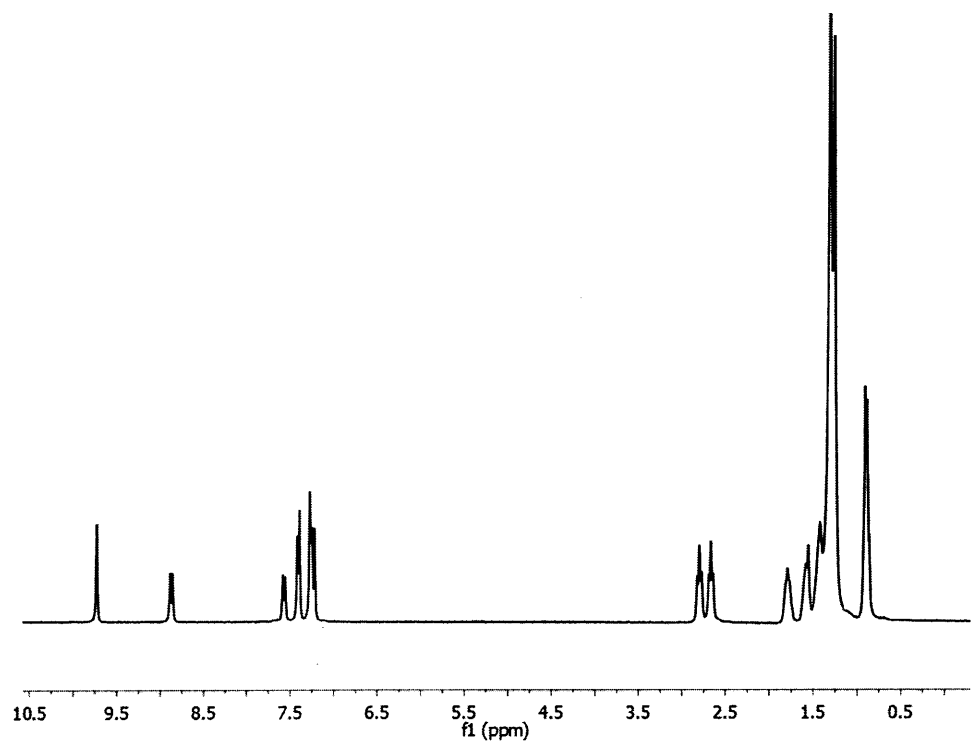


Figure 5.A.32. ^1H -NMR spectrum of **30** (300 MHz, CDCl_3).

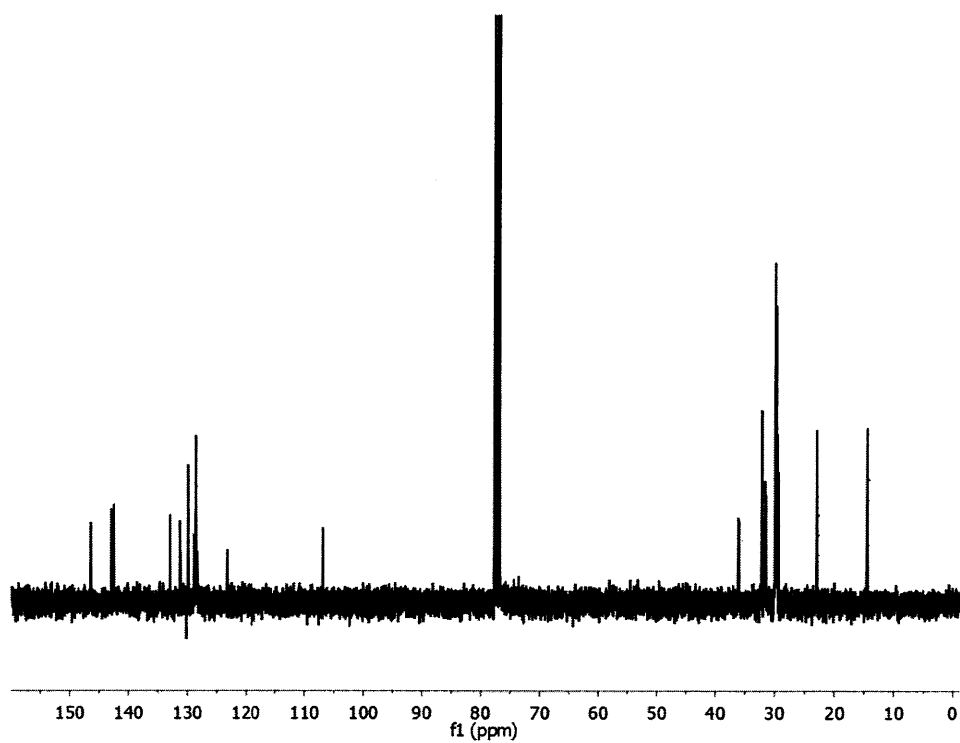


Figure 5.A.33. ^{13}C -NMR spectrum of **30** (300 MHz, CDCl_3).

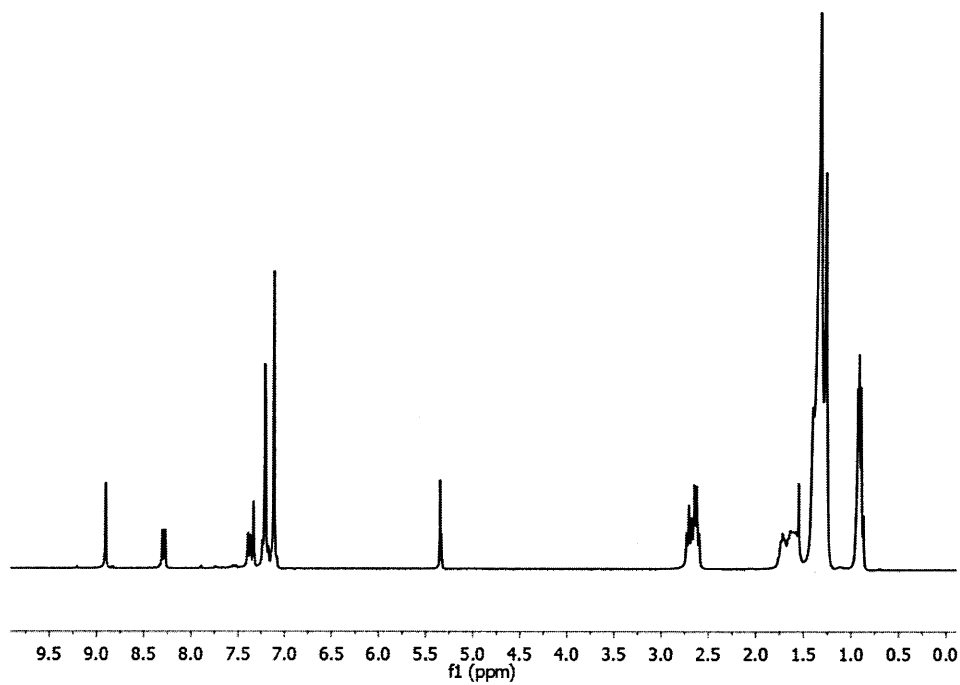


Figure 5.A.34. ^1H -NMR spectrum of **31** (300 MHz, CD_2Cl_2).

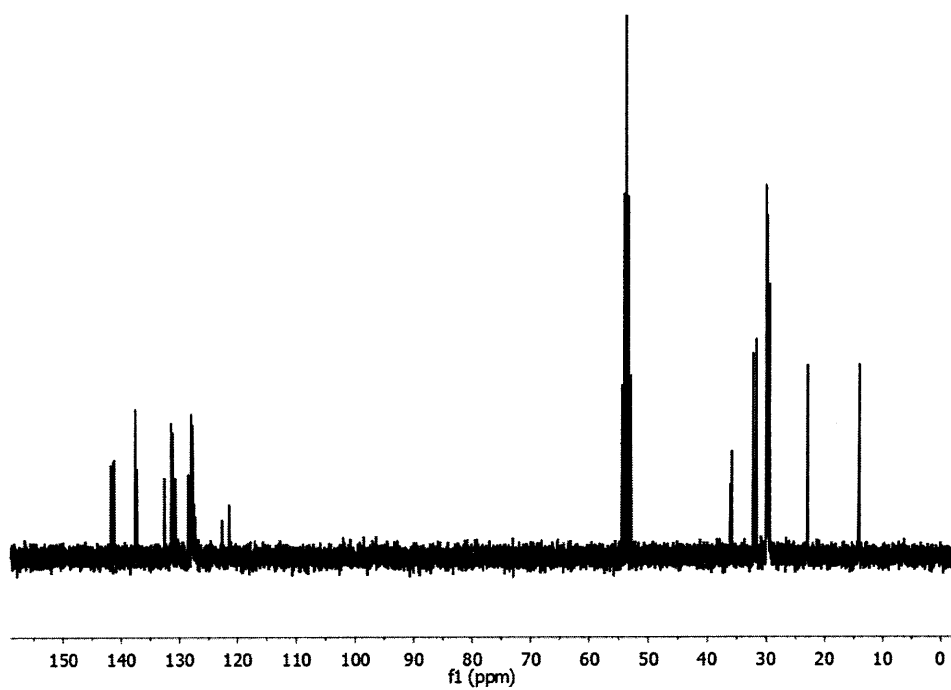


Figure 5.A.35. ^{13}C -NMR spectrum of 31 (300 MHz, CD_2Cl_2).

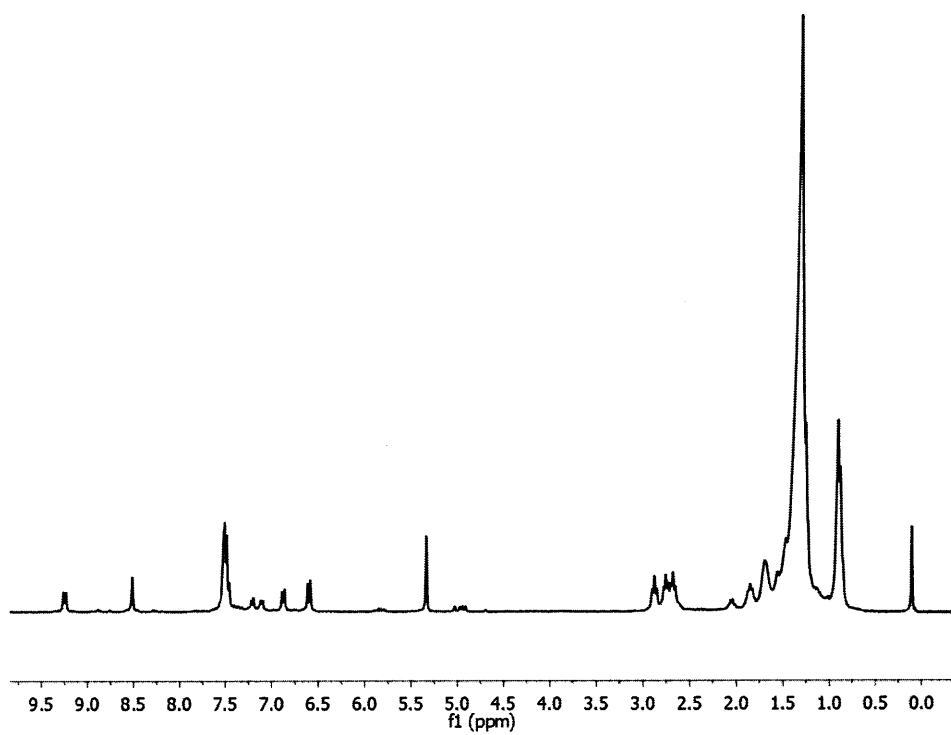


Figure 5.A.36. ^1H -NMR spectrum of 32 (300 MHz, CD_2Cl_2).

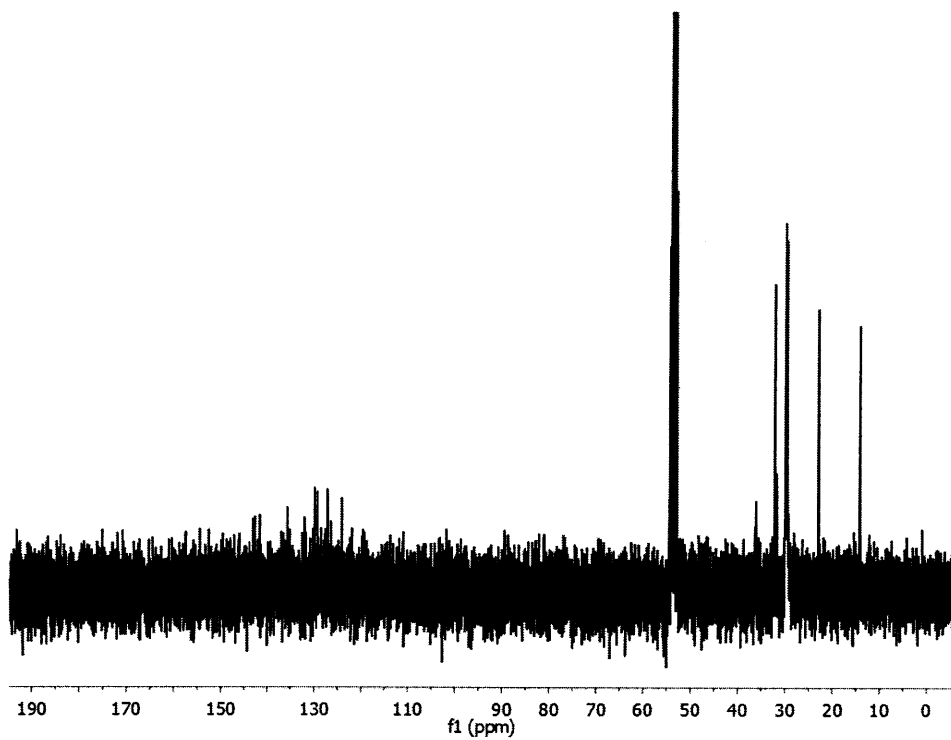


Figure 5.A.37. ^{13}C -NMR spectrum of **32** (300 MHz, CD_2Cl_2).

Curriculum Vitae

Julian M. W. Chan

EDUCATION

Massachusetts Institute of Technology

Cambridge, MA

Ph.D., Organic Chemistry

Expected June 2010

Thesis title: Design and Synthesis of Conjugated Macrocycles and Polymers

University of Illinois at Urbana-Champaign

Urbana-Champaign, IL

B.S., Chemistry, *summa cum laude*

May 2005

RESEARCH EXPERIENCE

Graduate Research Assistant with Professor Timothy M. Swager

2005-2010

Department of Chemistry, Massachusetts Institute of Technology

Design and synthesis of J-aggregating dibenz[*a,j*]anthracene-based macrocycles for potential application in electronic devices. Synthesis of highly functionalized cyclohexa-*m*-phenylenes, featuring a one-step, six-fold Suzuki macrocyclization. Synthesis of conjugated stair-stepped polymers containing dibenz[*a,h*]anthracene subunits. Designing novel J-aggregating conjugated polymers.

Undergraduate Research Assistant with Professor Eric Oldfield

2002-2005

Department of Chemistry, University of Illinois at Urbana-Champaign

Synthesized a library of structurally diversified bisphosphonates for use as anti-parasitic agents and bone-resorption drugs. Synthesized bisphosphonate and pyrophosphate compounds for use as T-cell stimulators. Prepared several transition metal–drug complexes for anti-tumor trials.

PUBLICATIONS

1. Chan, J. M. W., Kooi, S. E., Swager, T. M. "Synthesis of Stair-stepped Polymers Containing Dibenz[*a,h*]anthracene Subunits." *Macromolecules* **2010**, *43*, 2789-2793.
2. Chan, J. M. W., Tischler, J. R., Kooi, S. E., Bulović, V., Swager, T. M. "Synthesis of J-Aggregating Dibenz[*a,j*]anthracene-Based Macrocycles." *J. Am. Chem. Soc.* **2009**, *131*, 5659-5666.
3. Chan, J. M. W., Swager, T. M. "Synthesis of arylolethynylated cyclohexa-meta-phenylenes via sixfold Suzuki coupling." *Tetrahedron Lett.* **2008**, *49*, 4912-4914.
4. Song, Y., Chan, J. M. W., Tovian, Z., Secrest, A., Nagy, E., Krysiak, K., Bergan, K., Parniak, M. A., Oldfield, E. "Bisphosphonate inhibitors of ATP-mediated HIV-1 reverse

transcriptase catalyzed excision of chain-terminating 3'-azido, 3'-deoxythymidine: A QSAR investigation." *Bioorg. Med. Chem.* **2008**, *16*, 8959-8967.

5. Hudock, M. P., Sanz-Rodriguez, C. E., Song, Y., **Chan, J. M. W.**, Zhang, Y., Odeh, S., Kosztowski, T., Leon-Rossell, A., Concepcion, J. L.; Yardley, V., Croft, S. L., Urbina, J. A., Oldfield, E. "Inhibition of Trypanosoma cruzi Hexokinase by Bisphosphonates." *J. Med. Chem.* **2006**, *49*, 215-223.
6. Kotsikorou, E., Song, Y., **Chan, J. M. W.**, Faelens, S., Tovian, Z., Broderick, E., Bakalara, N., Docampo, R., Oldfield, E. "Bisphosphonate Inhibition of the Exopolyphosphatase Activity of the Trypanosoma brucei Soluble Vacuolar Pyrophosphatase." *J. Med. Chem.* **2005**, *48*, 6128-6139.
7. Sanders, J. M., Song, Y., **Chan, J. M. W.**, Jennings, S., Kosztowski, T., Odeh, S., Flessner, R., Kotsikorou, E., Meints, G., Gomez, A. O., Gonzalez-Pacanowska, D., Raker, A. M., Wang, H., Morita, C. T., Oldfield, E. "Pyridinium-1-yl Bisphosphonates are Potent Inhibitors of Farnesyl Diphosphate Synthase." *J. Med. Chem.* **2005**, *48*, 2957-2963.
8. Ling, Y., Sahota, G., Odeh, S., **Chan, J. M. W.**, Araujo, F. G., Moreno, S. N. J., Silvia, N. J., Oldfield, E. "Bisphosphonate Inhibitors of Toxoplasma gondi Growth: In Vitro, QSAR and In Vivo Investigations." *J. Med. Chem.* **2005**, *48*, 3130-3140.
9. Sanders, J. M., Ghosh, S., **Chan, J. M. W.**, Meints, G. A., Wang, H., Raker, A. M., Song, Y., Colantino, A., Burzynska, A., Kafarski, P., Morita, C. T., Oldfield, E. "Quantitative Structure-Activity Relationships for γ,δ T-Cell Activation by Bisphosphonates." *J. Med. Chem.* **2004**, *47*, 375-384.
10. Ghosh, S., **Chan, J. M. W.**, Lea, C. R., Meints, G. A., Lewis, J. C., Tovian, Z. S., Flessner, R. M., Loftus, T. C., Bruchhaus, I., Kendrick, H., Croft, S. L., Kemp, R. G., Kobayashi, S., Nozaki, T., Oldfield, E. "Effects of bisphosphonates on the growth of Entamoeba histolytica and Plasmodium species in vitro and in vivo." *J. Med. Chem.* **2004**, *47*, 175-187.

PRESENTATIONS

1. **Chan, J. M. W.**, Swager, T. M. "Synthesis of functionalized hexa-*m*-phenylenes." *Poster presented*, 234th ACS National Meeting, Boston, MA, **2007**.
2. **Chan, J. M. W.**, Swager, T. M. "Synthesis of novel Kekulene-type Torands." *Poster presented*, 21st International Liquid Crystal Conference, Keystone, CO, **2006**.

PATENT APPLICATIONS

1. Sanders, J. M., Song, Y., **Chan, J. M. W.**, Oldfield, E., Zhang, Y. "Bisphosphonate compounds and methods for bone resorption diseases, cancer, bone pain, immune disorders and infectious diseases." PCT/US2005/036425.

Acknowledgments

I would like to thank my research advisor Professor Tim Swager for accepting me into his group, for being so patient throughout the entire duration of my graduate student life, and for granting me unparalleled freedom to conduct scientific research, without which the work described herein would not have been possible. It should also be mentioned that Tim's frequent provision of career counseling as well as general advice for professional and personal growth went well beyond the call of duty.

I must also acknowledge the other members of my thesis committee, Professors Rick Danheiser and Mounji Bawendi, for their helpful suggestions and advice. In particular, I thank Prof. Danheiser for all the helpful career advice provided during our annual meetings.

I am also indebted to all my fellow Swager group members for offering their help and advice whenever I was in need. Special thanks go out to former postdocs Koushik Venkatesan and Kazunori Sugiyasu, who not only offered me their insight in a professional capacity, but also for being there as friends during the first half of my Ph.D. program. I also thank my current office/bay-mates Wang Fei, Liu Shuang, Mindy Levine, and Rebecca Parkhurst for their company and for helping make tough days go by faster. I shall also not forget all the help and advice that Jean Bouffard, Andrew Satrijo and Changsik Song have given me over e-mail even well after they had left the group.

I also thank my collaborators Yaakov Tischler of Bulović group and Steven Kooi of the ISN for rendering their expertise in physics and instrumentation, Yaakov in particular for sharing his knowledge and helping me better understand the physical aspects of J-aggregates.

Of course, nothing would have been possible without the unwavering love and support of my parents (Chan Yat Peng and Ng Soi Hong) and sister (Lesley Chan) throughout the course of my life. My parents have always been there for me, not only in terms of providing me with a good education and financial support, but also in the form of emotional support during difficult periods. I dedicate this thesis to them, and hope that whatever I have accomplished to date and in the future will stand testimony to the fact that all their hard work and sacrifice over the years have not been in vain. My family has been, and will always be, a positive influence in my life.

Last but not least, I express my gratitude to my fiancée Tong Puiyee for being there for me over the past three years with all her love and support, and also for showing infinite patience in waiting for me to graduate. I can only regret the fact that my hectic research schedule had taken away a lot of the time and attention that she rightfully deserves.

